

EFFECT OF ADDITION OF GRAPHENE OXIDE ON CEMENT MORTAR

Thesis submitted by

SURAJIT BISWAS

Doctor of Philosophy (Engineering)

**Department of Civil Engineering
Faculty Council of Engineering & Technology
Jadavpur University
Kolkata, India
2024**

JADAVPUR UNIVERSITY
KOLKATA – 700 032, INDIA

INDEX NO: 04/18/E

1. Title of the thesis: Effect of addition of graphene oxide on cement mortar.

2. Name, Designation & Institution of the Supervisor:

Dr. Saroj Mandal

Professor

Department of Civil Engineering

Jadavpur University,

Kolkata 700032, India

3. List of publications:

Journal Publications

[1] **Surajit Biswas** and Saroj Mandal, Mechanical and micro-structural study of cement mortar with graphene oxide, Journal of Building Pathology and Rehabilitation (2022) 7:87.
<https://doi.org/10.1007/s41024-022-00232-8>.

[2] **Surajit Biswas**, Sk. Aakash Hossain, and Saroj Mandal, Fly ash-based Cement-Sand Mortar with Graphene Oxide nano-sheet: An Experimental Study on Strength, Durability and Microstructural Properties, Journal of Materials Science, (Communicated).

4. List of Patents – Nil

5. List of Publications in International Conference Proceedings:

[1] **Surajit Biswas** and Saroj Mandal, Effect of Graphene oxide Addition on Cement-Sand Mortar, 12th Structural Engineering Convention - An International Event (SEC 2022)/ASPS Conference Proceedings 1: 135-138 (2022).

[2] **Surajit Biswas** and Saroj Mandal, Graphene Oxide Modified Cement Mortar, 2nd International Conference on Futuristic and Sustainable Aspects in Engineering and Technology/AIP Conference Proceedings 2721, 020033 (2023).

6. List of Presentations at National/International Conference

[1] **Surajit Biswas**, Ashis Majee, and Saroj Mandal, Study on the mechanical properties of cement-sand mortar with graphene oxide addition, Proceedings of International Conference on Energy and Sustainable Development Jointly organized by Jadavpur University and The Institution of Engineers, India, February 14-15 (2020).

[2] **Surajit Biswas** and Saroj Mandal, Utilization of Graphene Oxide to Enhance the Mechanical Properties of Cement-Sand Mortar. Revolutions in Concrete Construction: Vision 2050. Delhi, India (2022).

STATEMENT OF ORIGINALITY

SHRI SURAJIT BISWAS registered on 4th June 2018 do hereby declare that this thesis entitled “**EFFECT OF ADDITION OF GRAPHENE OXIDE ON CEMENT MORTAR**” contains a literature survey and original research work done by the undersigned candidate as part of Doctoral studies.

All information in this thesis been obtained and presented in accordance with existing academic rules and ethical conduct. I declare that, as required by these rules and conduct, I have fully cited and referred all materials and results that are not original to this work.

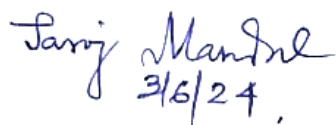
I also declare that I have checked this thesis as per the “Policy on Anti Plagiarism, Jadavpur University, 2019”, and the level of similarity as checked by iThenticate software is 7 %.

Signature of Candidate:



Date: 03/06/2024

**Certified by Supervisor:
(Signature with date, seal)**



Dr. Saroj Mandal
Professor
Civil Engineering Department
JADAVPUR UNIVERSITY
Kolkata-32

Dr. Saroj Mandal

Professor

Department of Civil Engineering

Jadavpur University

Kolkata 700032

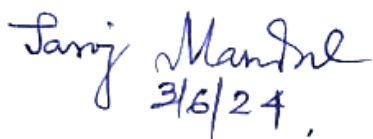
India

CERTIFICATE FROM THE SUPERVISOR

This is to certify that the thesis entitled “**EFFECT OF ADDITION OF GRAPHENE OXIDE ON CEMENT MORTAR**”, Index No. 04/18/E, submitted by **Shri SURAJIT BISWAS**, who got his name registered on 4th June, 2018 for the award of Ph.D. (Engg.) degree of Jadavpur University is absolutely based upon his own work under the supervision of **Dr. Saroj Mandal** and that neither his thesis nor any part of the thesis has been submitted for any degree/diploma or any other academic award anywhere before.

Certified by Supervisor:

(Signature with date, seal)



Saroj Mandal
3/6/24,

Dr. Saroj Mandal

Professor

Department of Civil Engineering

Jadavpur University

Kolkata 700032

India

Dr. Saroj Mandal
Professor
Civil Engineering Department
JADAVPUR UNIVERSITY
Kolkata-32

**Dedicated
To
My Father**

DECLARATION

This work has not previously been submitted for a degree or diploma in any University. To the best of my knowledge and belief, the thesis contains no material previously published or written by another person except where due reference is made in the thesis itself.

Surajit Biswas
03/06/2024

SURAJIT BISWAS

ACKNOWLEDGEMENTS

The person who upheld me from nowhere and believed that I could continue his high-end research legacy, the person I will be beyond grateful forever to, is my supervisor Dr. Saroj Mandal. Without him, my research journey would never start. He has extended his supervision, mentorship, and unwavering support throughout my doctoral journey, and taught me how to push oneself beyond his comfort zone.

I would like to express my gratitude to Dr. Papita Das, Professor, Department of Chemical Engineering, Jadavpur University, and Dr. Brajadulal Chattopadhyay, Professor, Department of Physics, Jadavpur University for their support and for allowing me to access their laboratories.

I am deeply grateful for the unwavering love and support I have received from my mother, Rita Biswas, throughout my doctoral journey.

Expressing gratitude to Uncle Mr. Gurubar Biswas and Aunt Mrs. Suchismita Biswas Roy for their unwavering support throughout my doctoral journey. They have not only provided encouragement but also taught me the importance of pushing oneself beyond the comfort zone.

I am grateful for the affection and support I have received during my doctoral journey from all of my cousins, sisters, and brothers, especially Kankan Biswas.

I am grateful to my fellow researchers Biplab Ranjan Adhikari, Sayak Nandi, Saikat Sarkar, Aritra Majumder, Saptarshi Roy, Souvik Roy, Sourish Mukherjee, Arkadeb Saha, Rakesh Sikder, Debasis Sahu, Mainak Maity, Achinta Mandal, and Poushali Chakraborty for their affection and support throughout my doctoral journey.

I thank all the teaching and non-teaching staff members of the Department of Civil Engineering, Jadavpur University.

Last but not least, I extend my heartfelt thanks to all my friends for their love and support, especially Prosenjit Ghosh.

SURAJIT BISWAS

ABSTRACT

Graphene oxide (GO) is a derivative of graphene, which has a single layer of carbon atoms arranged in a two-dimensional honeycomb lattice. Each carbon atom's bonding within this is hybridized sp^2 with the inclusion of π -orbitals. Each graphene unit cell contains two orbitals that are scattered to form two bonds, each of which might be referred to as bonding and antibonding. Over the past few decades, GO has drawn attention for its use as a reinforcing element in cement-based construction materials. There are very limited studies on the effect of GO addition in cement based materials. Previous studies indicate the GO addition in cement along with different types of dispersing agents or chemicals and minerals. Thus, an attempt has been taken to use GO without such chemicals or minerals in cement sand mortar using two different types of cement such as Ordinary Portland Cement (OPC) and Portland Pozzolana Cement (PPC). The mechanical strength, durability, and micro-structure properties of mortar having the cement-sand ratio of 1:2 and 1:3 (by weight) with and without GO have been studied experimentally. The different proportions of GO (0.03–0.06% by weight of cement) were incorporated into the cement mortar matrix. The water-to-cement ratio was fixed at 0.45.

The uniform dry mixing of GO in cement mortar is quite difficult. The GO nanoparticles tend to agglomerate and form clusters in the presence of water due to their hydrophobic nature and strong Van der Waals interactions between individual nanoparticles. Thus, the most significant process for uniform mixing of GO in cement composites is the sonication of GO with water and subsequent addition in the matrix. During sonication, it breaks down the agglomeration and promotes dispersion and exfoliation. In this present study, GO was mixed with water at a ratio of 1:200 (by weight), and it was sonicated for 45–60 minutes using a UP100H ultrasonic processor, no additional chemicals or dispersion agents were used.

The results of the flow table test indicated that for all types of mortar mixes using either OPC or PPC, the workability in terms of the final flow diameter of the flow table is reduced with the

addition of GO compared to the control mortar mix (without GO). The maximum reduction was noted with the addition of 0.03% of GO for all mixes. In general, the addition of GO increases the compressive strength of the OPC or PPC based cement sand mortar up to an optimum limit. This is due to the filling up of nano pores and the GO acts as nanofibers within the matrix arresting the initial micro cracks as per microstructural study. The optimum amount of GO in terms of maximum compressive strength was 0.05% and 0.04% by weight of cement, for OPC and PPC based cement-sand mortars, respectively. The flexural and split tensile strength of such mortars show similar results. The Young's modulus of OPC or PPC based cement-sand mortar is also enhanced with the addition of a small amount of GO.

The durability study also indicated that the optimum amount of GO addition in the cement-sand mortar was 0.05% and 0.04% by weight of cement, for OPC or PPC based cement-sand mortars as in the case of strength. The rate of water absorption of GO modified OPC or PPC based cement mortar was lower than the control sample. Similarly, the amount of charge passing through the specimens in the RCPT test was found lower for GO modified cement mortar. However, the GO modified OPC and PPC based cement-sand mortar have almost similar resistance against acid attack for a limited period of 56 days compared to the control.

The MIP test result of OPC and PPC based cement mortar confirmed that the incorporation of the optimum amount of GO, by filling of large pore area reduces the total pore volume and refines the pore structure of cement mortar. The results of XRD analysis reported that the formation of more C-S-H gel in GO based cement mortar both in OPC or PPC with respect to their corresponding control mortar. As per the FESEM test, a distinct change in the morphology of GO modified OPC or PPC based cement mortar is detected as compared to their corresponding control where the former had a large amount of denser crystal. The elemental analysis by EDX indicated that the percentages of carbon atoms and silicon atoms in cement mortar changed noticeably with the addition of a small amount of GO.

Although, the addition of appropriate amount GO to cement-sand mortar enhanced the strength and durability, but long-term effects are not studied. The optimum limit for the cement sand mixture will change depending on the mix proportion and the chemical composition of GO. Despite its high cost, wider applications of GO in different fields will definitely reduce the price over time.

CONTENTS

Sl No.	Page No
CHAPTER -1: INTRODUCTION	
1.0 General View	1
1.2 Graphene oxide (GO)	3
1.3 Mechanical properties of Graphene oxide	6
1.4 Background	7
1.5 Goals	8
1.6 Research objectives	9
CHAPTER - 2: REVIEW OF LITERATURE	
2.0 General View	15
2.1 History of GO	15
2.2 Source of GO	16
2.3 Current Trend of Research on Cementitious Materials	17
2.4 Review on GO Modified Cement Composites	17
2.4.1 Workability	17
2.4.2 Compressive strength	22
2.4.3 Tensile strength	39
2.4.4 Flexural strength	42
2.4.5 Young modulus (E value)	50
2.4.6 Durability	52
2.4.6.1 Water absorption	53
2.4.6.2 Rapid chloride ion penetration test (RCPT)	55
2.4.6.3 Acid resistance test	57
2.4.7 Micro-structural analysis	59
2.4.7.1 Mercury Intrusion Porosimetry (MIP)	59
2.4.7.2 X-Ray Diffraction analysis (XRD)	62
2.4.7.3 Scanning Electron Microscopy (SEM)	65
2.5 Aim of The Present Study	70
CHAPTER - 3: INSTRUMENT & APPARATUS	
3.0 General View	78
3.1 Ultrasonic Probe Sonicator	78
3.3 Compressive Strength and Split Tensile Strength Test	79
3.3 Flexural Strength Test	80
3.4 Flow Table Test	81
3.5 Ultrasonic Pulse Velocity test (UPV)	82
3.6 Chloride Ion Penetration Test (RCPT)	83
3.7 X-ray Diffraction (XRD)	84
3.8 Field Emission Scanning Electron Microscope (FESEM)	86
3.9 Mercury Intrusion Porosimetry (MIP)	87
CHAPTER - 4: MATERIALS AND METHODS	
4.0 General View	88
4.1 Materials	88
4.1.1 Graphene oxide (GO)	88

4.1.2 Cement	89
4.1.3 Fine aggregate (Sand)	90
4.1.4 Water	91
4.2 Experimental Program	91
4.2.1 Characterization of GO	91
4.2.2 Dispersion of GO	91
4.2.3 Preparation GO modified cement mortar	92
4.3 Sample Preparation	93
4.3.1 Flow test	93
4.3.2 Compressive strength test	94
4.3.3 Split tensile strength test	96
4.3.4 Flexural strength test	96
4.3.5 Measurement of young modulus (E value)	97
4.3.6 Ultrasound pulse velocity (UPV) test	98
4.3.7 Rapid chloride penetration Test (RCPT)	98
4.3.8 Sorptivity test	98
4.3.9 Acid resistance test	99
4.3.10 Mercury intrusion porosity (MIP) test	99
4.3.11 X-ray diffraction analysis (XRD)	99
4.3.12 Field emission scanning electron microscopy (FESEM) and energy dispersive X-Ray (EDX) analysis	100
 CHAPTER - 5: RESULTS AND DISCUSSION	
5.0 General View	102
5.1 Characterization of GO	102
5.2 Flow Table Test	104
5.3 Compressive Strength Test	107
5.4 Split Tensile Strength	113
5.5 Flexural Strength	118
5.6 Measurement of Young Modulus (E value)	124
5.7 Ultrasonic Pulse Velocity Test (UPV)	125
5.8 Sorptivity Test	126
5.9 Rapid Chloride Penetration Test (RCPT)	130
5.10 Acid Resistance Test	131
5.11 Mercury Intrusion Porosimetry (MIP) Test	137
5.12 X-ray Diffraction Analysis (XRD)	139
5.13 Field Emission Scanning Electron Microscopy Analysis (FESEM)	141
5.14 Energy Dispersive X-Ray Analysis (EDX)	143
5.15 Limitations	144
 CHAPTER - 6: CONCLUSION & FUTURE SCOPE	
6.1 Conclusion	147
6.2 Future scope of the study	150

LIST OF FIGURES

CHAPTER-1: INTRODUCTION

	Page No
Fig. 1.1: Morphological images of (a) nanorods, (b) nanowires, and (c) nanotubes (A.A. Ghassan 2020).	3
Fig. 1.2: Images of (a) Titanium oxide, (b) Carbon nanotube, and (c) Nano silica	3
Fig. 1.3: Chemical single layer structure of GO. (Nasrollahzadeh et al. 2015).	4
Fig. 1.4: Modified Hummer's method for GO synthesis.	6

CHAPTER-2: REVIEW OF LITERATURE

Fig. 2.1: Mini slump flow at 10 min after lifting the mini core (Kai Gong et al. 2015).	18
Fig. 2.2: Impact of PC, GO, and PC+GO on the fluidity cement pastes (Li Zhao et al., 2018).	20
Fig. 2.3: Fluidity behaviour of GO modified fly-ash based cement mortar with PCs and CNTs (Jianqing Gong et al. 2020).	20
Fig. 2.4: Fluidity behaviour of GO modified cement mortar with SF, FA, and PCs (C. Liu et al. 2021).	21
Fig. 2.5: Slump test results of GO modified cement mortar with PCs (X. Hong et al. 2023).	22
Fig. 2.6: Compressive strength of plain cement and GO-cement samples at different curing ages (Q. Wang et al., 2015).	23
Fig. 2.7: Compressive strength of plain cement and GO-cement samples at different curing ages (Z. Pan et al., 2013).	24
Fig. 2.8: Compressive strength of plain cement and GO-cement samples at different curing ages (K. Gong et al., 2015).	25
Fig. 2.9: Compressive strength of GO modified cement mortar at different curing ages (S. Sharma and N. C. Kothiyal, 2015).	26
Fig. 2.10: Compressive strength of hardened cement paste with and without GONPs (M.M. Mokhtar et al. 2017).	27
Fig. 2.11: Compressive strength of GO modified cement paste at different curing ages (H. Yang et al. 2017).	28
Fig. 2.12: Compressive strength of cement paste of (a) Dry-mix method, and (b)Wet-mix method (J. An et al., 2018).	28
Fig. 2.13: Compressive strength of different mixes of cement mortar at 7 days curing age (L. Zhao et al., 2018).	29
Fig. 2.14: Compressive strength of different mixes at different curing ages (S. Sharma et al. 2018).	31
Fig. 2.15: Compressive strength of cement past with and without GO at different curing ages (G. Xu et al. 2019).	32

Fig. 2.16:	Compressive strength of GO modified cement paste with 0.04% of GO at different curing ages (A.M. Sabziparvar 2019).	33
Fig. 2.17:	Compressive strength and flexural strength of GO modified cement-sand mortar with different w/c ratios (H. Peng et al. 2019).	33
Fig. 2.18:	Compressive strength of GO modified fly-ash based with PCs and CNTs at different curing ages (J. Gong et al. 2020).	34
Fig. 2.19	Compressive strength of GO modified cement mortar with SF, PCs, FA at different ages of curing ages (C. Liu et al. 2021).	36
Fig. 2.20:	Compressive strength of GO modified cement mortar with SF (P. Vasudevareddy et al. 2022).	38
Fig. 2.21:	Compressive strength of GO modified cement mortar with PCs (X. Hong et al. 2023).	39
Fig. 2.22:	Compressive strength of GO modified cement mortar (a) with and (b) without SP at different curing ages (L. Djenaoucine et al. 2023).	39
Fig. 2.23:	Indirect tensile strength of plan cement paste and GONPs modified cement paste after 28 days hydration (M.M. Mokhtar et al. 2017).	41
Fig. 2.24:	Tensile strength of different mixes at different curing ages (S. Sharma et al. 2018).	42
Fig. 2.25:	Split tensile strength behaviour of GO modified cement mortar with nano-silica (P. Vasudevareddy et al. 2022).	43
Fig. 2.26:	Flexural strength of GO modified cement paste with 0.04% of GO at different curing ages (A.M. Sabziparvar 2019).	45
Fig. 2.27:	Flexural strength of GO modified cement mortar with SF, PCs, FA at different ages (C. Liu et al. 2021).	47
Fig. 2.28:	Flexural strength of cement mortar with GO and TiO ₂ -rGO at different curing ages (X. Qi et al. 2021).	48
Fig. 2.29:	Flexural strength behaviour of GO modified cement mortar with nano-silica (P. Vasudevareddy et al. 2022).	49
Fig. 2.30:	Flexural strength of GO modified cement mortar at different curing ages (A. Bagheri et al. 2022).	50
Fig. 2.31:	Flexural strength of concrete with different percentages of GO (Z. Cheng et al. 2023).	50
Fig. 2.32:	Dynamic elastic modulus relative (%) at different temperatures (S. Han et al. 2022).	52
Fig. 2.33:	Modulus of elasticity of cement mortar with GO and PVA (N. Bheel et al. 2023).	52

Fig. 2.34:	Water absorption curve of GO modified cement-sand mortar along with soaking time, (A) total water absorption (wtot), and (B) average water absorption (wpr) (J. Luo et al. 2021).	54
Fig. 2.35:	Water absorption curve of cement mortar with GO and TiO ₂ -RGO at different (X. Qi et al. 2021).	55
Fig. 2.36:	Sorptivity test results of GO modified cement-sand mortar (A. Bagheri et al. 2022).	55
Fig. 2.37:	RCPT test results of cement mortar with GO and TiO ₂ -RGO (X. Qi et al. 2021).	56
Fig. 2.38:	RCPT test of concrete with different percentages of GO (Z. Cheng et al. 2023).	57
Fig. 2.39:	RCPT test results of cement mortar with different percentages of GO and PVA fibre (N. Bheel et al. 2023).	57
Fig. 2.40:	Weight loss curve of GO modified cement mortar with nano-silica (P. Vasudevareddy et al. 2022).	59
Fig. 2.41:	Pore-size distribution curves of plain and GONPs modified cement paste after 28 days hydration (M.M. Mokhtar et al. 2017).	60
Fig. 2.42:	Pore size distribution of various GO-containing RFA mortar after 28 days (W. J. Long et al. 2018).	61
Fig. 2.43:	Pore size distribution of cement mortar with GO and TiO ₂ -rGO (X. Qi et al. 2021).	62
Fig. 2.44:	XRD results of different GO modified cement paste, peaks are produced by Ca(OH) ₂ , peaks 2 are produced by C ₃ S and C ₂ S phases (H. Yang et al., 2017).	63
Fig. 2.45:	XRD pattern of cement pastes with different concentration of GONPs (M.M. Mokhtar et al. 2017).	64
Fig. 2.46:	XRD pattern of GO modified FA based cement mortar after 28 days curing (S. Sharma et al. 2018).	65
Fig. 2.47:	SEM image of GO modified cement mortar (at 7 days) with small quantity of PC (L. Zhao et al., 2016).	66
Fig. 2.48:	SEM image of cement paste containing 0.2% of GO (H. Yang et al. 2017).	66
Fig. 2.49:	SEM images of cement mortar with different percentages of GO (H. Peng et al. 2019).	68

CHAPTER-3: INSTRUMENT & APPARATUS

Fig. 3.1:	Ultrasonic probe sonicator.	79
Fig. 3.2:	Compressive strength and split tensile strength test set up.	80
Fig. 3.3:	Graphical set up of flexural strength test.	80
Fig. 3.4:	Flexural strength test set-up.	81

Fig. 3.5:	Flow table test set up.	82
Fig. 3.6:	UPV test set up.	83
Fig. 3.7:	RCPT test set up.	84
Fig. 3.8:	Graphical presentation of XRD test.	85
Fig. 3.9:	XRD test arrangement	85
Fig. 3.10:	FESEM analysis setup.	87

CHAPTER-4: MATERIALS AND METHODS

Fig. 4.1:	Graphene oxide nanoparticles.	88
Fig. 4.2:	Powder form of cement.	89
Fig. 4.3:	Dry fine aggregates (sand).	90
Fig. 4.4:	Dispersed GO after sonication.	92
Fig 4.5:	Flow chart of GO modified sample preparation	93
Fig. 4.6:	Flow test of mortar.	94
Fig. 4.7:	Mortar cube specimens.	94
Fig. 4.8:	Cylindrical mortar specimens.	96
Fig. 4.9:	Beam specimens for flexural strength test.	97

CHAPTER-5: RESULTS AND DISCUSSION

Fig. 5.1a:	XRD analysis of GO.	103
Fig. 5.1b:	FT-IR spectra of GO.	103
Fig. 5.1c:	SEM image of GO	103
Fig. 5.2a:	Flow table test results of GO modified OPC 1:2 cement-sand mortar mixes.	104
Fig. 5.2b:	Flow table test results of GO modified OPC 1:3 cement-sand mortar mixes.	105
Fig. 5.2c:	Flow table test results of GO modified PPC 1:2 cement-sand mortar mixes.	105
Fig. 5.2d:	Flow table test results of GO modified PPC 1:2 cement-sand mortar mixes.	106
Fig. 5.3a:	Compressive strength of GO modified OPC 1:2 cement-sand mortar mixes with different curing ages.	108
Fig. 5.3b:	Compressive strength of GO modified OPC 1:3 cement-sand mortar mixes with different curing ages.	109
Fig. 5.3c:	Compressive strength of GO modified PPC 1:2 cement-sand mortar mixes with different curing ages.	111
Fig. 5.3d:	Compressive strength of GO modified PPC 1:3 cement-sand mortar mixes with different curing ages.	112
Fig. 5.4a:	Split tensile strength behaviour of OPC based mortar of 1:2 (cement: sand) ratio with/without GO after 28 days of curing.	115
Fig. 5.4b:	Split tensile strength behaviour of OPC based mortar of 1:3 cement-sand ratio with/without GO after 28 days of curing.	116

Fig. 5.4c:	Split tensile strength behaviour of PPC based mortar of 1:2 cement-sand ratio with/without GO after 28 days of curing.	117
Fig. 5.4d:	Split tensile strength behaviour of PPC based mortar of 1:3 cement-sand ratio with/without GO after 28 days of curing.	118
Fig. 5.5a:	Flexural strength behaviour of OPC 1:2 cement-sand ratio mortar with/without GO after 28 days curing.	120
Fig. 5.5b:	Flexural strength behaviour of OPC 1:3 cement-sand ratio mortar with/without GO after 28 days of curing.	121
Fig. 5.5c:	Flexural strength behaviour of PPC 1:2 cement-sand ratio mortar with/without GO after 28 days of curing.	122
Fig. 5.5d:	Flexural strength behaviour of PPC 1:2 cement-sand ratio mortar with/without GO after 28 days of curing.	123
Fig. 5.6:	Modulus of elasticity of different cement based (OPC and PPC) mortar with different dosages of GO.	125
Fig. 5.7:	Ultrasonic pulse velocity test result of GO modified OPC and PPC based cement-sand mortar.	126
Fig. 5.8a:	Sorptivity test result of GO modified cement-sand mortar using OPC with cement and sand ratio 1:2.	128
Fig. 5.8b:	Sorptivity test result of GO modified cement-sand mortar using OPC with cement and sand ratio 1:3.	128
Fig. 5.8c:	Sorptivity test result of GO modified cement-sand mortar using PPC with cement and sand ratio 1:3.	129
Fig. 5.8d:	Sorptivity test result of GO modified cement-sand mortar using PPC with cement and sand ratio 1:3.	129
Fig. 5.9:	Charged passed through different cement based (OPC and PPC) mortar with different dosages of GO.	130
Fig. 5.10a:	Acid resistance behaviour of different mixes of OPC based 1:2 cement-sand ratio mortar with different percentages of GO.	132
Fig. 5.10b:	Acid resistance behaviour of different mixes of OPC based 1:3 cement-sand ratio mortar with different percentages of GO.	133
Fig. 5.10c:	Acid resistance behaviour of different mixes of PPC based 1:2 cement-sand ratio mortar with different percentages of GO.	133
Fig. 5.10d:	Acid resistance behaviour of different mixes of PPC based 1:3 cement-sand ratio mortar with different percentages of GO.	134
Fig. 5.11a:	MIP test results OPC 1:2 cement-sand ratio control mortar and GO modified mortar with 0.05% of GO	138
Fig. 5.11b:	MIP test results PPC 1:2 cement-sand ratio control mortar and GO modified mortar with 0.04% of GO.	139

Fig. 5.12a:	XRD analysis results of OPC based 1:2 cement-sand ratio control mortar and GO modified cement-sand mortar with 0.05% of GO.	140
Fig. 5.12b:	XRD analysis results of PPC based 1:2 cement-sand ratio control mortar and GO modified cement-sand mortar with 0.04% of GO.	141
Fig. 5.13a:	FESEM image of OPC based 1:2 ratio cement-sand mortar (a) control sample and (b) GO modified cement mortar with 0.05% of GO.	142
Fig. 5.13b:	FESEM image of PPC based 1:2 ratio cement-sand mortar (a) control sample and (b) GO modified cement mortar with 0.04% of GO.	142
Fig. 5.14a:	EDX analysis results of OPC based 1:2 cement-sand ratio (a) control mortar and (b) GO modified cement-sand mortar with 0.05% of GO.	143
Fig. 5.14b:	EDS analysis results of PPC based 1:2 cement-sand ratio (a) control mortar and (b) GO modified cement-sand mortar with 0.04% of GO.	144

LIST OF TABLES

CHAPTER-2: REVIEW OF LITERATURE

		Page No
Table 2.1:	Technical parameters of GOD.	30
Table 2.2:	Elemental analysis GO.	32
Table 2.3:	Elemental Analysis of Graphene Oxide (GO).	36
Table 2.4:	Chemical composition of Graphene Oxide (GO).	37
Table 2.5:	Physical Properties of Graphene Oxide.	37
Table 2.6:	Chemical composition of Graphene Oxide (GO).	39
Table 2.7:	Chemical composition of GONF (edged oxidized).	44
Table 2.8:	Properties of GO nanosheets	49

CHAPTER-4: MATERIALS AND METHODS

Table 4.1:	Technical parameters of GO	89
Table 4.2:	Chemical composition Ordinary Portland cement (OPC) 53 grade.	90
Table 4.3:	Chemical composition of Portland Pozzolana cement (PPC).	90
Table 4.4:	Details of different cement-sand mortar mixture.	95

CHAPTER-5: RESULTS AND DISCUSSION

Table 5.1:	Details of compressive strength of OPC based 1:2 cement mortar with/without GO.	109
Table 5.2:	Details of compressive strength of OPC based 1:3 cement mortar with/without GO.	110
Table 5.3:	Details of compressive strength of PPC based 1:2 cement mortar with/without GO.	112
Table 5.4:	Details of compressive strength of PPC based 1:3 cement mortar with/without GO.	113
Table 5.5:	Details of split tensile strength of OPC based 1:2 cement mortar with/without GO.	115
Table 5.6:	Details of split tensile strength of OPC based 1:3 cement mortar with/without GO.	116
Table 5.7:	Details of split tensile strength of PPC based 1:2 cement mortar with/without GO.	117
Table 5.8:	Details of split tensile strength of PPC based 1:3 cement mortar with/without GO.	118
Table 5.9:	Details of flexural strength of OPC based 1:2 cement mortar with/without GO.	120
Table 5.10:	Details of flexural strength of OPC based 1:3 cement mortar with/without GO.	121
Table 5.11:	Details of flexural strength of PPC based 1:2 cement mortar with/without GO.	122
Table 5.12:	Details of flexural strength of PPC based 1:2 cement mortar with/without GO.	123

Table 5.13:	Details of strength reduction of OPC based 1:2 cement-sand mortar mixes with GO.	134
Table 5.14:	Details of strength reduction of OPC based 1:3 cement-sand mortar mixes with GO.	135
Table 5.15:	Details of strength reduction of PPC based 1:2 cement-sand mortar mixes with GO.	135
Table 5.16:	Details of strength reduction of PPC based 1:3 cement-sand mortar mixes with GO.	135
Table 5.17:	Details of mass loss of OPC based 1:2 cement-sand different mortar mixes with GO.	136
Table 5.18:	Details of mass loss of OPC based 1:3 cement-sand different mortar mixes with GO.	136
Table 5.19:	Details of mass loss of PPC based 1:2 cement-sand different mortar mixes with GO.	136
Table 5.20:	Details of mass loss of PPC based 1:3 cement-sand different mortar mixes with GO.	137

ABBREVIATIONS

HPC	High Performance Concrete
UHPC	Ultra High-Performance Concrete
CNT	Carbon nanotubes
GO	Graphene oxide
CVD	Chemical Vapour Deposition
MPa	Mega Pascal
kN	Kilo Newton
M	Meter
PC	Polycarboxylate superplasticizer
E	Young Modulus
F _{ck}	Compressive strength
OPC	Ordinary Portland Cement
PPC	Portland Pozzolana Cement
MIP	Mercury Intrusion Porosity
FESEM	Field Emission Scanning Electron Microscopy
EDX	Energy Dispersive X-Ray
XRD	X-ray diffraction analysis
GONF	Graphene oxide nanoflakes
WRA	Water reducing agents
LS	sodium lignosulfonate
PNS	Polycondensate of b-naphthalene sulfonate formaldehyde
GOD	Graphene oxide Nanosheets dispersion
MK	Metakaolin
SF	Silica Fume
FA	Fly ash
GONPs	Graphene oxide nanoplatelets
GONF	Graphene oxide nanoflake
RFA	Recycled fine aggregate
SDS	Sodium dodecyl sulphate
NSF	Naphthalene-based superplasticizer
rGO	Reduced graphene oxide
ASR	Alkali-silica reaction
PG	Pyrex glass
SP	Superplasticizer
w/c	Water to cement ratio
PVA	Oil-coated polyvinyl alcohol
RCPT	Rapid Chloride ion Penetration Test
CTM	Compressive testing machine
UPV	Ultrasonic Pulse Velocity test
PDF	Preder Diffraction File
BSE	Back-scattered Electrons

Chapter - 1



INTRODUCTION

1.0 General View

Developing nations are working extremely hard to make significant progress in the housing and industrial sectors. Massive construction projects are necessary for progress. Cement-based materials are, widely recognized as one of the most significant building materials due to their straightforward construction method, low energy consumption, and large variety of raw materials from which they may be created [1]. It passes through hydration to become a solid substance with remarkable structural qualities. It is made of cement, sand, water, and occasionally extra components. The composition and proportions of cement-sand mortar/concrete can vary depending on the specific application and desired characteristics. Typically, it includes Portland cement as a binder combined with fine sand as the aggregate. Initiating hydration with water enables the cement to bind with the sand particles and harden. However, the usage of typical concrete is restricted in certain construction areas due to its inadequate self-weight, tensile strength, tensile strain, and quasi-brittle nature.

To increase the mechanical performance of cement composites, it is now normal practice to incorporate reinforcing elements. The use of fibers to reinforce or repair concrete structures rather than more traditional materials has become a major concern over the past few decades [2–5]. Although the strength can be significantly increased by these reinforcing materials, cracking and durability are still a problem. Since the introduction of nanotechnology, extensive research has been discovered to be involved in the hunt for novel and effective materials on the nanoscale (10^{-9} m) [6]. In fact, nanotechnology was ultimately applied in different field of engineering, and these materials may soon revolutionize construction field also. Therefore, it is thought that this could potentially revolutionize the construction industry. There are successful nanotechnology applications being used today that would have been nearly

impossible without the usage of nanoparticles [7]. Recent study explores the challenges of the manufacture of construction materials, (notably concrete) and their treatment with nanotechnologies, the general mechanisms of development of the structure of a hardened cement composite and the influence of a treatment of its components [8]. The introduction of nanotechnology to the cement industry has already shown that it has an impact on the mechanical properties and that the performance of reinforced concrete can be improved by nanomaterials, producing High Performance Concrete (HPC) or Ultra High-Performance Concrete (UHPC), which makes concrete durable [9]. Nanomaterials interact strongly at their interfaces with the cement matrix due to their small particle sizes and high specific surface areas. They can be easily combined with cement to create cement-based nanocomposites, which can be used to increase mechanical performance, lengthen service life, and/or minimize cement dosage.

Recently, construction industries have been using nanotechnology to improve their overall performance. Nanoscience studies how a material's macroscale qualities are influenced by its nanoscale structure, whereas nano-engineering focuses on creating materials with improved mechanical properties by utilizing nanoparticles. The development of various nanomaterials, including nanoparticles, nanotubes, nanorods, and nano surfaces, as a result of nanotechnology [10–12]. Fig 1.1 shows the image of different types of nanomaterials such as nanorods, nanotubes, and nanowires [13]. It depends on activities that take place at the micro- and nanoscale how cement-based structures behave mechanically, including how strong, stiff, hard, robust, and durable they are. Recent studies have demonstrated that a minor addition of nanoparticles, such as nano-silica [14,15], carbon nanotubes (CNT) [16,17] and nano titanium dioxide (TiO₂) [18,19], the mechanical characteristics of cementitious materials can be significantly impacted. Not only did it effect on the mechanical characteristics, but it also changed micro-structural properties. Fig. 1.1 shows the images of (a) titanium oxide, (b) carbon

nanotubes, and (c) nano-silica. Graphene oxide (GO), a carbon-based nanomaterial, has recently gained interest for its ultrahigh mechanical properties and high specific surface area to incorporate into cement composites.

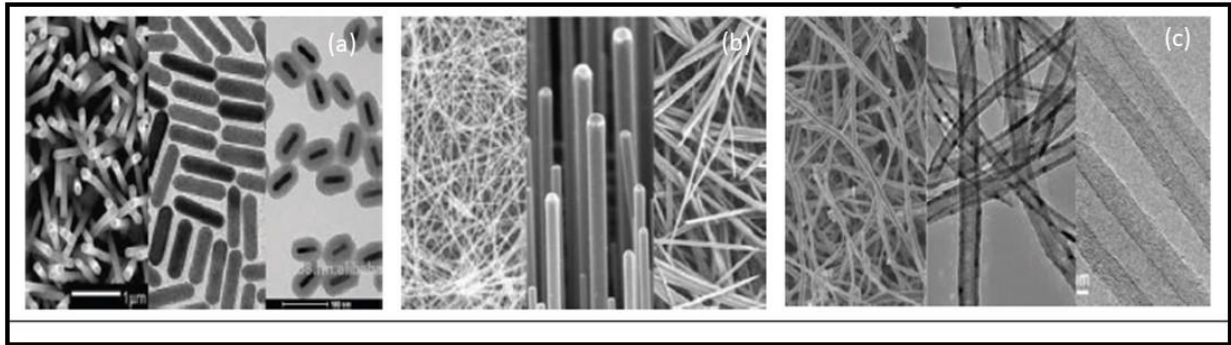


Fig. 1.1: Morphological images of (a) nanorods, (b) nanowires, and (c) nanotubes (A.A. Ghassan 2020).

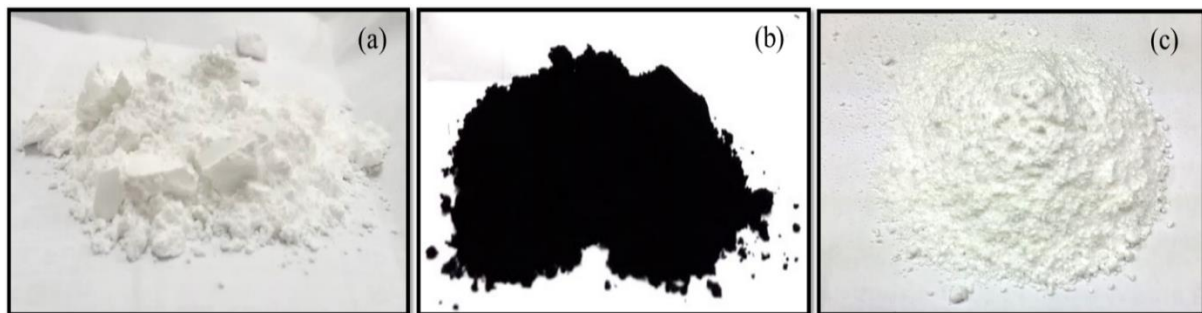


Fig. 1.2: Images of (a) Titanium oxide, (b) Carbon nanotube, and (c) Nano silica

1.1 Graphene Oxide (GO)

GO is a derivative of graphene, which is a single layer of carbon atoms arranged in a two-dimensional honeycomb lattice. Each carbon atom's bonding within this is hybridized sp^2 with the inclusion of π -orbitals. Each graphene unit cell contains two orbitals that are scattered to form two bonds, each of which might be referred to as bonding and antibonding [20]. It has oxygen-containing functional groups ($=O$, $-OH$, $-O-$, and $-COOH$) linked to both the layer's outside and the plane's edges [21]. GO is a type of 2D carbon material that can have either a single layer or a multilayer structure. Graphene oxide is a structure with one layer. A two-

layered GO is a structure with two layers of graphene oxide. GO with less than five layers and more than two layers is known as few-layered GO. Multilayered GO is known as GO with five to ten layers, and graphite oxide is known as GO with eleven layers or more [22]. Graphite can be oxidized to become graphite oxide, which can then be exfoliated to form GO. The method of synthesis, which affects the number and nature of oxygen-containing groups that are produced in the generated GO and has a significant impact on the material's characteristics. Contrary to graphene, GO is hydrophilic, making the preparation of suspensions based on water or organic solvents relatively easy. Because GO has several oxygen functions on its surface, it can be used as a starting point for the creation of graphene derivatives including fluorographene, bromographene, and many more. It is interesting to note that GO can also be applied to cutting-edge applications including medicine delivery, high-temperature materials, and building materials [23]. Fig. 1.1 shows the chemical structure of single layered GO.

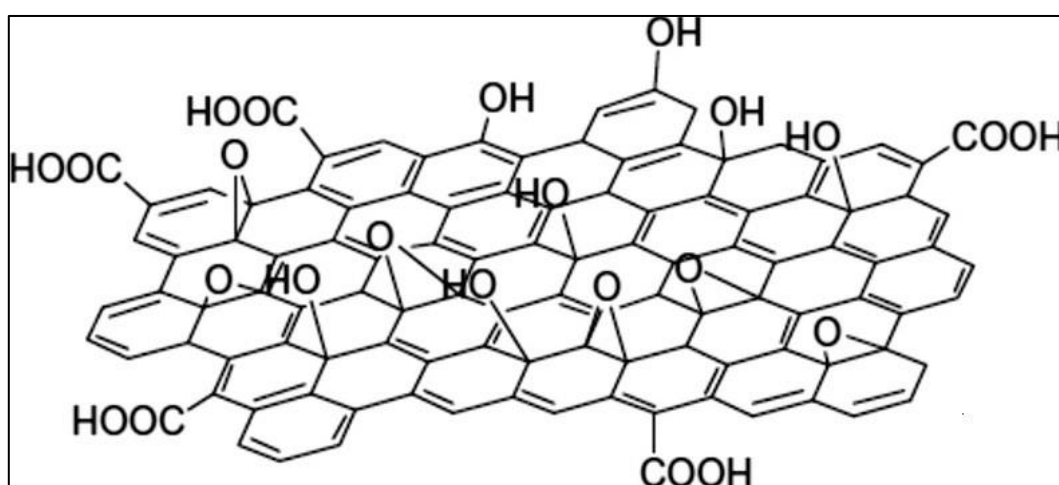


Fig 1.3: Chemical structure of single layer of GO. (Nasrollahzadeh et al. 2015) [24].

Basically, there are two categories of GO synthesis: "top-down" methods [25,26]. and "bottom-up" methods [27–30]. Top-down methods involve extracting layers of graphene derivatives from a carbon source, usually graphite, whereas bottom-up methods use simple carbon molecules to create pristine graphene [31–35]. Scotch tape exfoliation [36] liquid-phase exfoliation in various solvents [37], or chemical synthesis employing redox reactions [25,26]

are examples of top-down techniques. On another hand, bottom-up methods include Chemical Vapour Deposition (CVD) and molecular beam epitaxy [28–30,38]. The original synthesis of GO is frequently credited to Brodie, Staudenmaier, Hummers and Offeman, all of whom produced graphite oxide by oxidizing graphite using different methods. The original two methods were improved upon by Hummers and Offeman in several ways to make them safer. These improvements included the use of KMnO_4 as an oxidizer (instead of KClO_3 , which produces toxic ClO_2 gas) and the addition of sodium nitrate (to form nitric acid in situ rather than using nitric acid as a solvent). This is typically employed (or, in most cases, somewhat modified) for producing the GO due to the Hummers' method's safer and more scalable nature [39]. A "modified Hummer's method" is a technique that alters or enhances the synthesis route provided by Hummers, but the precise definition of this phrase is not standardized [40]. Generally, a carbon source (commonly graphite flakes or powders) is added to a protonated solvent (such as sulfuric acid, phosphoric acid, or a mixture of these), and then a potent oxidizing agent (often KMnO_4) is added. After a dilution step, it is usual to treat the resulting mixture with H_2O_2 to get rid of any metal ions from the oxidizer; this causes yellow bubbling, which turns into a yellow-brown liquid eventually. The resultant solids are then separated, and subjected to further removal of any metal species by treatment with diluted hydrochloric acid, and the solution is centrifuged and rinsed with water numerous times until the pH of the solution is nearly neutral [39]. Depending on the requirements of each researcher, the general synthesis route can be changed. It is important to remember, for instance, that a modified version of Hummer's approach will allow one to predict the size and shape of the producing graphene oxide based on the size and shape of the carbon source [40]. This typically indicates that the average lateral dimension of the resulting GO sheets will depend on the average diameter of the graphite powders employed in the synthesis, though other carbon sources can be used.



Fig. 1.4: Modified Hummer's method for GO synthesis.

1.2 Mechanical Properties of Graphene oxide

Graphene oxide is an oxidized form of graphene, consisting of graphene sheets with oxygen-containing functional groups attached to its basal planes and edges. These functional groups, such as hydroxyl, epoxide, and carboxyl groups, impart unique mechanical properties to graphene oxide. Generally, the degree of oxidation, the density and distribution of functional groups, the synthesis method, and the processing conditions all affect the mechanical properties of graphene oxide. Some major mechanical properties are given below-

- **Tensile strength:** Graphene oxide exhibits high tensile strength, which refers to its ability to withstand pulling forces without breaking. However, the tensile strength of graphene oxide is generally lower than that of pristine graphene due to the presence of defects and functional groups introduced during the oxidation process. It has been determined that GO has a tensile strength of 130 GPa [41,42].
- **Flexibility:** Graphene oxide is a relatively flexible material, despite only possessing two dimensions. The flexibility of graphene is ascribed to the existence of oxygen functional groups, which produce kinks and defects in the structure and allow deformation and bending [43].

- **Young's Modulus:** Young's modulus measures the stiffness of a material under tension or compression. Graphene oxide typically has a lower Young's modulus compared to pristine graphene due to the presence of defects and functional groups, which disrupt the sp² carbon network and reduce the overall stiffness. Using molecular dynamics analysis, the young modulus of Graphene oxide was calculated with a value of 1.0 TPa [44,45].
- **Fracture Toughness:** Graphene oxide exhibits high fracture toughness, which is its ability to resist crack propagation and fracture. The presence of functional groups and defects can lead to energy dissipation mechanisms that enhance fracture toughness compared to pristine graphene. Depending on the type of sample, the fracture toughness of GO, as determined by various techniques, ranges from 4 to 20 MPa M^{1/2} [46, 47].
- **Mechanical Reinforcement:** Incorporating graphene oxide into polymer matrices or other materials can improve mechanical qualities including stiffness, strength, and toughness, making it an efficient reinforcing material in composite systems [48].

1.3 Background

There is little information in the literature about how GO affects on the mechanical, durability, and microstructural properties of cement composites without any other chemicals and minerals [49–52]. It has been reported that the mechanical characteristics of cement composite were noticeably improved by introducing of an appropriate amount of GO with superplasticizers. [50,51,53]. It has been established that the compressive strength was increased by 29% compared to the control using GO modified cement mortar with 7% silica fume [54]. With the inclusion of GO with Polycarboxylate superplasticizer (PC) with a solid content of 40%, the compressive strength of cement mortar enhanced by 38% compared to the control [55]. It has been noted that the introduction of a small amount of GO improves the microstructure of cementitious materials [56,57]. Through the use of GO in cementitious materials is an exciting

area of research. According to a previous study, the mechanical properties of cement paste, such as compressive strength and flexural strength, were improved by 77% and 21%, respectively, with the introduction of 0.2% of GO by mass of cement [58]. Most of the previous studies are limited to strength only, there is almost no literature on the durability of GO based cement composites. In terms of durability, a previous study reported that the ion penetration of cementitious materials reduced with the inclusion of a small amount of GO [59]. It has been reported that with the inclusion of a small of GO, the resistance attack against acidic water was higher than the control [60 61].

In general, the Young Modulus (E) of cement based materials increases with the proportion of shear root of compressive strength of concrete. As an example for concrete as per IS: 456;200, $E = 5000\sqrt{F_{ck}}$. A lot of high-rise buildings are being constructed with high strength concrete, having limited “ E ” value. In general, increases the size of the vertical members by reducing useable space. Therefore, it is necessary to improve the “ E ” value of such materials. An attempt has been made to improve the “ E ” value of cement based composite by using a small amount of GO.

However, there is no systematic study on the effects of the addition of GO on cement-sand mortar. The aim of the present study is discussed in the next section based on the above background of GO modified cement composites.

1.4 Goals

The aim of the current study is to significantly move forward the development of GO-modified cement mortar and to encourage its application in real-world situations. The development of high strength and more durable cement composite will be achieved from the usage of GO modified cement mortar for actual uses. The cost of GO synthesis is quite expensive till now. The primary goal of the present research work is to produce a cement composite with a high

strength and improved durability using a very small amount of GO by weight of cement without any other dispersing agents. Another goal of the research is to study the micro-structural properties of this cement mortar treated with GO.

1.5 Research Objectives

The following are the main objectives of the study:

- To disperse the GO in water without any depressing agents by using a prob sonicator.
- To develop the GO modified cement-sand mortar with different cement-sand ratios (1:2 and 1:3) by using different types of cement such as Ordinary Portland Cement (OPC) and Portland Pozzolana Cement (PPC) with different dosages of GO, ranging from 0.03% to 0.06% by weight of cement. The workability of such cement-sand mortar has been included.
- Mechanical strength (such as compressive strength, split tensile strength, and flexural strength) study of GO modified cement-sand mortar.
- To improve the young modulus (E) of cement-sand mortar with GO.
- Durability study of GO modified cement-sand mortar.
- Pore size distribution study of GO modified cement-sand mortar by Mercury Intrusion Porosity (MIP) test.
- Morphological study of GO modified cement-sand mortar by using Field Emission Scanning Electron Microscopy (FESEM) with Energy Dispersive X-Ray (EDX) and X-ray diffraction analysis (XRD).

References

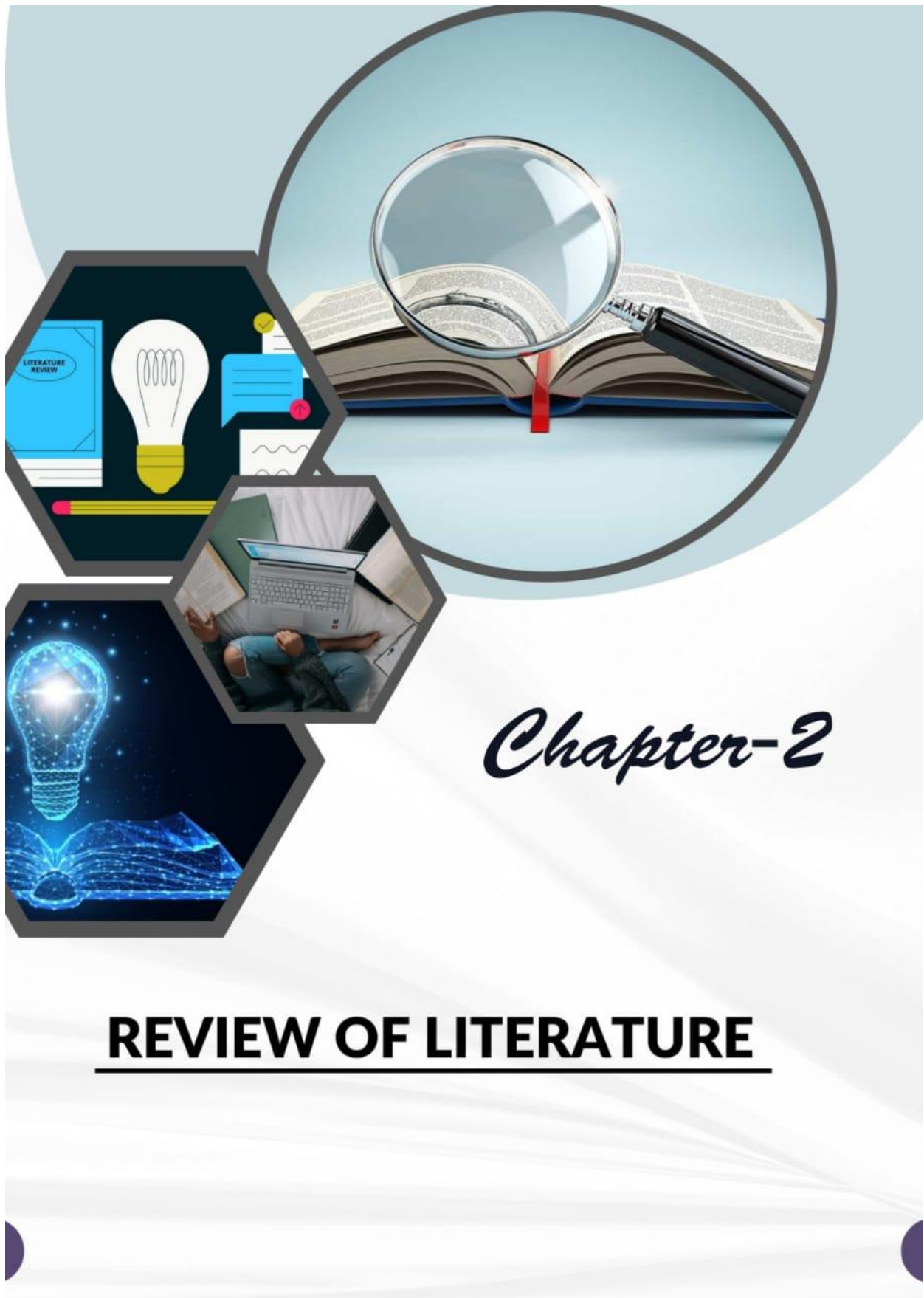
- [1] K. Sreeja, T. Naresh Kumar, Effect of graphene oxide on fresh, hardened and mechanical properties of cement mortar, *Mater Today Proc* 46 (2021) 2235–2239. <https://doi.org/10.1016/j.matpr.2021.03.574>.
- [2] J. Ahmad, R.A. González-Lezcano, A. Majdi, N. Ben Kahla, A.F. Deifalla, M.A. El-Shorbagy, Glass Fibers Reinforced Concrete: Overview on Mechanical, Durability and Microstructure Analysis, *Materials* 15 (2022) 5111. <https://doi.org/10.3390/ma15155111>.
- [3] K. Thanushan, Y. Yogananth, P. Sangeeth, J.G. Coonghe, N. Sathiparan, Strength and Durability Characteristics of Coconut Fibre Reinforced Earth Cement Blocks, *Journal of Natural Fibers* 18 (2021) 773–788. <https://doi.org/10.1080/15440478.2019.1652220>.
- [4] A. Okeola, S. Abuodha, J. Mwero, Experimental Investigation of the Physical and Mechanical Properties of Sisal Fiber-Reinforced Concrete, *Fibers* 6 (2018) 53. <https://doi.org/10.3390/fib6030053>.
- [5] S.M. Mousavi, M.M. Ranjbar, R. Madandoust, Combined effects of steel fibers and water to cementitious materials ratio on the fracture behavior and brittleness of high strength concrete, *Eng Fract Mech* 216 (2019) 106517. <https://doi.org/10.1016/j.engfracmech.2019.106517>.
- [6] G. Liu, C. Zhang, M. Zhao, W. Guo, Q. Luo, Comparison of Nanomaterials with Other Unconventional Materials Used as Additives for Soil Improvement in the Context of Sustainable Development: A Review, *Nanomaterials* 11 (2020) 15. <https://doi.org/10.3390/nano11010015>.
- [7] P. Sikora, M. Abd Elrahman, D. Stephan, The Influence of Nanomaterials on the Thermal Resistance of Cement-Based Composites—A Review, *Nanomaterials* 8 (2018) 465. <https://doi.org/10.3390/nano8070465>.
- [8] E. Rabiaa, R.A.S. Mohamed, W.H. Sofi, T.A. Tawfik, Developing Geopolymer Concrete Properties by Using Nanomaterials and Steel Fibers, *Advances in Materials Science and Engineering* 2020 (2020) 1–12. <https://doi.org/10.1155/2020/5186091>.
- [9] N. Lovecchio, F. Shaikh, M. Rosano, R. Ceravolo, W. Biswas, Environmental assessment of supplementary cementitious materials and engineered nanomaterials concrete, *AIMS Environ Sci* 7 (2020) 13–30. <https://doi.org/10.3934/environsci.2020002>.
- [10] Y. Gao, H.W. Jing, S.J. Chen, M.R. Du, W.Q. Chen, W.H. Duan, Influence of ultrasonication on the dispersion and enhancing effect of graphene oxide–carbon nanotube hybrid nanoreinforcement in cementitious composite, *Compos B Eng* 164 (2019) 45–53. <https://doi.org/10.1016/j.compositesb.2018.11.066>.
- [11] L. Laím, H. Caetano, A. Santiago, Review: Effects of nanoparticles in cementitious construction materials at ambient and high temperatures, *Journal of Building Engineering* 35 (2021) 102008. <https://doi.org/10.1016/j.job.2020.102008>.
- [12] F. Torabian Isfahani, E. Redaelli, F. Lollini, W. Li, L. Bertolini, Effects of Nanosilica on Compressive Strength and Durability Properties of Concrete with Different Water to Binder Ratios, *Advances in Materials Science and Engineering* 2016 (2016) 1–16. <https://doi.org/10.1155/2016/8453567>.

- [13] A. Abdulkareem Ghassan, N.-A. Mijan, Y. Hin Taufiq-Yap, Nanomaterials: An Overview of Nanorods Synthesis and Optimization, in: *Nanorods and Nanocomposites*, IntechOpen, 2020. <https://doi.org/10.5772/intechopen.84550>.
- [14] A. P. P., D.K. Nayak, B. Sangoju, R. Kumar, V. Kumar, Effect of nano-silica in concrete; a review, *Constr Build Mater* 278 (2021) 122347. <https://doi.org/10.1016/j.conbuildmat.2021.122347>.
- [15] P. Zhang, J. Su, J. Guo, S. Hu, Influence of carbon nanotube on properties of concrete: A review, *Constr Build Mater* 369 (2023) 130388. <https://doi.org/10.1016/j.conbuildmat.2023.130388>.
- [16] G. Li, X. Shi, Y. Gao, J. Ning, W. Chen, X. Wei, J. Wang, S. Yang, Reinforcing effects of carbon nanotubes on cement-based grouting materials under dynamic impact loading, *Constr Build Mater* 382 (2023) 131083. <https://doi.org/10.1016/j.conbuildmat.2023.131083>.
- [17] S.K. Adhikary, Ž. Rudžionis, R. Rajapriya, The Effect of Carbon Nanotubes on the Flowability, Mechanical, Microstructural and Durability Properties of Cementitious Composite: An Overview, *Sustainability* 12 (2020) 8362. <https://doi.org/10.3390/su12208362>.
- [18] M. Daniyal, S. Akhtar, A. Azam, Effect of nano-TiO₂ on the properties of cementitious composites under different exposure environments, *Journal of Materials Research and Technology* 8 (2019) 6158–6172. <https://doi.org/10.1016/j.jmrt.2019.10.010>.
- [19] M.S. Döndüren, M.G. Al-Hagri, A review of the effect and optimization of use of nano-TiO₂ in cementitious composites, *Research on Engineering Structures and Materials* (2022). <https://doi.org/10.17515/resm2022.348st1005>.
- [20] D.S. Shin, H.G. Kim, H.S. Ahn, H.Y. Jeong, Y.-J. Kim, D. Odkhuu, N. Tsogbadrakh, H.-B.-R. Lee, B.H. Kim, Distribution of oxygen functional groups of graphene oxide obtained from low-temperature atomic layer deposition of titanium oxide, *RSC Adv* 7 (2017) 13979–13984. <https://doi.org/10.1039/C7RA00114B>.
- [21] C. Qiu, L. Jiang, Y. Gao, L. Sheng, Effects of oxygen-containing functional groups on carbon materials in supercapacitors: A review, *Mater Des* 230 (2023) 111952. <https://doi.org/10.1016/j.matdes.2023.111952>.
- [22] V. Kumar, A. Kumar, D.-J. Lee, S.-S. Park, Estimation of Number of Graphene Layers Using Different Methods: A Focused Review, *Materials* 14 (2021) 4590. <https://doi.org/10.3390/ma14164590>.
- [23] A. Jiříčková, O. Jankovský, Z. Sofer, D. Sedmidubský, Synthesis and Applications of Graphene Oxide, *Materials* 15 (2022) 920. <https://doi.org/10.3390/ma15030920>.
- [24] M. Nasrollahzadeh, F. Babaei, P. Fakhri, B. Jaleh, Synthesis, characterization, structural, optical properties and catalytic activity of reduced graphene oxide/copper nanocomposites, *RSC Adv* 5 (2015) 10782–10789. <https://doi.org/10.1039/C4RA12552E>.
- [25] M.N. Chernysheva, A.Yu. Rychagov, D.Yu. Kornilov, S.V. Tkachev, S.P. Gubin, Investigation of sulfuric acid intercalation into thermally expanded graphite in order to optimize the synthesis of electrochemical graphene oxide, *Journal of Electroanalytical Chemistry* 858 (2020) 113774. <https://doi.org/10.1016/j.jelechem.2019.113774>.
- [26] K.K.H. De Silva, H.-H. Huang, M. Yoshimura, Progress of reduction of graphene oxide by ascorbic acid, *Appl Surf Sci* 447 (2018) 338–346. <https://doi.org/10.1016/j.apsusc.2018.03.243>.

- [27] S. Ganguly, S. Ghosh, P. Das, T.K. Das, S.K. Ghosh, N.C. Das, Poly(N-vinylpyrrolidone)-stabilized colloidal graphene-reinforced poly(ethylene-co-methyl acrylate) to mitigate electromagnetic radiation pollution, *Polymer Bulletin* 77 (2020) 2923–2943. <https://doi.org/10.1007/s00289-019-02892-y>.
- [28] V.T. Nguyen, Y.C. Kim, Y.H. Ahn, S. Lee, J.-Y. Park, Large-area growth of high-quality graphene/MoS₂ vertical heterostructures by chemical vapor deposition with nucleation control, *Carbon* N Y 168 (2020) 580–587. <https://doi.org/10.1016/j.carbon.2020.07.014>.
- [29] M.Ye. Svavil'nyi, V.Ye. Panarin, A.A. Shkola, A.S. Nikolenko, V.V. Strelchuk, Plasma Enhanced Chemical Vapor Deposition synthesis of graphene-like structures from plasma state of CO₂ gas, *Carbon* N Y 167 (2020) 132–139. <https://doi.org/10.1016/j.carbon.2020.05.057>.
- [30] J. Yu, Z. Hao, J. Deng, X. Li, L. Wang, Y. Luo, J. Wang, C. Sun, Y. Han, B. Xiong, H. Li, Low-temperature van der Waals epitaxy of GaN films on graphene through AlN buffer by plasma-assisted molecular beam epitaxy, *J Alloys Compd* 855 (2021) 157508. <https://doi.org/10.1016/j.jallcom.2020.157508>.
- [31] J. Yu, Z. Hao, J. Deng, X. Li, L. Wang, Y. Luo, J. Wang, C. Sun, Y. Han, B. Xiong, H. Li, Low-temperature van der Waals epitaxy of GaN films on graphene through AlN buffer by plasma-assisted molecular beam epitaxy, *J Alloys Compd* 855 (2021) 157508. <https://doi.org/10.1016/j.jallcom.2020.157508>.
- [32] M.Ye. Svavil'nyi, V.Ye. Panarin, A.A. Shkola, A.S. Nikolenko, V.V. Strelchuk, Plasma Enhanced Chemical Vapor Deposition synthesis of graphene-like structures from plasma state of CO₂ gas, *Carbon* N Y 167 (2020) 132–139. <https://doi.org/10.1016/j.carbon.2020.05.057>.
- [33] C.K. Chua, M. Pumera, Chemical reduction of graphene oxide: a synthetic chemistry viewpoint, *Chem. Soc. Rev.* 43 (2014) 291–312. <https://doi.org/10.1039/C3CS60303B>.
- [34] Z. Wang, J. Liu, W. Wang, H. Chen, Z. Liu, Q. Yu, H. Zeng, L. Sun, Aqueous phase preparation of graphene with low defect density and adjustable layers, *Chemical Communications* 49 (2013) 10835. <https://doi.org/10.1039/c3cc46809g>.
- [35] J. Yu, Z. Hao, J. Deng, W. Yu, L. Wang, Y. Luo, J. Wang, C. Sun, Y. Han, B. Xiong, H. Li, Influence of nitridation on III-nitride films grown on graphene/quartz substrates by plasma-assisted molecular beam epitaxy, *J Cryst Growth* 547 (2020) 125805. <https://doi.org/10.1016/j.jcrysgro.2020.125805>.
- [36] K.S. Novoselov, A.K. Geim, S. V. Morozov, D. Jiang, Y. Zhang, S. V. Dubonos, I. V. Grigorieva, A.A. Firsov, Electric Field Effect in Atomically Thin Carbon Films, *Science* (1979) 306 (2004) 666–669. <https://doi.org/10.1126/science.1102896>.
- [37] Y. Hernandez, V. Nicolosi, M. Lotya, F.M. Blighe, Z. Sun, S. De, I.T. McGovern, B. Holland, M. Byrne, Y.K. Gun'Ko, J.J. Boland, P. Niraj, G. Duesberg, S. Krishnamurthy, R. Goodhue, J. Hutchison, V. Scardaci, A.C. Ferrari, J.N. Coleman, High-yield production of graphene by liquid-phase exfoliation of graphite, *Nat Nanotechnol* 3 (2008) 563–568. <https://doi.org/10.1038/nnano.2008.215>.
- [38] S. Lee, W.K. Park, Y. Yoon, B. Baek, J.S. Yoo, S. Bin Kwon, D.H. Kim, Y.J. Hong, B.K. Kang, D.H. Yoon, W.S. Yang, Quality improvement of fast-synthesized graphene films by rapid thermal chemical vapor deposition for mass production, *Materials Science and Engineering: B* 242 (2019) 63–68. <https://doi.org/10.1016/j.mseb.2019.03.004>.

- [39] A.T. Smith, A.M. LaChance, S. Zeng, B. Liu, L. Sun, Synthesis, properties, and applications of graphene oxide/reduced graphene oxide and their nanocomposites, *Nano Materials Science* 1 (2019) 31–47. <https://doi.org/10.1016/j.nanoms.2019.02.004>.
- [40] F. Pendolino, N. Armata, *Graphene Oxide in Environmental Remediation Process*, Springer International Publishing, Cham, 2017. <https://doi.org/10.1007/978-3-319-60429-9>.
- [41] C. Shen, S.O. Oyadiji, The processing and analysis of graphene and the strength enhancement effect of graphene-based filler materials: A review, *Materials Today Physics* 15 (2020) 100257. <https://doi.org/10.1016/j.mtphys.2020.100257>.
- [42] C. Lee, X. Wei, J.W. Kysar, J. Hone, Measurement of the Elastic Properties and Intrinsic Strength of Monolayer Graphene, *Science* (1979) 321 (2008) 385–388. <https://doi.org/10.1126/science.1157996>.
- [43] P. Poulin, R. Jalili, W. Neri, F. Nallet, T. Divoux, A. Colin, S.H. Aboutalebi, G. Wallace, C. Zakri, Superflexibility of graphene oxide, *Proceedings of the National Academy of Sciences* 113 (2016) 11088–11093. <https://doi.org/10.1073/pnas.1605121113>.
- [44] A.R. Khoei, M.S. Khorrami, Mechanical properties of graphene oxide: A molecular dynamics study, *Fullerenes, Nanotubes and Carbon Nanostructures* 24 (2016) 594–603. <https://doi.org/10.1080/1536383X.2016.1208180>.
- [45] Z. Ni, H. Bu, M. Zou, H. Yi, K. Bi, Y. Chen, Anisotropic mechanical properties of graphene sheets from molecular dynamics, *Physica B Condens Matter* 405 (2010) 1301–1306. <https://doi.org/10.1016/j.physb.2009.11.071>.
- [46] Z. Zhang, X. Zhang, Y. Wang, Y. Wang, Y. Zhang, C. Xu, Z. Zou, Z. Wu, Y. Xia, P. Zhao, H.T. Wang, Crack Propagation and Fracture Toughness of Graphene Probed by Raman Spectroscopy, *ACS Nano* 13 (2019) 10327–10332. <https://doi.org/10.1021/acs.nano.9b03999>.
- [47] C. Ramírez, 10 years of research on toughness enhancement of structural ceramics by graphene, *Philosophical Transactions of the Royal Society A: Mathematical, Physical and Engineering Sciences* 380 (2022). <https://doi.org/10.1098/rsta.2022.0006>.
- [48] B.L. Dasari, M. Morshed, J.M. Nouri, D. Brabazon, S. Naher, Mechanical properties of graphene oxide reinforced aluminium matrix composites, *Compos B Eng* 145 (2018) 136–144. <https://doi.org/10.1016/j.compositesb.2018.03.022>.
- [49] A. Anwar, X. Liu, L. Zhang, Nano-cementitious composites modified with Graphene Oxide – a review, *Thin-Walled Structures* 183 (2023) 110326. <https://doi.org/10.1016/j.tws.2022.110326>.
- [50] S. Prabavathy, K. Jeyasubramanian, S. Prasanth, G.S. Hikku, R.B.J. Robert, Enhancement in behavioral properties of cement mortar cubes admixed with reduced graphene oxide, *Journal of Building Engineering* 28 (2020) 101082. <https://doi.org/10.1016/j.jobbe.2019.101082>.
- [51] G. Li, J.B. Yuan, Y.H. Zhang, N. Zhang, K.M. Liew, Microstructure and mechanical performance of graphene reinforced cementitious composites, *Compos Part A Appl Sci Manuf* 114 (2018) 188–195. <https://doi.org/10.1016/j.compositesa.2018.08.026>.
- [52] M. Muthu, N. Ukrainczyk, E. Koenders, Effect of graphene oxide dosage on the deterioration properties of cement pastes exposed to an intense nitric acid environment, *Constr Build Mater* 269 (2021) 121272. <https://doi.org/10.1016/j.conbuildmat.2020.121272>.

- [53] A. Mohammed, N.T.K. Al-Saadi, Ultra-High Early Strength Cementitious Grout Suitable for Additive Manufacturing Applications Fabricated by Using Graphene Oxide and Viscosity Modifying Agents, *Polymers (Basel)* 12 (2020) 2900. <https://doi.org/10.3390/polym12122900>.
- [54] A. Abdullah, M. Taha, M. Rashwan, M. Fahmy, Efficient Use of Graphene Oxide and Silica Fume in Cement-Based Composites, *Materials* 14 (2021) 6541. <https://doi.org/10.3390/ma14216541>.
- [55] L. Zhao, X. Guo, Y. Liu, C. Ge, L. Guo, X. Shu, J. Liu, Synergistic effects of silica nanoparticles/polycarboxylate superplasticizer modified graphene oxide on mechanical behavior and hydration process of cement composites, *RSC Adv* 7 (2017) 16688–16702. <https://doi.org/10.1039/C7RA01716B>.
- [56] H. Yang, M. Monasterio, H. Cui, N. Han, Experimental study of the effects of graphene oxide on microstructure and properties of cement paste composite, *Compos Part A Appl Sci Manuf* 102 (2017) 263–272. <https://doi.org/10.1016/j.compositesa.2017.07.022>.
- [57] M.M. Mokhtar, S.A. Abo-El-Enein, M.Y. Hassaan, M.S. Morsy, M.H. Khalil, Mechanical performance, pore structure and micro-structural characteristics of graphene oxide nano platelets reinforced cement, *Constr Build Mater* 138 (2017) 333–339. <https://doi.org/10.1016/j.conbuildmat.2017.02.021>.
- [58] W.-J. Long, J.-J. Wei, F. Xing, K.H. Khayat, Enhanced dynamic mechanical properties of cement paste modified with graphene oxide nanosheets and its reinforcing mechanism, *Cem Concr Compos* 93 (2018) 127–139. <https://doi.org/10.1016/j.cemconcomp.2018.07.001>.
- [59] X. Qi, S. Zhang, T. Wang, S. Guo, R. Ren, Effect of High-Dispersible Graphene on the Strength and Durability of Cement Mortars, *Materials* 14 (2021) 915. <https://doi.org/10.3390/ma14040915>.
- [60] K. Chintalapudi, R.M.R. Pannem, Enhanced chemical resistance to sulphuric acid attack by reinforcing Graphene Oxide in Ordinary and Portland Pozzolana cement mortars, *Case Studies in Construction Materials* 17 (2022) e01452. <https://doi.org/10.1016/j.cscm.2022.e01452>.
- [61] P. Vasudevareddy, K. Chandrasekhar Reddy, Effect of graphene oxide and nano silica on mechanical and durability properties of cement mortar, *Mater Today Proc* 60 (2022) 1042–1050. <https://doi.org/10.1016/j.matpr.2022.01.234>.



Chapter-2

REVIEW OF LITERATURE

REVIEW OF LITERATURE

2.0 General View

This chapter briefly discusses the history of Graphene oxide (GO) and its use in the cement-sand composite. This chapter additionally covers the ongoing study into the development of GO-modified cement-sand composite and its application.

2.1 History of GO

Many incredible discoveries were made in the 19th century, including those involving new materials, electromagnetic phenomena, electrodynamics, and many others. **Benjamin Collins Brodie**, a chemist, focused on highly layered morphology of reduced graphite oxide in this line as early as 1859 after confirming the atomic weight of graphite in a Royal Society of London publication [1]. However, a German chemist named **C. Schafhaeutl** attempted to oxidize graphitic sheets to graphite oxide considerably earlier, around 1840. More recently, there has been a debate over who should be given the initial honor for the first oxidation of graphite [2]. Initial study on graphite demonstrates unequivocally that **P.R. Wallace** was the first to foresee the electrical properties of a single sheet of graphite (today known as graphene) in the 1940s. At this time, graphene has been found to have several extraordinary properties, confirming the accuracy of **Wallace's** predictions. Thus, the structure of graphite is strongly related to the discovery of graphene oxide and graphene as well as their possible applications [3,4]. Hummers and Offeman published a different process for graphite oxidation in 1958. For this, potassium permanganate was added to a suspension of sodium nitrate, graphite powder, and sulfuric acid that had been cooled to 0°C in an ice bath. In order to decrease manganese dioxide to colorless soluble manganese sulphate, the suspension was further diluted with hot water and treated with H₂O₂ (3%) as it thickened while stirring. The diluted suspension was then filtered and given numerous warm water washes. Centrifugation was used to obtain

graphite oxide powder, and afterward 40°C dehydration with phosphorus pentoxide in a vacuum [5]. Since the beginning of the 2000s, there has been a growing of scientific interest in carbon nanotubes and fullerenes as well as an expansion of hardware capabilities for the analysis of nanomaterials. It has been reported that the high values of the mobility of charge carriers in graphene, was one of the papers published during this time. The Nobel Prize in Physics was given to K. **Novoselov** and A. **Geim** in 2010 for their "pioneering experiments involving the two-dimensional material graphene." [6]. However, it has been reported that introducing GO can improve the properties of hardened composites [7–10].

2.2 Source of GO

Graphene oxide (GO) is a layered carbon structure with functional groups comprising oxygen (=O, -OH, -O-, and -COOH) bonded to the layer's edges as well as its two opposite sides. The structure of GO can be either single or multilayered, like that of any other 2D carbon material. Graphite oxide can be produced through oxidizing graphite, and then this graphite oxide can be exfoliated to generate the GO. The technique of synthesis, which affects the amount and variety of oxygen-containing groups in the developed the GO, has a significant impact on the characteristics of material [11]. According to Siaw et al. [12], GO can be synthesized from industrial waste material by utilizing leaching and a modified version of Hummers' method. Through the application of 6 M HCl in a leaching solution with a solid to liquid ratio of 1:10 for 210 minutes at 70 °C, it is possible to successfully eliminate the pollutants present in industrial waste. Then, by using concentrated H₂SO₄ and KMnO₄, GO was synthesized by using a modified Hummers method.

2.3 Current Trend of Research on Cementitious Materials

The construction sector has been utilizing nanotechnology to enhance its materials throughout the past few decades. Towards the beginning of the 21st century, GO attracted the interest of

researchers due to its high specific surface area and amazing mechanical properties to incorporate in cement composites as nano reinforcing material [7,13–30]. However, studies on the GO modified cement composite are very limited. In order to use GO as a reinforcing nano-material in cementitious materials and its applications, a comprehensive evaluation of these properties is essential.

2.4 Review on GO Modified Cement Composites

Limited previous studies reported that the addition of GO on cement composites, influences the mechanical properties such as the compressive strength of hardened cementitious materials. Most of the studies have reported on the effect of GO addition on the workability, compressive strength, flexural strength, and tensile strength. A very few literature is available on durability and microstructure analysis on these areas. With this background a comprehensive review of past literature on GO modified cement composites is presented. Workability, mechanical properties, such as compressive strength, tensile strength, flexural strength, Young's modulus (E), durability properties, and micro-structural properties are presented.

2.4.1 Workability

It is generally established that the more fluid the cement based material, the higher the slump, and although the slump is commonly used as an indicator of water content, it is also commonly utilized as a measure of concrete consistency. The workability of GO modified cement composites is measured mainly by slump test and flow test.

K. Gong et al. (2015) observed that the addition of GO into cement paste the workability in terms of flow was lower than the control paste (Fig. 2.1). It was noted that the inclusion of 0.03% of GO by weight of cement reduced the workability by around 34% [31].

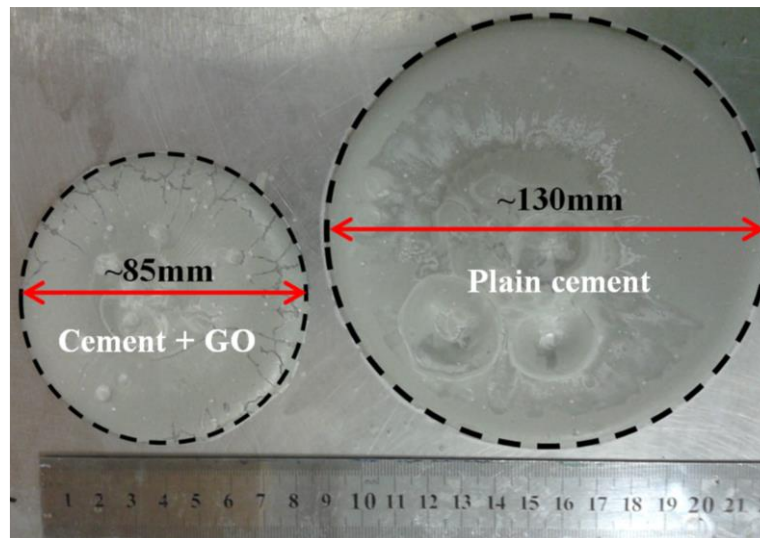


Fig. 2.1: Mini slump flow at 10 min after lifting the mini core (Kai Gong et al. 2015).

In accordance with *Z. Pan et al. (2015)*; the workability of cement paste was reduced by 41% with the addition of 0.05% of GO by weight of cement, with respect to the control. This could be the effect of a GO sheet's large surface area, which reduces the amount of water available in the fresh mix while the GO sheets are wet [32].

Q. Wang et al. (2015) reported that the inclusion of a small amount of GO reduced the workability remarkability of cement paste. The GO surface chemistry and nanoscale size effect could be the cause of the fluidity decline [33].

According to *L. Zhao et al. (2016)*; the addition of a small quantity of GO in cement paste, with PC does not reduce the fluidity of cement mortar. Addition of 0.022% GO, by weight of cement and the GO to polycarboxylate superplasticizer (PC) mass ratio of 0.1, fluidity increased by 13% compared to the similar plain cement mortar. The improvement in fluidity can be possible by PC's electrostatic repulsion and steric hindrance effect [34].

Z. Lu et al. (2017) measured the fluidity of plain cement paste and GO modified cement paste. It was reported that the fluidity of cement paste was significantly decreased with the inclusion

of GO. The maximum reduction was noted by 23% with the addition of 0.08% GO addition, by weight of cement [35].

J. An et al. (2018) reported that the use of the mini-slump test, and the addition of Graphene oxide nanoflakes (GONF) decreased the fluidity of cement paste. Physical and chemical characteristics of GONF are used to clarify a potential cause for the lowering of fluidity. With the addition of 0.1% of GO, by weight of cement, the maximum reduction was reported by 40% when compared to the control [36].

L. Zhao et al. (2018) showed that the addition of a small amount of GO such as 0.05% by weight of cement with three types of water reducing agents (WRA) such as sodium lignosulfonate (LS), polycondensate of b-naphthalene sulfonate formaldehyde (PNS) and polycarboxylate superplasticizer (PC), reduced the fluidity of cement paste (Fig. 2.2). Based on the GO concentration and the recommended dosage by the manufacturer, a total of three WRA to GO mass ratios (5: 1, 10:1, and 20:1) were investigated [37].

According to *R. Roy et al.* (2018), when a small amount of Graphene oxide Nanosheets dispersion (GOD) was introduced to cement-sand mortar, the mortar's fluidity decreased. Cement was partially substituted 20% by Metakaolin (MK) and 10% by Silica Fume (SF). It illustrates how the mortar's cohesion increases with the amount of GOD substance [38].

With 10% PCs and 0.02% CNTs by weight of cement, *J. Gong et al.* (2020) investigated the fluidity behaviour of GO modified fly-ash based cement-sand mortar through a mini-slump test (Fig. 2.3). It was observed that the inclusion of GO, the fluidity of fly-ash based cement-sand mortar was significantly decreased with increased GO quantity. The maximum reduction was noted by 40% with 0.1% GO addition by weight of cement [39].

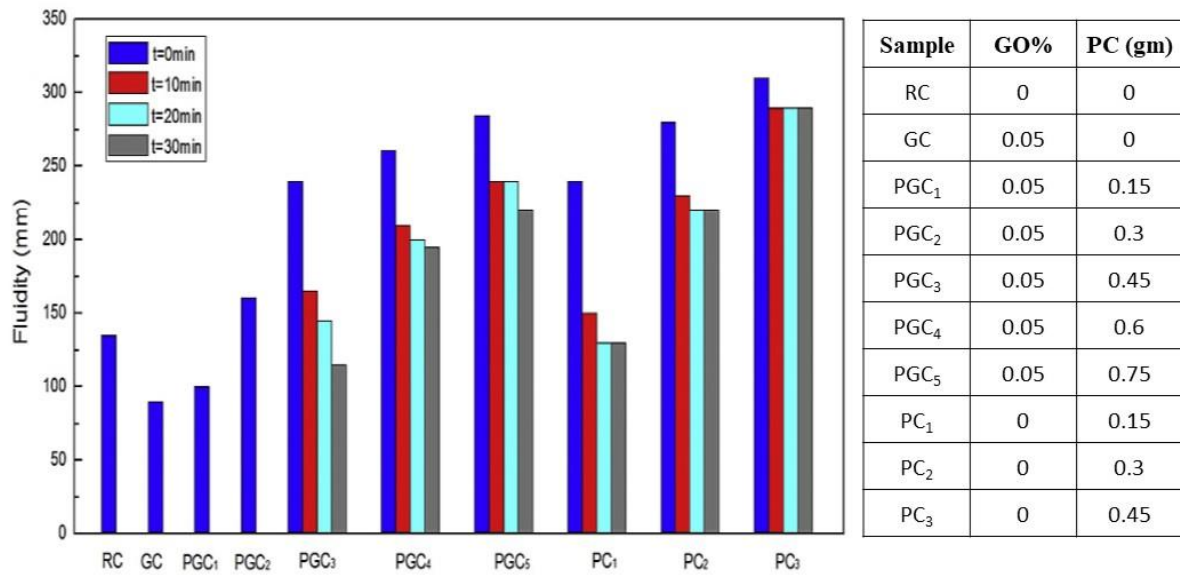


Fig. 2.2: Impact of PC, GO, and PC+GO on the fluidity cement pastes (Li Zhao et al., 2018).

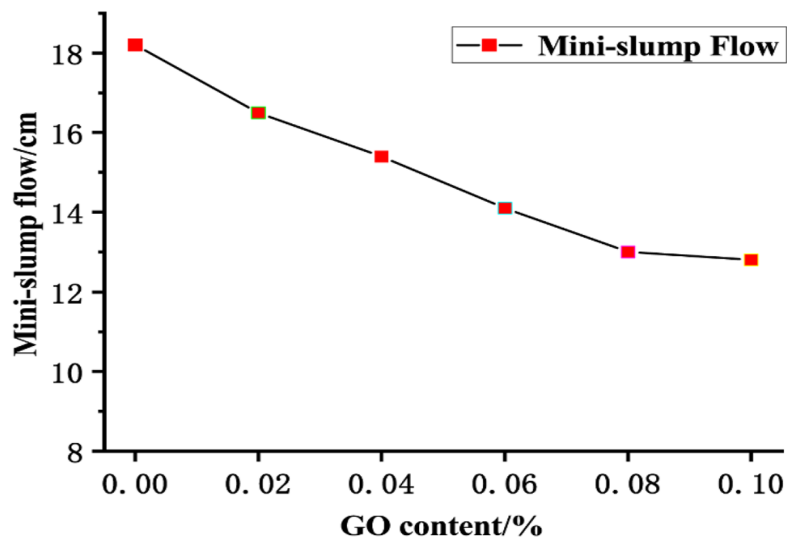


Fig. 2.3: Fluidity behaviour of GO modified fly-ash based cement mortar with PC and CNTs (Jianqing Gong et al. 2020).

The fluidity behaviour of GO-modified cement-sand mortar was studied by *C. Liu et al.* (2021) using SF, FA, and PC (Fig. 2.4). The result of the fluidity behaviour test reported contradictory results that there were almost no changes in the fluidity behaviour cement-sand mortar due to GO addition [40], but previous studies reported that GO can absorb free water on its surface area and thereby reduces the fluidity. [41–44].

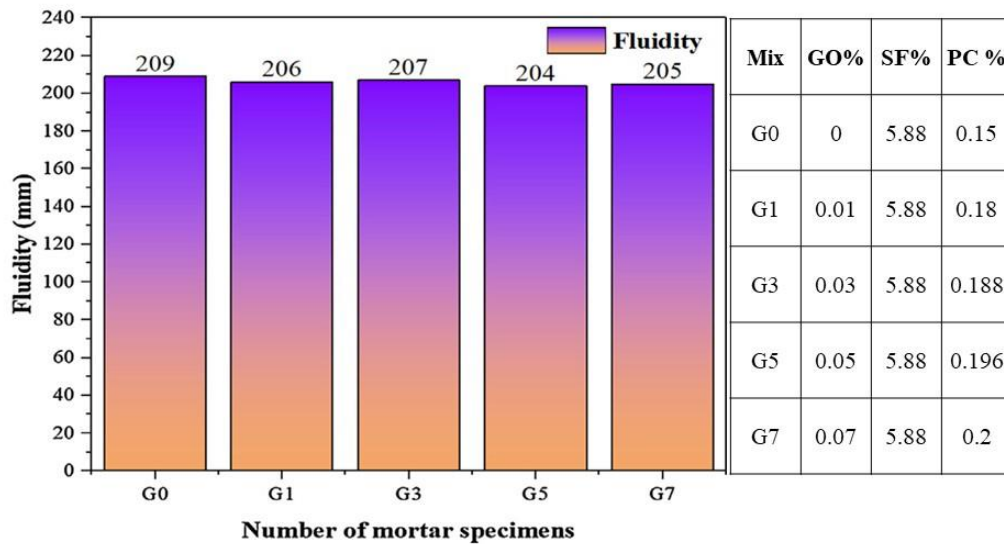


Fig. 2.4: Fluidity behaviour of GO modified cement mortar with SF, FA, and PC (C. Liu et al. 2021).

K. Chintalapudi et al. (2022) used a flow test to study the fluidity behaviour of OPC and PPC cement-sand mortar with 0.04% of GO by weight of cement. According to the flow table test results, the addition of GO increased marginally the fluidity of cement-sand mortar by 4% and 10% for PPC and OPC, respectively, when compared to the control sample. The O-containing functional groups on the surface of GO Nanosheet enables the improved fluidity of cement mortar. [45].

X. Hong et al. (2023) examined the workability of cement-sand mortar by slump test with the addition of a small amount of GO, shale ceramsite, and shale pottery sand with PCs (2% by weight of cement). According to the results of the slump test, the addition of GO and other additives lowered the slump value in comparison to the control (Fig. 2.5). The maximum reduction was noted by 30% with the addition of 0.06% GO. The slump value has declined for two main reasons. First, shale ceramsite is a type of coarse aggregate that has a rough surface, plenty of pores, and the ability to absorb water from cement slurry. Second, because of its huge surface area, the addition of GO may decrease the fluidity of fresh cement composites [46].

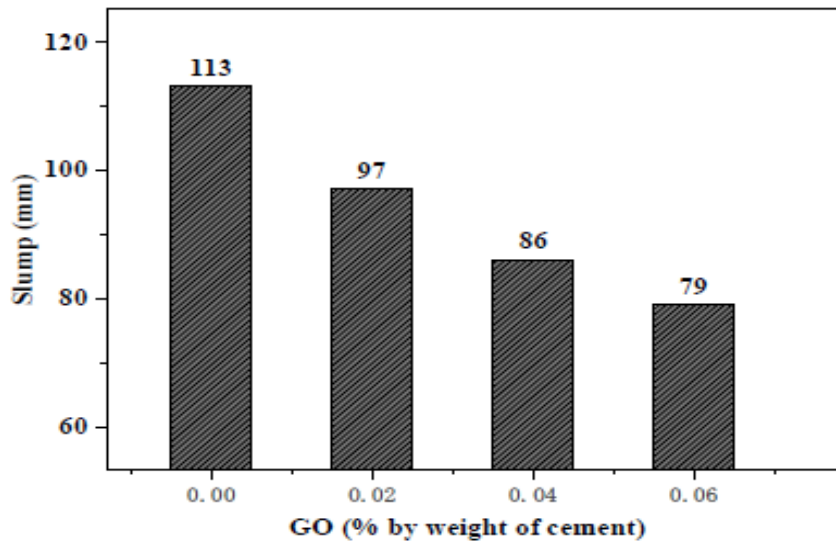


Fig. 2.5: Slump test results of GO modified cement mortar with PC (X. Hong et al. 2023).

2.4.2 Compressive strength

One of the most important parameters in a typical cement composite is its compressive strength. The compressive strength of hardened cementitious materials is influenced by several factors, including type of cement, cement content, the ratio of cement to aggregates (fine or coarse aggregates), the ratio of cement to water, etc. Similar to this, GO modified cement composite's compressive strength is supposed to be influenced by several parameters, such as dosages of GO, types of GO, addition of other admixtures (mineral and Chemical) etc.

According to *S. Lv et al. (2014)*, the compressive strength enhanced with the addition of GO in cement paste only, compared to the control with the addition of PC based admixture. The optimal improvement of the compressive GO modified cement paste was achieved by adding 0.04% GO by weight of cement with 0.2% PC. The maximum enhancement of compressive strength was noted by 34.5%. The possible reason for such enhancement the hydration crystals are primarily bar-like and flower-like crystals, as well as their aggregates and crosslinking [47]. The above study is limited to the cement paste only without using any aggregate.

In comparison with the control cement paste, *Q. Wang et al.* (2015) showed that the compressive strength increased with the addition of a small amount of GO (Fig. 2.6). The maximum enhancement was noted by 52.4%, 46.5%, and 40.4% at 3 days, 7 days, and 28 days of curing with the addition of 0.05% GO by weight of cement, respectively. Based on the experimental results it was reported that the GO can speed up the hydrated products' nucleation, growth, and phase separation, encourage the hydration process. Also the matrix frequently connect the crystals, all of which may change the pore structure and increase the strength of the hardened cement paste [33].

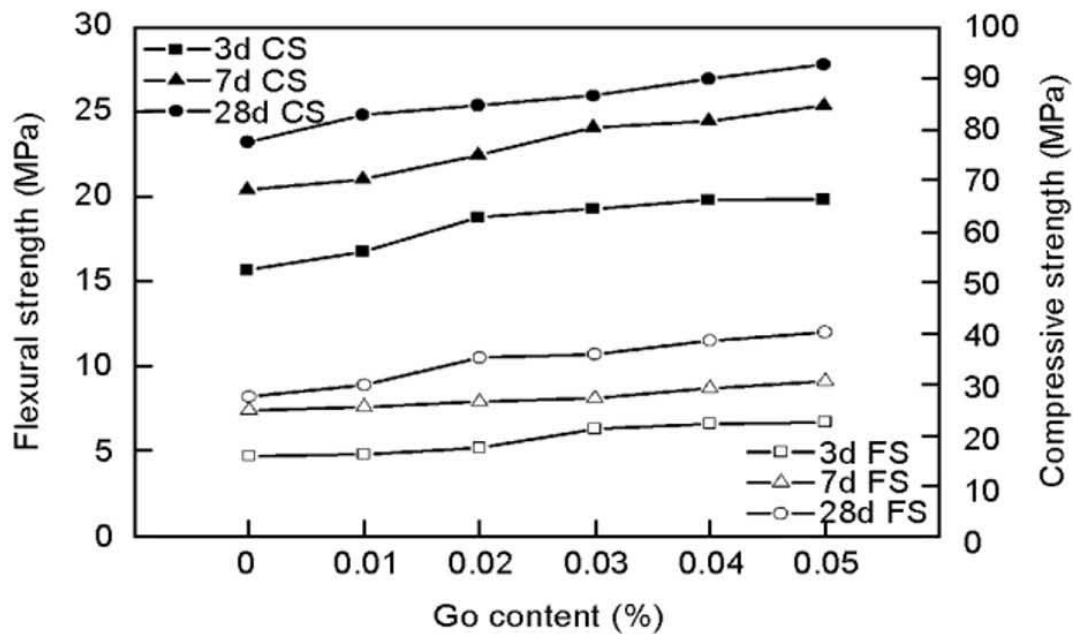


Fig. 2.6: Compressive strength of plain cement and GO-cement samples at different curing ages (Q. Wang et al., 2015).

Z. Pan et al. (2015) reported that the inclusion of a small amount of GO sheets enhanced the compressive strength of cement paste noticeably (Fig. 2.7). The graphite powder (10 g), $K_2S_2O_8$ (5 g) and P_2O_5 (5 g) were added to 60ml concentrated H_2SO_4 (80 °C) in an ice bath to prepare GO. The resulting mixture was cooled to room temperature over a period of 6 h. The addition of 0.05% GO was observed to increase compressive strength by 15-33% when compared to the

control. The samples reinforced with GO sheets show higher compressive strengths than their counterparts made of normal cement paste, indicating this may be the reason for the high compressive strength [32].

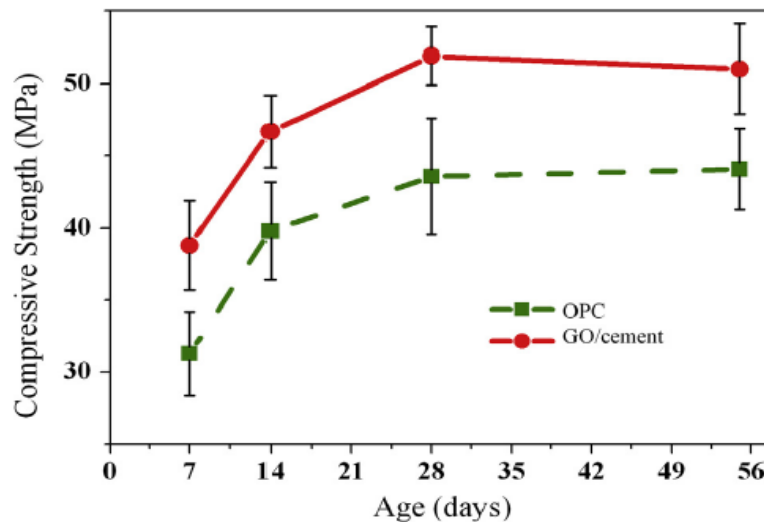


Fig. 2.7: Compressive strength of plain cement and GO-cement samples at different curing ages (Z. Pan et al., 2013).

K. Gong *et al.* (2015) reported that the inclusion of 0.03% of GO, increased the compressive strength of cement paste consistently at all curing ages, up to 28 days of curing ages (Fig. 2.8). The water/cement ratio was kept constant at 0.5 for with/without GO cement paste. The maximum enhancement was observed by 46% compared to control. The increase in hydration degree presence of GO nanoparticles may lead to the refinement of pore structure, which can contribute to enhanced strength [48].

In terms of mechanical qualities such as the compressive strength of cement-sand mortar, S. Sharma, and N. C. Kothiyal (2015) demonstrated a greater improvement (Fig. 2.9). The percentage of compressive strength increased from 35% to 86% for different concentrations of GO nanosheets such as 0.125%, 0.25%, 0.5% and 1% by weight of cement, were added into the cement-sand mortar, with small quantity Glenium as a PCs (0.2% to 0.6%) compared to the control sample [49].

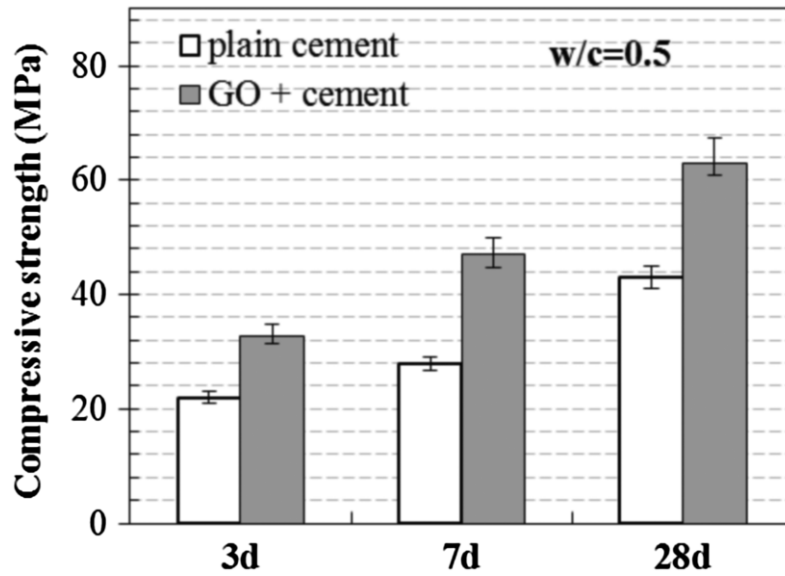


Fig. 2.8: Compressive strength of plain cement and GO-cement samples at different curing ages (K. Gong et al., 2015).

According to *Li Zhao et al.* (2016), GO-cement composites perform better than plain-cement composites in terms of strength across all ages. With the introduction of 0.22% of GO, with the GO to PC mass ratio of 0.1, the compressive strength increased by 17.68% compared to the control sample, after 28 days of curing. The internal curing action of GO can be used to explain the long-term improvement in the GO-cement sample. When the amount of free water in the cement matrix is unable to meet the requirements of continuous hydration, the water absorbed by GO surfaces progressively releases for additional hydration, leading to long-term improvement [34].

M.M. Mokhtar et al. (2017) reported that the compressive strength of hardened cement paste enhanced at all curing ages with the addition of Graphene oxide nanoplatelets (GONPs) compared to plain cement (Ordinary Portland Cement) paste (Fig. 2.10). GONPs were synthesized according to the modified Hummer's technique from graphite. The maximum enhancement of compressive strength was reported by 13% with the addition of 0.02% of GONPs, by weight of cement. Further, the compressive strength gradually decreases with the increased weight of GONPs. The possible reason for the enhancement of strength may be the

high aspect ratio and 2D sheet-like shape of GONPs; improving the hydration process and creating strong interfacial forces [50].

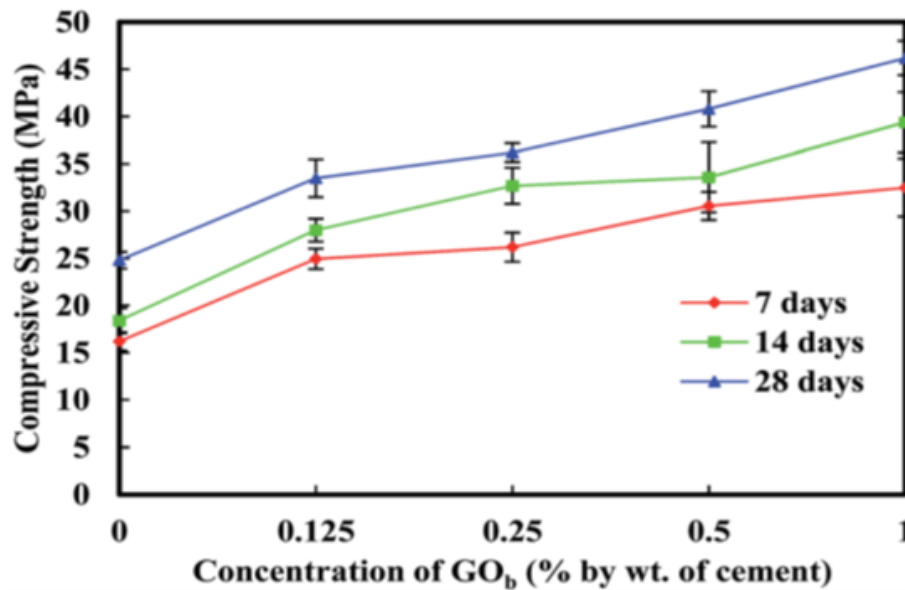


Fig. 2.9: Compressive strength of GO modified cement mortar at different curing ages

(S. Sharma and N. C. Kothiyal, 2015).

In accordance with *H. Yang et al. (2017)*, GO additions with a small quantity of PCs enhanced the compressive strength of cement paste (ordinary portland cement), particularly in early ages. Go was added along with PC based admixture and antifoaming agent in the cement paste. With the addition of 0.15% and 0.2% GO by weight of cement, the compressive strengths of the cement paste increased by 30.7% and 42.3% after 3 days compared to the control sample (Fig. 2.11). The improvements in compressive strength significantly decreased with the curing age, reaching 7.4% and 11.2% after 28 days for additions of 0.15 and 0.2% GO, respectively. However, the introduction of 0.2% GO, by weight of cement, showed the highest compressive strength improvement at all curing ages. GO sheets bonded with OPC hydration products may have strengthened their bonding, which could account for future gains in mechanical strength. [51].

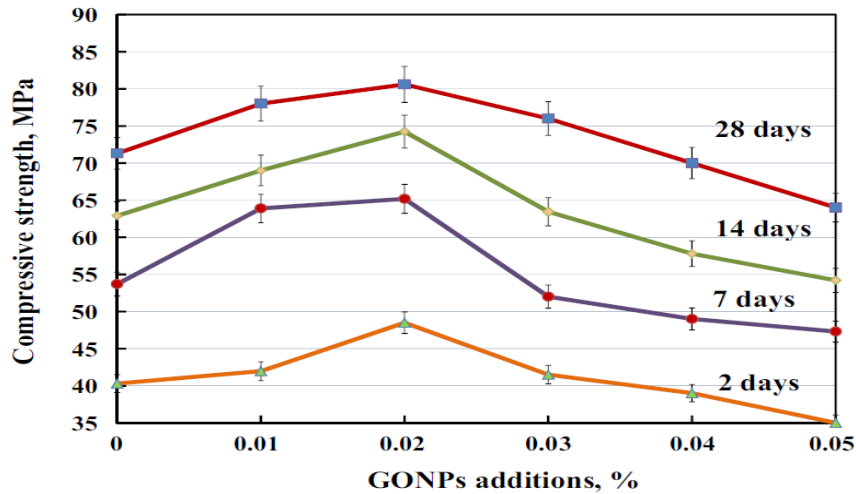


Fig. 2.10: Compressive strength of hardened cement paste with and without GONPs (M.M. Mokhtar et al. 2017).

J. An et al. (2018) concluded that the compressive strength of cement paste may increase with the addition of Graphene oxide nanoflake (GONF). The optimum percentage was noted 0.05% of GONF by weight of cement (Ordinary Portland Cement) , Dry-mix, and Wet-mix design methods (Fig. 2.12 (a) and (b)). Dry-mix design indicates the GONF is mixed with cement as a dry power while Wet-mix design signifies that the GONF as a solution (after sonication of GONF with water) is mixed with cement. Dry-mix is more practical and effective for concrete mix due to the ease of preparation. For the Dry-mix method maximum enhancement of compressive strength of cement paste was noted around 19% compared to the control sample, after 28 days. On the other hand, for the Wet-mix method, after 28 days, the compressive strength increased around by 25% compared to the control. It may be possible that the GONF is a two-dimensional material that strengthens cement composite by interlocking with its hydration products of cement composites [36].

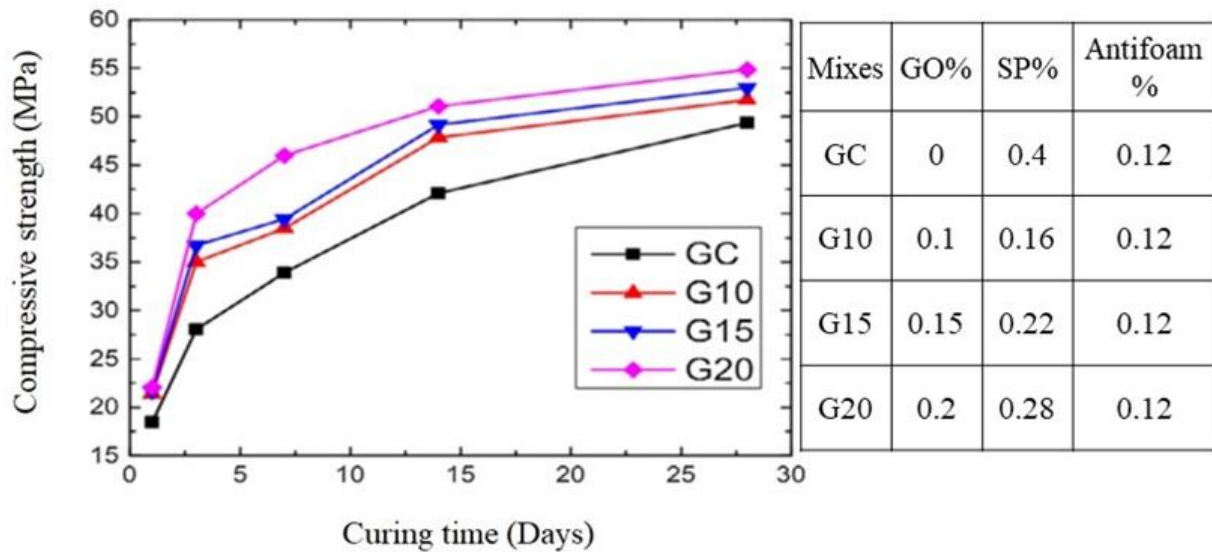


Fig. 2.11: Compressive strength of GO modified cement paste at different curing ages (H. Yang et al. 2017).

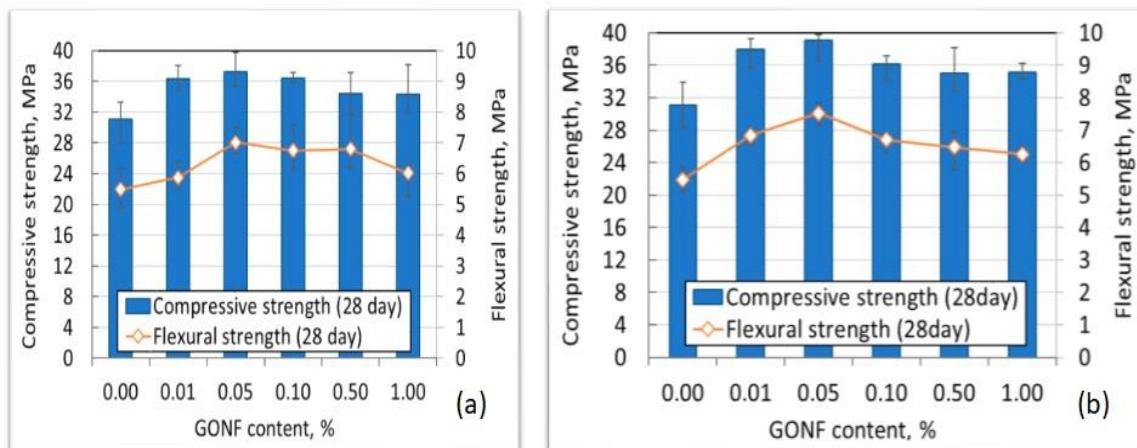


Fig. 2.12: Compressive strength of cement paste of (a) Dry-mix method, and (b)Wet-mix method (J. An et al., 2018).

L. Zhao et al. (2018) reported that the inclusion of a small amount of GO by weight of Portland cement, along with PC (having fixed percentage), achieved high compressive strength of cement sand composites (Fig. 2.13). The sand used was fine having a maximum size of 2mm. The ratio of cement: sand was 1:3 by weight and water cement ratio was fixed at 0.5. The results have shown that GO with PC reached a high level of reinforcement at a low

concentration, demonstrating that GO can be a potential nano-reinforcement in cement composites [37]. However, they had not reported the results of 28 days of strength.

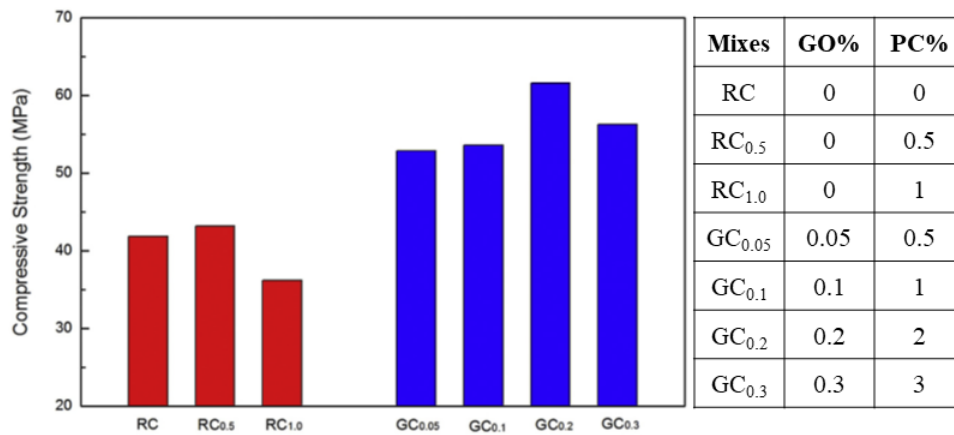


Fig. 2.13: Compressive strength of different mixes of cement mortar at 7 days curing age (L. Zhao et al., 2018).

R. Roy et al. (2018) reported that the inclusion of a small amount of Graphene Oxide Nanosheets dispersions (GOD) in OPC cement-sand mortar (cement-sand ratio 1:3), where cement partially replaced 10% by Silica Fume (SF) and 20% by Metakaolin (MK), the compressive strength of cement mortar increased at all curing ages compared to the control sample. The technical parameters of GOD are presented in table 2.1. The maximum enhancement of compressive strength was recorded for 0.05% GOD addition by weight of cement. The results indicated that the increase in strength was impacted by three elements. These are the pozzolanic reaction of MK and SF with the lime generated by the hydration reaction, the filler effect, and the acceleration of OPC hydration [38].

In comparison to the control sample, in which cement was replaced 30% by fly ash (FA) class F, *S. Sharma et al.* (2018) found that the incorporation of a minor quantity of GO with superplasticizer (SP) increases the compressive strength of cement-sand mortar (cement-sand ratio 1:3) at all curing ages (Fig. 2.14). After 28 days of curing age, the maximum compressive

strength gained by 35% compared to control mortar with the addition of 0.125% of GO and 0.1% SP. After that, when the concentration of GO in FA-based mortar mixes increases, the compressive strength decreases. After 28 days, the percentage improvement in compressive strength for 0.25, 0.50%, and 1.0% GO addition compared to the control mix was found to be 23.5%, 19.1%, and 9%, respectively. The improvement in strength may be possible due to nano filling activity of GO [52]. It is noted that the improvement of strength is comparatively less with addition of GOD in flyash based mortar compared to OPC based mortar.

Table 2.1: Technical parameters of GOD.

Properties	Description
Graphene Oxide Nanosheets content	1%
Fineness	<5 μm
Colour	Greyish Liquid
Dispersibility	Water, Ethanol, IPA- (Polar solvents)
pH	7
Surface Tension	35 dyne/cm
Viscosity	15 Pa.S (25°C)
Boiling Point	100°C
Density	0.89 mg/ml at 25°C

G. Xu et al. (2019) concluded that addition of 0.02% GO by weight of the cement the compressive strength of the OPC cement paste increased remarkably at all curing ages compared to the control sample (Fig. 2.15). The water/cement ratio was kept the same at 0.35 for with/without GO cement paste. The maximum enhancement was noted at 3 days curing ages by 34%. The compressive strength increased at 7 days and 28 days curing ages are around 27% and 29% compared to the control sample respectively. The results suggested that the addition of GO may change the hydration products of cement paste, which may have an impact on the mechanical properties [54]. However, it seems that there is an optimum percentage of GO addition for OPC based cement paste.

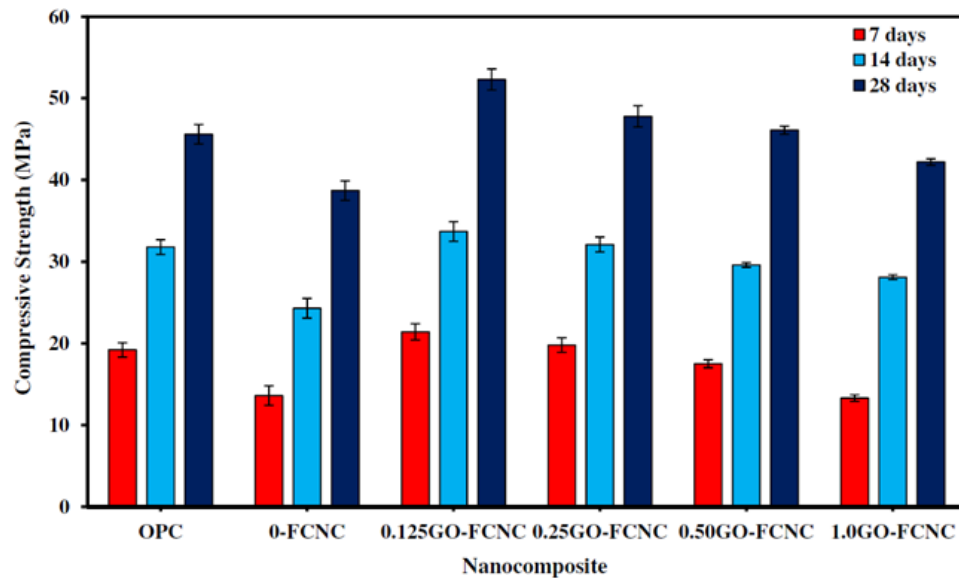


Fig. 2.14: Compressive strength of different mixes GO modified cement mortar with SP at different curing ages (S. Sharma et al. 2018).

A.M. Sabziparvar (2019) studied the effect of the addition of GO to cement paste along with polycarboxylate ether based superplasticizer (PCE), sodium dodecyl sulfate (SDS), naphthalene-based superplasticizer (NSF), and an alkyl ammonium salt of a high molecular weight copolymer that is sold as BYK 9076. It was observed that the compressive strength of GO modified OPC cement mortar (cement-sand ratio 1:3) enhanced at all curing ages compared to the control (Fig. 2.16). Table 2.2 presents the elemental analysis of GO was used throughout in this study. The water/cement ratio was kept constant at 0.38. The maximum enhancement was observed by 44% with the addition of 0.04 of GO after 28 days of curing. The better dispersion of GO with the presence of SDS, NSF, PC, and BYK 9076 is the most possible reason for the higher compressive strength of GO modified cement composite [55].

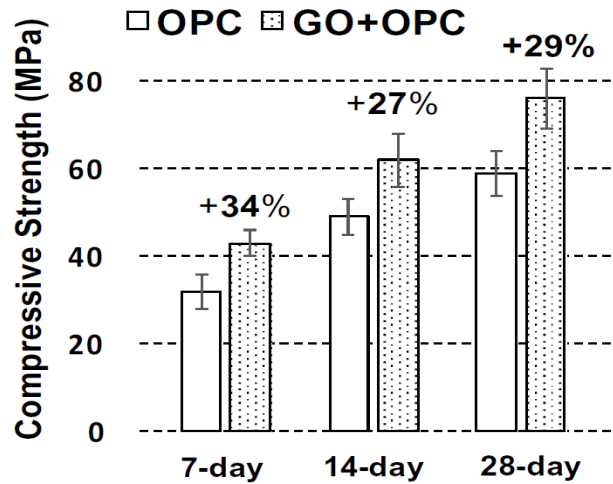


Fig. 2.15: Compressive strength of cement past with and without GO at different curing ages (G. Xu et al. 2019).

Table 2.2: Elemental analysis GO.

Element (by weight)	Carbon	Oxygen	Sulfur	Nitrogen
%	58–63	33–38	1–2	0–2

The compressive strength behaviour of cement-sand mortar was investigated by *H. Peng et al.* (2019) with small amount of GO (0%, 0.01%, 0.03%, and 0.05% by weight of cement) added and a varied water/cement ratio (w/c 0.3, 0.35, 0.4, 0.45, and 0.5) with 0.2% of PCs by weight of cement (Fig. 2.17a and 2.17b). The maximum compressive strength was noted for 0.01% GO addition by weight of cement by 5.16% compared to the control sample. Further addition of GO results in significantly decreased compressive strength of GO modified cement-sand mortar compared to the control sample due to GO nanoparticle agglomeration. The result indicated that GO absorbs a significant quantity of water, therefore decreasing the cement's degree of hydration. Consequently, appropriately increasing the w/c ratio will provide sufficient improved cement hydration by providing free water. Conversely, a higher w/c ratio could make it easier for GO to disperse throughout the cement matrix. Additionally, GO may

effectively fill the cement mortar's micropores as a nanomaterial, strengthening the mortar's structure [56].

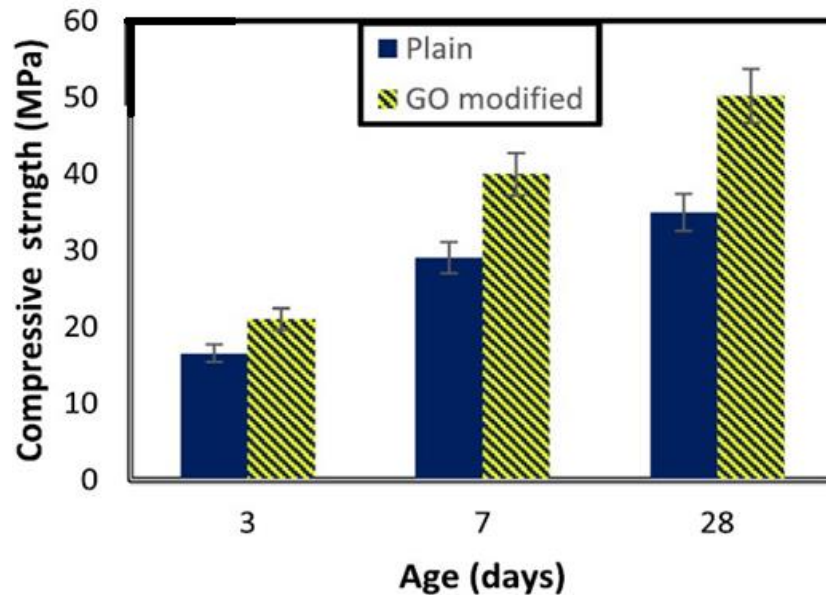


Fig. 2.16: Compressive strength of GO modified OPC cement mortar with 0.04% of GO with the presence of SDS, NSF, PC, and BYK 9076 at different curing ages (A.M. Sabziparvar 2019).

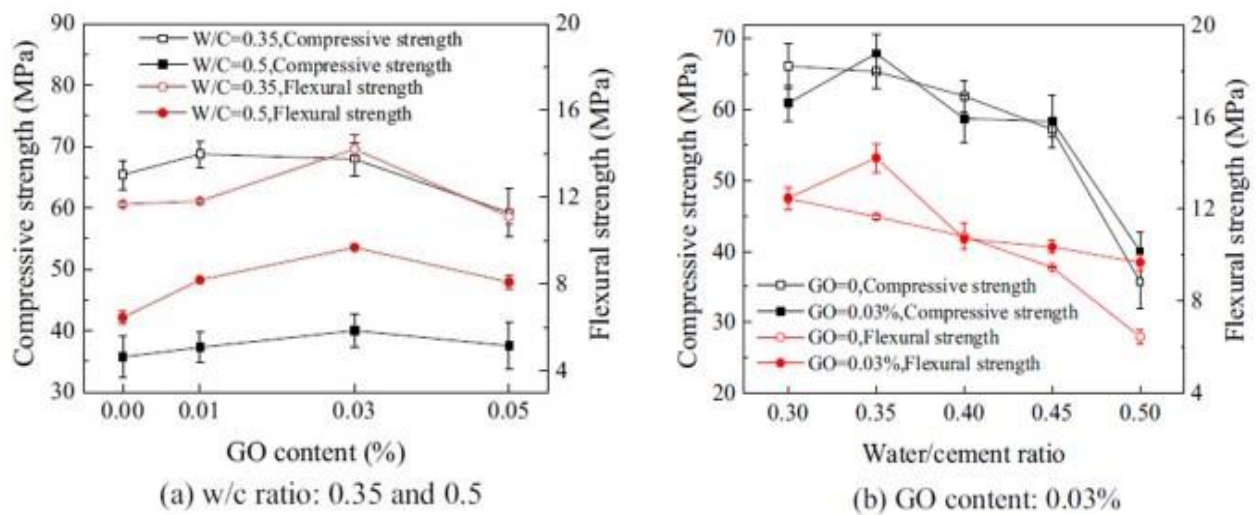


Fig. 2.17: Compressive strength and flexural strength of GO modified cement-sand mortar with different w/c ratios (H. Peng et al. 2019).

J. Gong et al. (2020) studied the compressive strength of GO modified fly-ash based cement-sand mortar with 10% water reducing agent used was QS-H8011L polycarboxylates (PC) and

0.02% of multi walled Carbon nanotubes (CNTs) by weight of cement (Fig. 2.18). The quantity of GO that was included in the cement-sand mortar were 0.02%, 0.04%, 0.06%, 0.08%, and 0.1% by weight of cement. The compressive strength of cement-sand mortar was increased significantly up to 0.08% GO added by weight of cement. The maximum enhancement was observed by 41% with 0.08% GO addition after 28 days, compared to the control. Further, in addition of GO such as 0.1%, compressive strength was higher than the control but lower than the 0.08% GO addition [39]. These results can be explained by the simple fact that the presence of CNTs and high GO increased the number of harmful holes in the specimen and decreased the compressive strength [57,58].

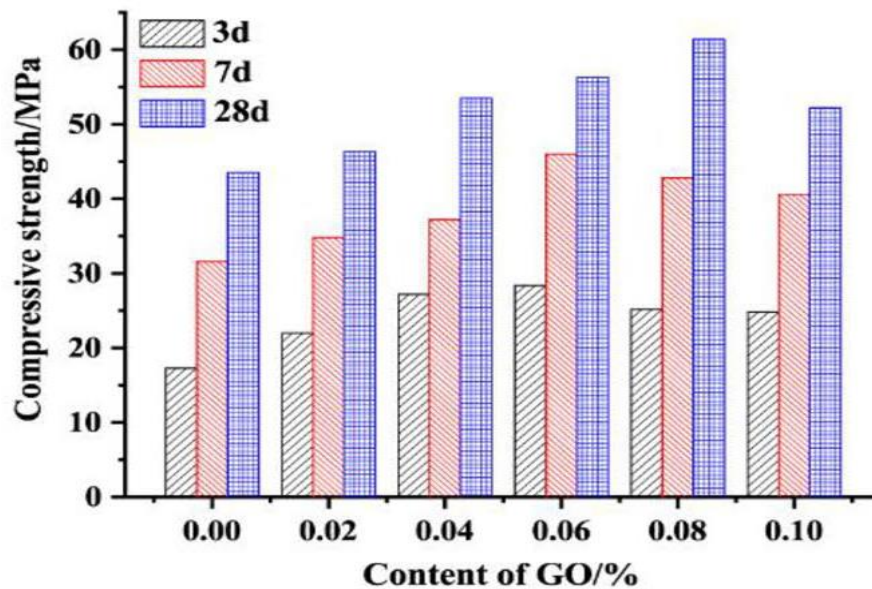


Fig. 2.18: Compressive strength of GO modified fly-ash based CNTs at different curing ages (J. Gong et al. 2020).

The effects of the addition of reduced graphene oxide (rGO) and polycarboxylate ether (0.08%) in structural cement concrete were the subject of a study conducted by B. M. Chufa et al. (2020). The rGO dosage was varied from 0.1% to 5% and the water/cement ratio was kept constant at 0.46. For the purpose of developing a uniform solution, rGO is suspended in distilled water and sonicated for 3 hours to prepare the rGO-concrete composites. After 28 days of curing, it was observed that a 0.5% rGO addition increased compressive strength by 44%

compared to the control. Compressive strength was higher with further rGO addition compared to the control, although it was still lower than with 0.5% rGO modified concrete. The presence of rGO nanoparticles in the cement composite may have refined its microstructure, possibly leading to an increase in strength [59].

The Alkali-silica reaction (ASR) of Portland cement-sand mortar was investigated by *J. Luo et al.* (2021) using Pyrex glass (PG) and GO (0.02% and 0.04% by weight of cement). The sand-cement mass ratio at 2.25 and water/ cement ratio was taken as 0.47 for all mixes. Fine aggregate, such as tuning sand was 25% and 50% replaced by PG by weight. In both cases with and without PG, it was found that the inclusion of GO enhanced the compressive strength of the GO-modified cement-sand mortar. In comparison to the control sample, the highest enhancement was observed around 43% with the addition of 0.04% GO without PG. The compressive strength of cement mortar increased with PG was added in place of sand in comparison to the control sample, however, it was still lower than adding 0.04% GO. An increase in mechanical strength occurs even with relatively small amounts of GO incorporation due to the nano-nucleation and interlocking effect of nanoscale GO, which leads to denser textiles and less pore structures of mortar [60].

The compressive strength of GO-modified cement-sand mortar was investigated by *C. Liu et al.* (2021) using SF, FA, and PC (Fig. 2.19). The GO dosage varies by 0.00%, 0.01%, 0.03%, 0.05%, and 0.07%, and the water/cement ratio was kept constant at 0.4. Table 2.3 presents the elemental analysis of GO was used throughout in this study. The time of ultrasonication of GO solution were varied from 10 min to 30 min. The result indicated that the compressive strength of cement-sand mortar increased with the inclusion of a certain amount of GO. After 28 days, maximum enhancement was seen by 12% with the addition of 0.03% GO in comparison to the control sample. The result indicated that the GO can promote cement hydration and help to

improve the microstructure [40]. It is noted that the improvement in strength is not so comparable.

Table 2.3: Elemental Analysis of Graphene Oxide (GO).

Carbon	Hydrogen	Nitrogen	Sulfur	Oxygen
49–56%	1–2%	0–1%	2–4%	41–50%

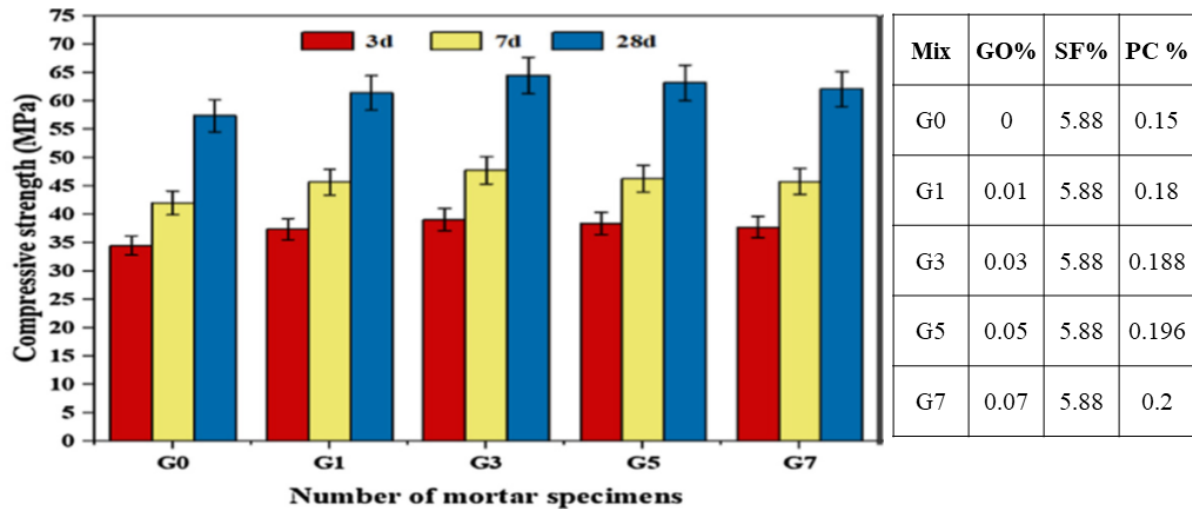


Fig. 2.19 Compressive strength of GO modified cement mortar with SF, PCs, and FA at different ages of curing ages (C. Liu et al. 2021).

X. Qi et al. (2021) studied the compressive strength of cement-sand mortar with GO and TiO₂-rGO. The cement-sand ratio was 1:3 and the water-cement ratio was kept constant at 0.42 for all mixes. The amount of GO and TiO₂-rGO were taken as 0.01%, 0.03%, and 0.05% by weight of cement. The result indicated that with the addition of GO and TiO₂-rGO, the compressive strength increased at all curing ages compared to the control. Compared to the control, the results showed that the inclusion of GO and TiO₂-rGO enhanced the compressive strength at all curing ages. For both mixes, the maximum enhancement was observed at 11% and 28% with a 0.03% GO addition by weight of cement. Growing nuclei for cement mortar hydration, which is advantageous for creating dense structures, may have contributed to the strength increase [61]. Cement mortar strength can be increased by using GO to control moisture and

create dense, flower-like microstructures [33,62]. It is also noted that the increase in strength is limited with the addition of GO.

In comparison to the control sample at all curing ages, *P. Vasudevareddy et al. (2022)* found that the addition of GO with a small amount of nano-silica enhanced the compressive strength of cement-sand mortar (Fig. 2.20). The chemical composition and physical properties of GO is presented at table 2.4 and table 2.5. The amount of GO dosages varies from 0.03%, 0.05%, 0.07%, and 0.09% by weight of cement. The percentage of nano silica was used 1.5%, 3%, 4.5%, and 6%. The cement-sand ratio was 1:3 and the water/cement ratio was kept constant 0.45 throughout the experimental study. After 28 days of curing, a maximum increase of 27% was observed for 0.07% GO addition with 4.5% nano-silica by weight of cement [63]. No explanation for the improvement of 27% is not provided.

Table 2.4: Chemical composition of Graphene Oxide (GO).

Carbon	Nitrogen	Sulfur	Oxygen
10%	3%	8%	78%

Table 2.5: Physical Properties of Graphene Oxide.

Parameters	Approximate values
Product Purity	99%
Number of layers	3–6
Surface area	greater than 120 m ² /g
Thickness	0.8–2 nm
Bulk density	0.121 g/cc
Electrical Conductivity	Insulator
Length	1–2 μm
Specific gravity	1.053

X. Hong et al. (2023) studied the compressive strength behaviour of cement-sand mortar with GO, Shale ceramsite (shale ceramsite to cement ratio 1.29), and shale pottery (shale pottery to cement ratio 1) sand with superplasticizer (SP) (2% by weight of cement). The dosage of GO

was varied as 0.02, 0.04 and 0.06%. the water/cement ratio was kept constant at 0.35 for all mixes. The result indicated that the addition of GO increased the compressive strength of cement mortar at all curing ages compared to the control sample (Fig. 2.21). After 28 days of curing and the addition of 0.06% GO by weight of cement, the specimens compressive strength improved by a maximum of 25%. This could be the result of GO speeding up the hydration of cement [46].

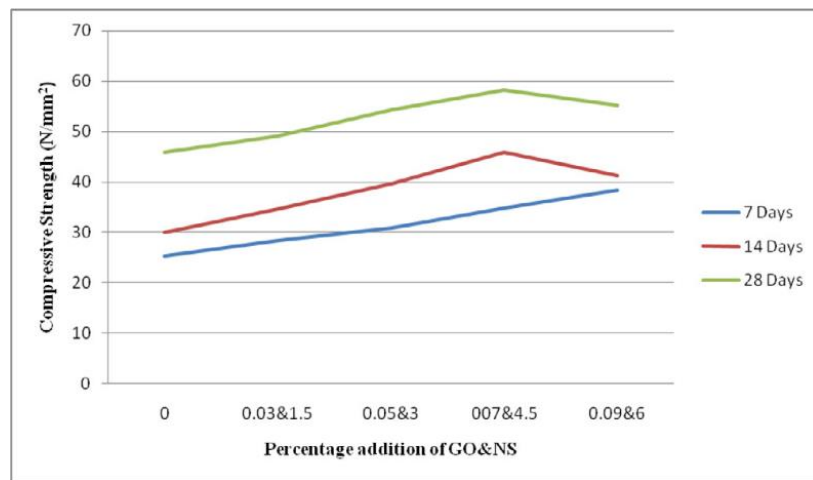


Fig. 2.20: Compressive strength of GO modified cement mortar with SF (P. Vasudevareddy et al. 2022).

L. Djenaoucine et al. (2023) studied the compressive strength of GO modified cement mortar with and without superplasticizer (SP) (2% by weight of cement) (Fig. 2.22). The GO dosages taken as 0.0005%, 0.005%, and 0.05% by weight of cement. The cement-sand ratio was taken 1:3 and water/cement ratio was kept constant at 0.05 for all mixes. The chemical composition of Graphene Oxide (GO) is presented in table 2.6. The mixture comprises 2 grams of GO dissolved in 1.125 liters of water. According to the experimental results, the GO did not increase compressive strength at early curing ages, such as 2 days and 7 days curing ages. After 28 days of curing, all GO modified cement mortar with and without SP improved the compressive compared to the control sample. The beneficial effects of SP in obtaining a decent GO dispersion were reported [64].

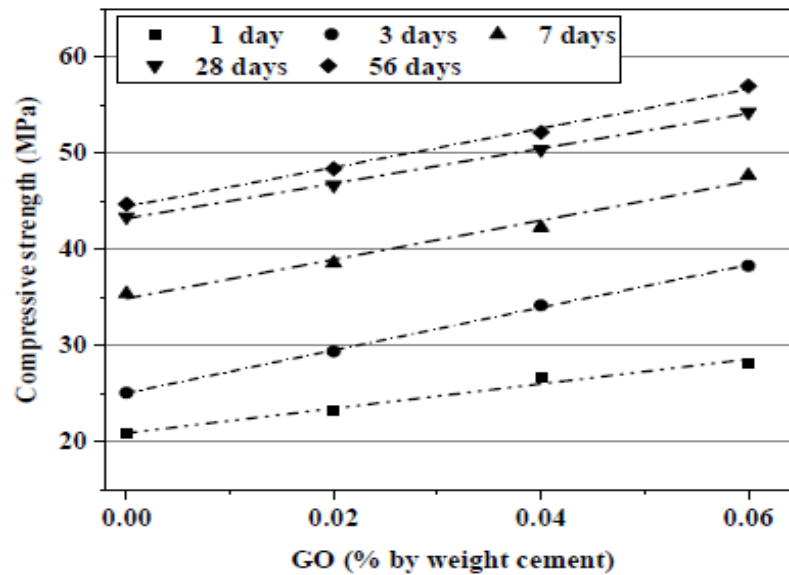


Fig. 2.21: Compressive strength of GO modified cement mortar with PCs (X. Hong et al. 2023).

Table 2.6: Chemical composition of Graphene Oxide (GO).

Element	Carbon	Hydrogen	Nitrogen	Sulfur	Oxygen
%	49-56	0-1	0-1	0-2	41-50

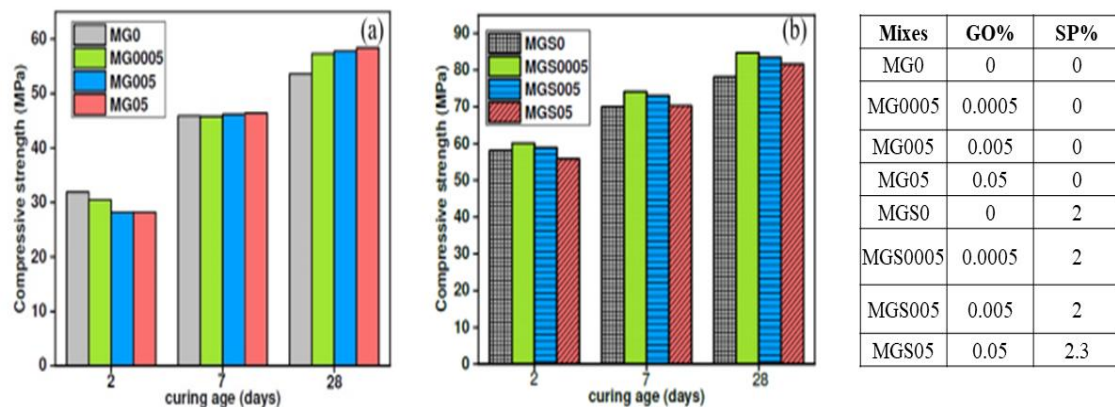


Fig. 2.22: Compressive strength of GO modified cement mortar (a) with and (b) without SP at different curing ages (L. Djenaoucine et al. 2023).

2.4.3 Tensile strength

The ability of a material to sustain pulling or stretching forces without breaking or deforming is determined by the tensile strength, which is a crucial mechanical characteristic of cement composites. Cement composite is not often expected to withstand direct tension due to its weak

tensile strength and brittle nature. Frequently used in construction and civil engineering, cement composites are made by combining cementitious materials (such Portland cement) with a variety of aggregates, reinforcing fibers, and additives.

K. Gong et al. (2015) reported that the split tensile strength of GO modified cement paste is higher than the control. The water/cement ratio was kept constant at 0.5 for with/without GO cement paste. It was observed that with the presence of 0.03% by weight of cement, split tensile strength enhanced more than 50%. The possible reason for the higher strength of cement is the reinforcing effect of GO [48].

M.M. Mokhtar et al. (2017) measured the tensile strength of hardened OPC cement paste with and without Graphene oxide nanoplatelets (GONPs) by indirect tensile strength method. The GONPs dosage varied from 0.01% to 0.05% by weight of cement. The water/cement ratio also varied as 0.25, 0.283, 0.292, 0.300, 0.302 and 0.307. The tensile strength was significantly increased up to 0.03% of GONPs addition (Fig. 2.23). The maximum enhancement of tensile strength was noted 41% higher than the plan cement sample with the addition of 0.03% of GONPs, by weight of cement. Furthermore, the enhancement of dosages of GONPs reduced the tensile strength. the tensile strength increment may be possible due to the strong interaction bond between GONPs and the crack of cement paste [50].

S. Sharma et al. (2018) discovered that the tensile strength of OPC based cement-sand mortar was enhanced by the small amount of GO combined with a polycarboxylate ether based superplasticizer (PC), as compared to the control sample, where fly ash (FA) was used in place of cement to replace 30% of the cement at all curing ages (Fig. 2.24). The maximum tensile strength was observed after 28 days with a 0.125% GO addition and 0.1% PC by weight of cement. This is approximately 96% higher than that of the control mix. Further, with more addition of GO such as 0.25%, 0.50%, and 1.0%, tensile strength enhanced by roughly 60%,

24%, and -8%, respectively, compared to the control mix. The nanofiller effect of GO is the possible reason for higher tensile strength [52].

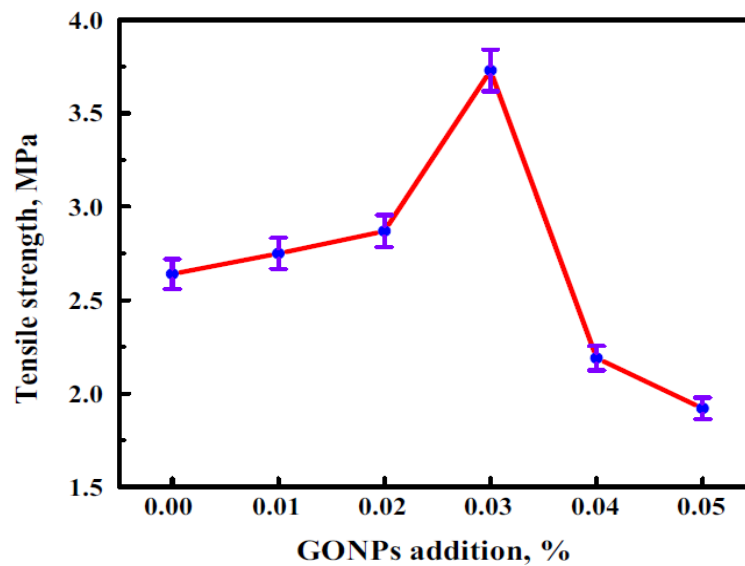


Fig. 2.23: Indirect tensile strength of plan cement paste and GONPs modified cement paste after 28 days hydration (M.M. Mokhtar et al. 2017).

An investigation on reduced graphene oxide (rGO) in structural cement concrete was carried out by *B. M. Chufa et al. (2020)*. The rGO dosage was varied from 0.1% to 5% and the water/cement ratio was kept constant at 0.46. For the purpose of developing a uniform solution, rGO is suspended in distilled water and sonicated for 3 hours to prepare the rGO-concrete composites. The results showed that a 0.5% rGO inclusion improved tensile strength by 73% after 28 days compared to the control. Tensile strength was lower with further rGO addition than with 0.5% rGO modified concrete, but higher than the control. The addition of rGO nanoparticles to the cement composite might improve its microstructure and increase strength [59].

P. Vasudevareddy et al. (2022) reported that the inclusion of GO with a small amount of nano-silica improved the split tensile strength of cement-sand mortar compared with the control sample at all curing ages (Fig. 2.25). The dosage of GO varies from 0.03%, 0.05%, 0.07%, to

0.09% by weight of cement, while the percentage of nano-silica ranges from 1.5%, 3%, 4.5%, to 6%. The cement-sand ratio remained at 1:3, with a constant water/cement ratio of 0.45 throughout the experimental study. A maximum enhancement of 22% was noted for 0.07% GO addition with 4.5% nano-silica by weight of cement after 28 days of curing [63].

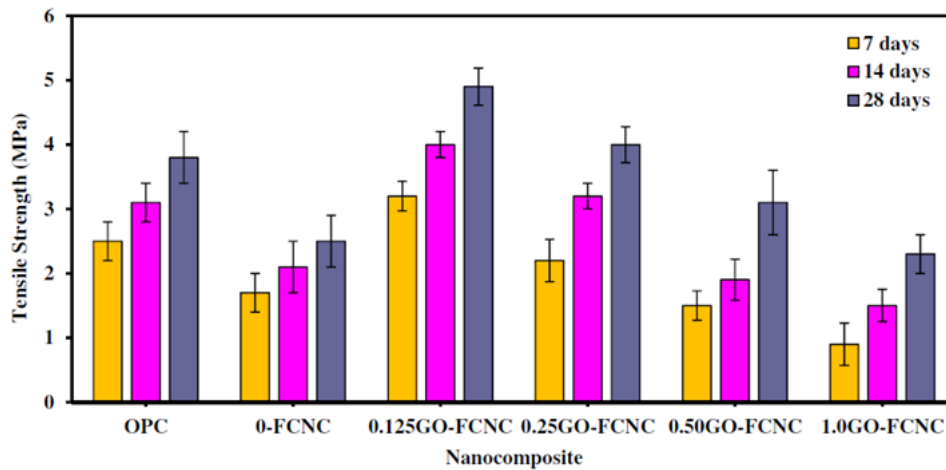


Fig. 2.24: Tensile strength of different mixes at different curing ages (S. Sharma et al. 2018).

2.4.4 Flexural strength

The flexural strength of cement composites is a fundamental mechanical property that characterizes a material's ability to resist bending or flexural forces without fracturing. This property is essential in the construction and civil engineering, as it helps assess the performance and durability of cement-based materials, such as concrete and mortar when subjected to various structural loads.

S. Lv et al. (2014), reported that the flexural strength of cement paste increased with the addition of small quantity of GO along with Polycarboxylate superplasticizer (PC, 20%) by weight of cement. The dosage of GO varied from 0.01% to 0.06% by weight of cement, and the water/cement ratio was fixed at 0.3. By incorporating 0.03% of GO by weight of cement, the flexural strength of GO modified cement paste was improved by around 43% compared to

the control sample. The densification of hydration crystals through interlacing with GO may be responsible for the enhancement of flexural strength [47].

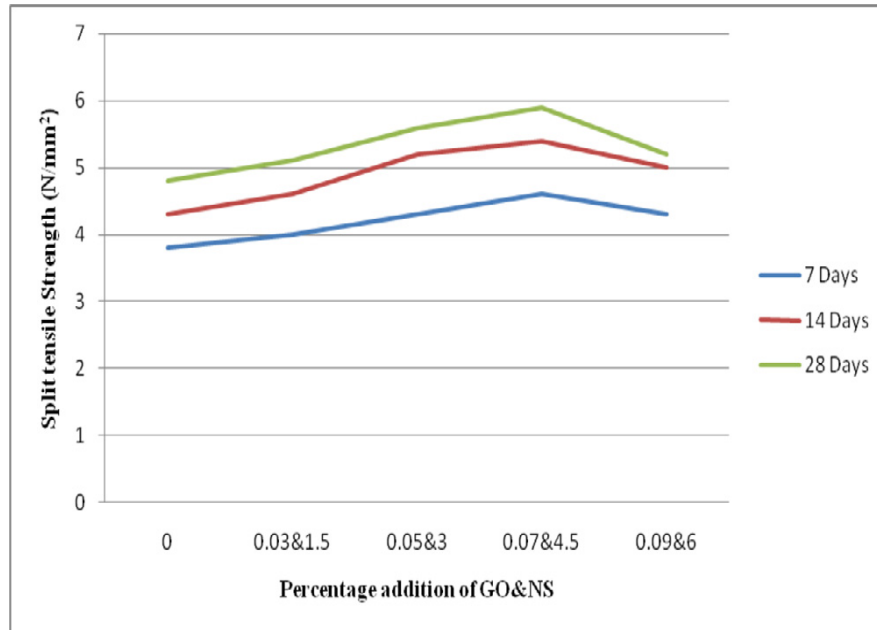


Fig. 2.25: Split tensile strength behaviour of GO modified cement mortar with nano-silica (P. Vasudevareddy et al. 2022).

L. Zhao et al. (2016) studied the flexural strength behaviour of GO modified cement mortar with the GO to PC mass ratio of 0.1. The percentage of GO was fixed 0.022% by weight of cement, the cement-sand ratio was taken 1:3, and the water/cement ratio was kept constant at 0.42. With the addition of 0.022% GO, the flexural strength of GO-cement composites significantly improved at 7 days and 28 days, by 22.03% and 22.55%, respectively. The results of the flexural strength test showed that GO nanosheets have a sizable toughening impact on cement composites. It is proposed that GO nanosheets are essential for the elimination of pre-flaws and the fine-tuning of cracks [34].

J. An et al. (2018) reported the same pattern GONF addition for the flexural strength of OPC based cement paste by Dry-mix and Wet-mix methods (Fig. 2.12 (a) and 2.12 (b)). The Chemical composition of GONF is presented in Table 2.7. The inclusion of 0.05% of GONF

by weight of cement resulted in a maximum improvement of 28% and 37% for the flexural strength of cement paste for dry-mix and wet-mix methods, respectively. The possible reason for enhancement of is the interlocking of hydration products of cement composite and GONF [36].

Table 2.7: Chemical composition of GONF (edged oxidized).

Oxygen	Non-Oxygen Composition						
	Carbon	Silicon	Sulphur	Calcium	Potassium	Chromium	Copper
5~10%	>99.8%	<40 ppm	<60 ppm	<5 ppm	<30 ppm	<125 ppm	<5 ppm

In according with *R. Roy et al.* (2018), the flexural strength of cement mortar enhanced at all curing ages when Graphene Oxide Nanosheets dispersions (GOD) were added in modest amount to cement-sand mortar. In this case, cement was partially replaced with 10% Silica Fume (SF) and 20% Metakaolin (MK). The technical parameters of GOD are already presented in table 2.1. The highest observed increase in flexural strength was found at 0.1% GOD addition by weight of cement. The results indicated that the filler effect of GOD, the accelerated hydration of OPC, and the pozzolanic reaction of MK and SF with the lime produced by the hydration reaction are responsible for generated the high strength [38].

W. J. Long et al. (2018) found that the incorporation of a small quantity of GO by weight of cement with a tiny amount of polycarboxylate-based ether (PCE) superplasticizer Sika TMS-YJ-1 (GO:PCE ratio 3:1) improved the compressive strength of cement mortar (cement sand ratio 1:3) where recycled fine aggregate (RFA) was used. The water/cement ratio was kept constant 0.66. The inclusion of 0.2% GO resulted in the highest improvement in flexural strength across all curing ages. When comparing the flexural strength of the RFA mortar with 0.2 % of GO addition to that of the mortar without GO, the results showed improvements of 20.0% and 47.5% at 14 and 28 days, respectively. The results suggested that the interaction

between GO and cement matrix is the possible reason for the improvement of the flexural strength [53].

An alkylammonium salt of a high molecular weight copolymer marketed under the name BYK 9076, PCE, SDS, and NSF were the materials used in *A.M. Sabziparvar et al. (2019)* investigation on the effects of addition of GO to cement paste (Fig. 2.26). When comparing the GO-modified cement paste to the plain samples, no appreciable differences were seen in the flexural strength [55].

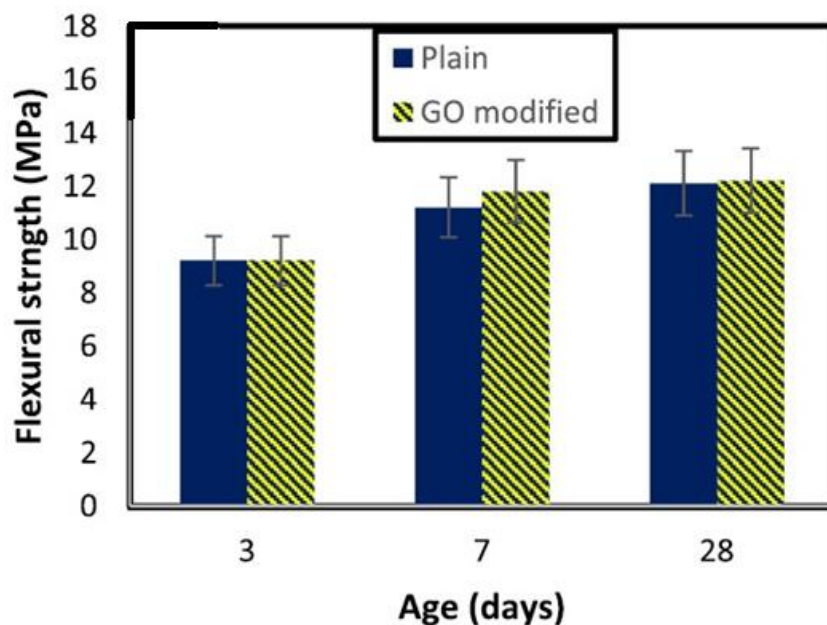


Fig. 2.26: Flexural strength of GO modified cement paste with 0.04% of GO at different curing ages (A.M. Sabziparvar 2019).

H. Peng et al. (2019) examined the flexural strength behaviour of cement-sand mortar with small amount of GO (0%, 0.01%, 0.03%, and 0.05% by weight of cement) added and a varied water/cement ratio (w/c 0.3, 0.35, 0.4, 0.45, and 0.5) with 0.2% of PCs by weight of cement (Fig. 2.17a and 2.17b). The maximum enhancement was noted by 21.86% with 0.03% GO addition by weight of cement, compared to the control sample. The results suggested that GO absorbs water, reducing cement hydration. Adjusting the w/c ratio can enhance hydration by

providing more free water. Conversely, a higher w/c ratio promoted GO dispersion. Additionally, as a nanomaterial, GO may fill micropores, reinforcing the mortar's structure [56].

A study by *B. M. Chufa et al.* (2020) focused on reduced graphene oxide (rGO) in structural cement concrete. The rGO dosage was varied from 0.1% to 5% and the water/cement ratio was kept constant at 0.46. For the purpose of developing a uniform solution, rGO is suspended in distilled water and sonicated for 3 hours to prepare the rGO-concrete composites. In comparison to the control, the results demonstrated that the 0.5% rGO inclusion increased the flexural strength by 51% after 28 days. Flexural strength increased with further rGO addition in comparison to control, although it remained lower than that of concrete treated with 0.5% rGO. The cement composite's microstructure may have been improved by the addition of rGO nanoparticles, possibly leading to an increase in strength [59].

Pyrex glass (PG) and GO (0.02% and 0.04% by weight of cement) were used by *J. Luo et al.* (2021) to study the ASR of cement-sand mortar. 25% and 50% by weight of PG was substituted for fine aggregate, such as tuning sand. For all mixes, the sand-cement mass ratio was fixed at 2.25 and the water/cement ratio was kept constant at 0.47. It was found that introducing GO improved the flexural strength of the GO-modified cement-sand mortar in both scenarios—with and without PG. The highest enhancement was observed around 24% with 0.04% GO without PG added, as compared to the control sample. Introducing PG instead of sand improved the flexural strength of cement mortar compared to the control sample, but it was still lower than the 0.04% GO added sample. The result suggests that small amounts of GO enhance mechanical strength by promoting nano-nucleation and interlocking effects [60].

The flexural strength of GO-modified cement-sand mortar was investigated by *C. Liu et al.* (2021) using SF, FA, and PC (Fig. 2.27). The GO dosage varies by 0.00%, 0.01%, 0.03%,

0.05%, and 0.07% and the water/cement ratio was kept constant at 0.4. Table 2.2 presents the elemental analysis of GO that was used throughout this study. The result of the flexural strength test result indicated that with the inclusion of a small amount of GO, the flexural strength increased significantly up to 0.05% compared to the control sample. The maximum enhancement was observed by 16% with the addition of 0.05% GO after 28 days. The result indicated that the GO can enhance the microstructure and promote cement hydration [40].

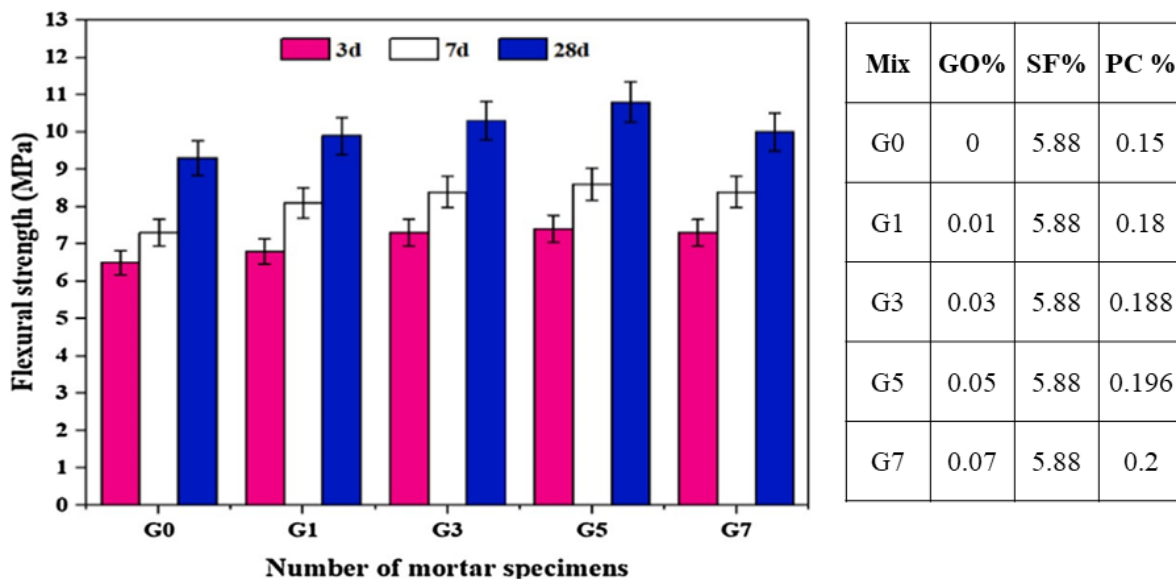


Fig. 2.27: Flexural strength of GO modified cement mortar with SF, PC, FA at different ages (C. Liu et al. 2021).

The flexural strength of cement-sand mortar incorporating GO and TiO₂-rGO was investigated by *X. Qi et al. (2021)* and reported that the flexural strength increased compared to both mixes compared to the control (Fig. 2.28). For each mix, the water-to-cement ratio was maintained at 0.42 and the cement-to-sand ratio was set at 1:3. GO and TiO₂-rGO concentrations were taken to be 0.01%, 0.03%, and 0.05% of the cement's weight. The highest enhancement was found to be 11% and 24% for the addition of GO (0.03%) and TiO₂-rGO (0.03%), respectively, after 28 days of curing, as compared to the control sample. Growing nuclei for cement mortar

hydration, which is advantageous for creating dense structures, may have contributed to the strength increase [61].

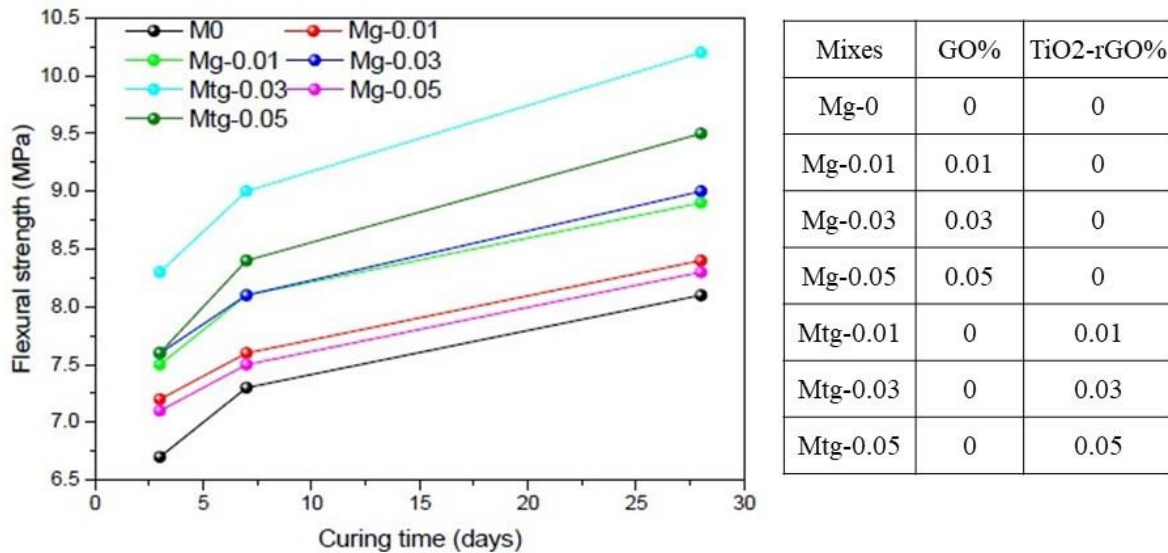


Fig. 2.28: Flexural strength of cement mortar with GO and TiO₂-rGO at different curing ages (X. Qi et al. 2021).

P. Vasudevareddy et al. (2022) found that at all curing ages, the flexural strength of cement-sand mortar was enhanced by the addition of GO combined with a modest quantity of nano-silica, as compared to the control sample (Fig. 2.29). The amount of GO dosages nano-silica varies from 0.03%, 0.05%, 0.07%, and 0.09% by weight of cement. The percentage of nano silica was used 1.5%, 3%, 4.5%, and 6%. The cement-sand ratio was 1:3 and the water/cement ratio was kept constant throughout the experimental study. There was a maximum enhancement by 13% compared to the control sample for 0.07% of GO addition with 4.5% nano-silica by weight of cement after 28 days of cure [63].

According to *A. Bagheri et al.* (2022), the flexural strength of GO modified cement mortar is higher than the control sample at 7 days and 28 days of curing ages (Fig. 2.30). the dosage of GO varied as 0.01%, 0.03%, and 0.05% by weight of cement. The cement-sand ratio was fixed at 1:1.15, and the water/cement ratio was kept constant at 0.45. The properties of GO are presented in Table 2.8. The maximum enhancement was observed by 57% compared to the

control after 28 days of curing. The structural refinement of GO-reinforced cement composites may be the root cause of the strength improvement [65]. Nucleated GO nanosheets have the ability to fill up matrix pores and reduce the volume of big pores [31,66].

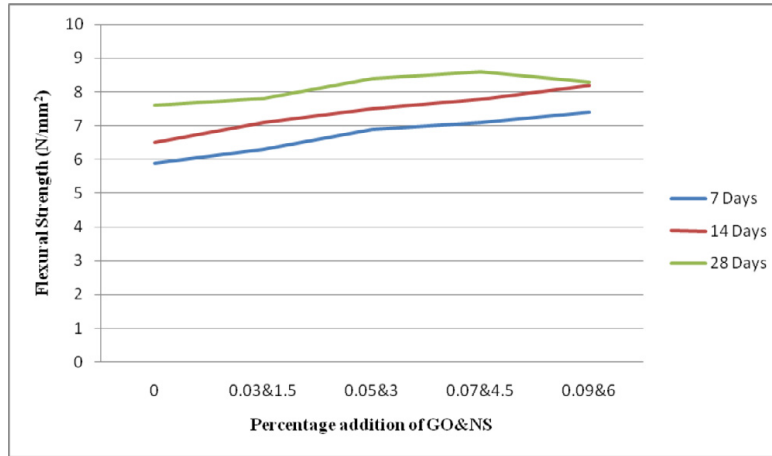


Fig. 2.29: Flexural strength behaviour of GO modified cement mortar with nano-silica (P. Vasudevareddy et al. 2022).

Table 2.8: Properties of GO nanosheets.

Properties	Purity (%)	Density (kg/ m ³)	Aspect ratio	Surface area (m ² kg ⁻¹)
Values	99.9	2.2 x 10 ³	1000	3.5 ×10 ⁵

According to Z. Cheng *et al.* (2023); the flexural strength of concrete increased with the addition of a small amount of GO with increases in curing ages (Fig. 2.31). the dosages of GO varied by 0.01%, 0.03%, and 0.05% by weight of cement. GO was dissolved in distilled water and treated with a 300W ultrasonic cleaner for 60 minutes to achieve dispersion. The maximum enhancement was observed with the addition of 0.03% of GO by 17.38%, 12.73%, 16.35%, and 18.05% at 3 days, 7 days, 14 days, and 28 days of curing ages, respectively. Further, addition of more amount of GO such as 0.05%, reduced the flexural strength. The enrichment

of the C element in high GO content makes it difficult for it to be properly distributed into cement-based products, which lowers the mechanical characteristics [67].

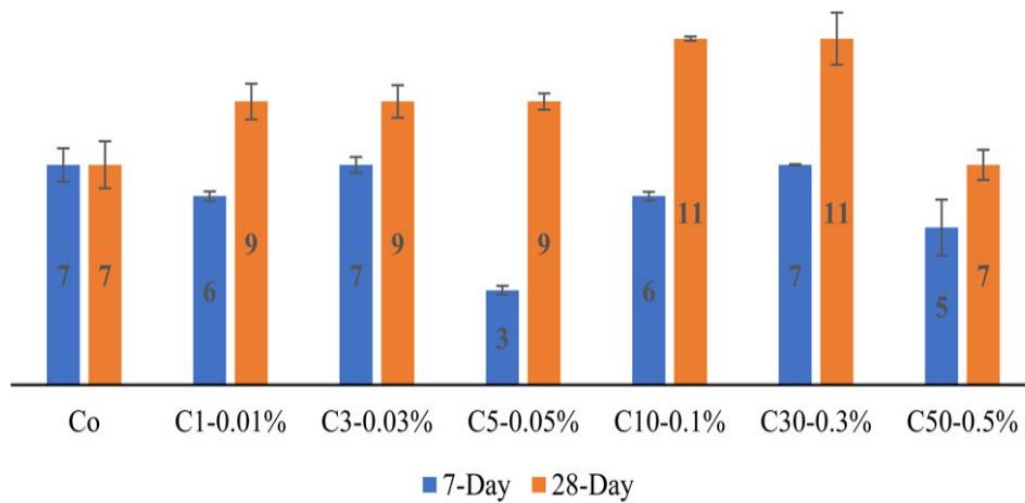


Fig. 2.30: Flexural strength of GO modified cement mortar at different curing ages (A. Bagheri et al. 2022).

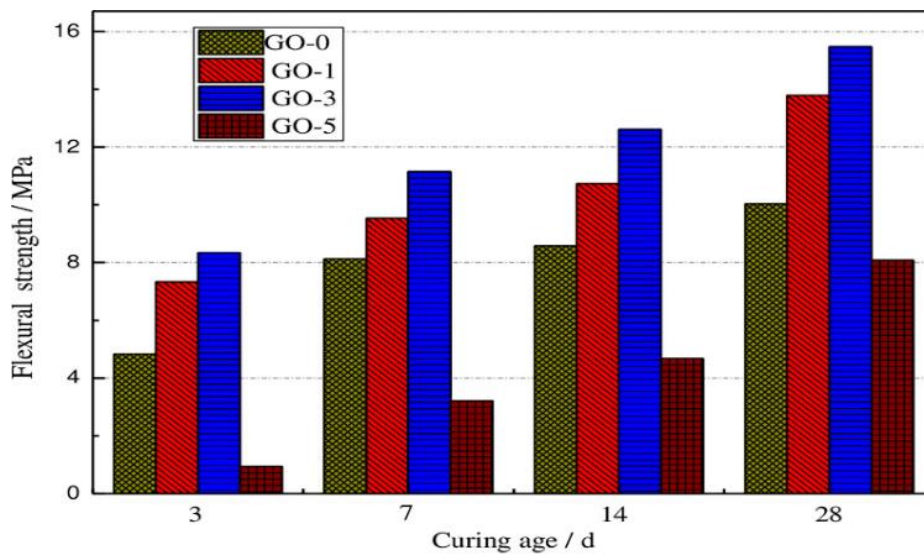


Fig. 2.31: Flexural strength of concrete with different percentages of GO (Z. Cheng et al. 2023).

2.4.5 Young modulus (E value)

The ratio of stress to strain within the elastic limit is known as the Young's modulus, and it indicates the stiffness or resistance of cement composites to deformation under stress. The

rigidity of cement particles and the reinforcing qualities of other elements like fibers or aggregates cause cement composites to generally have high Young's modulus. It is a crucial characteristic in structural engineering and construction that measures the capacity of a material to bear compressive or tensile stresses without permanent deformation. A brief overview of the modulus of elasticity of GO modified cement composites is provided in this section that is related to the present study. It may be mentioned that there is a very few literature available on the E values of GO modified mortars.

S. Han et al. (2022) measured the dynamic modulus of elasticity of cement mortar by Dynamic Young's modulus measurement equipment with the addition of 0.1% to 0.03% of GO by weight of cement (Fig. 2.32). the cement-sand ratio mortar was taken 1:3, and water/cement ratio was kept constant at 0.5. The results of this experimental study indicated that the addition of GO does not influence at normal temperatures such as at 20°C, it is almost similar to the control. But at higher temperatures, GO modified showed a better result than the control [68]. *N. Bheel et al. (2023)* measured the modulus of elasticity of cement mortar using GO and oil-coated polyvinyl alcohol (PVA) according to ASTM C469 (Fig. 2.33). The GO dosage varied as 0.05%, 0.065%, and 0.08% by weight of cement and PVA fibre volume fraction at 1%, 1.5%, and 2%. The cement-sand ration was takes as 1:1.2 and the water/cement ratio was kept constant at 0.66. The result indicated that the addition of GO with PVA increased the elastic modulus of cement mortar with respect to the control. The maximum enhancement was noted by 33.9% compared to the control, with the addition of 0.05% of GO with 1% of PVA. The enhancement of the Young Modulus is of cement composite is possible due to the presence of GO and PVA produced the more compact and tough hardened cement matrix and lead to enhances the E-value [69].

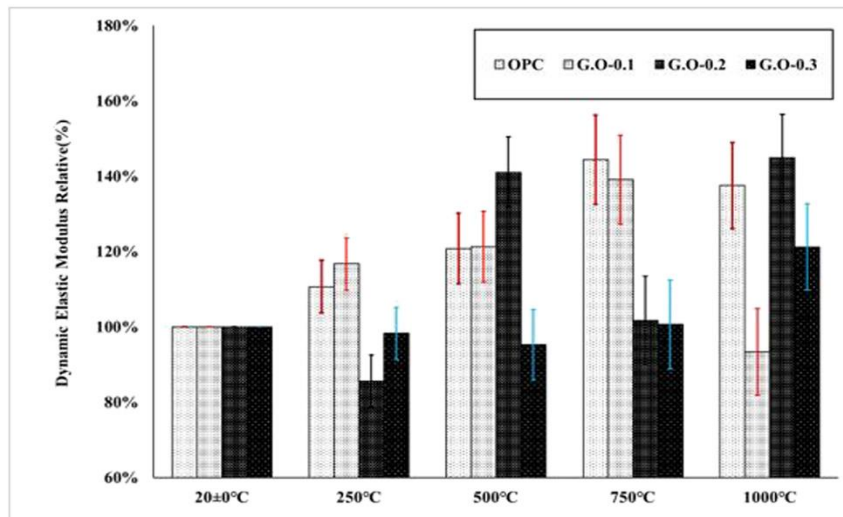


Fig. 2.32: Dynamic elastic modulus relative (%) at different temperatures (S. Han et al. 2022).

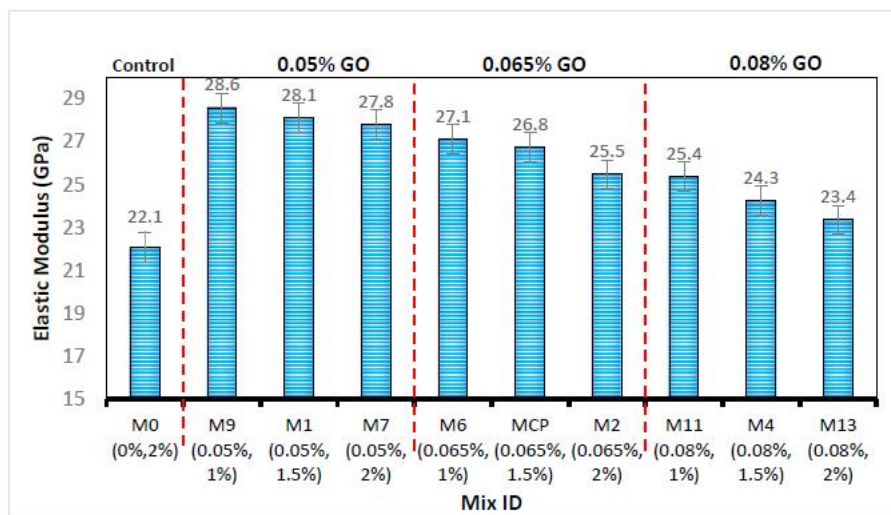


Fig. 2.33: Modulus of elasticity of cement mortar with GO and PVA (N. Bheel et al. 2023).

2.4.6 Durability

In the process of developing cement and concrete composites, durability is the crucial goal that is attracting the attention of scientists, engineers, and technicians worldwide. The service and safety of structures depend greatly on the durability of cement and concrete composites. It also helps to minimize maintenance expenses and resource waste that arises from inadequate durability in a structure's latter stages [70]. This section provides a brief review of the durability of GO-modified cement composites that is related to the current study.

2.4.6.1 Water absorption

The amount of water absorbed under specific conditions can be determined through water absorption. This test provides important information on the material's water absorption capacity, which is essential to comprehending its ability to adapt to environmental variations and durability.

G.T. Shamanth et al. (2017) used the sorptivity test to investigate the durability such as to measure the water absorption rate of the GO-modified cement mortar (GO=0.1% by weight of cement). The result showed that the primary absorption rate of the GO-modified cement-sand mortar (up to 24 hours) and secondary absorption rate (up to 9 days) were found to be comparable to those of the control sample [71].

J. Luo et al. (2021) used Pyrex glass (PG) and GO (0.02% and 0.04% by weight of cement) to investigate the durability through a water absorption test. Fine aggregate, such as tuning sand were 25% and 50% replaced by PG by weight (Fig. 2.34). The results indicated that the average water absorption of the GO modified cement-sand mortar with 0.04% of GO is lower than that of the control, with the exception that the average water absorption at 1-hour soaking time is 2.53% higher than the average water absorption at the same soaking time. The total water absorption of the GO modified cement mortar with 0.04% GO along with soaking time was steadily higher than that of the baseline without GO [60]. The surface of the cured GO modified mortar specimen will probably still have a large number of open holes. The GO dispersed in the hydration texture surrounding the pore is hydrophilic by nature and will adhere to many water molecules, leading to substantially greater total water absorption during the initial soaking [72,73].

X. Qi *et al.* (2021) studied the durability of cement mortar with GO and TiO₂-rGO through water absorption test by the standard test method proposed by Bamforth (Fig. 2.35). The results indicated that while the capillary water absorption of each sample increases with time, the capillary water absorbability of the samples gradually decreases. Additionally, cement mortars containing GO or TiO₂-rGO have significantly lower water absorbability than control samples. The water absorbability of cement mortar tended to decrease with the GO content increased. The lowest rate of water absorption was noted with the addition of 0.03% GO. This behaviour is also observed in the cement mortar samples that were combined with TiO₂-rGO. The possible reason for the low absorbability is the less amount of pore volume present in GO and TiO₂-rGO treated cement composite [61].

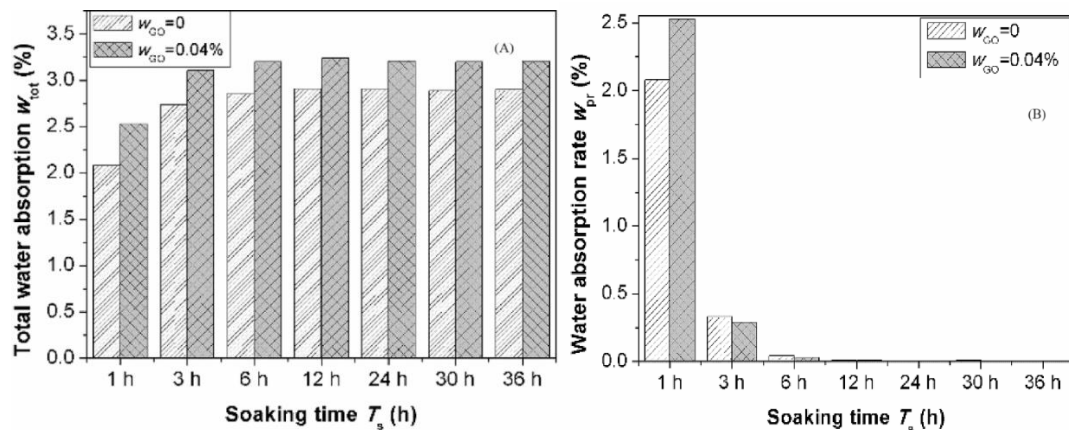


Fig. 2.34: Water absorption curve of GO modified cement-sand mortar along with soaking time, (A) total water absorption (w_{tot}), and (B) average water absorption (w_{pr}) (J. Luo et al. 2021).

A. Bagheri *et al.* (2022) studied the durability of cement mortar with GO by sorptivity test. The sorptivity test results showed that the addition of GO reduced the both initial (up to 6 hours) and final (up to 7 days) rate of water absorption (Fig. 2.36). The specimen that contained 0.03% GO performed the best in terms of initial and secondary absorption rates, reduced up to 88% and 66% compared to the control sample, respectively. The results suggested that the low water absorption could be attributed to the homogenous and uniform microstructure [65].

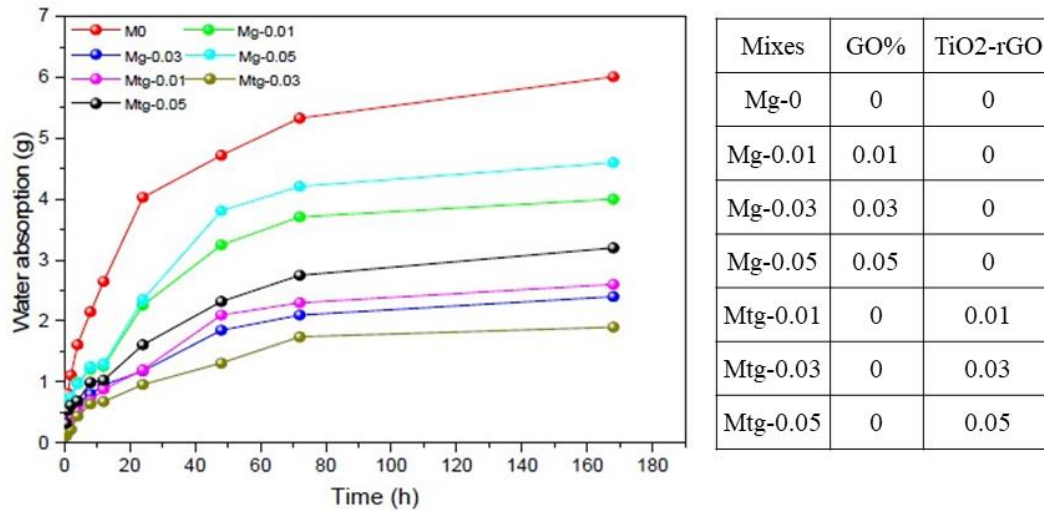


Fig. 2.35: Water absorption curve of cement mortar with GO and TiO₂-RGO at different (X. Qi et al. 2021).

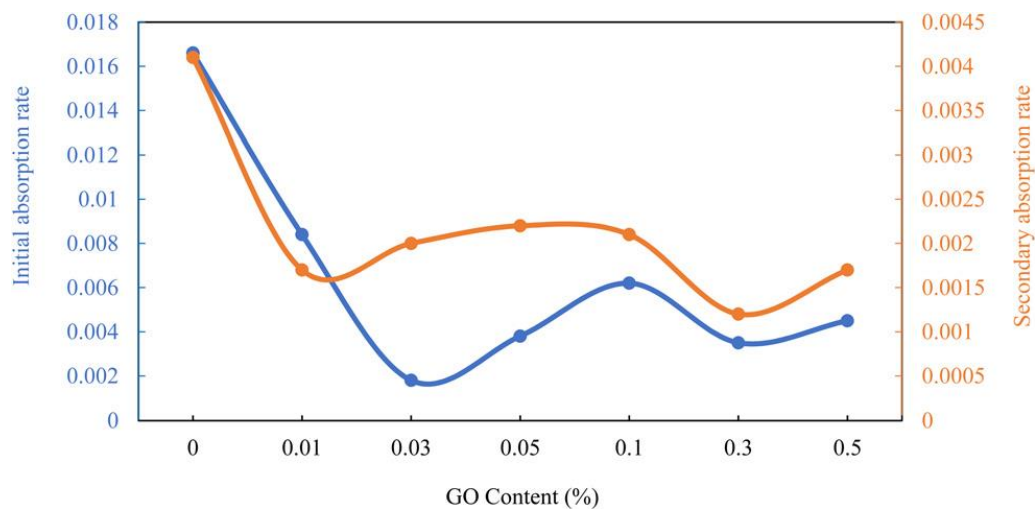


Fig. 2.36: Sorptivity test results of GO modified cement-sand mortar (A. Bagheri et al. 2022).

2.4.6.2 Rapid chloride ion penetration test (RCPT)

The resistance to chloride ion penetration is determined through the Rapid Chloride Permeability Test (RCPT). The ability of concrete to resist the penetration of chloride ions is shown electrically by RCPT. It additionally gives the ability to forecast the service life of concrete structures. For the purposes of durability-based quality control, a concrete specimen

is subjected to a constant voltage (V) for six hours, during which time the current that passes through the concrete is measured to determine the coulombs.

X. Qi *et al.* (2021) used the RCPT test to examine the durability of cement mortar with GO and TiO₂-rGO (Fig. 2.37). The results indicated that the chloride ion content decreased as GO increased by up to 0.03%. The chloride level reached minimum and maximum values with the addition of 0.03% and 0.05% GO, respectively. The distribution of the chloride ion content in cement mortar samples with TiO₂-rGO was similar to that of mortar samples with GO [61].

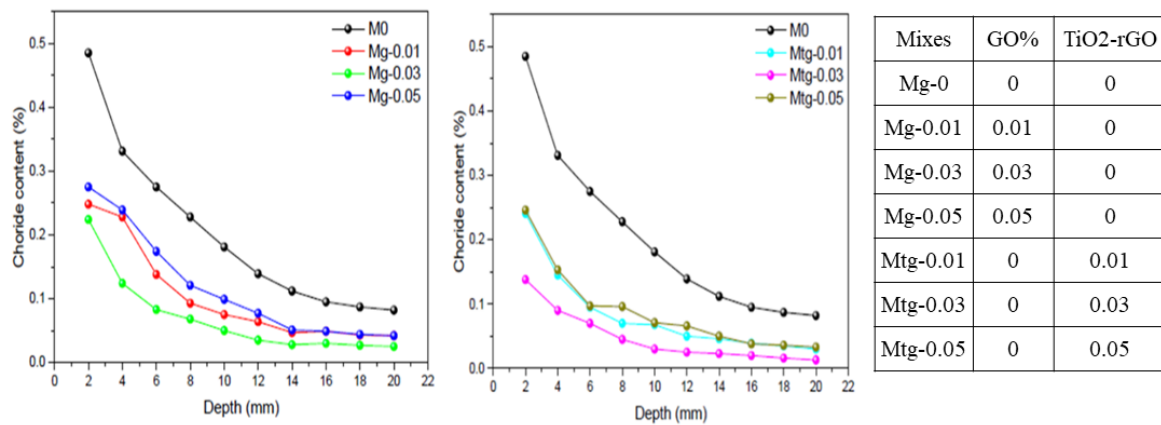


Fig. 2.37: RCPT test results of cement mortar with GO and TiO₂-RGO (X. Qi *et al.* 2021).

Z. Chen *et al.* (2023) examined the durability of concrete by RCPT test by applying different amounts of voltages. The result indicated that the depth of chloride ion penetration reduces as the amount of GO increases (Fig. 2.38). The lowest ion penetration was noted with the addition of 3% of GO by 22% with respect to the control [67].

Considering the durability test, the RCPT test was carried out by N. Bheel *et al.* (2023). The result indicated that the amount of charge passing through the mortar specimens was substantially decreased by the addition of GO nanoparticles with PVA fibre (Fig. 2.39). The microstructural densification and reduced microporous interconnectivity of the GO-modified cement mortar are responsible for the reduction in RCPT values [69].

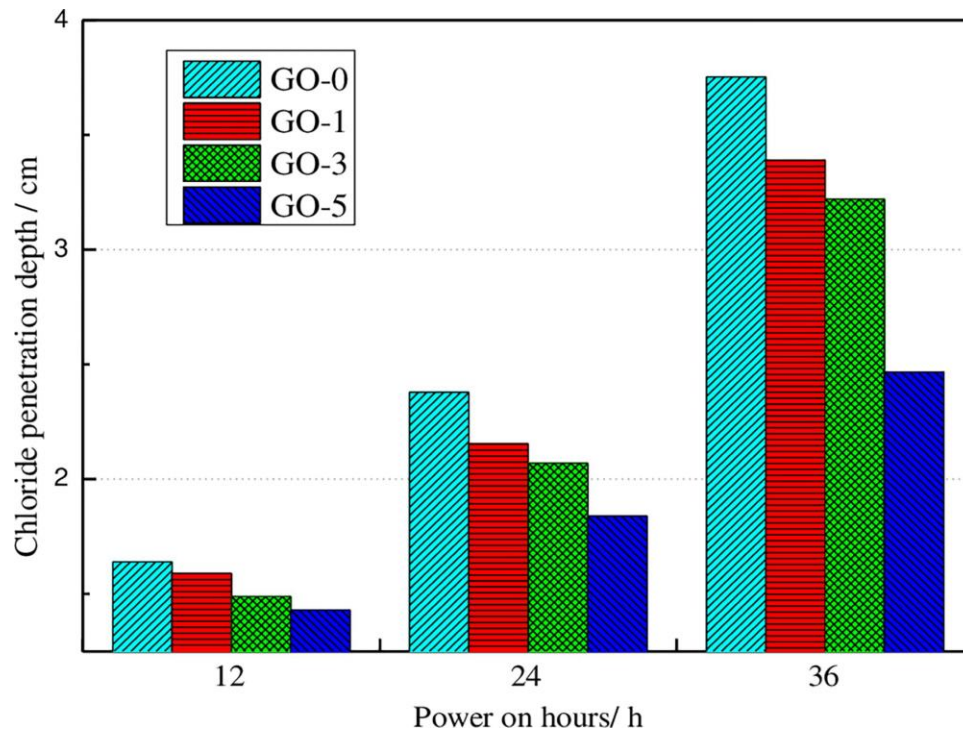


Fig. 2.38: RCPT test of concrete with different percentages of GO (Z. Cheng et al. 2023).

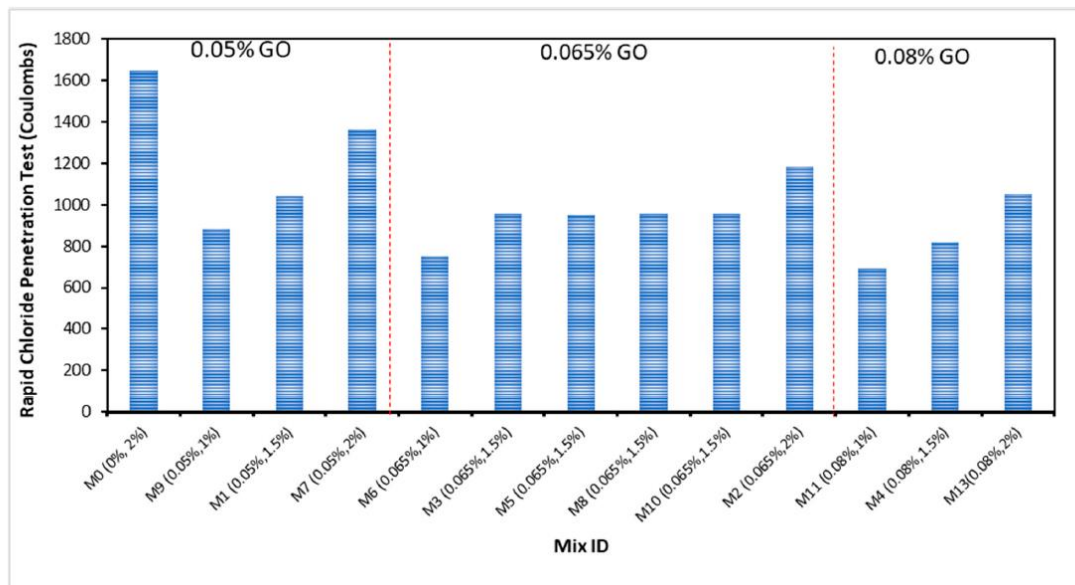


Fig. 2.39: RCPT test results of cement mortar with different percentages of GO and PVA fibre (N. Bheel et al. 2023).

2.4.6.3 Acid resistance test

The acid resistance test of cement composites assesses their ability to withstand exposure to acidic environments. This test involves immersing the cement sample in an acidic solution,

typically sulfuric acid, for a specified duration. After exposure, the sample is examined for any signs of deterioration, such as changes in weight, strength, or appearance. The test helps evaluate the durability of cement-based materials in acidic conditions, which is crucial for applications in industries like construction and infrastructure where exposure to acids may occur.

Through the use of an acid resistance test applying 0.04% GO by weight of cement, *K. Chintalapudi et al.* (2022) investigated the durability of OPC and PPC cement. PPC and GPPC specimens showed strong resistance at 3 and 7 days, but OPC and GOPC specimens showed a minor deterioration that resulted in a slight shift in colour to a yellowish/brown colour. In terms of mass loss, the GOPC specimen showed the less amount of weight loss, at 23.69%, while the OPC specimen showed the most weight loss, at 31.46%. The PPC and GPPC specimens exhibited 5.51% and 5.32% weight loss. Mechanical strength such as flexural strength showed lower by 44%, 20%, 16%, and 14% for OPC, GOPC, PPC, and GPPC samples respectively, after 28 days of acid water immersion [45].

The durability of cement-sand mortar was examined by *P. Vasudevareddy et al.* (2022) using an acid resistance test with a tiny quantity of GO and nano-silica by weight of cement. It was found that the GO modified cement mortar sample had a higher compressive strength than the control. The mass loss as a result of the acid water immersion also less than the control sample (2.40). The maximum compressive strength found with the addition of 0.07% GO with 4.5% of nano silica increased by 31% compared to the control sample, after 60 days of acid-water immersion. Minimum mass loss was also observed with the addition of 0.07% GO with 4.5% of nano silica [63].

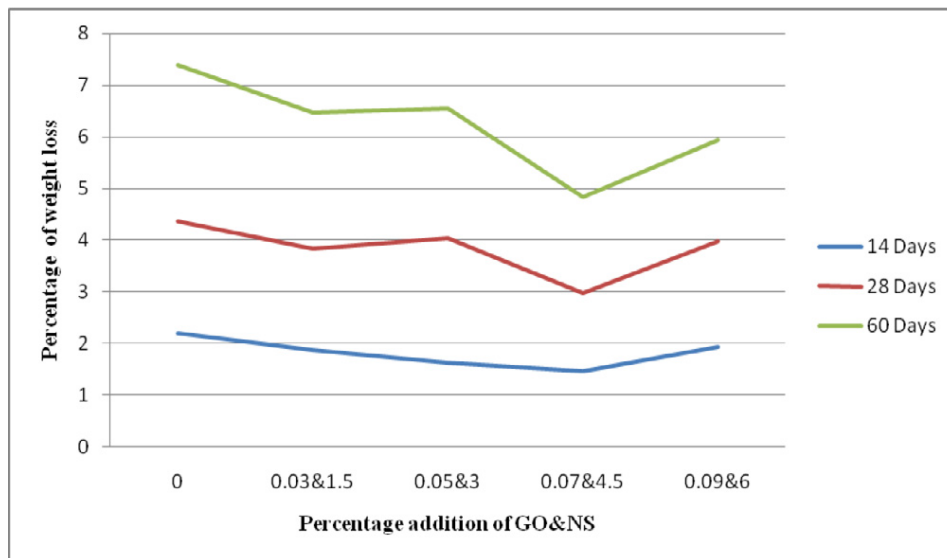


Fig. 2.40: Weight loss curve of GO modified cement mortar with nano-silica (P. Vasudevareddy et al. 2022).

2.4.7 Micro-structural analysis

Micro-structural analysis of cement composites involves examining the fine-scale structure of the material at the microscopic level. Techniques such as scanning electron microscopy (SEM), Mercury Intrusion Porosimetry (MIP), and X-ray diffraction analysis (XRD) are commonly used. This analysis provides insights into the distribution of phases, porosity, and the overall arrangement of cementitious components. Understanding the microstructure is crucial for assessing the material's properties, durability, and performance, offering valuable information for optimizing the design and composition of cement composites in construction and other applications.

2.4.7.1 Mercury intrusion porosimetry (MIP) test

The hydrated cement is an exceptionally porous substance with a constant range of pore diameters from nanometers to micrometers. Mercury Intrusion Porosimetry (MIP) is a standard procedure for researchers to use to describe the distribution of the pore sizes in cement-based materials. Even though it is a quick and straightforward indirect method, it has drawbacks when

used with materials whose pore geometry is unevenly distributed. Larger capillary pores (0.005–10mm) can be determined by MIP.

K. Gong et al. (2015) reported that the amount of gel pores ($d < 10$ nm) in the GO-cement sample was significantly higher than that of the plain cement. The amount of mercury that enters pores with a pore diameter of less than 10 nm is consistently higher in the GO cement sample, but the amount that enters pores with a pore diameter of more than 10 nm is consistently lower in the GO-cement sample. These results demonstrate that the incorporation of GO reduced the pore structure of cement paste [48].

M.M. Mokhtar et al. (2017) analysed the pore structure of cement paste with and without GONPs by MIP test (Fig. 2.41). The results indicated that the GONPs can effectively enhance the micro structural properties by decreasing pore size and increasing the compactness of the cement paste. The maximum compressive strength values were obtained with the highest concentration of GONPs (0.02% weight percent), which also produced the lowest intensity in the pore size distribution [50].

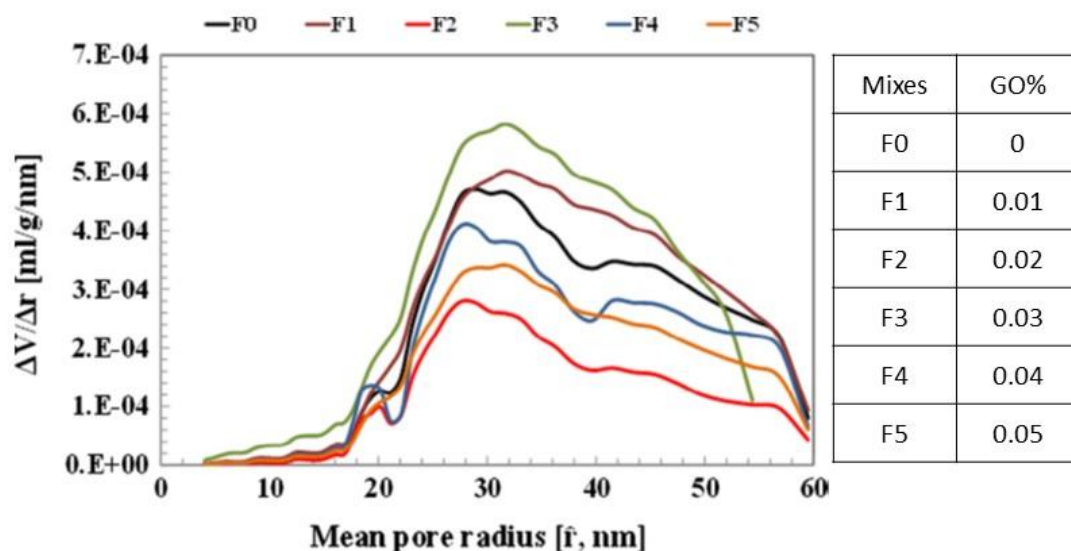


Fig. 2.41: Pore-size distribution curves of plain and GONPs modified cement paste after 28 days of hydration (M.M. Mokhtar et al. 2017).

W.J. Long et al. (2018) MIP was used to assess the porosity and pore size distribution of hardened RFA mortars with and without GO with a tiny amount of PCs (0.8% by weight of GO) (Fig. 2.42). The results demonstrated that the porosity and number of pores in mortar with varying pore size decreases with increasing GO content. The inclusion of GO may have initially accelerated the hydration process, which contributed to the higher density C-S-H gel, which could explain this alteration [53].

X. Qi et al. (2021) employed the MIP test to investigate the pore structure of cement-sand mortar with GO (GO= 0.03% by weight of cement) and TiO₂-rGO (GO= 0.03% by weight of cement). The result indicated that compared to the control, the average diameters of cement mortars containing GO and TiO₂-RGO are much smaller, with cement mortars containing TiO₂-rGO being the lowest (Fig. 2.43). The porosity of cement mortars containing GO and TiO₂-rGO decreased by roughly 26% and 40%, respectively, compared to the control. It is evident from the average pore size and porosity that TiO₂-rGO has a much greater effect than GO [61].

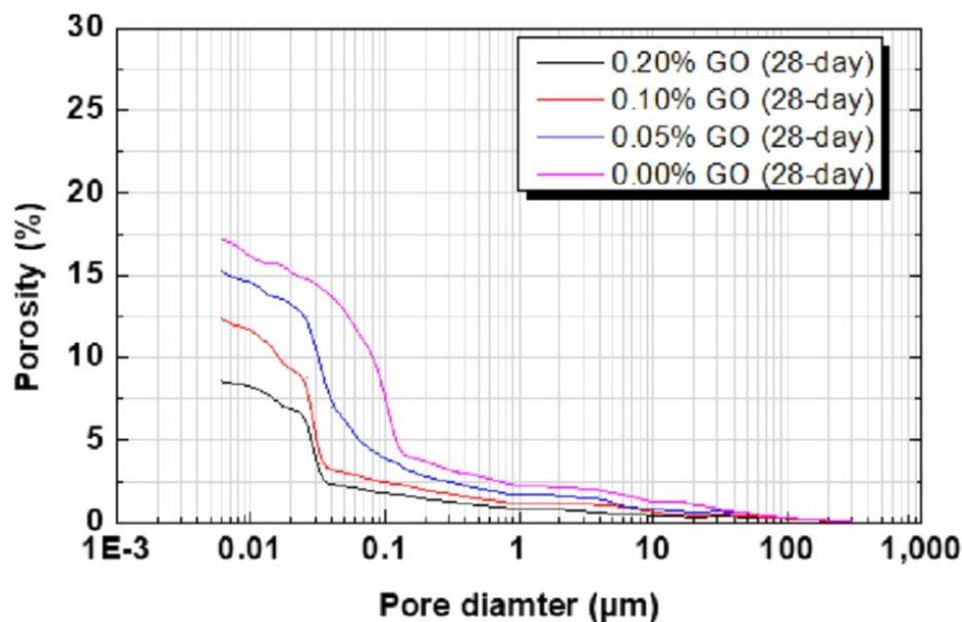


Fig. 2.42: Pore size distribution of various GO-containing RFA mortar after 28 days (W. J. Long et al. 2018).

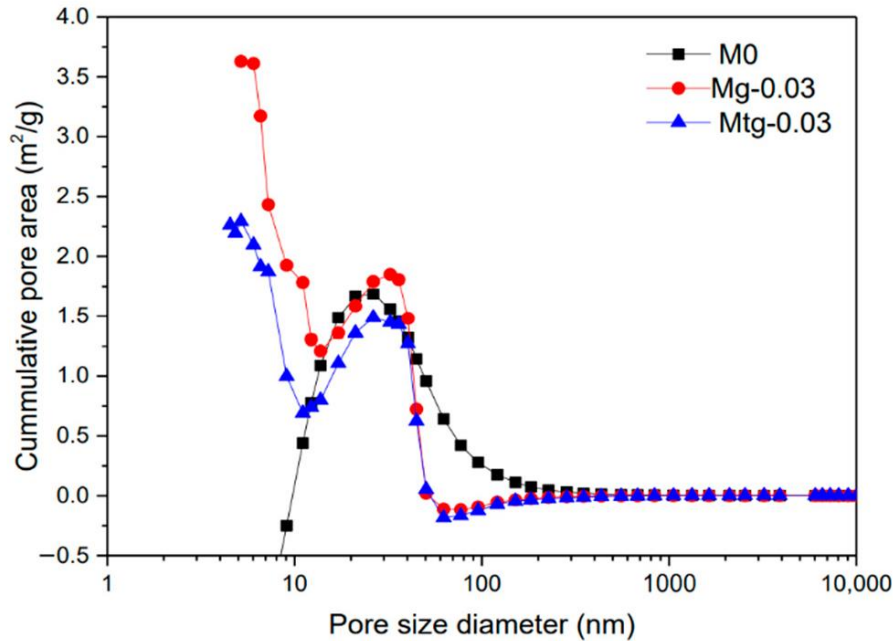


Fig. 2.43: Pore size distribution of cement mortar with GO and TiO₂-rGO (X. Qi et al. 2021).

2.4.7.2 X-ray diffraction analysis (XRD)

The basic concept of XRD analysis is the constructive interference of monochromatic X-rays with the crystalline sample. The sample is exposed to x-rays produced by a cathode ray tube, which are collimated, filtered to produce monochronic radiation, and directed at the sample. During the incident rays contact with the sample, useful interfaces are created.

L. Zhao et al. (2016) studied the crystal phase of normal cement paste and GO modified cement paste (containing 0.022% GO and 0.22% PC) by XRD analysis at 3 days, 7 days, and 28 days. At the same curing period, it was found that the intensities of the peaks corresponding to CH are higher in GO-cement composite than in plain-cement composite, indicating an increased degree of hydration [41].

The crystal phase of cement paste was studied by *H. Yang et al.* (2017) using GO dosages of 0.1%, 0.15%, and 0.2% by weight of cement (Fig. 2.44). Ca(OH)₂, dicalcium silicate (C2S), and tricalcium silicate (C3S) were discovered [7].

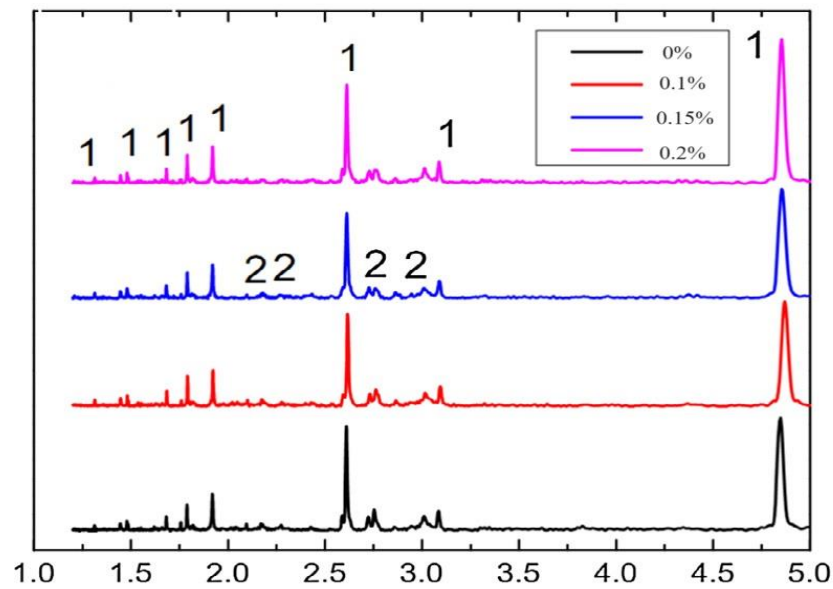


Fig. 2.44: XRD results of different GO modified cement paste, peaks are produced by $\text{Ca}(\text{OH})_2$, peaks 2 are produced by C_3S and C_2S phases (H. Yang et al., 2017).

M.M. Mokhtar et al. (2017) reported that the phases identified include the typical cement hydrates, such as calcium carboaluminate hydrate, CSH, and CH by XRD analysis of cement paste with GONPs (Fig. 2.45). Moreover, the reaction between the $-\text{COOH}$ functional groups and the C_3A phase results in an increase in calcium carboaluminate hydrate. The improved durability of the hardened cement pastes may be attributed to the rise in the hydrated phase of calcium carboaluminate [50].

S. Sharma et al. (2018) studied the crystal phase of normal GO modified FA based cement-sand mortar at 28 days (Fig. 2.46). It was evident from the results that adding GO to an FA-based cementitious matrix modified the basic crystallization rates. Peak intensities at $2\theta = 18.2, 34.2, 47.1, \text{ and } 50.1$ indicated an enhancement in the rate of production of C-H crystals due to GO addition, compared to the control. Two possibilities were suggested by the comparatively increased rate of C-H production brought about by the addition of GO. First, as GO content

risers, calcium silicate hydration improves. Secondly, in pozzolanic reactions, FA particles do not easily consume up C-H crystals [52].

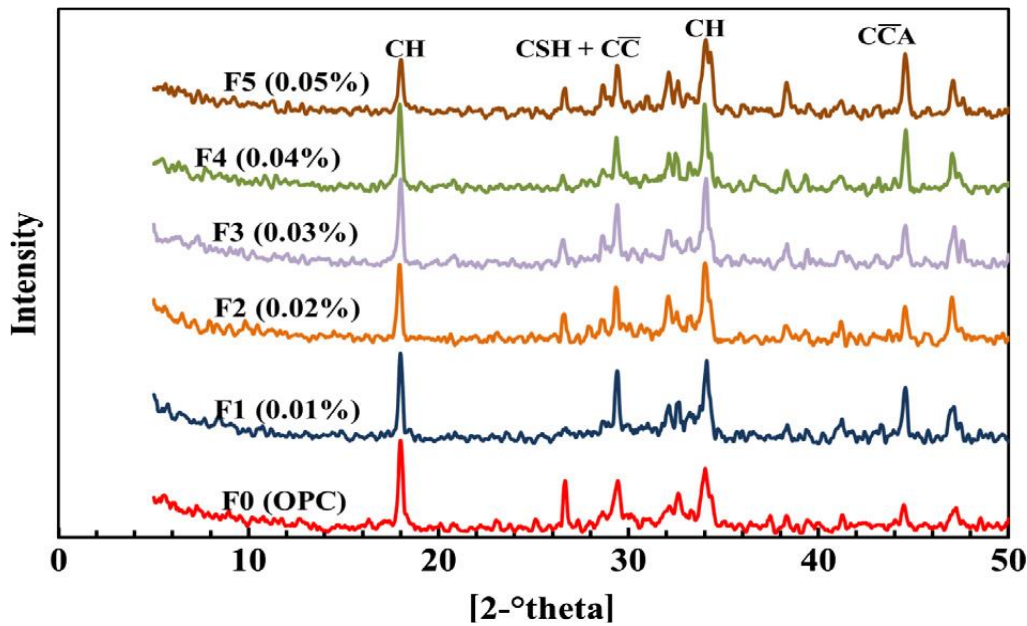


Fig. 2.45: XRD pattern of cement pastes with different concentrations of GONPs (M.M. Mokhtar et al. 2017).

The crystal phase of GO-modified cement paste (with 0.02% of GO by weight) has been studied by *G. Xu et al.* (2019) utilising the XRD pattern at 28 days. The XRD analysis results clearly demonstrated that with the addition of GO to the cement paste, the intensities of the CH peaks slightly decreased [54]. However, the results conflict with some other studies that concluded that the CH peaks' intensities increased with GO-modified OPC paste [74–76].

T. Janjaroen et al. (2022) evaluated the crystal phase of GO-modified cement paste using an XRD pattern at 28 days. A large diffraction peak that corresponded to the crystalline planes of (002) with a calculated d-spacing of 0.810 nm [77] emerged at 11.16° in the XRD pattern of GO sheets. Subsequently, the XRD patterns of GMT-0 (0% GO), GMT-0.01 (0.055% GO), GMT-0.03 (0.165% GO), GMT-0.05 (0.275% GO), and GMT-0.1 (0.555% GO) composites can identify the phases of the common cement hydrates, such as silicon dioxide (SiO₂), calcium

hydroxide ($\text{Ca}(\text{OH})_2$; Si), and ettringite ($\text{Ca}_6(\text{Al}(\text{OH})_6)_2(\text{SO}_4)_3 \cdot 26\text{H}_2\text{O}$; CA) [78]. The XRD data confirms the cement mortar's pure phase [79].

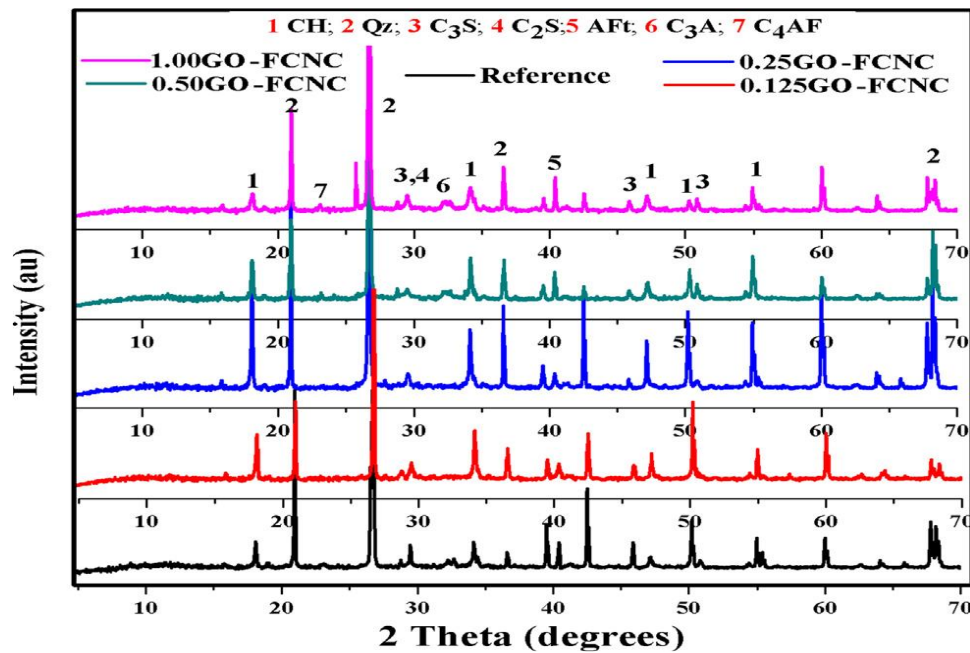


Fig. 2.46: XRD pattern of GO modified FA based cement mortar after 28 days curing (S.

Sharma et al. 2018).

2.4.7.3 Scanning electron microscopy (SEM) analysis

In the test procedure known as scanning electron microscopy (SEM), an electron beam scans a sample to produce a magnified image for analysis. When an electron interacts with a sample, it generates an immense amount of kinetic energy that emerges in different signals.

S. Sharma, and N. C. Kothiyal (2015) observed by SEM analysis that the addition of GO with a small amount of PCs, significantly increases the compressive strength of cement-based materials by regulating their microstructure and the quantities and forms of cement hydrates. Crystals can have a variety of morphologies, including columnar, platy, tentacular, and polyhedral [80].

L. Zhao et al. (2016) compared the micro-structural images of normal cement paste (Fig. 2.47 (a), and 2.47 (b)) and GO modified cement paste with small quantity of PC (Fig.2.47 (c), and

2.51 (d)) by SEM analysis. It was observed that the addition of GO, made the cement matrix more homogeneous and an abundance of flake-like CH crystals from precipitating is prevented. Furthermore, the formation of large capillary holes prevents free water from evaporating.

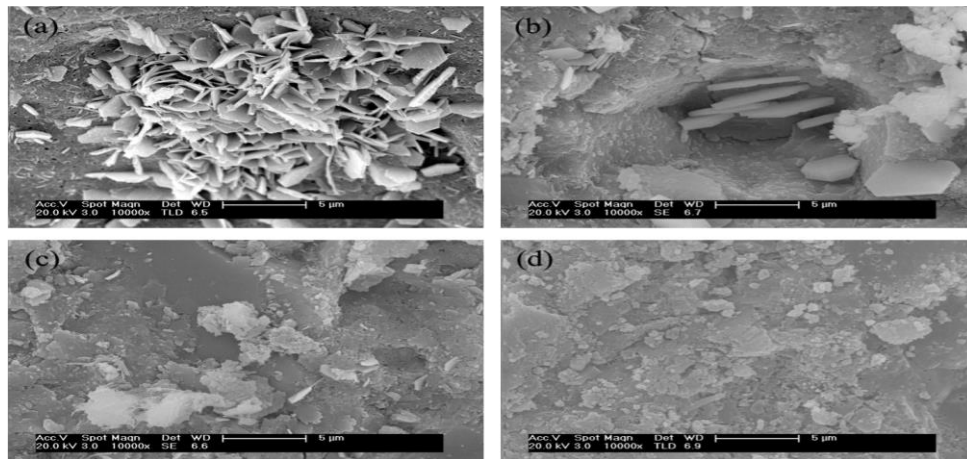


Fig. 2.47: SEM image of GO modified cement mortar (at 7 days) with small quantity of PC (L. Zhao et al., 2016).

SEM was utilized by *H. Yang et al.* (2017) to examine the microstructure of cement paste that has been treated with 0.2% of GO, by weight of cement (Fig. 2.48), and the agglomeration of GO into cement paste was observed. Even though aggregations hardly ever occurred, the fact that they were present in these samples suggests that GO's dispersion may have been increased even more to further enhance the mechanical properties. Moreover, crystals with needle-like shapes developed in the cement-based composite [81].

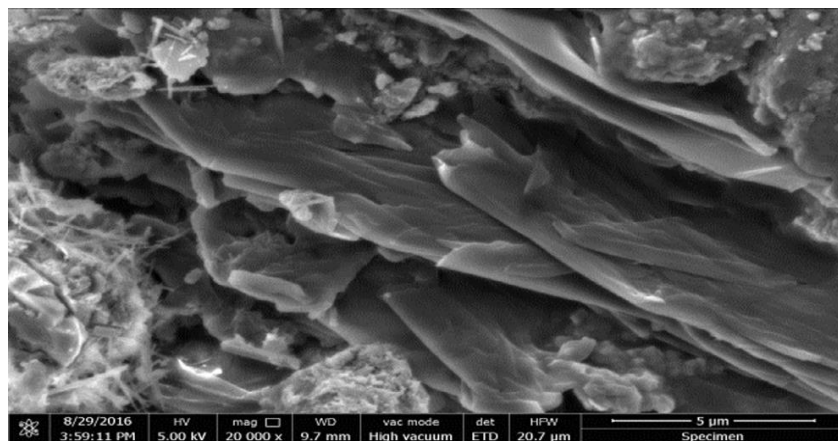


Fig. 2.48: SEM image of cement paste containing 0.2% of GO (H. Yang et al. 2017).

Z. Lu et al. (2017) utilized SEM analysis for a microstructural study of cement paste with and without GO for the period of 10 min. hydration. It observed that while some cement particles had started hydration but some are not. However, through the addition of GO, the cement particles' surfaces can be covered, bringing together the separate phases. More significantly, it was observed that the large amount of hydrated cement particles in GO modified cement paste compared to plain cement paste [35]. Overall, the GO modified cement paste exhibits more compact microstructures, faster early hydration, and comparatively higher crystal development when compared to the plain cement paste.

J. An et al. (2018) were used SEM to examine the microstructure of cement paste that has been treated with GONF (0.05% by weight of cement). From SEM images, the needle shaped ettringite that extends into the pores is easily visible [36].

S. Sharma et al. (2018) conducted FE-SEM investigations following varying curing durations of 7, 14, and 28 days to examine the impact of changes in GO concentration such as 0.5%, and 1.0% by weight of cement, on the microstructural behaviour and surface morphology of FA-based cement-sand mortars. As observed, the inclusion of GO nano particles causes the C-S-H gel to become tight and adherent because of the chemical bonding that may occur between oxygen-containing functionalities and C-S-H or C-H products, as well as the nanofiller effects of functionalized graphene sheets. For higher concentrations of GO, it was observed that GO particles were agglomerated and difficult to dispersion [52].

According *W. Long et al.* (2018); the interface between the paste and RFA in mortars containing GO is seen to be denser than in mortars without GO, as is evident from the observation. Because the interface was filled with more highly dense-hydrated products and GO itself, it is challenging to determine the diameter of the weak zone [53].

H. Peng et al. (2019) studied the microstructure of GO modified cement sand mortar with 0.2% of PCs by weight of cement (Fig. 2.49). The entire cement particle surface had fine foil-

like C-S-H gel (1 μm or so) with 0.01% GO distributed throughout. The C-S-H gel and plate-like C-H were densely interwoven to form a continuous structure. There were no noticeable big hydrated crystals or pores. The structure of the cured cement paste was significantly enhanced with 0.03% of GO. The C-S-H gel covered the surfaces of other crystals and cement particles in a nice order and was more uniform and compact. Multiple hydrates interacted to form a thick, homogenous structure with 0.05 % GO addition. [56].

S.C. Devi and R.A. Khan (2020) analysed the micro-structural of cement composite with/without GO by using SEM analysis. The results indicated that the addition of a small amount of GO improved the microstructure of concrete due to the presence of the densified hydrated crystal and lesser pore volume [82].

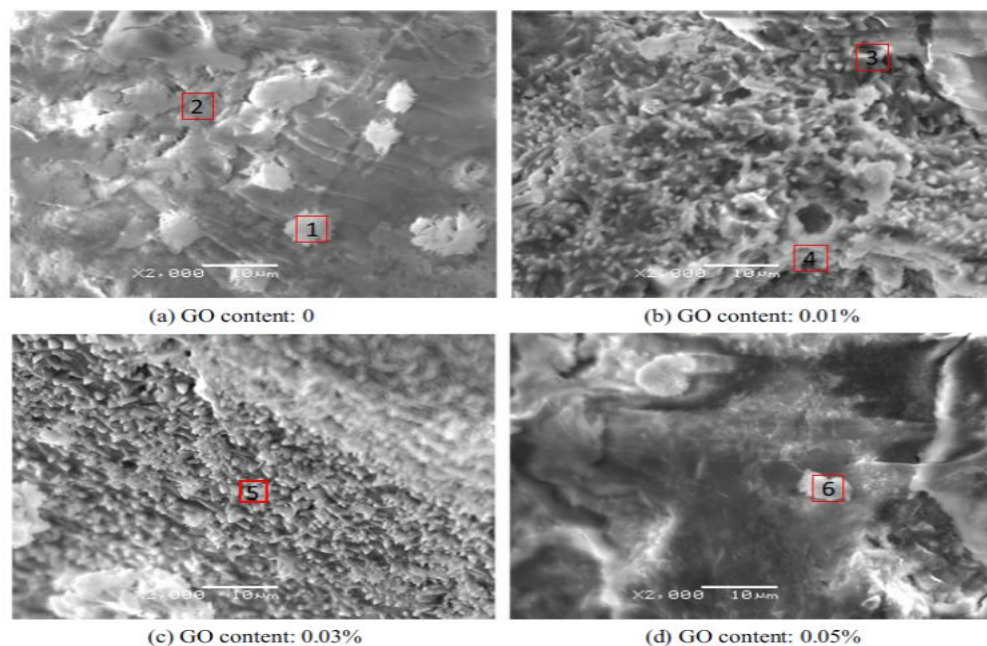


Fig. 2.49: SEM images of cement mortar with different percentages of GO (H. Peng et al. 2019).

S. Han et al. (2022) used the SEM analysis to examine the cement hydration crystal with the addition of 0.1% and 0.2% of GO at 28 days of curing age. The intensity of flower-shaped needle-like crystal-like structures was mostly influenced by the GO content, as seen by the

SEM image of the cement paste's microstructure. The flower-shaped needle-like crystal-like crystalline became thinner with the increase of GO concentration [68].

N. Bheel et al. (2023) reported that the inclusion of GO as a template to regulate the creation of cement hydration crystal products, smooth and compact the hardened cement paste's structure, and increase its strength. The porosity of the microstructure was greatly decreased by the addition of the 0.05% GO 1% of PVA. The capacity of GO to fill voids and accelerate the hydration reaction, which promotes the creation of several layers of hydration product, is the factor that produces the lower porosity [69].

2.5 Aim of The Present Study

Based on the review of literature on the GO modified cement composite, a thorough experimental programme has been adopted on the effects of GO addition on cement mortar using (a) Ordinary Portland Cement (OPC) and (b) fly-ash based cement, such as Portland Pozzolana Cement (PPC), with two different cement-sand ratio mortar mixes (1:2 and 1:3 by weight), Most of the previous literature is on the effect of GO on Ordinary Portland Cement. There is almost no literature on the effect of GO on fly ash based cement, Portland Pozzolana Cement. Thus, a comprehensive study on the addition of GO is needed. The basic aim is to disperse GO in water without any additives, including dispersing agents, chemicals, and minerals, and mixed with OPC and PPC based cement-sand mortar. The details of the study are as follows:

- To disperse the GO nanoparticles in water without any depressing agents by using a probe sonicator.
- To develop the GO modified cement-sand mortar with different cement-sand ratios (1:2 and 1:3) by using two types of cement such as Ordinary Portland Cement (OPC) and Pozzolanic Portland Cement (PPC) with varying dosages of

GO, ranging from 0.03% to 0.06% by weight of cement without use of any superplasticizers.

- To study the fluidity study of GO modified cement-sand mortar.
- To study the mechanical strength properties such as compressive strength, split tensile strength, flexural strength, and young modulus of (E value) cement mortar with and without GO.
- To study the durability properties in terms of RCPT, sorptivity, and acid resistance of GO modified cement-sand mortar.
- Pore size distribution study of GO modified cement-sand mortar by Mercury Intrusion Porosity (MIP) test.
- Morphological study of GO modified cement-sand mortar by using Field Emission Scanning Electron Microscopy (FESEM) with Energy Dispersive X-Ray (EDX) and X-Ray Diffraction analysis (XRD).

References

- [1] S.K. Tiwari, R.K. Mishra, S.K. Ha, A. Huczko, Evolution of Graphene Oxide and Graphene: From Imagination to Industrialization, *ChemNanoMat* 4 (2018) 598–620. <https://doi.org/10.1002/cnma.201800089>.
- [2] H.-P. Boehm, E. Stumpp, Citation errors concerning the first report on exfoliated graphite, *Carbon* 45 (2007) 1381–1383. <https://doi.org/10.1016/j.carbon.2006.12.016>.
- [3] A. De Adhikari, R. Oraon, S.K. Tiwari, N.K. Jena, J.H. Lee, N.H. Kim, G.C. Nayak, Polyaniline-Stabilized Intertwined Network-like Ferrocene/Graphene Nanoarchitecture for Supercapacitor Application, *Chem Asian J* 12 (2017) 900–909. <https://doi.org/10.1002/asia.201700124>.
- [4] T. Wang, D. Huang, Z. Yang, S. Xu, G. He, X. Li, N. Hu, G. Yin, D. He, L. Zhang, A Review on Graphene-Based Gas/Vapor Sensors with Unique Properties and Potential Applications, *Nanomicro Lett* 8 (2016) 95–119. <https://doi.org/10.1007/s40820-015-0073-1>.
- [5] D.Yu. Kornilov, S.P. Gubin, Graphene Oxide: Structure, Properties, Synthesis, and Reduction (A Review), *Russian Journal of Inorganic Chemistry* 65 (2020) 1965–1976. <https://doi.org/10.1134/S0036023620130021>.
- [6] K.S. Novoselov, A.K. Geim, S. V. Morozov, D. Jiang, M.I. Katsnelson, I. V. Grigorieva, S. V. Dubonos, A.A. Firsov, Two-dimensional gas of massless Dirac fermions in graphene, *Nature* 438 (2005) 197–200. <https://doi.org/10.1038/nature04233>.
- [7] H. Yang, M. Monasterio, H. Cui, N. Han, Experimental study of the effects of graphene oxide on microstructure and properties of cement paste composite, *Compos Part A Appl Sci Manuf* 102 (2017) 263–272. <https://doi.org/10.1016/j.compositesa.2017.07.022>.
- [8] A. Abdullah, M. Taha, M. Rashwan, M. Fahmy, Efficient Use of Graphene Oxide and Silica Fume in Cement-Based Composites, *Materials* 14 (2021) 6541. <https://doi.org/10.3390/ma14216541>.
- [9] M. Muthu, N. Ukrainczyk, E. Koenders, Effect of graphene oxide dosage on the deterioration properties of cement pastes exposed to an intense nitric acid environment, *Constr Build Mater* 269 (2021) 121272. <https://doi.org/10.1016/j.conbuildmat.2020.121272>.
- [10] G. Li, J.B. Yuan, Y.H. Zhang, N. Zhang, K.M. Liew, Microstructure and mechanical performance of graphene reinforced cementitious composites, *Compos Part A Appl Sci Manuf* 114 (2018) 188–195. <https://doi.org/10.1016/j.compositesa.2018.08.026>.
- [11] A. Jiříčková, O. Jankovský, Z. Sofer, D. Sedmidubský, Synthesis and Applications of Graphene Oxide, *Materials* 15 (2022) 920. <https://doi.org/10.3390/ma15030920>.
- [12] W.C. Siaw, T. Tsuji, N. Abdul Manaf, M.F. Abdul Patah, B. Mohamed Jan, Synthesis of graphene oxide from industrial waste, *IOP Conf Ser Mater Sci Eng* 778 (2020) 012050. <https://doi.org/10.1088/1757-899X/778/1/012050>.
- [13] K. Gong, Z. Pan, A.H. Korayem, L. Qiu, D. Li, F. Collins, C.M. Wang, W.H. Duan, Reinforcing Effects of Graphene Oxide on Portland Cement Paste, *Journal of Materials in Civil Engineering* 27 (2015). [https://doi.org/10.1061/\(ASCE\)MT.1943-5533.0001125](https://doi.org/10.1061/(ASCE)MT.1943-5533.0001125).

- [14] X. Li, Y.M. Liu, W.G. Li, C.Y. Li, J.G. Sanjayan, W.H. Duan, Z. Li, Effects of graphene oxide agglomerates on workability, hydration, microstructure and compressive strength of cement paste, *Constr Build Mater* 145 (2017) 402–410. <https://doi.org/10.1016/j.conbuildmat.2017.04.058>.
- [15] Y. Shang, D. Zhang, C. Yang, Y. Liu, Y. Liu, Effect of graphene oxide on the rheological properties of cement pastes, *Constr Build Mater* 96 (2015) 20–28. <https://doi.org/10.1016/j.conbuildmat.2015.07.181>.
- [16] S. Lv, Y. Ma, C. Qiu, Q. Zhou, Regulation of GO on cement hydration crystals and its toughening effect, *Magazine of Concrete Research* 65 (2013) 1246–1254. <https://doi.org/10.1680/mac.13.00190>.
- [17] A.M. Rashad, Effect of carbon nanotubes (CNTs) on the properties of traditional cementitious materials, *Constr Build Mater* 153 (2017) 81–101. <https://doi.org/10.1016/j.conbuildmat.2017.07.089>.
- [18] Y. Wang, J. Yang, D. Ouyang, Effect of Graphene Oxide on Mechanical Properties of Cement Mortar and its Strengthening Mechanism, *Materials* 12 (2019) 3753. <https://doi.org/10.3390/ma12223753>.
- [19] X. Zhu, X. Kang, Effect of graphene oxide (GO) on the hydration and dissolution of alite in a synthetic cement system, *J Mater Sci* 55 (2020) 3419–3433. <https://doi.org/10.1007/s10853-019-04266-1>.
- [20] Y. Gao, H.W. Jing, S.J. Chen, M.R. Du, W.Q. Chen, W.H. Duan, Influence of ultrasonication on the dispersion and enhancing effect of graphene oxide–carbon nanotube hybrid nanoreinforcement in cementitious composite, *Compos B Eng* 164 (2019) 45–53. <https://doi.org/10.1016/j.compositesb.2018.11.066>.
- [21] S.C. Devi, R.A. Khan, Effect of graphene oxide on mechanical and durability performance of concrete, *Journal of Building Engineering* 27 (2020) 101007. <https://doi.org/10.1016/j.job.2019.101007>.
- [22] S.C. Devi, R.A. Khan, Effect of graphene oxide on mechanical and durability performance of concrete, *Journal of Building Engineering* 27 (2020) 101007. <https://doi.org/10.1016/j.job.2019.101007>.
- [23] L. Zhao, X. Guo, Y. Liu, Y. Zhao, Z. Chen, Y. Zhang, L. Guo, X. Shu, J. Liu, Hydration kinetics, pore structure, 3D network calcium silicate hydrate, and mechanical behavior of graphene oxide reinforced cement composites, *Constr Build Mater* 190 (2018) 150–163. <https://doi.org/10.1016/j.conbuildmat.2018.09.105>.
- [24] S. Lv, J. Liu, T. Sun, Y. Ma, Q. Zhou, Effect of GO nanosheets on shapes of cement hydration crystals and their formation process, *Constr Build Mater* 64 (2014) 231–239. <https://doi.org/10.1016/j.conbuildmat.2014.04.061>.
- [25] C. Lin, W. Wei, Y.H. Hu, Catalytic behavior of graphene oxide for cement hydration process, *Journal of Physics and Chemistry of Solids* 89 (2016) 128–133. <https://doi.org/10.1016/j.jp.2015.11.002>.

- [26] L. Lu, P. Zhao, Z. Lu, A short discussion on how to effectively use graphene oxide to reinforce cementitious composites, *Constr Build Mater* 189 (2018) 33–41. <https://doi.org/10.1016/j.conbuildmat.2018.08.170>.
- [27] H. Qin, W. Wei, Y. Hang Hu, Synergistic effect of graphene-oxide-doping and microwave-curing on mechanical strength of cement, *Journal of Physics and Chemistry of Solids* 103 (2017) 67–72. <https://doi.org/10.1016/j.jpcs.2016.12.009>.
- [28] W.-J. Long, Y. Gu, B.-X. Xiao, Q. Zhang, F. Xing, Micro-mechanical properties and multi-scaled pore structure of graphene oxide cement paste: Synergistic application of nanoindentation, X-ray computed tomography, and SEM-EDS analysis, *Constr Build Mater* 179 (2018) 661–674. <https://doi.org/10.1016/j.conbuildmat.2018.05.229>.
- [29] A. Mashhadani, V. Pershin, Concrete Modification Using Graphene and Graphene Oxide, *Advanced Materials & Technologies* (2020) 046–056. <https://doi.org/10.17277/amt.2020.02.pp.046-056>.
- [30] G. Jing, J. Xu, J. Wu, S. Wang, X. Lu, X. Cheng, Z. Ye, Improving the cracking resistance of mortar by reduced graphene oxide, *Constr Build Mater* 310 (2021) 125150. <https://doi.org/10.1016/j.conbuildmat.2021.125150>.
- [31] K. Gong, Z. Pan, A.H. Korayem, L. Qiu, D. Li, F. Collins, C.M. Wang, W.H. Duan, Reinforcing Effects of Graphene Oxide on Portland Cement Paste, *Journal of Materials in Civil Engineering* 27 (2015). [https://doi.org/10.1061/\(ASCE\)MT.1943-5533.0001125](https://doi.org/10.1061/(ASCE)MT.1943-5533.0001125).
- [32] Z. Pan, L. He, L. Qiu, A.H. Korayem, G. Li, J.W. Zhu, F. Collins, D. Li, W.H. Duan, M.C. Wang, Mechanical properties and microstructure of a graphene oxide–cement composite, *Cem Concr Compos* 58 (2015) 140–147. <https://doi.org/10.1016/j.cemconcomp.2015.02.001>.
- [33] Q. Wang, J. Wang, C. Lu, B. Liu, K. Zhang, C. Li, Influence of graphene oxide additions on the microstructure and mechanical strength of cement, *New Carbon Materials* 30 (2015) 349–356. [https://doi.org/10.1016/S1872-5805\(15\)60194-9](https://doi.org/10.1016/S1872-5805(15)60194-9).
- [34] L. Zhao, X. Guo, C. Ge, Q. Li, L. Guo, X. Shu, J. Liu, Investigation of the effectiveness of PC@GO on the reinforcement for cement composites, *Constr Build Mater* 113 (2016) 470–478. <https://doi.org/10.1016/j.conbuildmat.2016.03.090>.
- [35] Z. Lu, X. Li, A. Hanif, B. Chen, P. Parthasarathy, J. Yu, Z. Li, Early-age interaction mechanism between the graphene oxide and cement hydrates, *Constr Build Mater* 152 (2017) 232–239. <https://doi.org/10.1016/j.conbuildmat.2017.06.176>.
- [36] J. An, M. McInnis, W. Chung, B. Nam, Feasibility of Using Graphene Oxide Nanoflake (GONF) as Additive of Cement Composite, *Applied Sciences* 8 (2018) 419. <https://doi.org/10.3390/app8030419>.
- [37] L. Zhao, X. Guo, Y. Liu, C. Ge, Z. Chen, L. Guo, X. Shu, J. Liu, Investigation of dispersion behavior of GO modified by different water reducing agents in cement pore solution, *Carbon N Y* 127 (2018) 255–269. <https://doi.org/10.1016/j.carbon.2017.11.016>.
- [38] R. Roy, A. Mitra, A.T. Ganesh, V. Sairam, Effect of Graphene Oxide Nanosheets dispersion in cement mortar composites incorporating Metakaolin and Silica Fume, *Constr Build Mater* 186 (2018) 514–524. <https://doi.org/10.1016/j.conbuildmat.2018.07.135>.

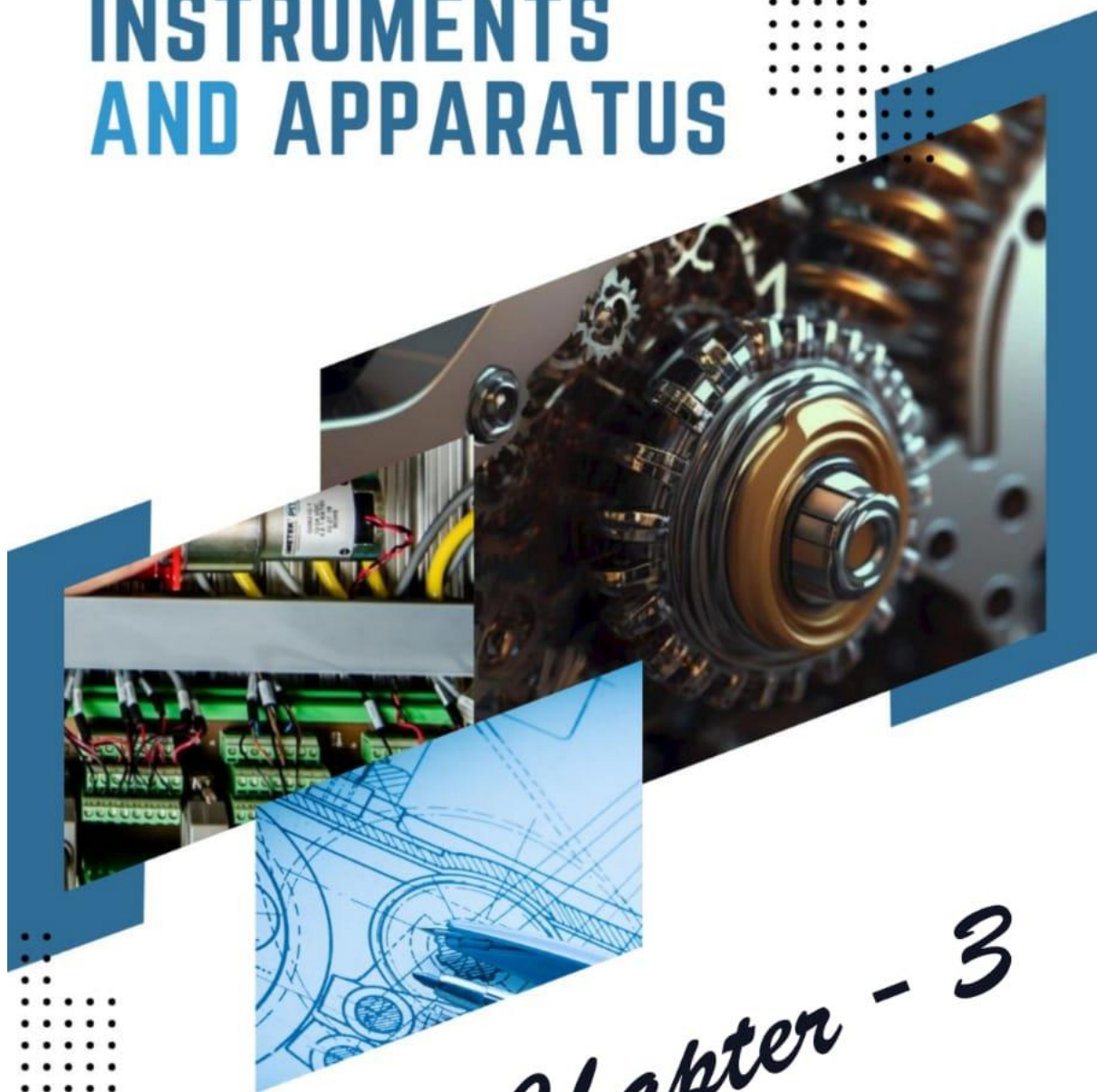
- [39] J. Gong, L. Lin, S. Fan, Modification of cementitious composites with graphene oxide and carbon nanotubes, *SN Appl Sci* 2 (2020) 1622. <https://doi.org/10.1007/s42452-020-03456-w>.
- [40] C. Liu, X. Huang, Y.-Y. Wu, X. Deng, Z. Zheng, The effect of graphene oxide on the mechanical properties, impermeability and corrosion resistance of cement mortar containing mineral admixtures, *Constr Build Mater* 288 (2021) 123059. <https://doi.org/10.1016/j.conbuildmat.2021.123059>.
- [41] L. Zhao, X. Guo, C. Ge, Q. Li, L. Guo, X. Shu, J. Liu, Investigation of the effectiveness of PC@GO on the reinforcement for cement composites, *Constr Build Mater* 113 (2016) 470–478. <https://doi.org/10.1016/j.conbuildmat.2016.03.090>.
- [42] G. Jing, J. Wu, T. Lei, S. Wang, V. Strokova, V. Nelyubova, M. Wang, Z. Ye, From graphene oxide to reduced graphene oxide: Enhanced hydration and compressive strength of cement composites, *Constr Build Mater* 248 (2020) 118699. <https://doi.org/10.1016/j.conbuildmat.2020.118699>.
- [43] Q. Zheng, B. Han, X. Cui, X. Yu, J. Ou, Graphene-engineered cementitious composites, *Nanomaterials and Nanotechnology* 7 (2017) 1847980417742304. <https://doi.org/10.1177/1847980417742304>.
- [44] Q. Wang, J. Wang, C. Lv, X. Cui, S. Li, X. Wang, Rheological behavior of fresh cement pastes with a graphene oxide additive, *New Carbon Materials* 31 (2016) 574–584. [https://doi.org/10.1016/S1872-5805\(16\)60033-1](https://doi.org/10.1016/S1872-5805(16)60033-1).
- [45] K. Chintalapudi, R.M.R. Pannem, Enhanced chemical resistance to sulphuric acid attack by reinforcing Graphene Oxide in Ordinary and Portland Pozzolana cement mortars, *Case Studies in Construction Materials* 17 (2022) e01452. <https://doi.org/10.1016/j.cscm.2022.e01452>.
- [46] X. Hong, J.C. Lee, M.Y. Chu, Q. Li, X. Daze, Effect of Graphene Oxide on compressive strength of Shale Ceramsite high strength lightweight aggregate concrete, *IOP Conf Ser Earth Environ Sci* 1205 (2023) 012049. <https://doi.org/10.1088/1755-1315/1205/1/012049>.
- [47] S. Lv, J. Liu, T. Sun, Y. Ma, Q. Zhou, Effect of GO nanosheets on shapes of cement hydration crystals and their formation process, *Constr Build Mater* 64 (2014) 231–239. <https://doi.org/10.1016/j.conbuildmat.2014.04.061>.
- [48] K. Gong, Z. Pan, A.H. Korayem, L. Qiu, D. Li, F. Collins, C.M. Wang, W.H. Duan, Reinforcing Effects of Graphene Oxide on Portland Cement Paste, *Journal of Materials in Civil Engineering* 27 (2015). [https://doi.org/10.1061/\(ASCE\)MT.1943-5533.0001125](https://doi.org/10.1061/(ASCE)MT.1943-5533.0001125).
- [49] S. Sharma, N.C. Kothiyal, Influence of graphene oxide as dispersed phase in cement mortar matrix in defining the crystal patterns of cement hydrates and its effect on mechanical, microstructural and crystallization properties, *RSC Adv* 5 (2015) 52642–52657. <https://doi.org/10.1039/C5RA08078A>.
- [50] M.M. Mokhtar, S.A. Abo-El-Enein, M.Y. Hassaan, M.S. Morsy, M.H. Khalil, Mechanical performance, pore structure and micro-structural characteristics of graphene oxide nano platelets reinforced cement, *Constr Build Mater* 138 (2017) 333–339. <https://doi.org/10.1016/j.conbuildmat.2017.02.021>.

- [51] H. Yang, M. Monasterio, H. Cui, N. Han, Experimental study of the effects of graphene oxide on microstructure and properties of cement paste composite, *Composites Part A: Applied Science and Manufacturing* 102 (2017) 263–272. <https://doi.org/10.1016/j.compositesa.2017.07.022>.
- [52] S. Sharma, D. Susan, N.C. Kothiyal, R. Kaur, Graphene oxide prepared from mechanically milled graphite: Effect on strength of novel fly-ash based cementitious matrix, *Constr Build Mater* 177 (2018) 10–22. <https://doi.org/10.1016/j.conbuildmat.2018.05.051>.
- [53] W.-J. Long, D. Zheng, H. Duan, N. Han, F. Xing, Performance enhancement and environmental impact of cement composites containing graphene oxide with recycled fine aggregates, *J Clean Prod* 194 (2018) 193–202. <https://doi.org/10.1016/j.jclepro.2018.05.108>.
- [54] G. Xu, S. Du, J. He, X. Shi, The role of admixed graphene oxide in a cement hydration system, *Carbon N Y* 148 (2019) 141–150. <https://doi.org/10.1016/j.carbon.2019.03.072>.
- [55] A.M. Sabziparvar, E. Hosseini, V. Chiniforush, A.H. Korayem, Barriers to achieving highly dispersed graphene oxide in cementitious composites: An experimental and computational study, *Constr Build Mater* 199 (2019) 269–278. <https://doi.org/10.1016/j.conbuildmat.2018.12.030>.
- [56] H. Peng, Y. Ge, C.S. Cai, Y. Zhang, Z. Liu, Mechanical properties and microstructure of graphene oxide cement-based composites, *Constr Build Mater* 194 (2019) 102–109. <https://doi.org/10.1016/j.conbuildmat.2018.10.234>.
- [57] Z. Pan, L. He, L. Qiu, A.H. Korayem, G. Li, J.W. Zhu, F. Collins, D. Li, W.H. Duan, M.C. Wang, Mechanical properties and microstructure of a graphene oxide–cement composite, *Cem Concr Compos* 58 (2015) 140–147. <https://doi.org/10.1016/j.cemconcomp.2015.02.001>.
- [58] W. Li, X. Li, S.J. Chen, Y.M. Liu, W.H. Duan, S.P. Shah, Effects of graphene oxide on early-age hydration and electrical resistivity of Portland cement paste, *Constr Build Mater* 136 (2017) 506–514. <https://doi.org/10.1016/j.conbuildmat.2017.01.066>.
- [59] M. Chufa, J. Mater, Effect of reinforcement of reduced graphene oxide on Mechanical Properties of Concrete nanocomposite, *J. Mater. Environ. Sci* 2020 (2020) 844–855. <http://www.jmaterenvironsci.com>.
- [60] J. Luo, C. Zhou, W. Li, S. Chen, A. Habibnejad Korayem, W. Duan, Using graphene oxide to improve physical property and control ASR expansion of cement mortar, *Constr Build Mater* 307 (2021) 125006. <https://doi.org/10.1016/j.conbuildmat.2021.125006>.
- [61] X. Qi, S. Zhang, T. Wang, S. Guo, R. Ren, Effect of High-Dispersible Graphene on the Strength and Durability of Cement Mortars, *Materials* 14 (2021) 915. <https://doi.org/10.3390/ma14040915>.
- [62] S. Lv, Y. Ma, C. Qiu, T. Sun, J. Liu, Q. Zhou, Effect of graphene oxide nanosheets of microstructure and mechanical properties of cement composites, *Constr Build Mater* 49 (2013) 121–127. <https://doi.org/10.1016/j.conbuildmat.2013.08.022>.
- [63] P. Vasudevareddy, K. Chandrasekhar Reddy, Effect of graphene oxide and nano silica on mechanical and durability properties of cement mortar, *Mater Today Proc* 60 (2022) 1042–1050. <https://doi.org/10.1016/j.matpr.2022.01.234>.

- [64] L. Djenaoucine, Á. Picazo, M. Ángel De La Rubia, A. Moragues, J.C. Gálvez, Effect of Graphene Oxide on Mechanical Properties and Durability of Cement Mortar, (2023). <https://doi.org/10.20944/preprints202307.2114.v1>.
- [65] A. Bagheri, E. Negahban, A. Asad, H.A. Abbasi, S.M. Raza, Graphene oxide-incorporated cementitious composites: a thorough investigation, *Mater Adv* 3 (2022) 9040–9051. <https://doi.org/10.1039/D2MA00169A>.
- [66] X. Li, Y.M. Liu, W.G. Li, C.Y. Li, J.G. Sanjayan, W.H. Duan, Z. Li, Effects of graphene oxide agglomerates on workability, hydration, microstructure and compressive strength of cement paste, *Constr Build Mater* 145 (2017) 402–410. <https://doi.org/10.1016/j.conbuildmat.2017.04.058>.
- [67] C. Chen, W. Zhang, H. Wu, C. Chen, B. Ma, Study on the damage resistance and deterioration behavior of GO concrete under the harsh environment, *PLoS One* 18 (2023) e0284186. <https://doi.org/10.1371/journal.pone.0284186>.
- [68] S. Han, M.S. Hossain, T. Ha, K.K. Yun, Graphene-oxide-reinforced cement composites mechanical and microstructural characteristics at elevated temperatures, *Nanotechnol Rev* 11 (2022) 3174–3194. <https://doi.org/10.1515/ntrev-2022-0495>.
- [69] N. Bheel, B.S. Mohammed, I. Abdulkadir, M.S. Liew, N.A.W.A. Zawawi, Effects of Graphene Oxide on the Properties of Engineered Cementitious Composites: Multi-Objective Optimization Technique Using RSM, *Buildings* 13 (2023) 2018. <https://doi.org/10.3390/buildings13082018>.
- [70] J. Yang, X. He, Durability and Sustainability of Cement and Concrete Composites, *Materials* 16 (2023) 5693. <https://doi.org/10.3390/ma16165693>.
- [71] R.V.R. S. T. Gowda, Microstructure modification of cementitious composites for enhanced engineering properties using nano-graphene oxide layers, *The Ind. Conc. Journ.* 91 (2017) 34–44.
- [72] L. Lavagna, D. Massella, E. Priola, M. Pavese, Relationship between oxygen content of graphene and mechanical properties of cement-based composites, *Cem Concr Compos* 115 (2021) 103851. <https://doi.org/10.1016/j.cemconcomp.2020.103851>.
- [73] D. Dimov, I. Amit, O. Gorrie, M.D. Barnes, N.J. Townsend, A.I.S. Neves, F. Withers, S. Russo, M.F. Craciun, Ultrahigh Performance Nanoengineered Graphene–Concrete Composites for Multifunctional Applications, *Adv Funct Mater* 28 (2018). <https://doi.org/10.1002/adfm.201705183>.
- [74] A. Anwar, X. Liu, L. Zhang, Nano-cementitious composites modified with Graphene Oxide – a review, *Thin-Walled Structures* 183 (2023) 110326. <https://doi.org/10.1016/j.tws.2022.110326>.
- [75] S. Han, M.S. Hossain, T. Ha, K.K. Yun, Graphene-oxide-reinforced cement composites mechanical and microstructural characteristics at elevated temperatures, *Nanotechnol Rev* 11 (2022) 3174–3194. <https://doi.org/10.1515/ntrev-2022-0495>.
- [76] P.V.R.K. Reddy, D.R. Prasad, Nano-reinforced cement composites and novel insights from graphene oxide: a review, *Bulletin of Materials Science* 47 (2024) 17. <https://doi.org/10.1007/s12034-023-03092-1>.

- [77] C. Phrompet, C. Sriwong, C. Ruttanapun, Mechanical, dielectric, thermal and antibacterial properties of reduced graphene oxide (rGO)-nanosized C3AH6 cement nanocomposites for smart cement-based materials, *Compos B Eng* 175 (2019) 107128. <https://doi.org/10.1016/j.compositesb.2019.107128>.
- [78] L. Wang, J. Wang, X. Qian, P. Chen, Y. Xu, J. Guo, An environmentally friendly method to improve the quality of recycled concrete aggregates, *Constr Build Mater* 144 (2017) 432–441. <https://doi.org/10.1016/j.conbuildmat.2017.03.191>.
- [79] T. Janjaroen, S. Khammahong, W. Tuichai, A. Karaphun, C. Phrompet, C. Sriwong, C. Ruttanapun, The Mechanical and Thermal Properties of Cement CAST Mortar/Graphene Oxide Composites Materials, *Int J Concr Struct Mater* 16 (2022) 34. <https://doi.org/10.1186/s40069-022-00521-z>.
- [80] Q. Wang, J. Wang, C. Lu, B. Liu, K. Zhang, C. Li, Influence of graphene oxide additions on the microstructure and mechanical strength of cement, *New Carbon Materials* 30 (2015) 349–356. [https://doi.org/10.1016/S1872-5805\(15\)60194-9](https://doi.org/10.1016/S1872-5805(15)60194-9).
- [81] H. Yang, M. Monasterio, H. Cui, N. Han, Experimental study of the effects of graphene oxide on microstructure and properties of cement paste composite, *Compos Part A Appl Sci Manuf* 102 (2017) 263–272. <https://doi.org/10.1016/j.compositesa.2017.07.022>.
- [82] S.C. Devi, R.A. Khan, Effect of graphene oxide on mechanical and durability performance of concrete, *Journal of Building Engineering* 27 (2020) 101007. <https://doi.org/10.1016/j.jobbe.2019.101007>.

INSTRUMENTS AND APPARATUS



Chapter - 3

INSTRUMENTS
AND APPARATUS

INSTRUMENTS AND APPARATUS

3.0 General View

The mechanical properties of cement mortar with or without GO, such as its compressive strength, split tensile strength, flexural strength, and Young's Modulus were measured according to Indian Standard IS 4031-6 (1988), Indian Standard IS 5816 (1999), American Association of State and Highway Transportation Officials AASHTO T 67-05, and Indian Standard IS 516-8 (2019). For the above-mentioned test, various types of specimens have been made and tested appropriately. To determine the flow behavior of cement mortar with/without GO, the flow test was conducted according to Indian Standard IS: 4031-4 (1988). Rapid Chloride Ion Penetration Test (RCPT) of GO modified cement-sand mortar conducted as per ASTM C1202. Field Emission Scanning Electron Microscope (FESEM) with Energy dispersive X-ray Spectroscopy (EDS), X-ray diffraction (XRD), and Mercury Intrusion Porosimetry (MIP) have been explored for micro-structure study. Most importantly, GO is dispersed in water by using Ultrasonic Probe Sonicator. Some important features and functioning principles of these instruments are briefly explained.

3.1 Ultrasonic Probe Sonicator

In a variety of scientific and industrial applications, an ultrasonic probe sonicator is an equipment used for sample homogenization, cell destruction, and particle size reduction. It uses high-frequency sound waves, or ultrasonics, produced by a probe to disturb particles or cells in a liquid. The technique is useful for effective sample preparation and processing in areas including biology, chemistry, and nanotechnology. The Hielscher Ultrasonic Processor-UP100H (Germany) was employed in the present study to produce a mixture of GO and water and to disperse the material (Fig. 3.1).



Fig. 3.1: Ultrasonic probe sonicator.

3.3 Compressive Strength and Split Tensile Strength Test

The ability of cement mortar to tolerate axial loads or forces that tend to compress or crush it is known as its compressive strength. This characteristic is crucial for evaluating the mortar's ability to support loads and maintain its structural integrity. In this present study, the compressive strength and split tensile strength of mortar specimens were measured according to Indian Standard IS 4031-6 (1988) and IS 5816 (1999) respectively, by compressive testing machine (CTM) (Aimil Ltd Mu-1) 2000 kN capacity (Fig. 3.2). For compressive strength test cube specimens placed CTM and the load was applied at a rate of $35\text{N/mm}^2/\text{minute}$. For split tensile strength cylindrical specimens were placed in CTM and the load was applied at a rate of $2.4\text{N/mm}^2/\text{minute}$. The experiments were carried out until the fracture specimens.



Fig. 3.2: Compressive strength and split tensile strength test set up.

3.3 Flexural Strength Test

The capacity of a material to resist the deformation or fracture under bending or flexural loads is known as flexural strength. Test specimens such as bar specimens were set up on a 10kN load frame of a beam testing equipment. The load is applied at one mid-point of the span. The load on the beam is increased by the load cell attached with the frame. The experiment is carried out until the cracks are observed. The graphical setup and experimental setup for the flexural strength test are shown in Fig. 3.3 and Fig. 3.4.

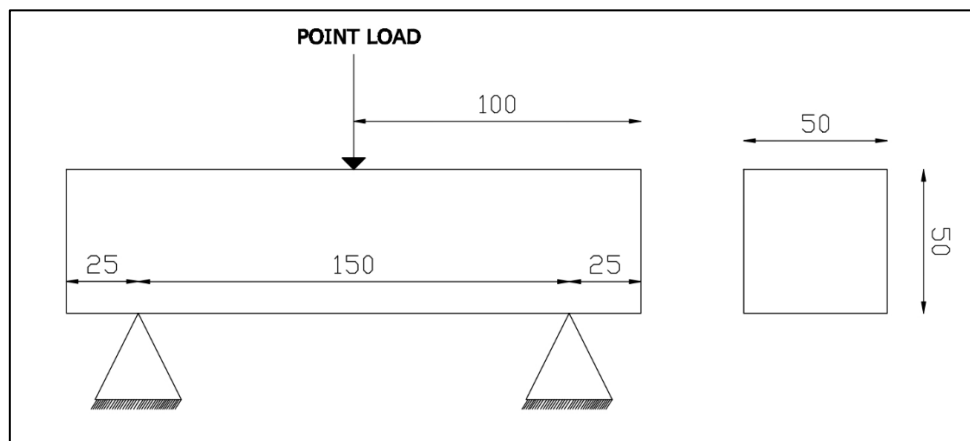


Fig. 3.3: Graphical setup of flexural strength test.



Fig. 3.4: Flexural strength test setup.

3.4 Flow Table Test

A common method to determine the workability of mortar or concrete is the flow table test. In this present study flow table test was conducted according to Indian Standard IS 4031(part-4). A mini-slump cone of 50 mm in height, 100 mm in bottom diameter, and 70 mm in top diameter was employed. The slump cone was placed on the center of the flow table and filled with fresh mortar. To ensure compaction, the newly mixed mortar was pressed down firmly by using a spatula. The slump cone was removed vertically to ensure no lateral disturbance. The flow table was immediately dropped 25 times in 15 seconds from a height of 12.5 mm, and the mortar mass's base diameter was then measured (Fig. 3.5). The flow can be defined as a change in the mortar mass's average base diameter as a percentage of its initial base diameter. This increase is recorded on at least six diameters at roughly equal spacing.



Fig. 3.5: Flow table test set up.

3.5 Ultrasonic Pulse Velocity test (UPV)

A non-destructive technique for evaluating the quality and integrity of concrete structures is the Ultrasonic Pulse Velocity (UPV) test. In this test, ultrasonic pulses are passed through concrete, and the length of time it takes for the waves to pass through is measured. The density and homogeneity of the concrete affect the wave's velocity, revealing information on the structural integrity of the material. The UPV test is frequently used to find defects in concrete elements, including delamination, voids, and cracks. Without causing any damage, it assists engineers and inspectors in evaluating a structure's overall condition. Lower velocities may indicate the presence of defects, while higher velocities often imply better quality and more uniform concrete. In this present study, a Pundit Lab UPV test machine is used.

An electroacoustic transducer produces the ultrasonic pulse. The pulse experiences several reflections at the borders of the various material phases within the concrete when it is introduced into the concrete through a transducer. The result is a complicated system of stress waves that consist of surface (Rayleigh), longitudinal (compressional), and shear (transverse) waves. The transducer that detects the onset of the longitudinal waves, which is the fastest.



Fig. 3.6: UPV test setup.

3.6 Chloride Ion Penetration Test (RCPT)

As per AASHTO T277 (2022), a water-saturated cylindrical specimen measuring 50 mm thick and 100 mm in diameter was used for the RCPT test. The specimen was sliced to have a 200 mm in length and 100 mm in diameter. The core specimens were put through RCPT by continuously applying 60 V. A PVC container served as the seal on either end of the core specimen (Fig. 3.7). One side of the container is filled with a solution of 3% sodium chloride (NaCl), and the other side is filled with a solution of 0.3 (M) sodium hydroxide (NaOH). This side of the cell should be connected to the cathode terminal of the power supply. The chloride ions with a negative charge will move in the direction of the positive terminal. A steady 60V voltage is supplied across the specimen in order to accelerate the test by increasing the rate of chloride penetration into the specimen.

The rubber gaskets and washers will be included to make it leak-proof. To hold the specimen tightly in place, stainless steel bolts with washers and nuts will be provided. Each cell will get electricity from the power supply via banana sockets, and current will be distributed via the brush. The tops of each cell will include openings for pouring chemicals and temperature

sensors. Lids are an effective way of sealing the opening. The capacity of the chemical chamber will be 250 milliliters.

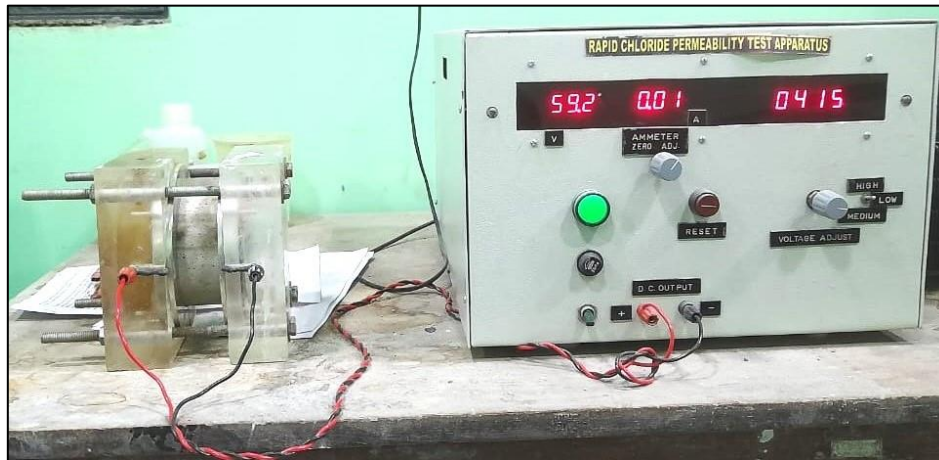


Fig. 3.7: RCPT test setup.

3.7 X-ray Diffraction (XRD)

To examine crystal structure and atomic spacing, X-ray diffraction is currently a widely used technique. It works by using constructive interference between monochronic X-rays and a crystalline sample. These X-rays are produced by a cathode ray tube, processed to produce monochromatic radiation, collimated concentrate, and directed towards the sample. In instances in which Bragg's Law ray ($2d \sin\theta = n\lambda$, where n is an integer, λ is the wavelength in angstroms, d is the interatomic spacing in angstroms, and θ is the diffraction angle in degrees) is satisfied, the interaction between the incident rays and the sample results in constructive interference as well as a diffracted ray. This law establishes a relationship between the diffraction angle and lattice spacing in a crystalline sample and the electromagnetic radiation wavelength. After that, these diffracted X-rays are located, examined, and counted. Due to the random orientation of the powdered materials, all possible diffraction directions of the lattice have to be determined by scanning the sample through a range of 2θ angles.

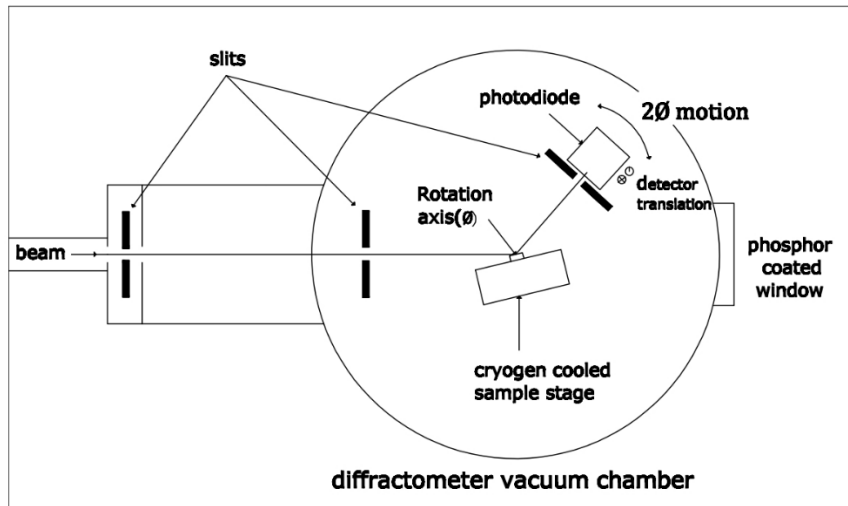


Fig. 3.8: Graphical presentation of XRD test.

The identification of the mineral is possible by the conversion of the diffraction peaks to d-spacings, as every mineral has a distinct set of d-spacings. The Preder Diffraction File (PDF), provided by the International Centre for Diffraction Data, contains d-spacing files for hundreds of thousands of inorganic elements. D-spacings of minerals can be found on a lot of other websites, like the American Mineralogist Crystal Structure Database. For the XRD examination of the GO-modified cement mortar and control sample in this investigation, a Bruker D8 ADVANCE instrument is employed (Fig. 3.9).

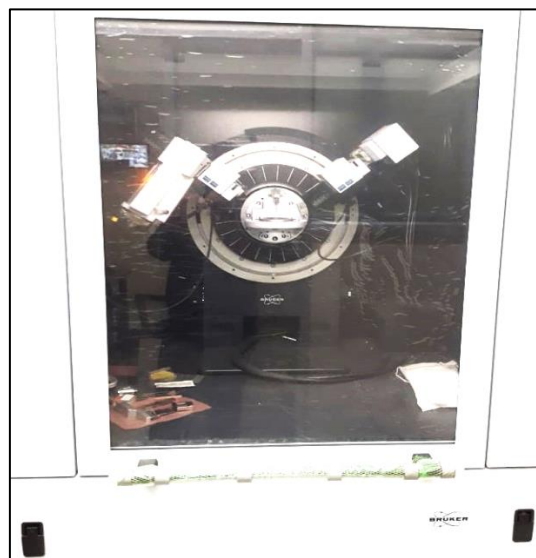


Fig. 3.9: XRD test arrangement.

3.8 Field Emission Scanning Electron Microscope (FESEM)

The non-destructive, versatile method of scanning electron microscopy provides a full understanding of the structure and composition of both natural and synthetic materials. The specimen in a scanning electron microscope is subjected to a narrow electron beam from an electron gun that rapidly moves over or scans the specimen's surface. The sample's surface topography, composition, and electrical conductivity are all provided by the signals that are produced when the electrons come in contact with the atoms that comprise the sample. The FESEM can provide a variety of signals, such as specimen current transmitted electrons, light (cathodoluminescence), distinctive X-rays, secondary electrons, and back-state electrons (BSE). Although secondary electron detectors are a basic feature of all FESEMs, but it is rare for a single machine to incorporate detectors for every possible signal. The signals are produced when atoms at or close to the sample's surface contact with the electron beam. Secondary electron imaging, or SEI, is the most widely used or standard form of detection. It can yield extremely high-resolution images of a sample surface, exposing features smaller than 1 nm in size. Because of its very narrow electron beam, SEM micrographs have a significant depth of field and a distinctive three-dimensional appearance that helps with comprehending a sample's surface structure.

Cementitious materials' morphology and microstructural examination have been studied using the INSPECT F50 SEM (FEL Europe BV, The Netherlands). FESEM is dried, coated with gold, and kept in desiccators before being examined with an INSPECT F50. It is elastic scattering that reflects back-scattered electrons (BSE) from the sample. Since the intensity of the BSE signal is closely correlated with the specimen's atomic number (Z), BSE is frequently utilised in analytical FESEM along with spectra generated from characteristic X-rays. Information regarding the distribution of various elements in the sample can be obtained from BSE images. When the electron beam removes an electron from the sample's inner shell, a higher-energy

electron fills the shell and releases energy, resulting in the characteristic X-rays. These qualities X-rays are utilised to determine the sample's composition and quantify its elemental abundance.



Fig. 3.10: FESEM analysis setup.

3.9 Mercury Intrusion Porosimetry (MIP)

The Mercury Intrusion Porosimetry (MIP) test is a technique used to characterize the pore structure of materials, including cement composites. It involves the intrusion of mercury into the pores of a sample at various pressures. The distribution of pore sizes in the material can be determined by measuring the amount of mercury that has intruded at each pressure level. Quantachrome make Poremaster 60 was used to conduct the test by applying different levels of pressure to a sample immersed in mercury. The specimens of cement mortar were broken into 3 to 6 mm particle sizes for the MIP test after 28 days of compression testing.



MATERIALS AND METHODS



Chapter - 4



MATERIALS AND METHODS

4.0 General View

The present study's experimental investigations were mostly carried out at the Concrete Technology Laboratory in the Civil Engineering Department at Jadavpur University, Kolkata, India. First, the specific materials used in this study, including GO, cement, and sand, are described in section 4.1. The next sections described briefly such as 4.2 and 4.3 include the characterization of GO, preparation of specimens, and experimental program to study the effects of GO on cement composite such as cement mortar, respectively.

4.1 Materials

4.1.1 Graphene Oxide (GO)

GO is a new found carbon based 2D nanomaterial. In cement-based composites, GO acts as a nano-reinforcement. It can be synthesized from graphite by strong oxidation and exfoliation [1]. The average lateral dimension 5-10 μ m and average thickness 0.8-1.6nm with 99% purity and black in colour (Fig. 4.1) GO was collected from M/s Ad-Nano Technologies Pvt. Karnataka, India. The technical properties of GO are presented in Table 4.1.



Fig. 4.1: Graphene oxide nanoparticles.

Table 4.1: Technical parameters of GO.

Descriptions	Purity (%)	Numbers of layers	Average thickness (z) (nm)	Average lateral dimension (x & y) (μm)	Surface area (m ² /g)	Carbon (%)	Oxygen (%)	Hydrogen (%)	Others (%)
Graphene oxide	>99	1-3 layers	0.8-1.6	5-10	450	60-80	15-32	0-2%	0-2

4.1.2 Cement

As a binder in construction, cement is an essential building material. It is a fine powder composed mainly of clay, limestone, and other minerals that, when mixed with water, goes through a process known as hydration (Fig. 4.2). At present different types of cement such as Ordinary Portland cement (OPC), Portland Pozzolana cement (PPC), Portland Slug cement (PSC), White cement, Quick setting cement, etc. are available. In this present study, two types of cement such as OPC grade 53 and PPC confirmed by Indian Standard IS: 269-2015 [2] and IS: 1489-2015 (part-I) [3] used for experimental study. The chemical composition of OPC and PPC cement is presented in Tables 4.2 and 4.3 respectively.



Fig. 4.2: Powder form of cement.

Table 4.2: Chemical composition Ordinary Portland cement (OPC) 53 grade.

Parameters	SiO ₂	Al ₂ O ₃	Fe ₂ O ₃	CaO	MgO	SO ₃	K ₂ O	Na ₂ O	Others
% (by mass)	21.94	4.95	3.74	62.33	2.08	2.22	0.44	0.32	1.98

Table 4.3: Chemical composition of Portland Pozzolana cement (PPC).

Parameters	SiO ₂	Al ₂ O ₃	Fe ₂ O ₃	CaO	MgO	SO ₃	K ₂ O	Na ₂ O	Others
% (By weight)	36.21	11.14	4.52	42.4	1.03	2.05	0.37	0.17	2.11

4.1.3 Fine aggregate (Sand)

A fine aggregate such as sand, is a collection of minerals that are left over after rocks crumble. Locally available river sand of Grade-II and a specific gravity of 2.66 confirmed by IS: 383-2016 [4] was used throughout this experimental study. The locally available river sand as fine aggregates are shown in Fig. 4.3.

**Fig. 4.3: Dry fine aggregates (sand).**

4.1.4 Water

Water fit for drinking is generally considered fit for construction work. Water should be free from acid, oils, alkalis vegetables, or other organic impurities. Soft water also produces weaker cement composites. In this present study, available tap water fit for drinking was used throughout the experimental study (confirmed by IS 456:200).

4.2 Experimental Program

4.2.1 Characterization of GO

Bruker D8 Advance X-ray diffractometer with Cu-K α radiation was used to perform X-ray diffraction (XRD) in order to analyse the amorphous GO nanoparticles sample. In the range of $2\theta = 5^\circ$ to 90° , the XRD spectrum was examined, and the peak positions were reported. A Zeiss system was subjected to the field emission scanning electron microscope (FESEM) characterization process. 10kV was the acceleration voltage. The existence of functional groups in the catalysts was ascertained by using a Perkin Elmer Spectrum Two spectrophotometer device operating in the 600–3600 cm⁻¹ scanning range.

4.2.2 Dispersion of GO

GO nanoparticles tend to agglomerate and form clusters in water due to their hydrophobic nature and strong van der Waals interactions between individual sheets. Perhaps the most significant process for making graphene oxide prepared for use in cement composites is sonication. It breaks down the agglomeration and promotes dispersion, exfoliation, and improved interaction of GO with the cement matrix, ultimately contributing to the enhanced performance of the composite material. In this present study, GO was mixed with water at a ratio of 1:200, and it was sonicated for 45–60 minutes using a UP100H ultrasonic processor, no additional chemicals or dispersion agents were used. The dispersed GO in water is shown in Fig. 4.4.

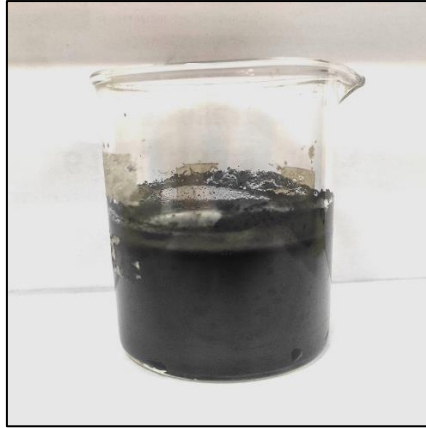


Fig. 4.4: Dispersed GO after sonication.

4.2.3 Preparation GO modified cement mortar

In this present study, GO modified cement-sand mortar was prepared by using two different types of cement such as OPC and PPC with two different cement-sand ratios 1:2 and 1:3. The preparation of GO modified sample are shown in Fig. 4.5. The percentages of GO in the mixes ranged from 0.0% to 0.06% by weight of cement. The water-to-cement ratio was kept fixed at 0.45. At first, the appropriate quantity of cement and sand are mixed thoroughly 3-4 minutes to get a uniform mixture in a plastic bowl. The sonicated suspension of GO and water was added to the dry mixture of cement and sand to form mortar. The mixing time was around 3-4 minutes to obtain the uniform colour of the mixture. In assembling the moulds ready for use, cover the joints between the halves of the mould with a thin film of petroleum jelly and apply a similar coating of petroleum jelly between the contact surface of the bottom of the mould and the base plate in order to ensure that no water escapes during compaction.

Three equal-thickness layers of cement mortar are poured into each mould. To remove trapped air and honeycombing, each layer of mortar compacts with a tamping rod by 25 strikes. Once the third layer has been compacted, use a trowel to smooth the top face and cut off the excess mortar. The test specimens were kept in the laboratory in moist air of at with a 90% relative humidity and at a temperature of $27 \pm 2^\circ\text{C}$ for 24 ± 1 hours from the water was added to the dry

ingredients. the cement mortar attained sufficient solidity after 24 hours to be extracted from the mould and submerged in water for curing before undergoing different testing. For each test 6 no of samples were prepared. Table 4.4 shows the details of different cement-sand mixtures with different percentages of GO.

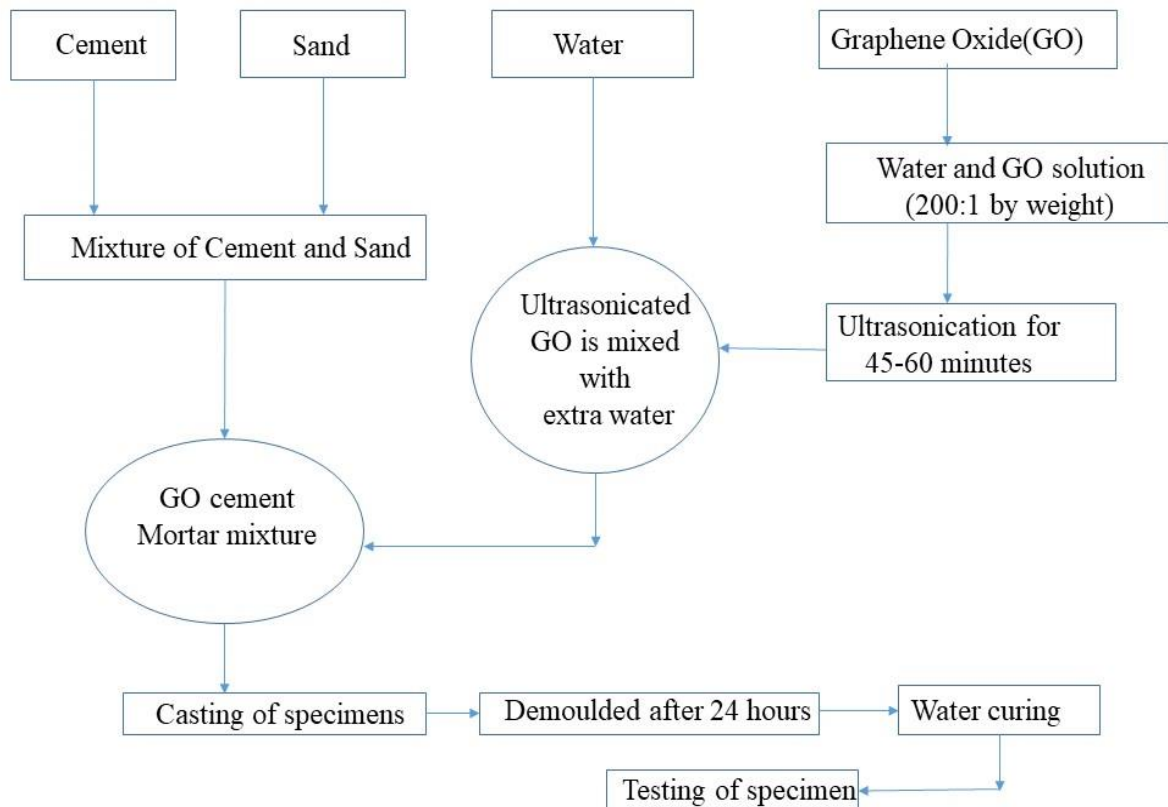


Fig 4.5: Flow chart of GO modified sample preparation.

4.3 Sample Preparation

4.3.1 Flow test

In accordance with IS 4031(part-4) [5], a flow table test was performed to determine the fluidity of fresh cement mortar using different addition percentages of GO. A slump cone of 50 mm in height, 100 mm in bottom diameter, and 70 mm in top diameter was used to measure the fluidity of different cement-sand mortar with and without GO. The cone was placed firmly on the flow

table, and the cone was then filled with fresh cement sand mortar mixtures. After the cone was removed, the fluidity was determined by measuring the initial and final diameters. Fig. 4.6 shows the flow test setup for mortar.

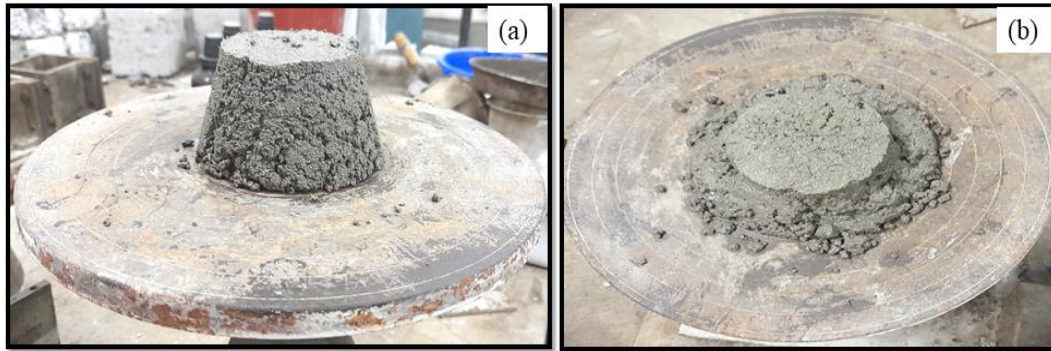


Fig. 4.6: Flow table test of mortar.

4.3.2 Compressive strength test

Standard cube specimens with dimensions of $70.6 \text{ mm} \times 70.6 \text{ mm} \times 70.6 \text{ mm}$ were prepared to study the compressive strength of various cement-sand mortar mixes with and without GO [6]. The compressive strength of the OPC and PPC based GO-modified cement mortar as well as the control sample have been measured on the cube specimens at 3 days, 7 days, and 28 days curing ages. A compressive strength testing machine has been used to determine the breaking load of samples. Fig. 4.7 shows the standard cube specimens.



Fig. 4.7: Mortar cube specimens.

Table 4.4: Details of different cement-sand mortar mixture.

Mixes	Types of Cement	Cement: sand (by weight)	Water: cement (by weight)	GO% by weight of cement	Types of mortar
1GM0	OPC	1:2	0.45	0	Without GO (Control)
1GM1				0.03	GO modified OPC mortar
1GM2				0.04	
1GM3				0.05	
1GM4				0.06	
2GM0	OPC	1:3	0.45	0	Without GO (Control)
2GM1				0.03	GO modified OPC mortar
2GM2				0.04	
2GM3				0.05	
2GM4				0.06	
2GM0	PPC	1:2	0.45	0	Without GO (Control)
3GM1				0.03	GO modified PPC mortar
3GM2				0.04	
3GM3				0.05	
3GM4				0.06	
4GM0	PPC	1:3	0.45	0	Without GO (Control)
4GM9				0.03	GO modified PPC mortar
4GM10				0.04	
4GM11				0.05	
4GM12				0.06	

4.3.3 Split tensile strength test

To determine the split tensile strength of GO modified OPC and PPC based cement mortar and control cylinder specimens of size 100 mm diameter and 200 mm height have been cast. All the cylinder specimens with and without GO have been tested after 28 days of curing. The cylinder is positioned horizontally between the loading surface of the compression testing machine, and the load is applied perpendicular to the cylinder's axis until it fractures. The small size of wood pieces has been utilised as packing material to prevent unexpected slip. The split tensile strength was calculated according to IS:5816-1999 [7]. Fig. 4.8 shows the standard cylindrical specimen for split tensile test.



Fig. 4.8: Cylindrical mortar specimens.

4.3.4 Flexural strength test

Beam specimens of 50 mm × 50 mm × 200 mm were used to determine the flexural strength of the cement mortar with and without GO. The flexural strength was determined by using the center point loading method (AASHTO T67) [8] with a span of 150 mm for all types of mixes after 28 days of curing. Six samples have been employed for each set of flexural strength testing. Fig. 4.9 shows the standard bar specimens for flexural strength test mortar samples.



Fig. 4.9: Beam specimens for flexural strength test.

4.3.5 Measurement of young modulus (E value)

The young modulus of cement mortar was determined using a cylinder with a diameter of 100 mm and a height of 200 mm, in accordance with IS: 516 (part-8)-2019 [9]. The all cylinder specimens have been tested by a compression testing machine. The basic stress equal to $1/9^{\text{th}}$ ($\sigma_b = f_c/9$) and ultimate stress equal to $1/3^{\text{rd}}$ ($\sigma_a = f_c/3$) of compressive strength of cube specimens after 28 days, and the corresponding strains ϵ_b and ϵ_a respectively measured. The modulus of elasticity is measured by using equation (1).

$$E = (\sigma_a - \sigma_b) / (\epsilon_a - \epsilon_b) \dots \dots \dots (1)$$

Where, σ_a ($f_c/3$) denotes the upper loading stress, in N/mm^2 ;

σ_b ($f_c/9$) is the basic stress, in N/mm^2

f_c is the compressive strength of cube specimens after 28 days

ϵ_a, ϵ_b = corresponding strain of σ_a and σ_b .

At first, the compressive strength of the cube specimen at 28 days was measured. Based on this σ_a and σ_b were fixed. The strain was measured corresponding to σ_a and σ_b .

4.3.6 Ultrasound Pulse Velocity (UPV) test

The Ultrasound Pulse Velocity (UPV) test of cement mortar with and without GO was carried out in accordance with IS:516 (Part 5)-2018 [10] to evaluate the quality of concrete and its packing characteristics. To perform the UPV test 70.6 mm× 70.6 mm× 70.6mm cube specimen was prepared. The test was performed after 28 days of curing. For each mixture, six samples have been used for UPV testing, and the average value has been taken.

4.3.7 Rapid Chloride Penetration Test (RCPT)

A cylindrical specimen with dimensions of 100 mm in diameter and 200 mm in height has been constructed for the chloride ion penetration test of cement mortar with and without GO. The cylindrical specimen had been cut to approximately 50 mm thickness after 28 days of curing. Over a period of six hours, the current flowing through the specimen at 60 volts has been recorded every 30-minute intervals, and the total charges in Coulombs have been recorded [11].

4.3.8 Sorptivity test

The sorptivity test was conducted following ASTM C1585-04 [12]. For every mixture, standard specimens, 50 mm sliced of 100 mm diameter and 200 mm cylinder has been made to conduct the sorptivity test. A waterproofing substance was applied to the external surface of mortar samples. The sliced specimen was kept in a water tray with its free surface submerged in water and supported appropriately. Throughout the testing period, the water level at the base of the cut specimen remained unchanged at 2±1 mm. The outcome of this test establishes the time dependence of water absorption in a single direction. The water absorption rate is calculated by equation (2)

$$I = \frac{\Delta M}{a \times d} \dots \dots \dots (2)$$

Where I =absorption in mm

ΔM = change in mass of the specimen

a = exposed area of specimen in mm^2

d = density of water in g/mm^3 .

A total 120 number of specimens were tested.

4.3.9 Acid resistance test

Standard cube specimens $70.6 \text{ mm} \times 70.6 \text{ mm} \times 70.6 \text{ mm}$ were prepared and submerged in an acid solution to test the acid resistance of cement-sand mortar with and without GO. The solution consisted of a 5% H_2SO_4 solution in water, and the specimens were submerged for 28 and 56 days to evaluate the resistance against acid attacks and their effects. The compressive strength and measured the mass of immersed cube specimens after 28 days, and 56 days [13].

4.3.10 Mercury Intrusion Porosity (MIP) test

After a 28-day compression test of mortar with and without GO, the Mercury Intrusion Porosimetry (MIP) test was conducted to measure the pore size distribution on broken materials with particles sized 3-6 mm in Quntachorme create Poremaster 60. The broken pieces were soaked in acetone to stop the hydration and were oven-dried.

4.3.11 X-ray Diffraction analysis (XRD)

The GO based cement mortar (OPC and PPC) and control samples processing acceptable suitable results of compressive strength of different mixtures (1GM0, 1GM3, 3GM0, and 3GM2) have been dried and sieved to make size less than $5\mu\text{m}$ for X-ray Diffraction (XRD) analysis using a diffractometer (Bruker AXS Inc, Model D8, WI, USA). The XRD spectrum has been examined in the region of $2\theta = 10^\circ$ to 70° . The peak positions are recorded and compared from the Joint Committee on Powder Diffraction Standard (JCPDS) file.

4.3.12 Field Emission Scanning Electron Microscopy (FESEM) and Energy Dispersive X-ray (EDX) analysis

Following the 28-day compression strength test, the fractured portions of the samples were dried, ground, and sieved to obtain finely powdered samples with uniform particle sizes below 5 μ m. These finely powdered samples were diluted with 99.9% ethanol to form a film on carbon tape and then placed under vacuum desiccators for evaporation. Finally, the dried samples were coated with gold and subjected to further analysis.

References

- [1] A. Jiříčková, O. Jankovský, Z. Sofer, D. Sedmidubský, Synthesis and Applications of Graphene Oxide, *Materials*. 15 (2022) 920. <https://doi.org/10.3390/ma15030920>.
- [2] IS: 269-2015 Ordinary Portland Cement Specification, Indian Standard Specification, Bureau of Indian Standards, New Delhi, India.
- [3] IS: 1489 (Part 1) 2015 Portland Pozzolana Cement Specification, Indian Standard Specification, Bureau of Indian Standards, New Delhi, India.
- [4] IS: 383-2016 Coarse and Fine Aggregate for Concrete Specification, Indian Standard Specification, Bureau of Indian Standards, New Delhi, India.
- [5] IS: 4031 (Part 4) 1988 Methods of Physical Tests for Hydraulic Cement, Indian Standard Specification, Bureau of Indian Standards, New Delhi, India.
- [6] IS: 4031 (part 7) Methods of Physical Tests for Hydraulic Cement, Indian Standard Specification, Bureau of Indian Standards, New Delhi, India.
- [7] IS: 5816 - 1999 Splitting Tensile Strength of Concrete Method of Test, Indian Standard Specification, Bureau of Indian Standards, New Delhi, India.
- [8] AASHTO T 67-05 Standard method of test for standard practices for force verification of testing machines, standard published by American Association of State and Highway Transportation Officials.
- [9] IS: 516 (part 8) 2019 Determination of Modulus of Elasticity and Poisson's Ratio in Compression, Indian Standard Specification, Bureau of Indian Standards, New Delhi, India.
- [10] IS: 516 (part 5) 2018 Non-Destructive Testing of Concrete, Indian Standard Specification, Bureau of Indian Standards, New Delhi, India.
- [11] AASHTO - T277 Standard Method of Test for Electrical Indication of Concrete's Ability to Resist Chloride Ion Penetration.
- [12] ASTM C1585 – 04. Standard Test Method for Measurement of Rate of Absorption of Water by Hydraulic-Cement Concretes.
- [13] P. Vasudevareddy, K. Chandrasekhar Reddy, Effect of graphene oxide and nano silica on mechanical and durability properties of cement mortar, *Mater Today Proc.* 60 (2022) 1042–1050. <https://doi.org/10.1016/j.matpr.2022.01.234>.

Chapter-5



RESULTS **AND** DISCUSSION

RESULTS AND DISCUSSION

5.0 General View

The aim of this study is to improve the properties of cement composite with the addition of a small amount of GO, without any other dispersion agents or chemicals and minerals. In this chapter, the results of the experimental study of cement based mortar samples with and without GO have been briefly presented and discussed. At first, the workability behaviour of GO modified OPC and PPC based cement mortars have been presented separately. Further, the mechanical properties, durability, and micro-structural studies of all typical mortar samples have been discussed.

5.1 Characterization of GO

Fig.5.1a highlights the XRD analysis result of GO nanoparticles. The characteristics XRD analysis peak for GO was observed at 10.54° corresponding to an interlayer distance of 0.42 nm width miller indices (001) [1]. The FT-IR spectra of GO are shown in Fig. 5.1b. The GO sample exhibits peaks of carbonyl (C=O), aromatic (C=C), carboxyl (-COOH), epoxy (C-O-C), and hydroxyl (-OH) groups. The -OH group is signified at 3434 cm^{-1} due to the presence of water molecules [2]. The transmission peak at 1627 cm^{-1} indicates the presence of the ketone group. The graphitic nature of GO due to the presence of sp^2 hybridization is exhibited by the presence of the peak at 1544 cm^{-1} [3]. The peak at 686 cm^{-1} appears due to the bonding vibration of the C-H bond [3]. The -COOH group appeared at 1055 cm^{-1} due to the presence of strong acids within GO during the synthesis process. The presence of the C-O-C group is proved by the presence of the transmission peak at 1406 cm^{-1} [4]. The SEM image of GO is presented in Fig. 5.1c. The SEM image of GO clearly indicates that the shape of GO is like a 2D sheet.

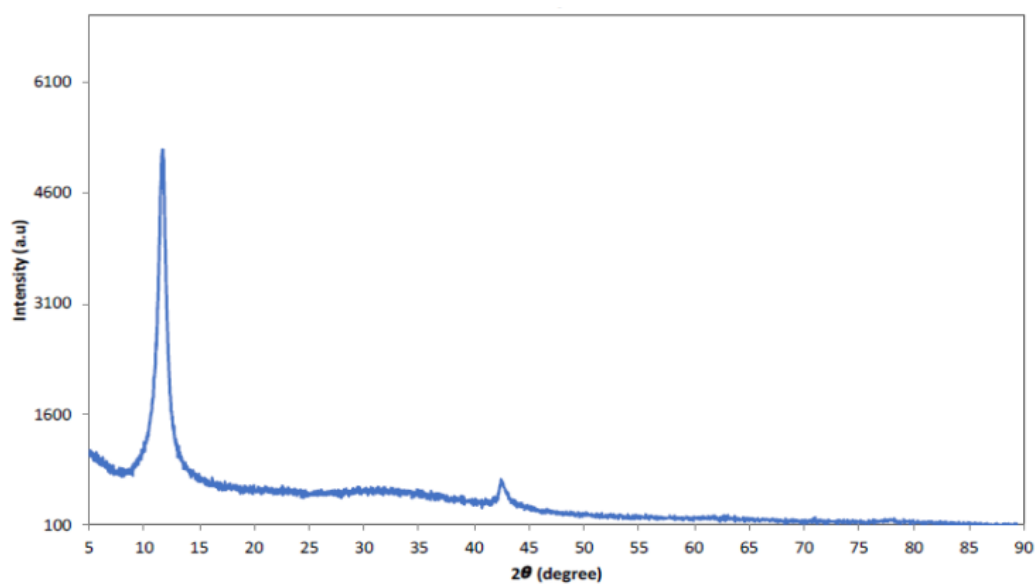


Fig. 5.1a: XRD analysis of GO.

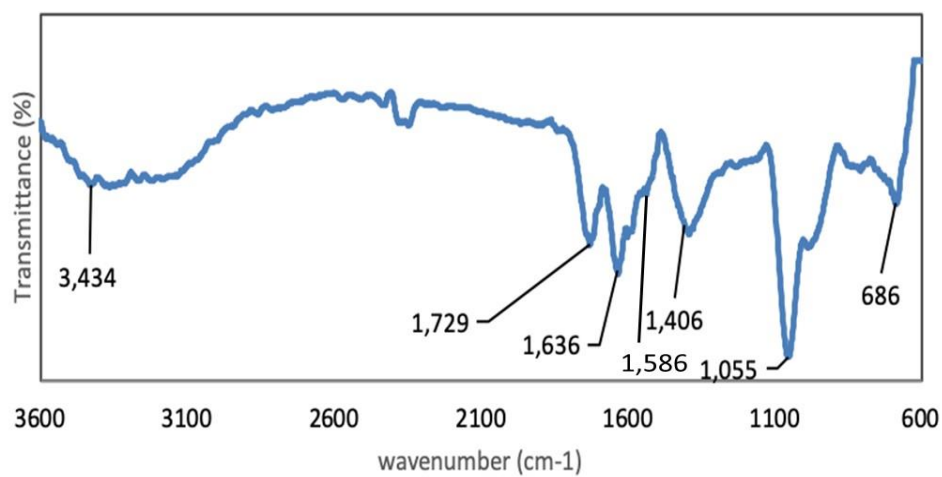


Fig. 5.1b: FT-IR spectra of GO.

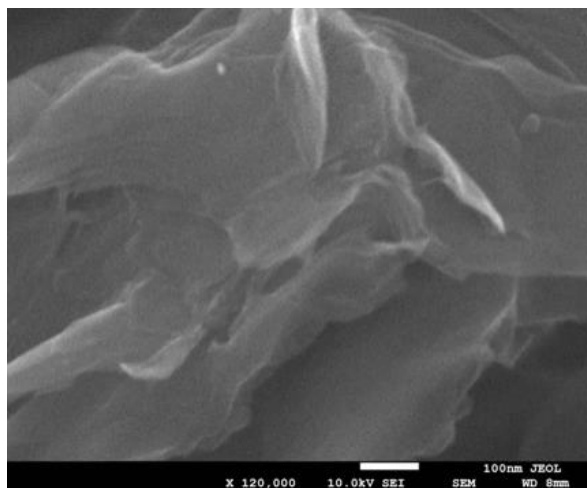


Fig. 5.1c: SEM image of GO.

5.2 Flow Table Test

The workability behaviour in terms of flow table test of 1:2 and 1:3 ratio cement-sand mortars based on OPC cement with different amounts of GO are shown in Fig. 5.2a, and Fig.5.2b, respectively. Similarly, Fig.5.2c and Fig.5.2d shows the workability behaviour of 1:2 and 1:3 ratio cement-sand mortar based on PPC cement, respectively. The results of the flow table test indicate that, for all types of mortar samples such as 1:2 and 1:3 cement-sand ratio, including OPC and PPC based cement mortars, the workability in terms of the final flow diameter of the flow table is reduced with the addition of GO compared to the control mortar mix (without GO). It may be noted that the average of the flow table test is based on six tests.

However, the maximum reduction is noted with the addition of 0.03% GO by weight of cement for all mixes. The highest reduction for OPC-based cement-sand mortar has been noted for 1:2 (1GM1) and 1:3 (2GM1) cement-sand mixtures by 23% and 15% compared to the control, respectively (Fig 5.2a and Fig. 5.2b).

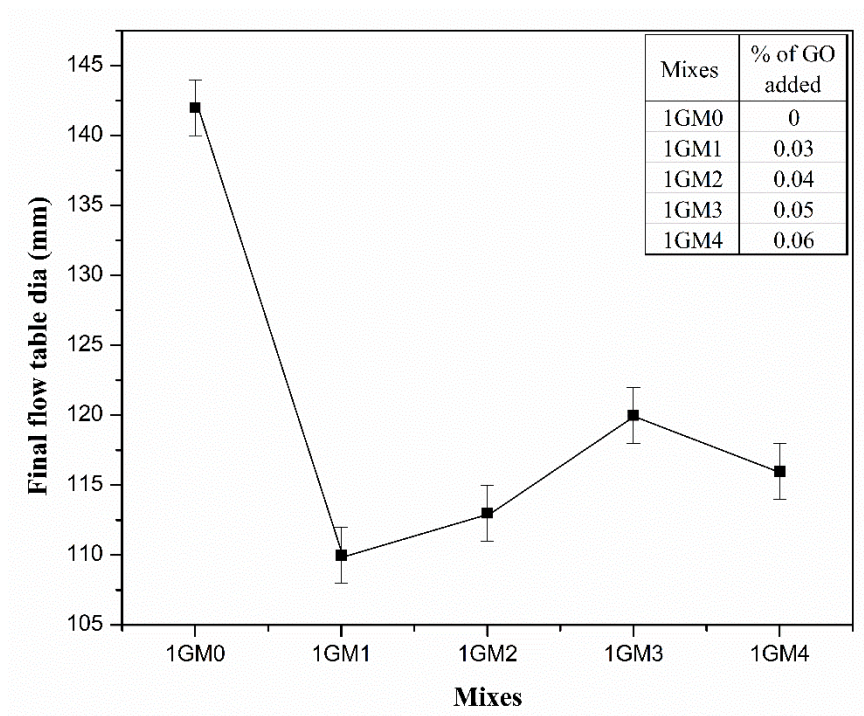


Fig. 5.2a: Flow table test results of GO modified OPC 1:2 cement-sand mortar mixes.

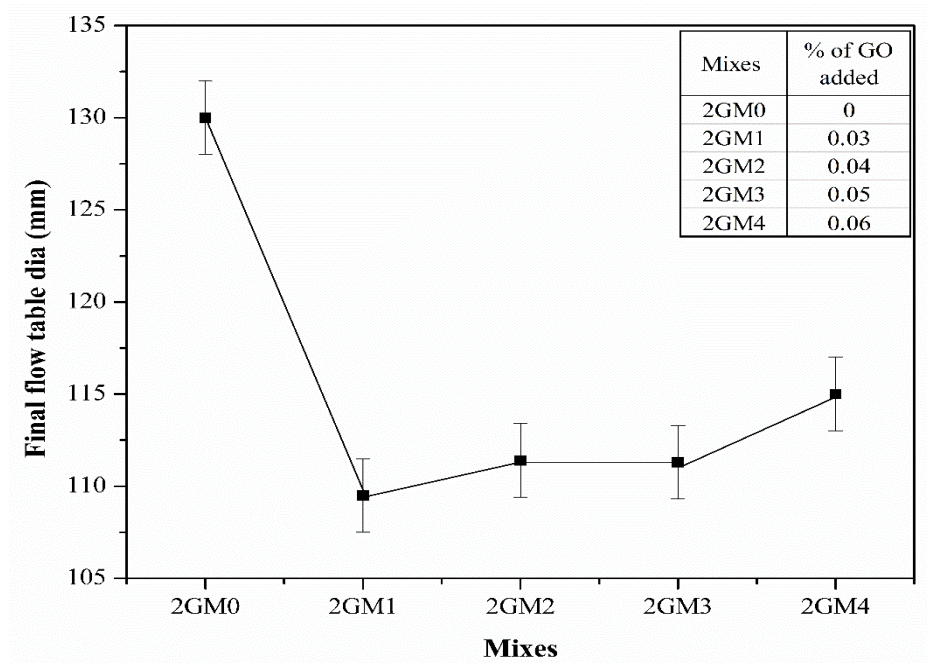


Fig. 5.2b: Flow table test results of GO modified OPC 1:3 cement-sand mortar mixes.

For PPC based cement-sand mortar maximum reduction is noted by 18% and 12% for 1:2 (3GM1) and 1:3 (4GM1) cement-sand ratio mortar compared to the control, respectively (Fig 5.2c and Fig. 5.2d).

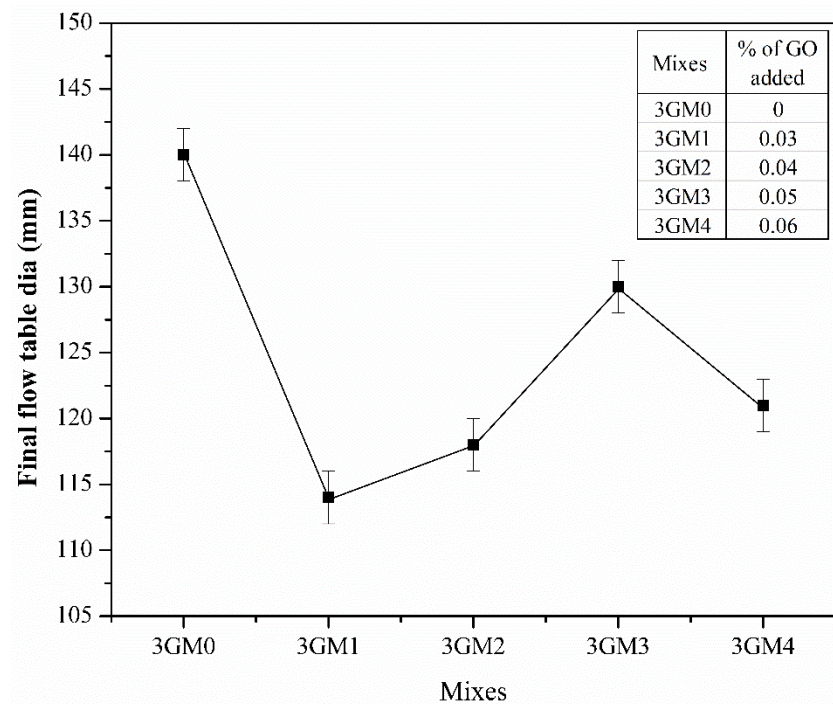


Fig. 5.2c: Flow table test results of GO modified PPC 1:2 cement-sand mortar mixes.

Moreover, the addition of more amount of GO such as 0.04%, 0.05%, and 0.06% for all types of mixtures such as OPC based 1:2, 1:3, and PPC based 1:2 and 1:3 cement-sand ratio mortar, the fluidity of cement-sand mortar reduced compared to the control sample but higher than the 0.03% of GO added cement-sand mortar. The large specific surface area of the GO nanosheet and its ability to absorb free water from its surface area is the main reason for the reduction in the fluidity of the GO modified cement-sand mortar. The agglomeration of GO nanoparticles may be the possible reason for the lower absorption with high dosages of GO. Similar results were also reported by previous studies [5–8]. This is due to the chemical composition of GO. It has been noted that the chemical composition of GO used throughout this study is almost similar to that of the previous researchers. A contradictory result was also reported by previous studies, such as GO cannot influence the fluidity behaviour of cement composites [9]. Therefore, it is always necessary to check the chemical composition of the GO, before use.

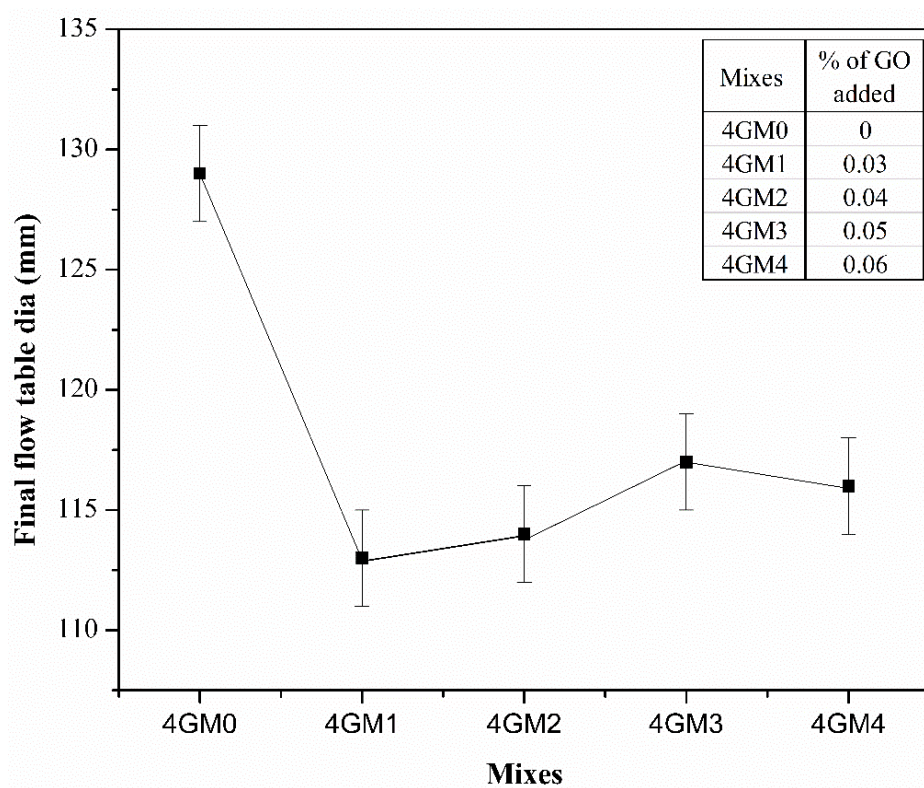


Fig. 5.2d: Flow table test results of GO modified PPC 1:2 cement-sand mortar mixes.

5.3 Compressive Strength Test

The compressive strength of OPC and PPC based different cement-sand mortar mixes, with and without GO is presented in Fig. Fig.5.3a, Fig.5.3b, Fig.5.3c, and Fig.5.3d. As usual, the compressive strength of each mortar mix (with/without GO) increases with the increase in curing age.

For OPC based 1:2 and 1:3 cement-sand mortar, it is noted that the compressive strength increases significantly up to 0.05% of GO addition by weight of cement, at all curing ages (3 days, 7 days, and 28 days). Furthermore, addition of 0.06% GO the compressive strength reduces drastically below the control mix (without GO) at all curing ages. The improvement in compressive strength is comparatively higher at initial age, such as at 3 days compared to that of 7 and 28 days. However, the maximum improvement is observed with the addition of 0.05% GO at all curing ages. In comparison to the control mix, the compressive strength of OPC 1:2 cement-sand mortar (Fig. 5.3a) increases by 49%, 25%, and 20% after 3 days, 7 days, and 28 days of curing ages, respectively, with the addition of 0.05% GO (1GM3). Addition of 0.03% and 0.04%, the compressive strength increases by 12% and 25% compared to the control at 3 days of curing age, respectively. After 7 days of curing age, compressive strength increases by 11% and 17% with the addition of 0.03% and 0.04% of GO, respectively. The improvement in compressive strength of mortar after 28 days of curing age is noted by 9% and 13% for 0.03% and 0.04% GO addition, respectively. Similarly, for OPC 1:3 cement-sand ratio mortar, with the addition of 0.05% GO(2GM3), the compressive strength increases by 27%, 19%, and 13% after 3 days, 7 days, and 28 days of curing ages, respectively, compared to the control mix (Fig. 5.3b). With the addition of 0.3% and 0.4% of GO, the compressive strength of cement-sand mortar increases by 18% and 22% after 3 days of curing age as compared to the control, respectively. The improvement in compressive strength of mortar at 7 days curing of age is

noted by 11% and 15% for 0.03% and 0.04% GO addition, respectively. After 28 days of curing age, incorporation of 0.03% and 0.04% of GO, improvement of the compressive strength is noted by 7% and 10%, respectively.

The compressive strength test results of cement mortar using PPC instead of OPC with different percentages of GO addition are shown in Fig 5.3c for cement sand ratio of 1:2 and in Fig 5.3d for cement sand ratio of 1:3. The compressive strength behavior of PPC based mortar sample with different percentages of GO addition has been almost similar to the OPC based GO modified cement-sand mortar. However, the optimum percentage of GO addition in PPC based mortar is 0.04% for both cement-sand ratios of 1:2 and 1:3. Addition of 0.05% GO, the compressive strength increases compared to the control mix, but lower than the 0.04% GO added mortar mixes at all curing ages. Moreover, the compressive strength showed similar results to the OPC-based cement-sand mortar with the addition of 0.06% of GO.

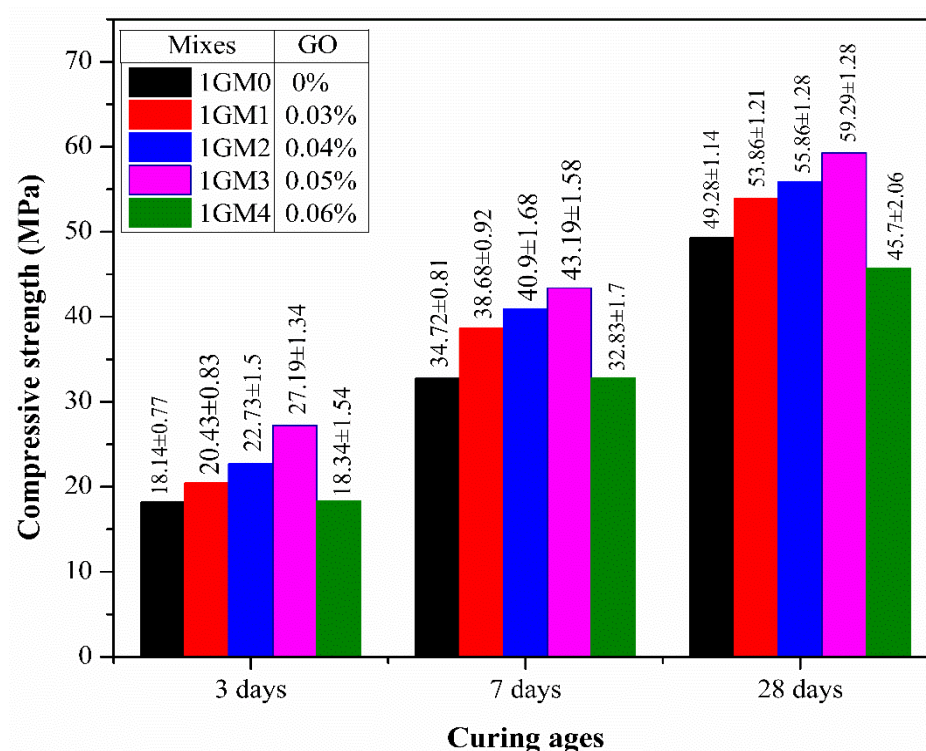


Fig. 5.3a: Compressive strength of GO modified OPC 1:2 cement-sand mortar mixes with different curing ages.

Table 5.1: Details of compressive strength of OPC based 1:2 cement mortar with/without GO.

Mixes	% of GO added	3 days of curing age		7 days of curing age		28 days of curing age	
		Compressive strength (MPa)	Enhancement %	Compressive strength (MPa)	Enhancement %	Compressive strength (MPa)	Enhancement %
1GM0	0	18.18	---	34.72	---	49.28	---
1GM1	0.03%	20.43	12.38	38.68	11.41	53.86	9.29
1GM2	0.04%	22.73	25.03	40.9	17.80	55.86	13.35
1GM3	0.05%	27.19	49.56	43.19	24.40	59.29	20.31
1GM4	0.06%	18.34	0.88	32.83	-5.44	45.7	-7.26

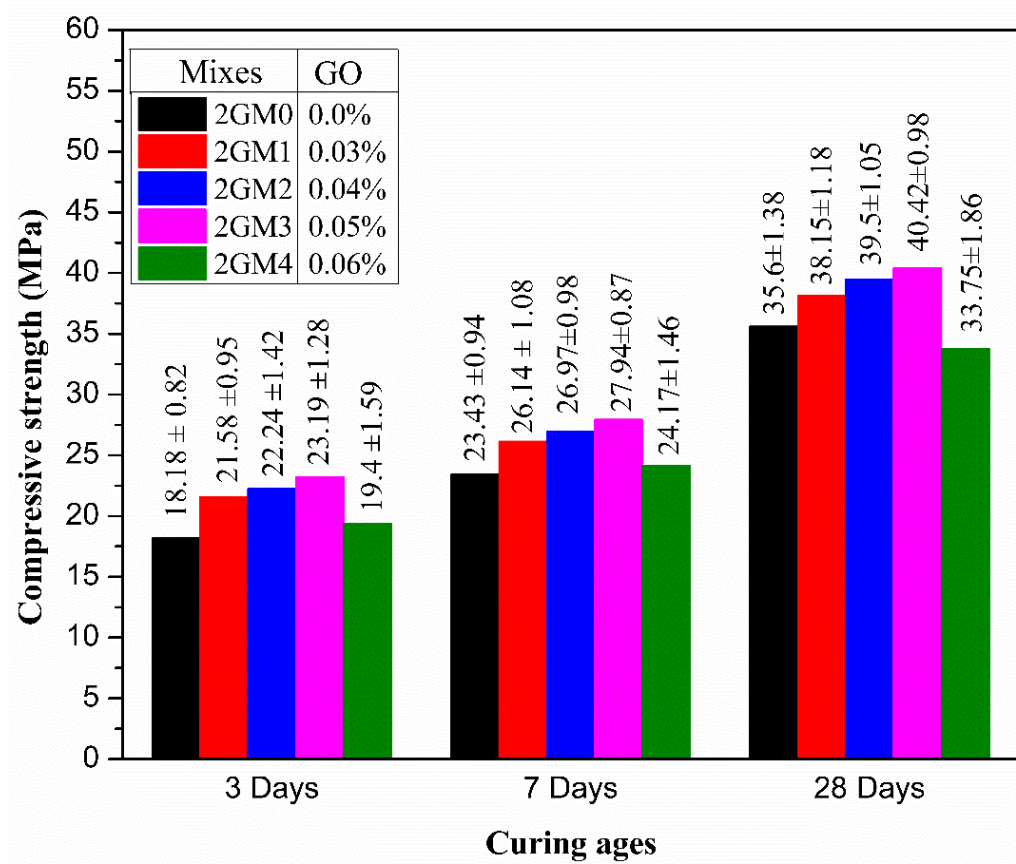


Fig. 5.3b: Compressive strength of GO modified OPC 1:3 cement-sand mortar mixes with different curing ages.

Table 5.2: Details of compressive strength of OPC based 1:3 cement mortar with/without GO.

Mixes	% of GO added	3 days of curing age		7 days of curing age		28 days of curing age	
		Compressive strength (MPa)	Enhancement %	Compressive strength (MPa)	Enhancement %	Compressive strength (MPa)	Enhancement %
2GM0	0	18.18	---	23.43	---	35.6	---
2GM1	0.03%	21.58	18.70	26.14	11.57	38.15	7.16
2GM2	0.04%	22.24	22.33	26.97	15.11	39.5	10.96
2GM3	0.05%	23.19	27.56	27.94	19.25	40.42	13.54
2GM4	0.06%	19.4	6.71	24.17	3.16	33.75	-5.20

Fig 5.3c shows the compressive strength behavior of PPC based 1:2 cement-sand ratio mortar with/without GO at different curing ages. For PPC 1:2 cement-sand ratio mortar, the compressive strength increases by 26%, 15%, and 12% at 3 days, 7 days, and 28 days of curing ages, with the addition of 0.04% GO compared to the control mix, respectively. After 3 days of curing age, the compressive strength of PPC based mortar is improved by 9% and 13%, as compare to the control mix with 0.03% and 0.05% of GO addition, respectively. The improvement in compressive strength of mortar at 7 days curing age is noted by 7% and 10% for 0.03% and 0.05% GO addition, respectively. After 28 days of curing age, incorporation of 0.03% and 0.04% of GO, compressive strength improves by 6% and 9%, respectively. Fig. 5.3d shows that the compressive strength of PPC based 1:3 cement-sand ratio mortar with/without GO at different curing ages such as 3 days, 7 days, and 28 days. After 3 days of curing age, the compressive strength increases by 12%, 29%, and 21% for 0.03%, 0.04%, and 0.05% GO addition, with respect to the control mix, respectively. The compressive strength improvement is noted after 7 days of curing age by 5%, 24%, and 10% for 0.03%, 0.04% and 0.05% GO addition, respectively. After 28 days of curing age, incorporation of 0.03%, 0.04%, and 0.05% of GO, compressive strength improves by 5%, 14%, and 9%, respectively.

As a consequence, the increase in compressive strength of GO modified OPC and PPC based cement mortar suggested that the bond developed between the GO and cement mortar is

effective under the loading condition. Also, the addition of GO has a positive impact on the degree of hydration shown by XRD analysis, FESEM analysis, and EDX analysis discussed later, which could directly transform into mechanical properties such as compressive strength. In addition, GO as a nan-scale material, can easily fill the pores of the cement mortar shown by MIP test elaborated later, making the material more solid and denser. Further, the nano-reinforcing effect of GO is mainly responsible for the enhancement of the compressive strength of GO modified cement mortar.

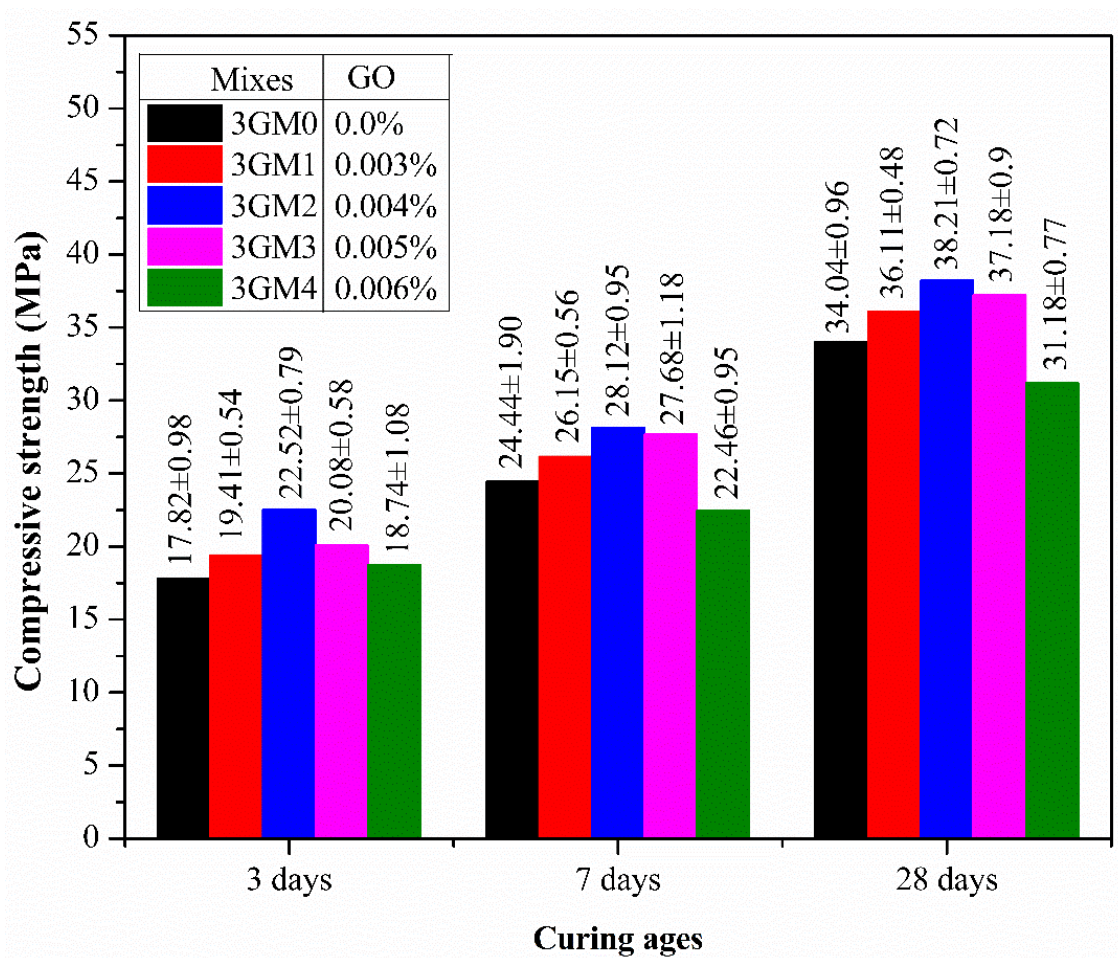


Fig. 5.3c: Compressive strength of GO modified PPC 1:2 cement-sand mortar mixes with different curing ages.

Table 5.3: Details of compressive strength of PPC based 1:2 cement mortar with/without GO.

Mixes	% of GO added	3 days of curing age		7 days of curing age		28 days of curing age	
		Compressive strength (MPa)	Enhancement %	Compressive strength (MPa)	Enhancement %	Compressive strength (MPa)	Enhancement %
3GM0	0	17.82	---	24.44	---	34.04	---
3GM1	0.03%	19.41	8.92	26.15	7.00	36.11	6.08
3GM2	0.04%	22.52	26.37	28.12	15.06	38.21	12.25
3GM3	0.05%	20.08	12.68	27.68	13.26	37.19	9.25
3GM4	0.06%	18.71	4.99	22.46	-8.10	31.18	-8.40

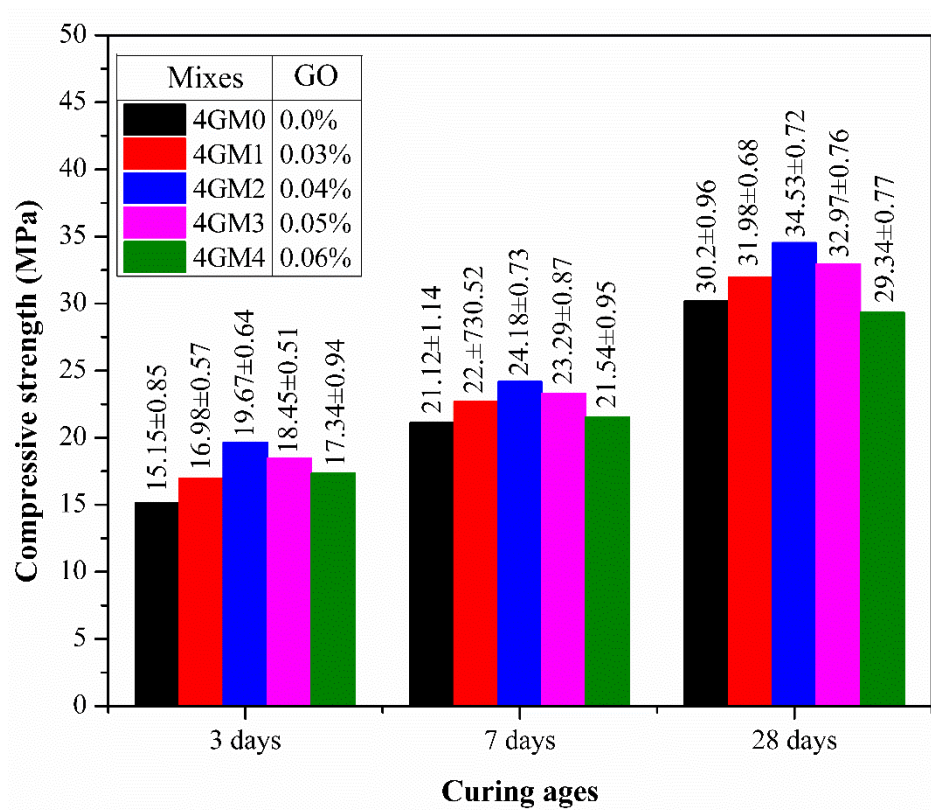


Fig. 5.3d: Compressive strength of GO modified PPC 1:3 cement-sand mortar mixes with different curing ages.

Table 5.4: Details of compressive strength of PPC based 1:3 cement mortar with/without GO.

Mixes	% of GO added	3 days of curing age		7 days of curing age		28 days of curing age	
		Compressive strength (MPa)	Enhancement %	Compressive strength (MPa)	Enhancement %	Compressive strength (MPa)	Enhancement %
4GM0	0	15.15	---	21.21	---	30.2	---
4GM1	0.03%	16.98	12.08	22.73	7.17	31.98	5.89
4GM2	0.04%	19.67	29.83	24.18	14.00	34.53	14.34
4GM3	0.05%	18.45	21.78	23.29	9.81	32.97	9.17
4GM4	0.06%	17.34	14.46	21.54	1.56	29.34	-2.85

5.4 Split Tensile Strength Test

The split tensile strength of OPC and PPC based both cement-sand ratio mortar with/without GO is shown in Fig 5.4a, Fig 5.4b, Fig. 5.4c, and Fig 5.4d, after 28 days of curing age. It is noted that the split tensile strength of OPC and PPC based both cement-sand mortar increases with the addition of a small quantity of GO concerning the control mix. Similar observations were also reported in previous literatures [10–12]. For OPC, both mixes such as 1:2 and 1:3 cement-sand ratio mortar split tensile strength significantly increases up to 0.05% of GO addition. For PPC based mortar, the maximum split tensile strength is noted with the addition of 0.04% GO addition, for both mixes such as 1:2 and 1:3 cement-sand ratio mortar.

Fig 5.4a shows the split tensile strength behaviour of OPC 1:2 cement-sand mortar with/without GO. The maximum enhancement of split tensile strength is noted by 27% with the addition of 0.05% GO addition, with respect to the control mix after 28 days of curing. With the inclusion of 0.03%, 0.04%, and 0.06% GO, the split tensile strength increases by 12%, 20%, and 15% compared to the control mix, respectively. The split tensile behaviour of OPC based 1:3 cement-sand mortar with/without GO is similar to the OPC based 1:2 mortar mixes, shown in Fig 5.4b. The maximum improvement of split tensile strength is recorded by 19% with 0.05% GO addition with respect to the control mix, after 28 days of curing ages. The enhancement is

observed for split tensile strength by 10%, 14%, and 9% concerning to the control for 0.03%, 0.04%, and 0.06% of GO addition, respectively.

Fig. 5.4c shows the split tensile strength behaviour of PPC based cement-sand mortar with/without GO after 28 days of curing age. The split tensile strength significantly enhances up to 0.04% GO addition. The maximum enhancement of split tensile strength is observed by 22% with respect to the control mix for 0.04% (3MG2) GO addition. With the inclusion of 0.03% GO, the split tensile strength increases by 10% after 28 days of curing. Further, more amount of GO incorporation such as 0.05% and 0.06%, split tensile of GO modified mortar reduces with respect to 0.04% of GO added mortar (3MG2), but enhances compared to control mix (3GM0) by 17% and 9% respectively. The split tensile behaviour of PPC based 1:3 cement-sand mortar with/without GO is similar to the PPC based 1:2 mortar mixes, shown in Fig 5.4d. The maximum enhancement of split tensile is noted by 20% with the inclusion of 0.04% GO (4MG2), with respect to the control mix after 28 days of curing. Addition of 0.03% (4MG1), 0.05% (4MG3), and 0.06% (4MG4) GO, the split tensile strength increases by 8%, 15%, and 10% compared to the control mix, after 28 days of curing age, respectively.

The improvement in tensile strength of the cement mortar based on PPC and GO modified OPC consequently indicated that the link formed between the cement mortar and GO is effective under the loading conditions. However, it is established that GO has a high tensile strength itself [13,14] and the GO shape is like a 2D nanosheets [15] which act as a fibre in nano-scale to arrest the macro-cracks of the cement composites thereby improving the tensile strength of cementitious materials.

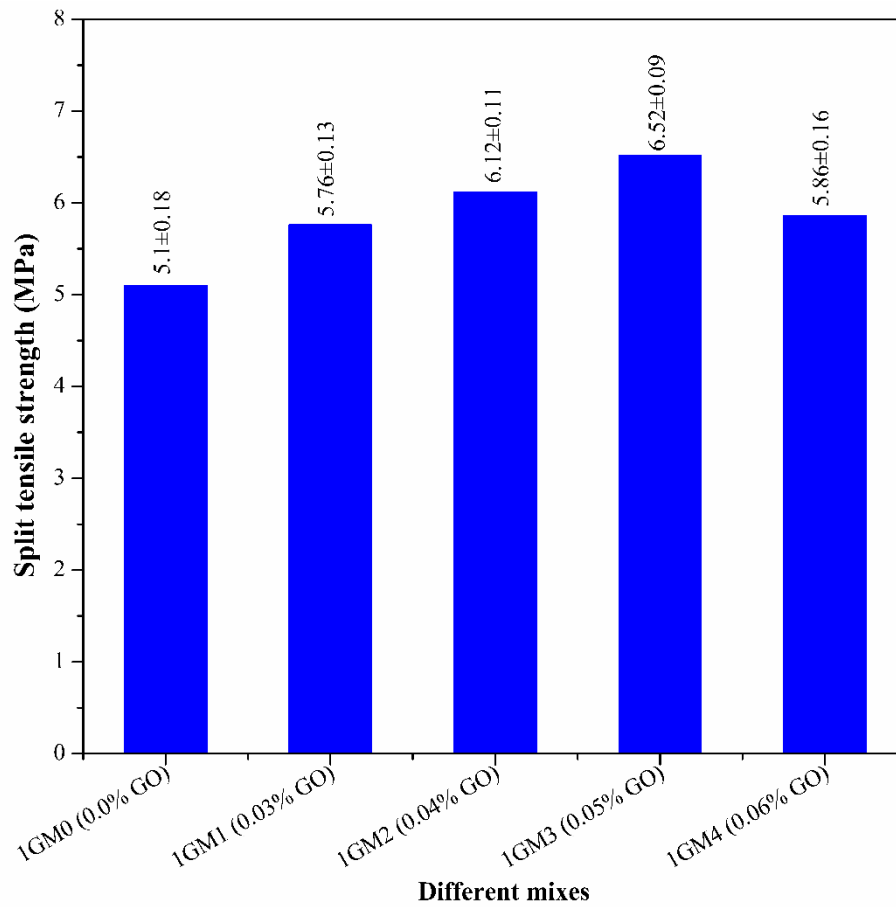


Fig. 5.4a: Split tensile strength behaviour of OPC based mortar of 1:2 (cement: sand) ratio with/without GO after 28 days of curing.

Table 5.5: Details of split tensile strength of OPC based 1:2 cement mortar with/without GO.

Mixes	% of GO added	Split tensile strength (MPa)	Enhancement %
1GM0	0	5.1	---
1GM1	0.03%	5.76	12.94
1GM2	0.04%	6.12	20.00
1GM3	0.05%	6.52	27.84
1GM4	0.06%	5.86	14.90

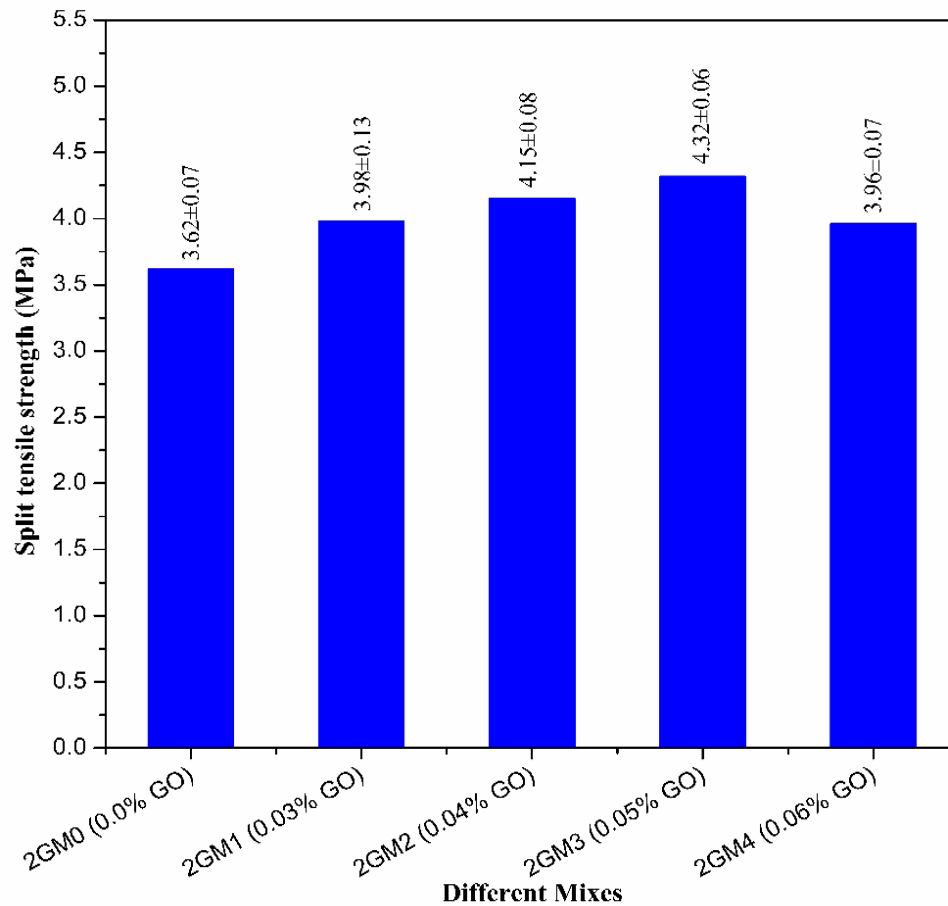


Fig. 5.4b: Split tensile strength behaviour of OPC based mortar of 1:3 cement-sand ratio with/without GO after 28 days of curing.

Table 5.6: Details of split tensile strength of OPC based 1:3 cement mortar with/without GO.

Mixes	% of GO added	Split tensile strength (MPa)	Enhancement %
2GM0	0	3.62	---
2GM1	0.03%	3.98	9.94
2GM2	0.04%	4.15	14.64
2GM3	0.05%	4.32	19.34
2GM4	0.06%	3.96	9.39

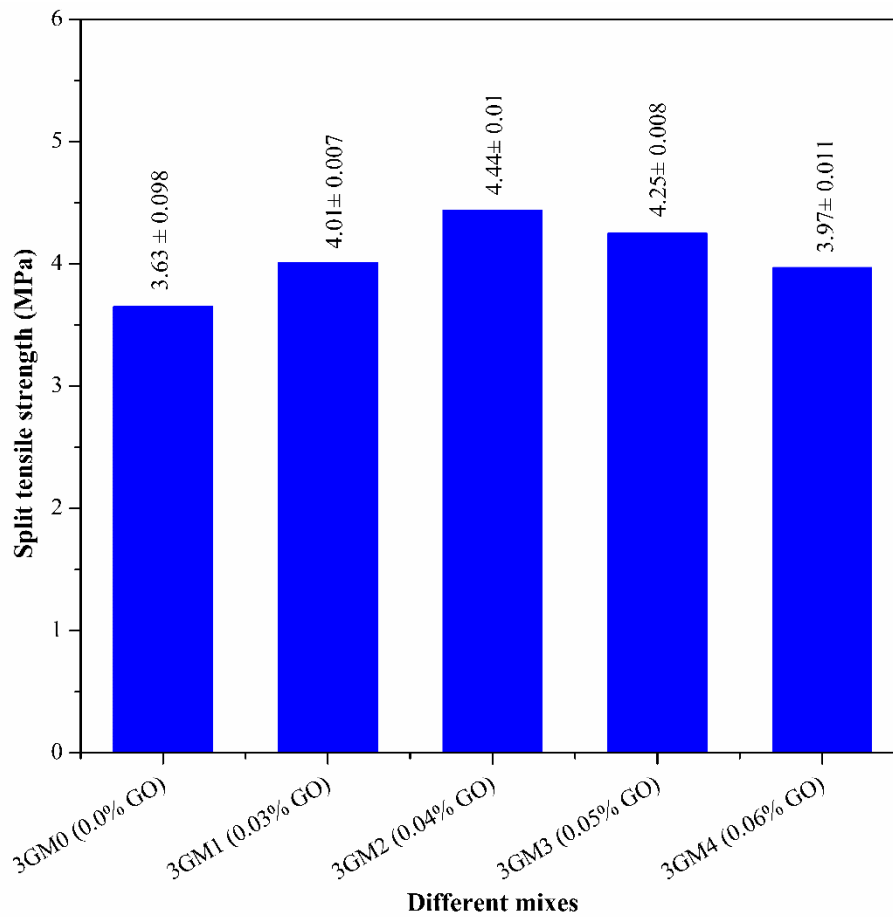


Fig. 5.4c: Split tensile strength behaviour of PPC based mortar of 1:2 cement-sand ratio with/without GO after 28 days of curing.

Table 5.7: Details of split tensile strength of PPC based 1:2 cement mortar with/without GO.

Mixes	% of GO added	Split tensile strength (MPa)	Enhancement %
3GM0	0	3.63	---
3GM1	0.03%	4.01	10.47
3GM2	0.04%	4.44	22.31
3GM3	0.05%	4.25	17.08
3GM4	0.06%	3.97	9.37

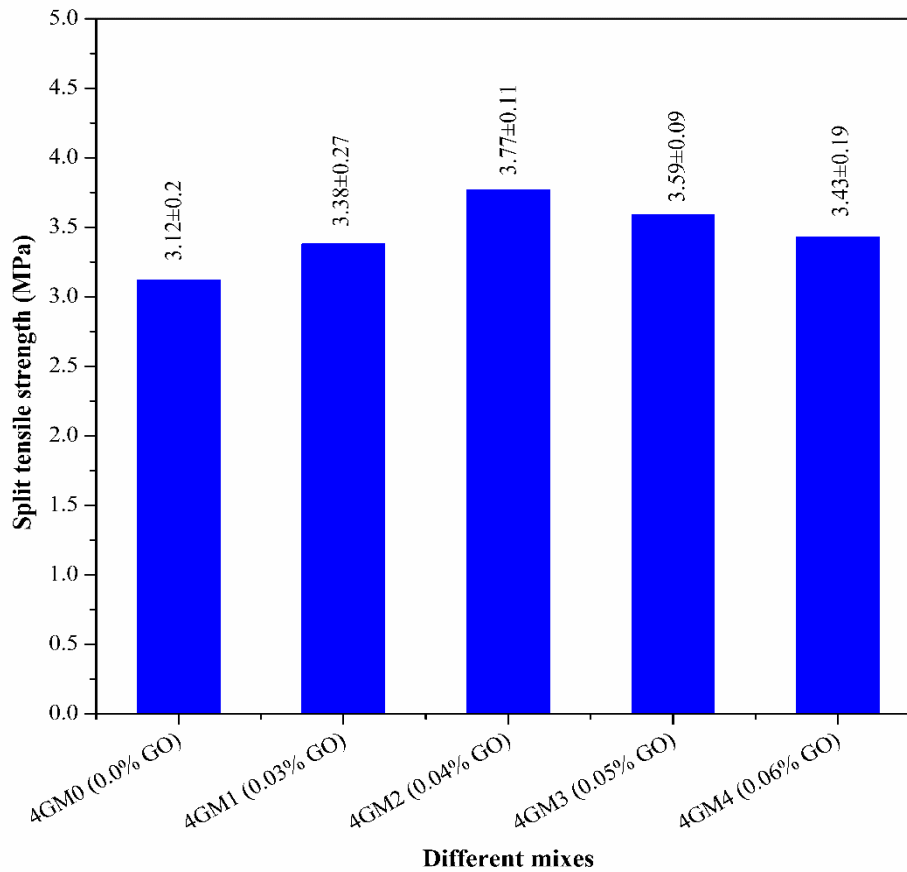


Fig. 5.4d: Split tensile strength behaviour of PPC based mortar of 1:3 cement-sand ratio with/without GO after 28 days of curing.

Table 5.8: Details of split tensile strength of PPC based 1:3 cement mortar with/without GO.

Mixes	% of GO added	Split tensile strength (MPa)	Enhancement %
4GM0	0	3.12	---
4GM1	0.03%	3.38	8.33
4GM2	0.04%	3.77	20.83
4GM3	0.05%	3.59	15.06
4GM4	0.06%	3.43	9.94

5.5 Flexural Strength Test

The flexural strength test result behaviour of GO modified cement-sand mortar shows a similar trend of split tensile test results. The flexural strength of OPC and PPC based GO modified cement-sand mortar and control mortar at 28 days are shown in Fig. 5.5a, 5.5b, 5.5c, and 5.5d.

It is noted that the flexural strength of both cement-sand mortar specimens increases with the inclusion of a small amount of GO nano-particles with respect to the control. The structural refinement of GO modified cement-sand mortar may be the root cause of strength improvement.

The flexural strength behaviour of the OPC-based 1:2 cement:sand ratio mortar with and without GO is shown in Fig. 5.5a. The maximum enhancement of flexural strength is noted with the 0.05% of GO addition by 26% compared to the control mix, after 28 days of curing. Further, with the addition of more amount of GO such as 0.06%, the flexural strength increases compared to control mortar but reduces compared to 0.05% of GO added mix (1GM3). With the incorporation of 0.03%, 0.04%, and 0.06% of GO the flexural strength is increased by 11%, 21%, and 15% with respect to the control mix, respectively. The flexural strength behaviour of OPC based 1:3 cement-sand ratio mortar with/without GO is shown in Fig. 5.5b. After 28 days of curing, it is noted that a 15% increase in flexural strength is achieved with 0.05% of GO addition compared to the control mix. The flexural strength increased by 9%, 12%, and 8% in comparison to the control mix with the addition of 0.03%, 0.04%, and 0.06% GO, respectively.

Fig. 5.5c shows the flexural strength behaviour of PPC based 1:2 cement-sand mortar with/without GO. As compared to the control mix, the flexural strength test result after 28 days of curing age shows the maximum improvement by 32% with 0.04% of GO addition (3GM2). Further, the addition of more amount of GO such as 0.05% and 0.06%, enhances the flexural strength with respect to the control but reduces compared to 0.04% of GO addition. In comparison to the control mix, the addition of 0.03%, 0.05%, and 0.06% of GO increased the flexural strength by 23%, 25%, and 17%, respectively. The flexural strength test result of PPC 1:3 cement-sand ratio mortar with/without GO shows the similar trend of PPC 1:2 cement-sand ratio mortar shown in Fig 5.5d. The maximum enhancement is noted with 0.04% GO addition by 20% compared to the control mortar (4GM0), after 28 days of curing age. In comparison to

the control mortar, the flexural strength improves by 5%, 17%, and 7% with the addition of 0.03%, 0.05%, and 0.06% GO, respectively.

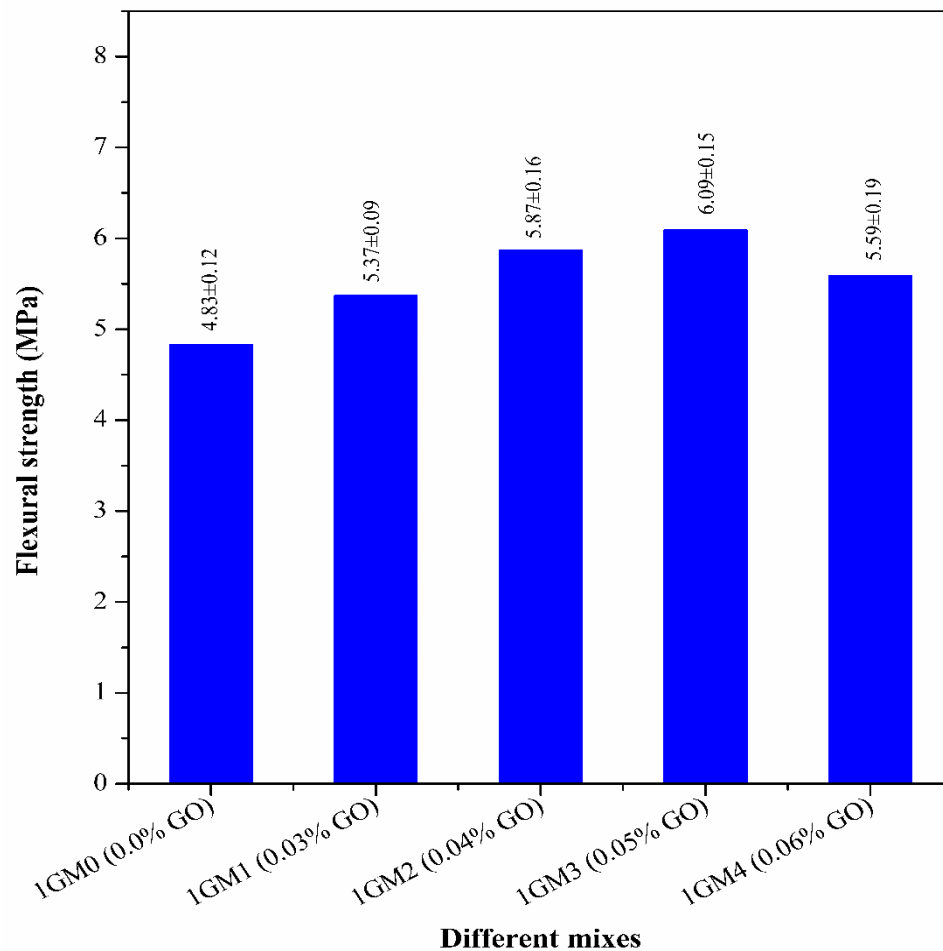


Fig. 5.5a: Flexural strength behaviour of OPC 1:2 cement-sand ratio mortar with/without GO after 28 days curing.

Table 5.9: Details of flexural strength of OPC based 1:2 cement mortar with/without GO.

Mixes	% of GO added	Flexural strength (MPa)	Enhancement %
1GM0	0	4.83	---
1GM1	0.03%	5.37	11.18
1GM2	0.04%	5.87	21.53
1GM3	0.05%	6.09	26.09
1GM4	0.06%	5.59	15.73

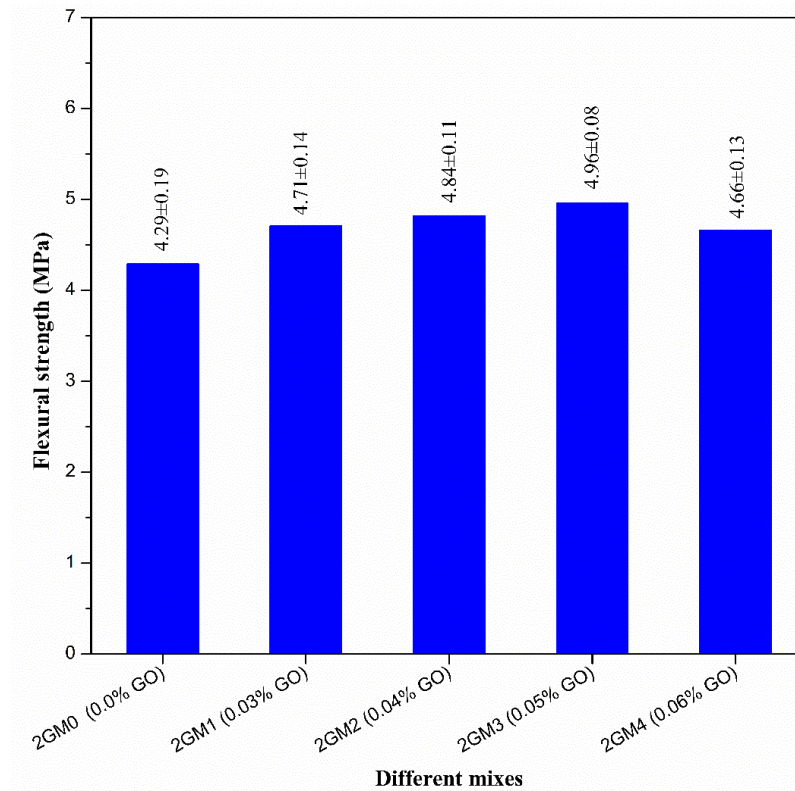


Fig. 5.5b: Flexural strength behaviour of OPC 1:3 cement-sand ratio mortar with/without GO after 28 days of curing.

According to XRD, FESEM, and EDX analyses all of which will be discussed later, the addition of GO positively affects the degree of hydration, which could translate into mechanical properties. Further, GO has been shown to have a high tensile strength on its own [9,10], and its shape is like a 2D nanosheets [11], which function as a nanoscale fibre that prevents the cement composites' macrocracks and increases the flexural strength of cementitious materials.

Table 5.10: Details of flexural strength of OPC based 1:3 cement mortar with/without GO.

Mixes	% of GO added	Flexural strength (MPa)	Enhancement %
2GM0	0	4.29	---
2GM1	0.03%	4.71	9.79
2GM2	0.04%	4.81	12.12
2GM3	0.05%	4.96	15.62
2GM4	0.06%	4.66	8.62

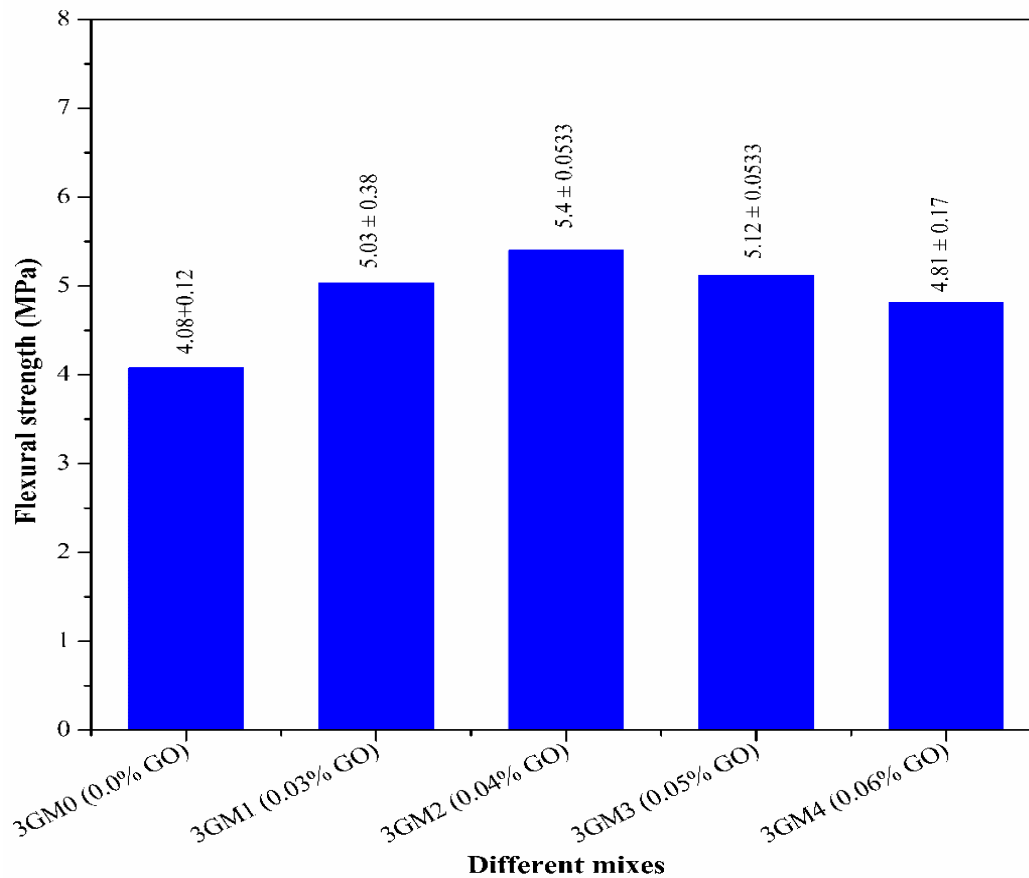


Fig. 5.5c: Flexural strength behaviour of PPC 1:2 cement-sand ratio mortar with/without GO after 28 days of curing.

Table 5.11: Details of flexural strength of PPC based 1:2 cement mortar with/without GO.

Mixes	% of GO added	Flexural strength (MPa)	Enhancement %
3GM0	0	4.08	---
3GM1	0.03%	5.03	23.28
3GM2	0.04%	5.4	32.35
3GM3	0.05%	5.12	25.49
3GM4	0.06%	4.81	17.89

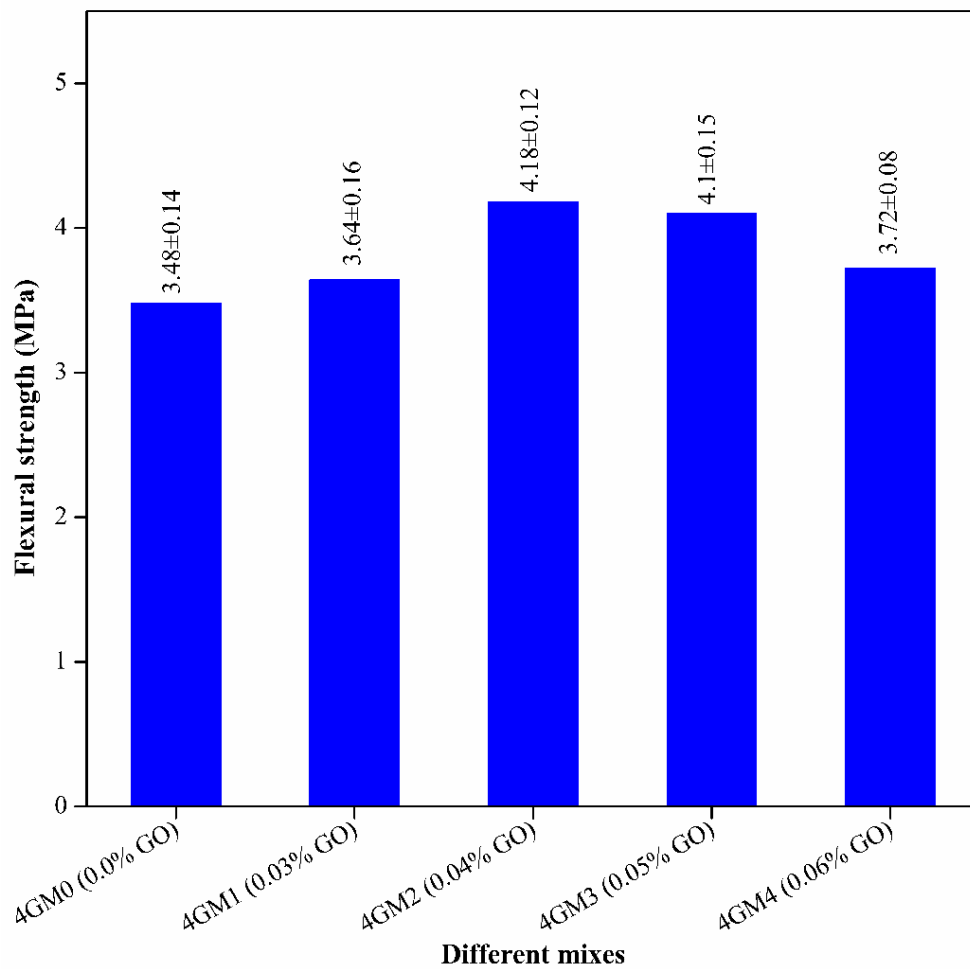


Fig. 5.5d: Flexural strength behaviour of PPC 1:2 cement-sand ratio mortar with/without GO after 28 days of curing.

Table 5.12: Details of flexural strength of PPC based 1:2 cement mortar with/without GO.

Mixes	% of GO added	Flexural strength (MPa)	Enhancement %
4GM0	0	4.83	---
4GM1	0.03%	5.37	11.18
4GM2	0.04%	5.87	21.53
4GM3	0.05%	6.09	26.09
4GM4	0.06%	5.59	15.73

5.6 Measurement of Young Modulus (E value)

The behaviour of the modulus of elasticity of OPC and PPC-based cement-sand control mortar and GO-modified mortar containing different percentages of GO, such as 0.03% to 0.06% is shown in Fig. 5.6. The young modulus of cement mortar has been measured by using a cylinder with a diameter of 100 mm and a height of 200 mm, in accordance with Indian Standard IS: 516 (part-8)-2019. It is observed that the inclusion of a small quantity of GO enhances the modulus of elasticity of cement-sand mortar prepared by both OPC and PPC cement concerning the control mortar, after 28 days of curing age. The enhancement in modulus of elasticity is possible for more compacted micro-structure, denser hydration products, and low pore volume of GO modified cement mortar due to the presence of a small quantity of GO which are reported by MIP test, FESEM analysis, and EDS analysis.

For OPC based mortar the optimum percentage is found 0.05% of GO for both types of mixes such as 1:2 and 1:3 cement-sand ratio mortar. The modulus of elasticity is enhanced by 23% and 17% for 1:2 and 1:3 cement-sand mortar with the addition of 0.05% GO, respectively. For OPC 1:2 cement-sand mortar, the modulus of elasticity is enhanced by 6% and 15% with the addition of 0.03% and 0.04% of GO, respectively. The inclusion of 0.03% and 0.04% of GO into OPC based 1:3 cement-sand mortar, the enhancement of elastic modulus is noted by 11% and 14%, respectively. Further, with the addition of more amount of GO such as 0.06%, the modulus of elasticity of OPC based 1:2 and 1:3 cement-sand ratio mortar is reduced by 12% and 6% concerning to the control mortar, respectively.

The behaviour of modulus elasticity of PPC based GO modified mortar shows the similar behaviour of OPC based GO modified mortar. The optimum percentage is noted 0.04% of GO for PPC based 1:2 and 1:3 cement-sand ratio mortar. The enhancement is observed by 16% and 24% for 1:2 and 1:3 cement-sand mortar with the incorporation of 0.04% of GO, respectively. The modulus of elasticity of PPC based 1:2 cement-sand mortar enhances by 7% and 12% with

the inclusion of 0.03% and 0.05% of GO concerning the control sample, respectively. For 1:3 PPC based cement-sand ratio mortar enhancement of modulus of elasticity is observed due to 0.03% and 0.05% of GO by 9% and 22% concerning the control sample, respectively.

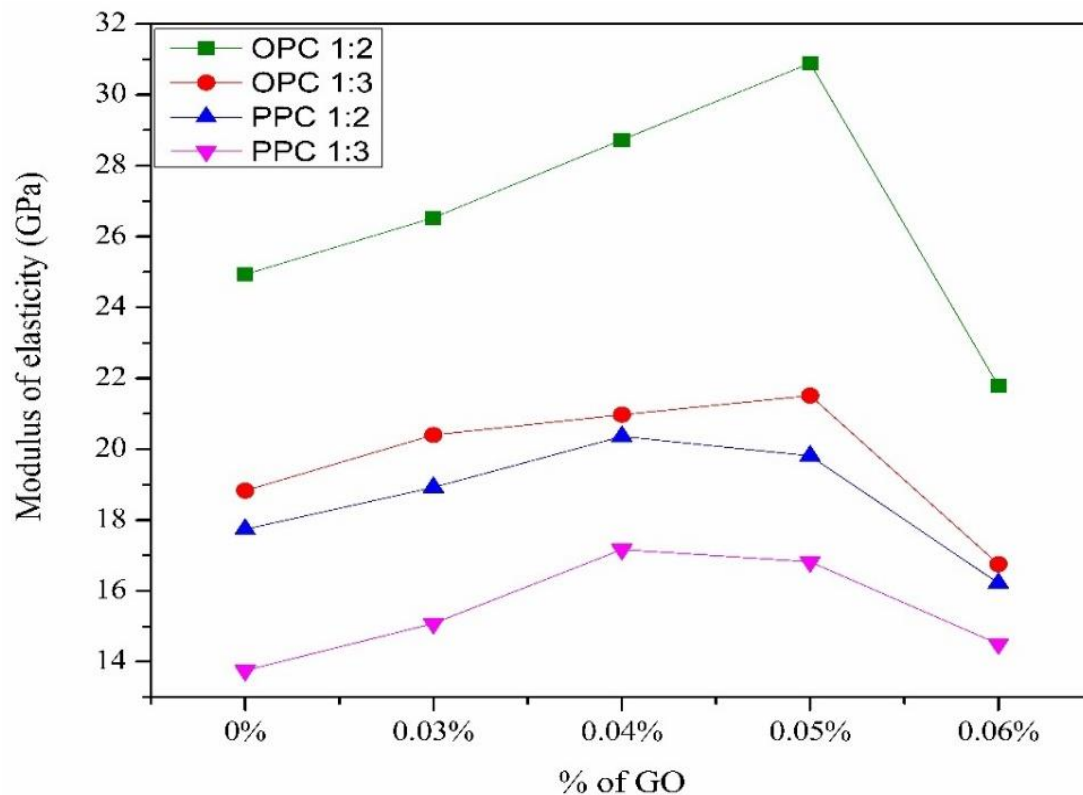


Fig. 5.6: Modulus of elasticity of different cement based (OPC and PPC) mortar with different dosages of GO.

5.7 Ultrasonic Pulse Velocity (UPV) Test

The ultrasonic pulse velocity test has conducted after 28 days of curing before the compressive strength test of standard cube specimens $70.06\text{mm} \times 70.06\text{mm} \times 70.06\text{mm}$. Fig. 5.7 shows the variation in ultrasonic pulse velocity test results of GO modified OPC and PPC based mortar with a cement-to-sand ratio of 1:2 and 1:3. The results indicate that the velocity of the ultrasonic pulse through GO based cement-sand mortar increases with the increase in the addition of different percentage of GO (0.03%, 0.4%, 0.05%, and 0.06%). Such an increase in pulse

velocity test results suggests that the cement mortar has solidified, strengthened, get densified micro-structure, and formed a strong link between the GO and the cement mortar. For OPC cement-sand ratios of 1:2 and 1:3, the pulse velocity reaches its maximum value at GO content of 0.05%. This supports the result of maximum compressive strength, split tensile strength, and flexural strength at the optimum percentage of GO addition. It is noted that the ultrasonic pulse velocity test results of PPC based cement mortar show the similar trend of OPC based GO modified cement-sand mortar. However, the addition of 0.04% GO for PPC-based cement mortar shows the highest pulse velocity for both 1:2 and 1:3 ratio mortar.

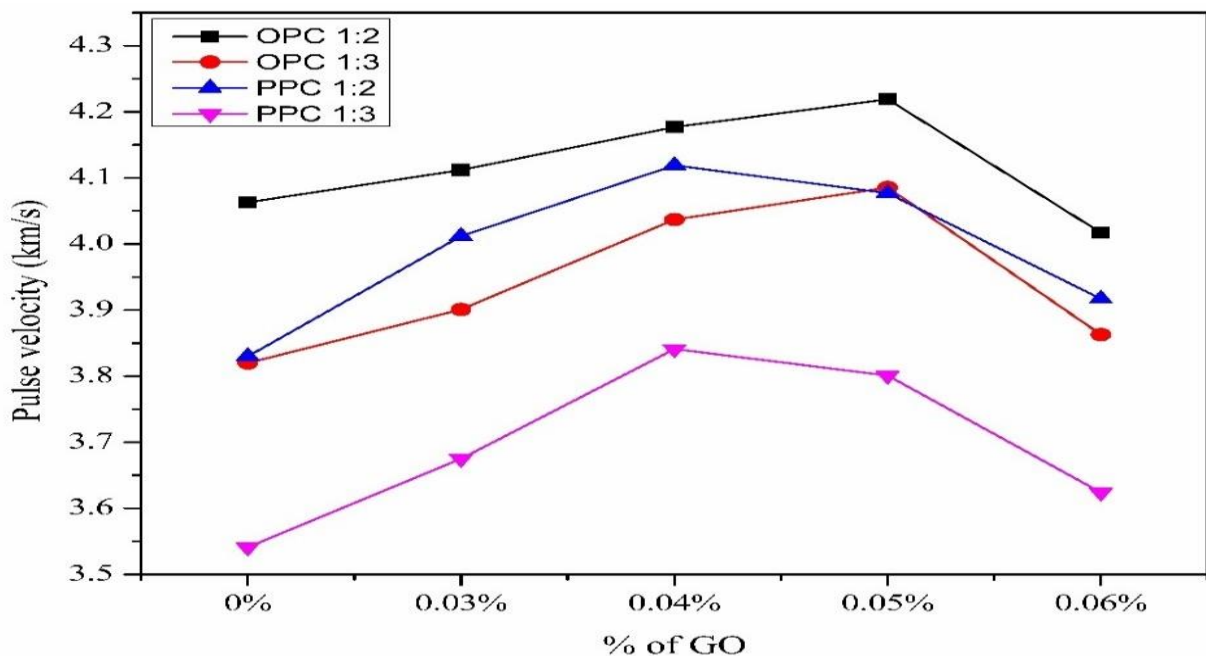


Fig. 5.7: Ultrasonic pulse velocity test result of GO modified OPC and PPC based cement-sand mortar.

5.8 Sorptivity Test

Figs. 5.8a and 5.8b show the results of the sorptivity test of cement mortar using OPC with cement sand ratios of 1:2 and 1:3 for different percentages of GO addition. This test measures the rate of water absorption, occurring due to capillary suction along a unidirectional rise, as a

function of time. It has been shown that the trend of water absorption rate of GO modified cement-sand mortar and control mix (without GO) are almost similar. The rate of water absorption of cement-sand mortar decreases with the respect of control mix due to the inclusion of different percentages of GO (0.03% to 0.06%). When the GO content is 0.06% and cement sand ratio is 1:2, the rate of absorption is less than the control mortar (without GO) up to 3 days after that rate of absorption is more than the control mortar (without GO). For GO addition of GO 0.06% and cement sand ratio 1:3, the rate of absorption of cement mortar fluctuated with the control mortar (without GO) all over the test period. The inclusion of 0.05% GO for both cement-sand ratios mortar of 1:2 and 1:3 results in the lowest rate of water absorption for OPC cement-sand mortar.

The sorptivity test results of GO-based cement mortar using PPC with a cement-sand ratio of 1:2 and 1:3 are shown in Fig. 5.8c and 5.8d. It is observed that the rate of water absorption of GO-based cement mortar decreases with the addition of increasing percentages (0.03% to 0.06%) of GO in cement mortar compared to the control mortar (without GO). The trend of water absorption rate of GO based OPC mortar and PPC mortar are almost similar. However, the optimum percentage of GO addition in PPC based mortar is 0.04% for both mixes 1:2 and 1:3 cement-sand mortar. The possible reason for low water absorption rate of GO modified cement-sand mortar is the presence of more amount and improved hydration products due to the addition of a small amount of GO [16,17]. Thus, at optimum GO content, cement mortar exhibits maximum strength improvement, less voids, compact microstructure, and more durable than the control mortar (without GO).

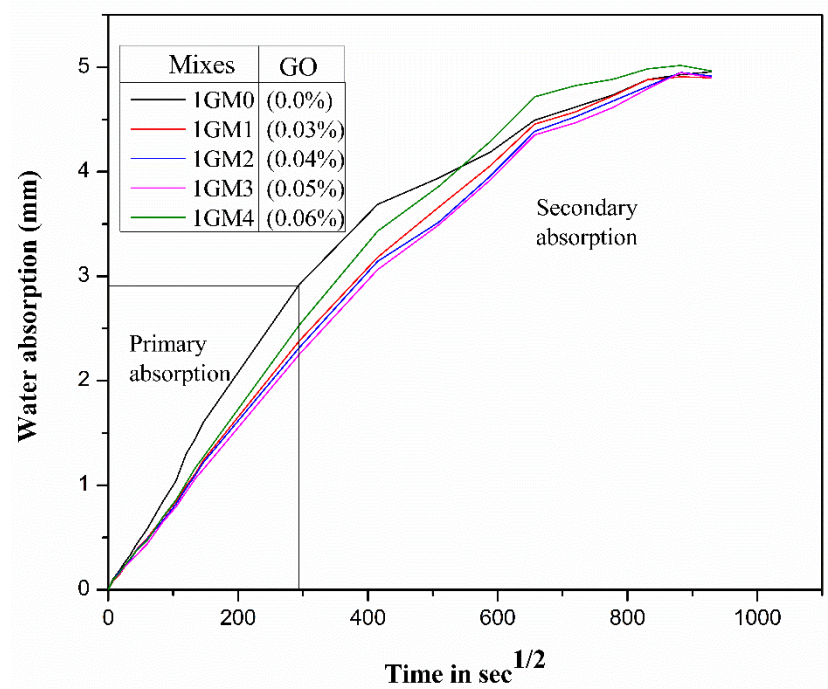


Fig. 5.8a: Sorptivity test result of GO modified cement-sand mortar using OPC with cement and sand ratio 1:2.

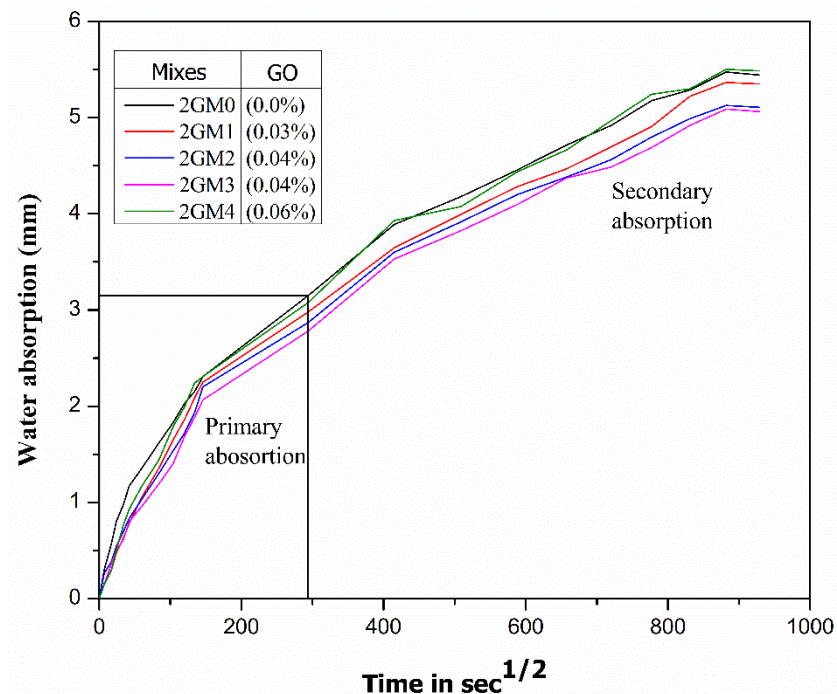


Fig. 5.8b: Sorptivity test result of GO modified cement-sand mortar using OPC with cement and sand ratio 1:3.

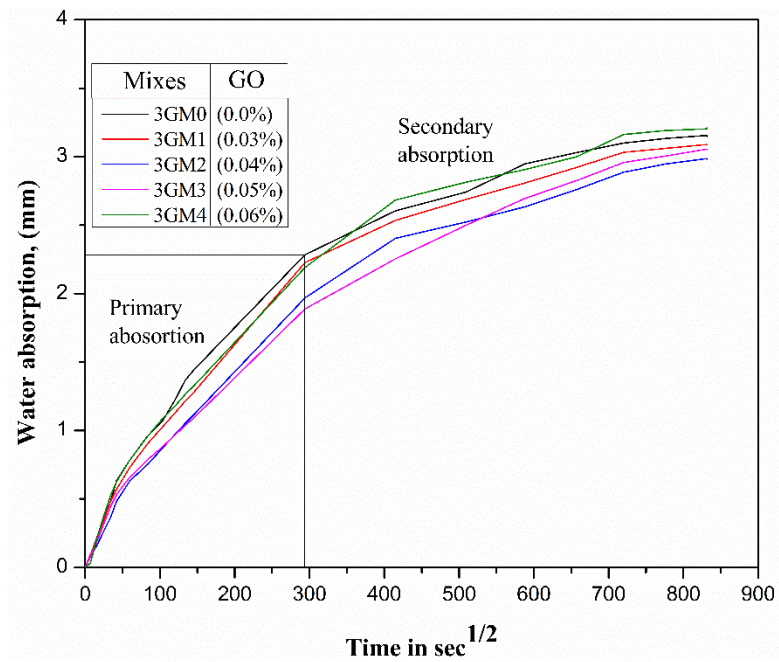


Fig. 5.8c: Sorptivity test result of GO modified cement-sand mortar using PPC with cement and sand ratio 1:3.

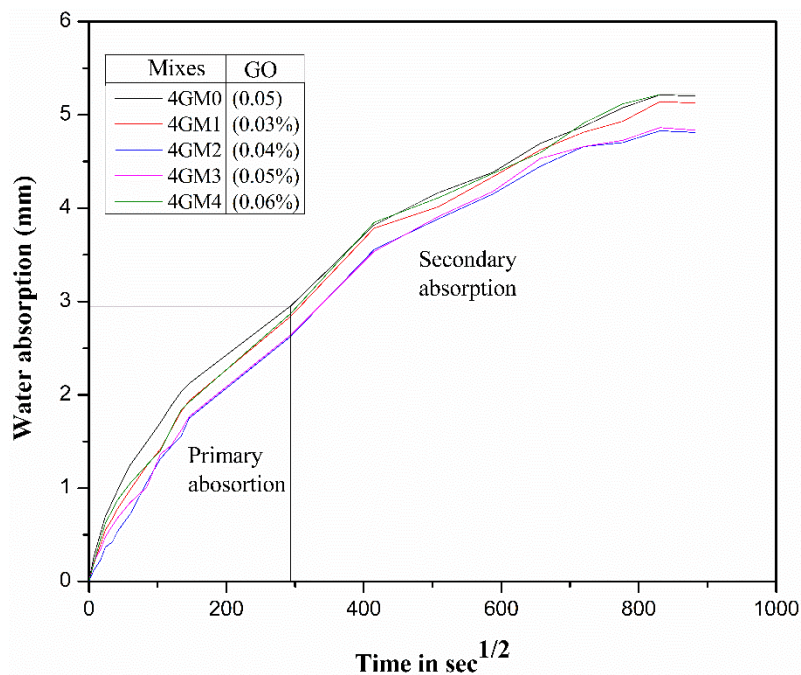


Fig. 5.8d: Sorptivity test result of GO modified cement-sand mortar using PPC with cement and sand ratio 1:3.

5.9 Rapid Chloride Penetration Test (RCPT)

The value of the chloride ion penetration test results for the 1:2 and 1:3 cement-sand ratio mortar by using both OPC and PPC for the GO modified cement mortar samples (28 days) are shown in Fig. 5.9. The amount of charge passed in RCPT for cement-sand mortar is decreased with the addition of a small amount of GO compared to control mix (without GO) for both type of cement (OPC and PPC) mortar. The large quantity of hydration products that filled the pore area/volume of the GO-modified mortar sample with a small quantity of GO may be a possible reason for the low charge passing through the samples [11,18,19]. It is observed that the lowest amount of charge passed with the addition of 0.05% GO, by 11% and 9% for OPC based 1:2 and 1:3 cement-sand ratio mortar with respect to the control, respectively. For PPC based cement mortar, for both 1:2 and 1:3 cement-sand ratio, the lowest amount of charge passed with the inclusion of 0.04% GO by 14% and 8% compared to the control sample, respectively.

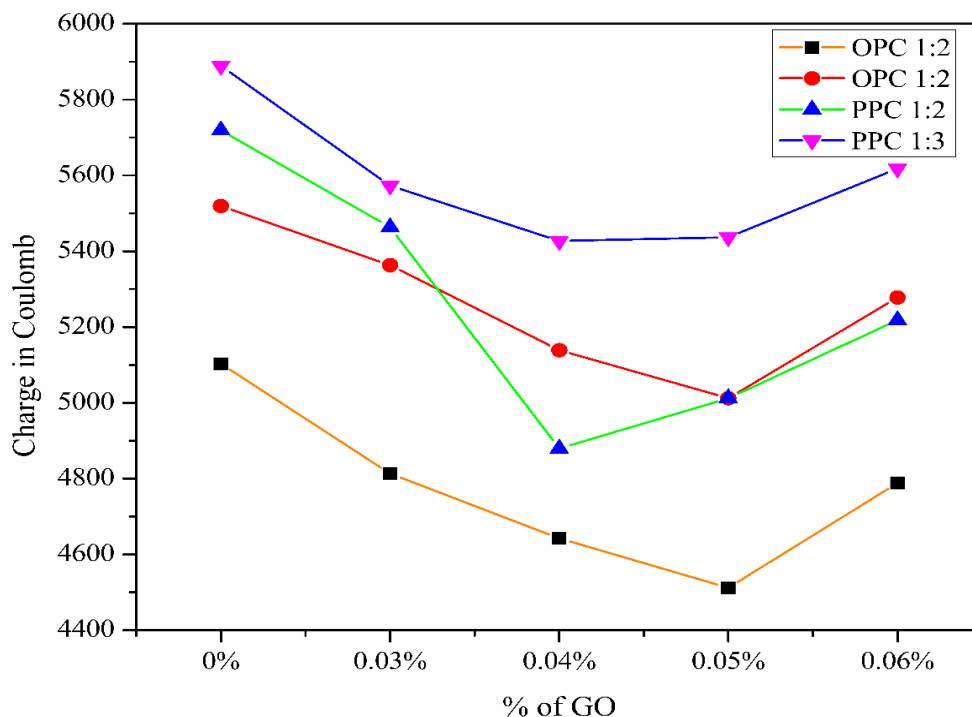


Fig. 5.9: Charged passed through different cement based (OPC and PPC) mortar with different dosages of GO.

5.10 Acid Resistance Test

The acid resistance test of OPC and PPC based cement-sand mortar with and without GO was observed by measuring compressive strength after immersing the standard cube sample in an acid/water solution (1:20, v/v). The compressive strength of GO modified OPC and PPC based mortar samples after 28 days and 56 days of acid water immersion is shown in Fig. 5.10a, 5.10b, 5.10c, and 5.10d. It is noted that there is no significant improvement in the resistance against the damage of hardened cement-sand mortar due to acid attack for GO modified mortar compared to the control sample (without GO)..

The compressive strength of OPC based 1:2 and 1:3 cement-sand ratios mortar with and without GO is shown in Fig. 5.10a and Fig. 5.10b after 28 days and 56 days in the acid water solution immersion. The maximum value of compressive strength was noted with the addition of 0.05% of GO, but the strength reduction is almost similar for the control and GO modified mortar samples after both 28 days and 56 days periods of acid water immersion. The lowest reduction of compressive is noted with the addition of 0.06% of GO (Tables 5.13 and 5.14). For OPC based 1:2 cement-sand mortar the reduction is noted by 5% low compared to the control, for 28 days and 56 days of acid water immersion. For OPC based 1:3 cement-sand mortar, the reduction is observed by 5% and 2% less than the control after 28 days and 56 days of acid water immersion, respectively.

For PPC-based GO modified mortar show a similar trend of GO modified OPC-based cement-sand against acid attack is observed. Fig. 5.10c and Fig. 5.10d show the acid resistance behaviour of different mixes of PPC based 1:2 and 1:3 cement-sand ratios mortar with different percentages of GO, respectively. After 28 days and 56 days of acid water immersion, the details behaviour of compressive strength tabulated in table 5.15 and table 5.16. The maximum compressive strength value was observed with the addition of 0.04% GO addition compared to the control after 28 days and 56 days of acid water immersion. It is noted that the addition of

0.06% of GO show lowest percentage of compressive strength decrease. For PPC 1:2 cement-sand ratio mortar the reduction is noted that 4% and 6% than the control, after 28 days and 56 days of acid water immersion. For 1:3 cement-sand ratio mortar, the reduction of compressive strength is noted around 3% low compared to control after both 28 days and 56 days of acid water immersion.

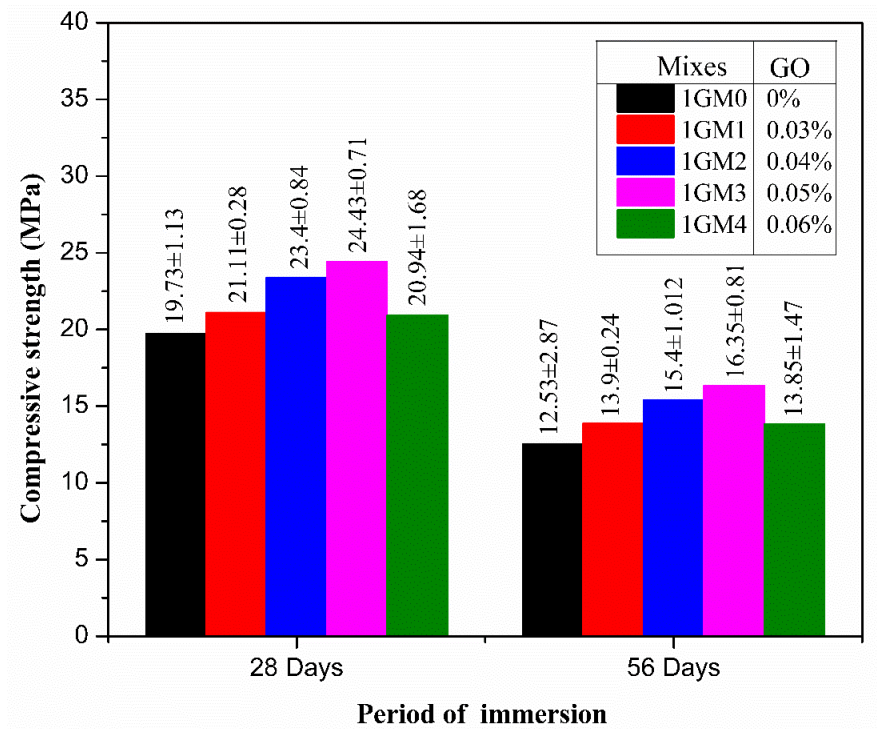


Fig. 5.10a: Acid resistance behaviour of different mixes of OPC based 1:2 cement-sand ratio mortar with different percentages of GO.

The mass loss was also observed for the control sample and GO-based modified mortar sample after 28 days and 56 days due to the immersion in acid/water solution. It is observed that for both OPC and PPC based cement-sand mortar, the loss of mass percentages (%) is similar for the control sample and the GO-modified cement-sand mortar sample. The details of mass loss for OPC and PPC based cement-sand mortar are presented in Tables 5.17, 5.18, 5.19, and 5.20.

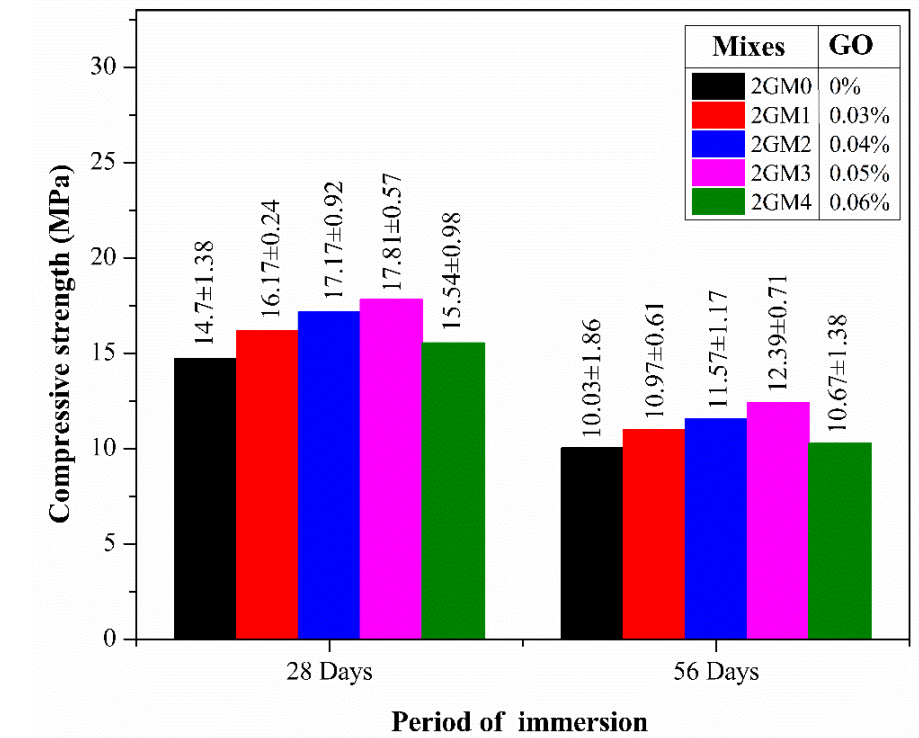


Fig. 5.10b: Acid resistance behaviour of different mixes of OPC based 1:3 cement-sand ratio mortar with different percentages of GO.

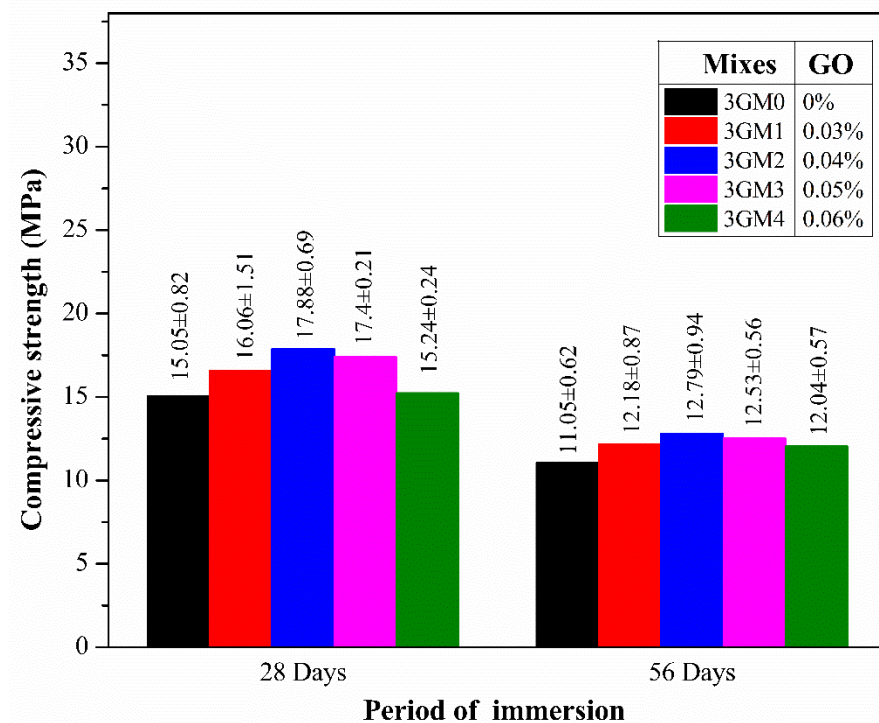


Fig. 5.10c: Acid resistance behaviour of different mixes of PPC based 1:2 cement-sand ratio mortar with different percentages of GO.

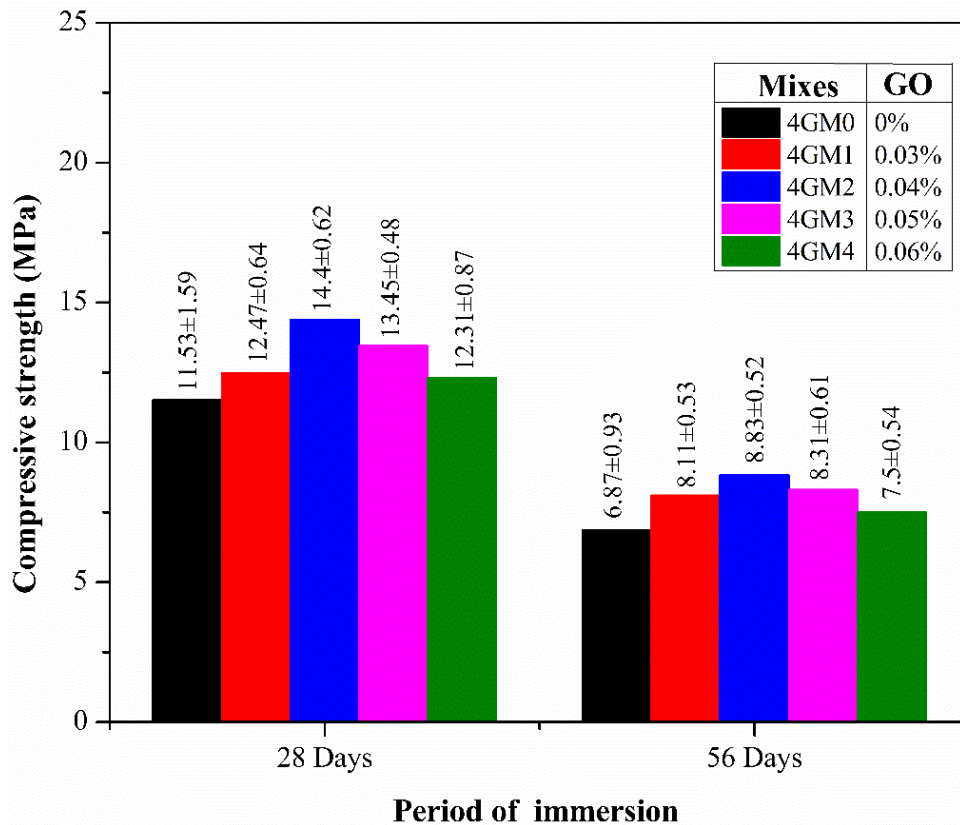


Fig. 5.10d: Acid resistance behaviour of different mixes of PPC based 1:3 cement-sand ratio mortar with different percentages of GO.

Table 5.13: Details of strength reduction of OPC based 1:2 cement-sand mortar mixes with GO.

Mixes	% of GO added	Initial strength (at 28 days of casting, MPa)	Strength after 28 days immersion (MPa)	% of strength reduction	Strength after 56 days immersion (MPa)	% of strength reduction
1GM0	0	49.28	19.73	59.96%	12.53	74.57%
1GM1	0.03	53.86	21.11	60.81%	13.9	74.19%
1GM2	0.04	55.86	23.4	58.11%	15.4	72.43%
1GM3	0.05	59.29	24.43	58.80%	16.35	72.42%
1GM4	0.06	45.7	20.94	54.18%	13.85	69.69%

Table 5.14: Details of strength reduction of OPC based 1:3 cement-sand mortar mixes with GO.

Mixes	% of GO added	Initial strength (at 28 days of casting, MPa)	Strength after 28 days immersion (MPa)	% of strength reduction	Strength after 56 days immersion (MPa)	% of strength reduction
2GM0	0	35.6	14.7	58.71%	10.03	71.83%
2GM1	0.03	38.15	16.17	57.61%	10.97	71.25%
2GM2	0.04	39.5	17.17	56.53%	11.57	70.71%
2GM3	0.05	40.42	17.81	55.94%	12.39	69.35%
2GM4	0.06	33.75	15.54	53.96%	10.27	69.57%

Table 5.15: Details of strength reduction of PPC based 1:2 cement-sand mortar mixes with GO.

Mixes	% of GO added	Initial strength (at 28 days of casting, MPa)	Strength after 28 days immersion (MPa)	% of strength reduction	Strength after 56 days immersion (MPa)	% of strength reduction
3GM0	0	34.04	15.03	55.85%	11.05	67.54%
3GM1	0.03	36.11	16.6	54.03%	12.18	66.27%
3GM2	0.04	38.21	17.88	53.21%	12.79	66.53%
3GM3	0.05	37.19	17.4	53.21%	12.53	66.31%
3GM4	0.06	31.18	15.24	51.12%	12.04	61.39%

Table 5.16: Details of strength reduction of PPC based 1:3 cement-sand mortar mixes with GO.

Mixes	% of GO added	Initial strength (at 28 days of casting, MPa)	Strength after 28 days immersion (MPa)	% of strength reduction	Strength after 56 days immersion (MPa)	% of strength reduction
4GM0	0	30.2	11.53	61.82%	6.87	77.25%
4GM1	0.03	31.98	12.47	61.01%	8.11	74.64%
4GM2	0.04	34.53	14.4	58.30%	8.83	74.43%
4GM3	0.05	32.97	13.45	59.21%	8.31	74.80%
4GM4	0.06	29.34	12.31	58.04%	7.5	74.44%

Table 5.17: Details of mass loss of OPC based 1:2 cement-sand different mortar mixes with GO.

Mixes	Initial weight (gm)	Weight after 28 days of immersion (gm)	% of mass change	Weight after 56 days of immersion (gm)	% of mass change
1GM0	784.5	727.3	7.86%	671.8	16.78%
1GM1	781.5	724.7	7.84%	668.4	16.92%
1GM2	779	725.1	7.43%	667.8	16.65%
1GM3	787.3	731.3	7.66%	681.2	15.58%
1GM4	787	732.5	7.44%	678.1	16.06%

Table 5.18: Details of mass loss of OPC based 1:3 cement-sand different mortar mixes with GO.

Mixes	Initial weight (gm)	Weight after 28 days of immersion (gm)	% of mass change	Weight after 56 days of immersion (gm)	% of mass change
2GM0	781.5	727.3	7.45%	662.8	17.91%
2GM1	783.7	725.7	7.99%	668.4	17.25%
2GM2	779	723.1	7.73%	665.8	17.00%
2GM3	783.2	730.3	7.24%	673.2	16.34%
2GM4	782	726.5	7.64%	670.1	16.70%

Table 5.19: Details of mass loss of PPC based 1:2 cement-sand different mortar mixes with GO.

Mixes	Initial weight (gm)	Weight after 28 days of immersion (gm)	% of mass change	Weight after 56 days of immersion (gm)	% of mass change
3GM0	774.5	720.3	7.52%	664.8	16.50%
3GM1	771.5	720.7	7.05%	668.4	15.42%
3GM2	775	729.1	6.30%	670.8	15.53%
3GM3	777.3	732.3	6.15%	669.2	16.15%
3GM4	777	726.5	6.95%	670.1	15.95%

Table 5.20: Details of mass loss of PPC based 1:3 cement-sand different mortar mixes with GO.

Mixes	Initial weight (gm)	Weight after 28 days of immersion (gm)	% of mass change	Weight after 56 days of immersion (gm)	% of mass change
4GM0	772.8	721.3	7.14%	665.8	16.07%
4GM1	768.5	717.7	7.08%	660.4	16.37%
4GM2	770	725.1	6.19%	664.8	15.82%
4GM3	778.3	731.3	6.43%	668.2	16.48%
4GM4	777	722.5	7.54%	670.1	15.95%

Based on the mechanical and durability test results the micro-structural study, including MIP test, XRD analysis, and FESEM analysis are carried out on OPC and PPC based 1:2 cement-sand ratio control mortar (without GO), such as 1GM0 and 3GM0, respectively, as well as OPC based with 0.05% of GO (1GM3) and PPC based 0.04% of GO (3GM2) 1:2 cement-sand mortar.

5.11 Mercury Intrusion Porosimetry (MIP) Test

The pore size distribution of both types of cement such as OPC and PPC based cement mortar (with/without GO) have been measured through the Mercury Intrusion Porosimetry (MIP) test after 28 days. Fig. 5.11a shows the OPC based 1:2 cement-sand control mortar and GO modified mortar with 0.05% of GO, in terms of $-dV/d(\log d)$ versus pore diameter (d) where V is pore volume. It is noted from the MIP test result that the volume of mercury intrusion is less in GO modified mortar compared to control mortar consistently. The large diameter pores were filled by GO agglomerates and the peak of the intruded amount of mercury shifted towards the finer pore diameter with the addition of GO into control cement-sand mortar. In comparison to the control sample, it indicates that the addition of GO modified the pore size distribution

and increased the gel pore volume of calcium silicate hydrate gel. It was clear that the critical pore size, which showed a high association with the material's permeability and diffusivity, is related to the peak of the MIP test curve [20,21].

The pore size distribution of PPC based 1:2 cement-sand ratio control mortar and GO modified cement-sand mortar with 0.04% of GO is shown in Fig. 5.11b. The MIP results of PPC based mortar sample show the similar trend of OPC based mortar sample. It indicates that the amount of mercury intrusion in GO-modified mortar is lower than in control. The peak of the intruded amount of mercury shifted towards the finer pore diameter with the addition of GO into the control cement-sand mortar.

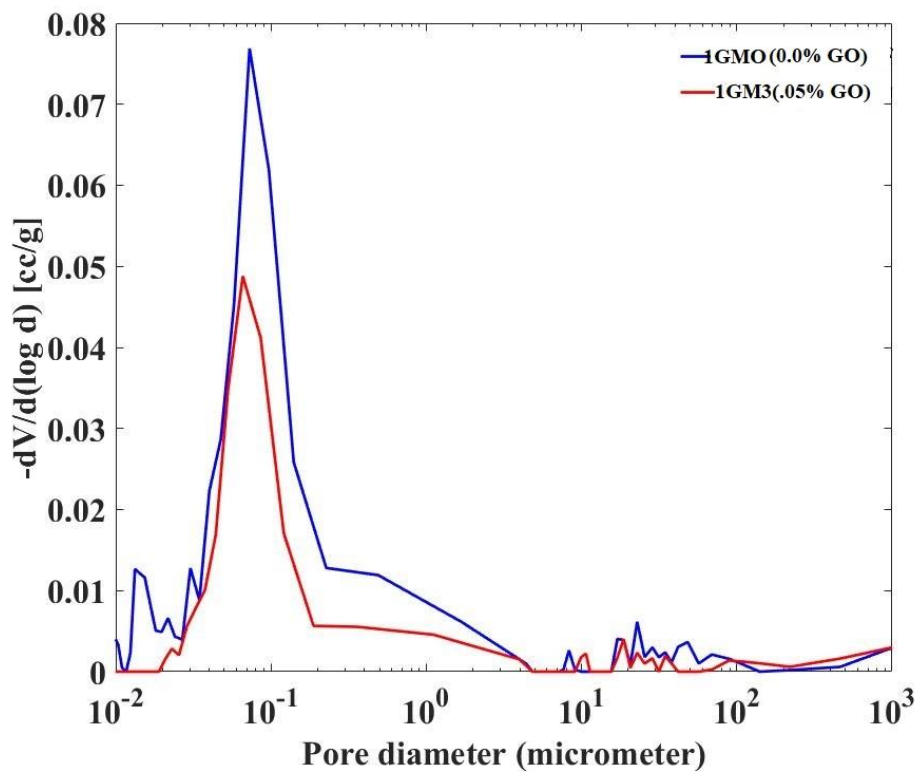


Fig. 5.11a: MIP test results OPC 1:2 cement-sand ratio control mortar and GO modified mortar with 0.05% of GO.

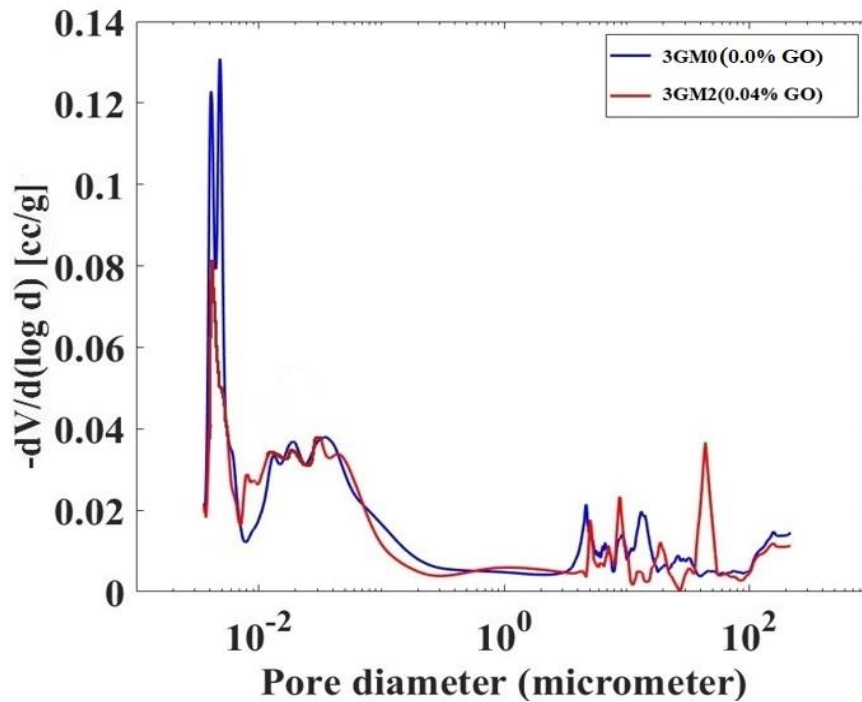


Fig. 5.11b: MIP test results PPC 1:2 cement-sand ratio control mortar and GO modified mortar with 0.04% of GO.

5.12 X-ray Diffraction Analysis (XRD)

The XRD analysis results for the OPC based 1:2 cement control mortar (without GO, 1GM0) and the GO modified cement-sand mortar (1GM3) with 0.05% GO are shown in Fig. 5.12a. The XRD analysis results clearly indicates that the higher and more peaks of C–S–H (JCPDS CARD: 14-0035) are observed in GO modified mortar (1GM3) compare to the control mortar sample (1GM0) at different values of 2θ . The significant peaks are occurs at $2\theta = 18.05^\circ, 20.9^\circ, 26.7^\circ, 28.05^\circ, 30.75^\circ, 34.15^\circ, 39.5^\circ, 50.15^\circ, 54.9^\circ, 60.0^\circ$, and 67.8° . According to these mineralogical results, GO can promote hydration processes. New compounds $\text{Ca}_4\text{Al}_2\text{SO}_{10}\text{H}_{20}$ (JCPDS CARD:45-0158), Boggsite (JCPDS CARD: 42–1379), Ankerite (JCPDS CARD: 41-0586), Gismondine (JCPDS CARD: 20-0452), Srebrodolskite (JCPDS CARD: 038-0408) and CSO (JCPDS CARD:15-0130) are formed due to incorporation of GO in cement mortar. Thus, the formation of Ankerite and Gismondine is highly responsible for

the early strength improvement. In general, gesmondine offers thermal stability and prevent decomposition of cement gel at high temperature.

Fig. 5.12b shows XRD analysis results of PPC based 1:2 ratio control mortar (GM0) and GO modified cement-sand mortar with 0.04% of GO (3GM2). The XRD analysis results clearly indicates that more C-S-H (JCPDS CARD: 14-0035) peaks are present in GO modified PPC based mortar sample at various diffraction angle values than the control sample. The significant picks are appeared at $2\theta = 10.5^\circ$, 18° , 20.8° , 26.6° , 27.9° , 50.1° , 59.9° , 67.7° , 68.2° , 73.4° and 76° . However, the increase of peaks was seen in the by-product of the cement hydration that was created through the reaction of the $-\text{COOH}$ functional groups with C_2S , C_3S phase. It is found that the inclusion of 0.04% GO into cement-sand mortar caused the formation of new compounds, such as Amstallite (JCPDS CARD: 41–1420), Brownmillerite (JCPDS CARD: 30–0226), Ettringite (JCPDS CARD: 41–1451), Boggsite (JCPDS CARD: 42–1379), and Gismondine (JCPDS CARD: 20-0452). Thus, the presence of Gismondine is a possible reason for mechanical strength improvement and long-term durability [22].

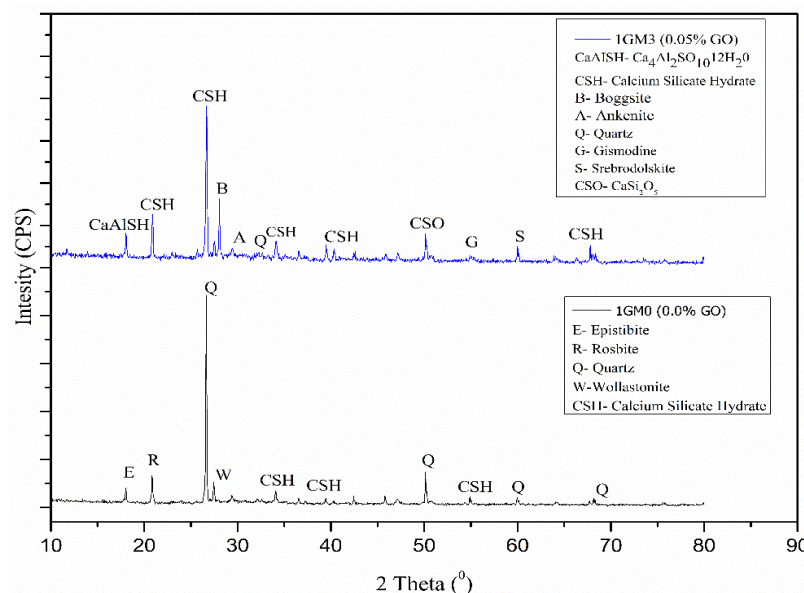


Fig. 5.12a: XRD analysis results of OPC based 1:2 cement-sand ratio control mortar and GO modified cement-sand mortar with 0.05% of GO.

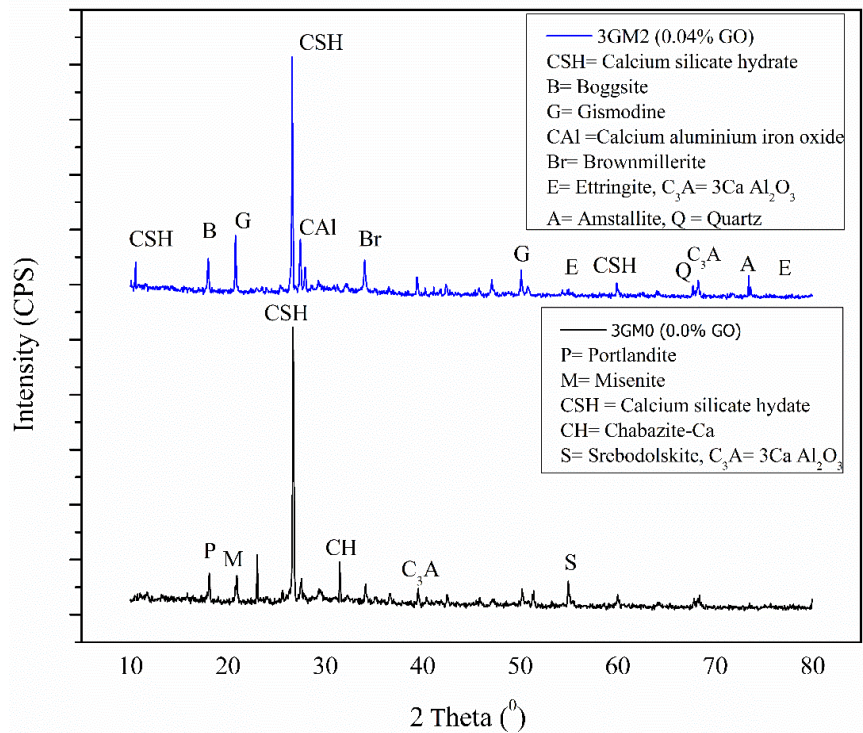


Fig. 5.12b: XRD analysis results of PPC based 1:2 cement-sand ratio control mortar and GO modified cement-sand mortar with 0.04% of GO.

5.13 Field Emission Scanning Electron Microscopy Analysis (FESEM)

Fig. 5.13a shows the morphology of the control mix (1GM0 without GO) and GO modified mix (1GM3) with 0.05% GO addition for OPC based 1:2 mortar by field emission scanning electron microscope (FESEM). There is an apparent distinction in the morphology of cement mortar containing 0.05% GO compared to the control, with significantly more dense and needle-shaped crystals. Further, it seems that the inclusion of GO was advantageous to interlocking cement hydration products like C-S-H gel and resulted in a more compacted microstructure of cement mortar, which in turn improves the mechanical and durability properties. In fact, the GO in the matrix accelerates the hydration reaction of cementitious materials and causes more heat generation [17]. It may be possible that the presence of GO enhances the mobility of ions in cement mortar, which subsequently increases the interaction of water with the cement particles and promotes the growth and formation of C-S-H into

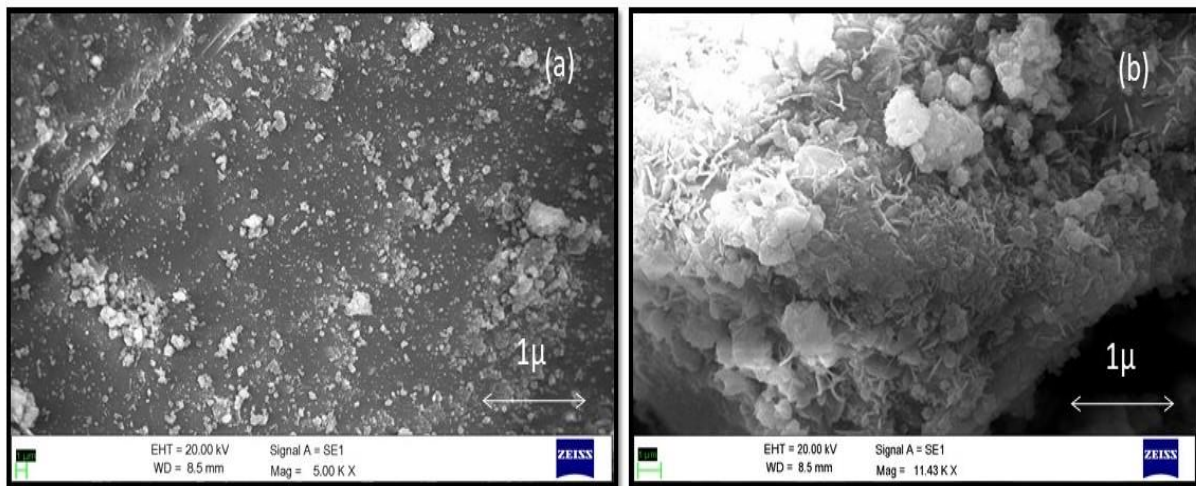


Fig. 5.13a: FESEM image of OPC based 1:2 ratio cement-sand mortar (a) control sample and (b) GO modified cement mortar with 0.05% of GO.

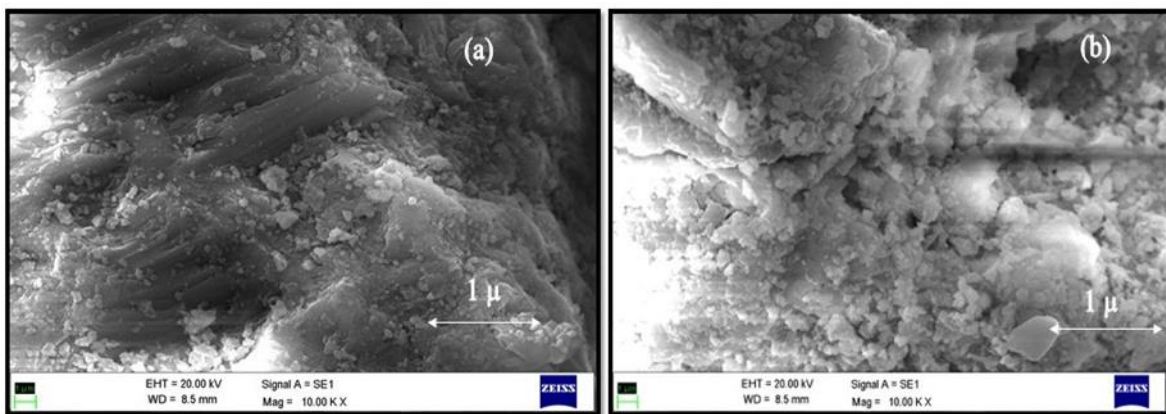


Fig. 5.13b: FESEM image of PPC based 1:2 ratio cement-sand mortar (a) control sample and (b) GO modified cement mortar with 0.04% of GO.

cement-sand mortar. It seems that these two effects have modified the pore structure of cement mortar with GO as reported earlier in the MIP test results.

Similarly, the morphology of the control mix (3GM0) and GO modified mix (3GM2) with the inclusion of 0.04% of GO for PPC based mortar of 1:2 cement mortar are examined by FESEM analysis as shown in Fig. 5.13b. A sharp difference in morphology of GO modified (3GM2) cement-sand mortar compared to the control mix (3GM0) is observed as in the case of OPC

based mortar sample. In the microstructure of GO modified cement mortar, there is a higher concentration and denser hydration products, such as C-S-H gel and a more compact microstructure that consequently led to enhanced mechanical and durability properties.

5.14 Energy Dispersive X-Ray Analysis (EDX)

Fig. 5.14a shows the EDX analysis results of control mortar (1GM0) and GO modified cement mortar (1GM3) with 0.05% of GO for OPC based 1:2 cement mortar. A significant difference in the elementary compositions as per EDX analysis is noted. The percentage of Carbon (C) and Silicon (Si) atoms is increased due to the addition of GO. The atomic percentage of C and Si is increased by about 1.3 times and more than 2 times in GO modified mortar compared to the control mix, respectively. Actually, the carbon content of GO increases the typical crystals in GO modified mortar, especially needle-shaped crystals [23]. Thus, the result of EDX analysis helps to demonstrate that the GO could participate in the formation of crystals, and also regulate the formation and growth of needle-shaped crystals, thereby further improving the mechanical properties such as compressive strength, tensile strength, etc.

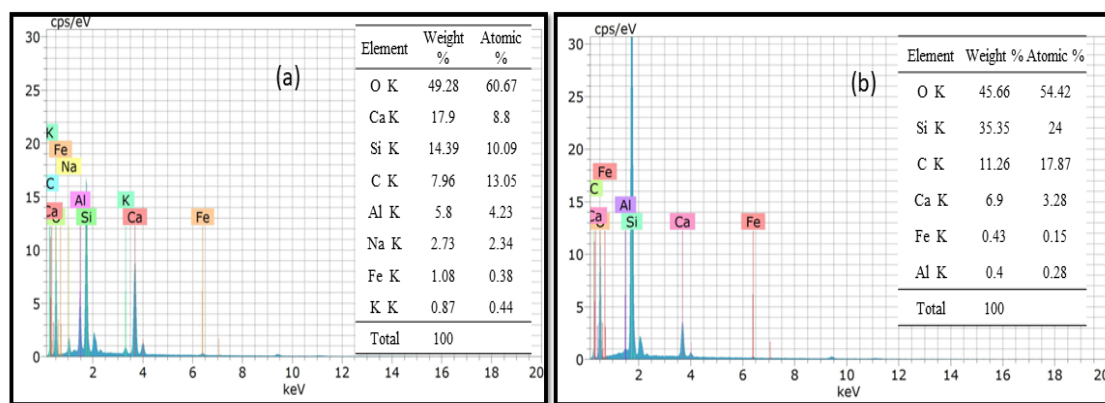


Fig. 5.14a: EDX analysis results of OPC based 1:2 cement-sand ratio (a) control mortar and (b) GO modified cement-sand mortar with 0.05% of GO.

The elemental analysis results of control mortar (3GM0) and GO modified mortar (3GM2) with 0.04% of GO for PPC based 1:2 cement-sand ratio are shown in Fig. 5.14b. The elemental

analysis of PPC based GO modified mortar shows the similar results of OPC based GO modified mortar. The Carbon (C) atom and Silicon (Si) atom percentages increase by about 1.6 times and 2 times in GO modified cement-sand mortar (0.04%) compared to the control mix, respectively.

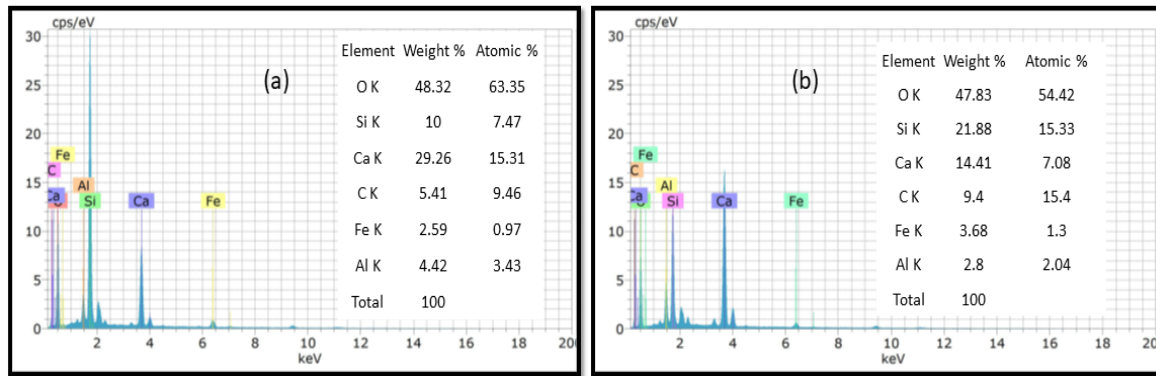


Fig. 5.14b: EDS analysis results of PPC based 1:2 cement-sand ratio (a) control mortar and (b) GO modified cement-sand mortar with 0.04% of GO.

5.15 Limitations

Based on the experimental study, it is noted that the addition of GO in cement-sand mortar with an optimal amount improves the overall strength and durability properties. Such improvement depends on the nature and composition of GO. The present study is limited to a particular type of GO. The long-term effect of GO addition in cement composite has not been studied. Further, it is well known that the cost of GO is comparatively high at present with respect to the cost of regular cement composites. It is expected that the price of GO will definitely reduce with more application of this material in different fields.

References

- [1] L. Zhao, X. Guo, C. Ge, Q. Li, L. Guo, X. Shu, J. Liu, Investigation of the effectiveness of PC@GO on the reinforcement for cement composites, *Constr Build Mater* 113 (2016) 470–478. <https://doi.org/10.1016/j.conbuildmat.2016.03.090>.
- [2] Sudesh, N. Kumar, S. Das, C. Bernhard, G.D. Varma, Effect of graphene oxide doping on superconducting properties of bulk MgB₂, *Supercond Sci Technol* 26 (2013) 095008. <https://doi.org/10.1088/0953-2048/26/9/095008>.
- [3] D. He, Z. Peng, W. Gong, Y. Luo, P. Zhao, L. Kong, Mechanism of a green graphene oxide reduction with reusable potassium carbonate, *RSC Adv* 5 (2015) 11966–11972. <https://doi.org/10.1039/C4RA14511A>.
- [4] V. Sharavath, S. Sarkar, S. Ghosh, One-pot hydrothermal synthesis of TiO₂/graphene nanocomposite with simultaneous nitrogen-doping for energy storage application, *Journal of Electroanalytical Chemistry* 829 (2018) 208–216. <https://doi.org/10.1016/j.jelechem.2018.09.056>.
- [5] Y. Suo, R. Guo, H. Xia, Y. Yang, F. Yan, Q. Ma, Study on modification mechanism of workability and mechanical properties for graphene oxide-reinforced cement composite, *Nanomaterials and Nanotechnology* 10 (2020) 184798042091260. <https://doi.org/10.1177/1847980420912601>.
- [6] H. Zeng, S. Qu, Y. Qin, Microstructure and transport properties of cement-based material enhanced by graphene oxide, *Magazine of Concrete Research* 73 (2021) 1011–1024. <https://doi.org/10.1680/jmacr.19.00558>.
- [7] K. Vallurupalli, W. Meng, J. Liu, K.H. Khayat, Effect of graphene oxide on rheology, hydration and strength development of cement paste, *Constr Build Mater* 265 (2020) 120311. <https://doi.org/10.1016/j.conbuildmat.2020.120311>.
- [8] A. Anwar, X. Liu, L. Zhang, Nano-cementitious composites modified with Graphene Oxide – a review, *Thin-Walled Structures* 183 (2023) 110326. <https://doi.org/10.1016/j.tws.2022.110326>.
- [9] J. Liu, L. Zhao, F. Chang, L. Chi, Mechanical properties and microstructure of multilayer graphene oxide cement mortar, *Frontiers of Structural and Civil Engineering* 15 (2021) 1058–1070. <https://doi.org/10.1007/s11709-021-0747-3>.
- [10] J. Wang, Y. Xu, X. Wu, P. Zhang, S. Hu, Advances of graphene- and graphene oxide-modified cementitious materials, *Nanotechnol Rev* 9 (2020) 465–477. <https://doi.org/10.1515/ntrev-2020-0041>.
- [11] S. Ganesh, C. Thambiliyagodage, S.V.T.J. Perera, R.K.N.D. Rajapakse, Influence of Laboratory Synthesized Graphene Oxide on the Morphology and Properties of Cement Mortar, *Nanomaterials* 13 (2022) 18. <https://doi.org/10.3390/nano13010018>.
- [12] S.K. Maurya, N.C. Kothiyal, Influence of physico-mechanical and electrical resistivity performance of high volume fly-ash cementitious mortar with low carbon, *Structural Concrete* 24 (2023) 7506–7523. <https://doi.org/10.1002/suco.202201240>.

- [13] C. Shen, S.O. Oyadiji, The processing and analysis of graphene and the strength enhancement effect of graphene-based filler materials: A review, *Materials Today Physics* 15 (2020) 100257. <https://doi.org/10.1016/j.mtphys.2020.100257>.
- [14] C. Lee, X. Wei, J.W. Kysar, J. Hone, Measurement of the Elastic Properties and Intrinsic Strength of Monolayer Graphene, *Science* (1979) 321 (2008) 385–388. <https://doi.org/10.1126/science.1157996>.
- [15] P. Poulin, R. Jalili, W. Neri, F. Nallet, T. Divoux, A. Colin, S.H. Aboutalebi, G. Wallace, C. Zakri, Superflexibility of graphene oxide, *Proceedings of the National Academy of Sciences* 113 (2016) 11088–11093. <https://doi.org/10.1073/pnas.1605121113>.
- [16] S. Meng, X. Ouyang, J. Fu, Y. Niu, Y. Ma, The role of graphene/graphene oxide in cement hydration, *Nanotechnol Rev* 10 (2021) 768–778. <https://doi.org/10.1515/ntrev-2021-0055>.
- [17] W. Baomin, D. Shuang, Effect and mechanism of graphene nanoplatelets on hydration reaction, mechanical properties and microstructure of cement composites, *Constr Build Mater* 228 (2019) 116720. <https://doi.org/10.1016/j.conbuildmat.2019.116720>.
- [18] X. Zhu, X. Kang, Effect of graphene oxide (GO) on the hydration and dissolution of alite in a synthetic cement system, *J Mater Sci* 55 (2020) 3419–3433. <https://doi.org/10.1007/s10853-019-04266-1>.
- [19] X. Kang, X. Zhu, X. Shu, J. Liu, Hydration of Clinker Phases in Portland Cement in the Presence of Graphene Oxide, *Journal of Materials in Civil Engineering* 34 (2022). [https://doi.org/10.1061/\(ASCE\)MT.1943-5533.0004063](https://doi.org/10.1061/(ASCE)MT.1943-5533.0004063).
- [20] P. Halamickova, R.J. Detwiler, C. Dale, P. Bentz, E.J. Garboczi, water permeability and chloride ion diffusion in portland cement mortars: relationship to sand content and critical pore diameter, *Cement and Concrete Research* 25 (1995) 790–802.
- [21] S. Diamond, Mercury porosimetry, *Cem Concr Res* 30 (2000) 1517–1525. [https://doi.org/10.1016/S0008-8846\(00\)00370-7](https://doi.org/10.1016/S0008-8846(00)00370-7).
- [22] V.E.L.K. Samen, R.C. Kaze, J.G. Deutou Nemaleu, H.K. Tchakoute, P. Meukam, E. Kamseu, C. Leonelli, Engineering properties, phase evolution and microstructure of the iron-rich aluminosilicates-cement based composites: Cleaner production of energy efficient and sustainable materials, *Cleaner Materials* 1 (2021) 100017. <https://doi.org/10.1016/j.clema.2021.100017>.
- [23] X. Hong, J.C. Lee, M.Y. Chu, Q. Li, X. Daze, Effect of Graphene Oxide on compressive strength of Shale Ceramsite high strength lightweight aggregate concrete, *IOP Conf Ser Earth Environ Sci* 1205 (2023) 012049. <https://doi.org/10.1088/1755-1315/1205/1/012049>.



CONCLUSION & FUTURE SCOPE

6.1 Conclusion

Based on experimental investigation on the effects of the addition of different percentages of GO, such as 0.03% to 0.06% by weight of cement, on cement mortar (with OPC or PPC) based 1:2 and 1:3 cement-sand mortar mixes the following conclusions are drawn:

- The GO is to be sonicated with water without any other dispersing agents, chemicals, and minerals to reduce the agglomeration and then the uniform mixture can be added in cement-sand mortar in optimum quantity as a reinforcing material.
- The workability of GO modified cement mortar for either OPC or PPC based cement-sand is reduced with respect to the control. For workability, 0.03% of GO addition is the threshold value (refer Fig. 5.2a – 5.2d). It should be mentioned that the GO has a high specific surface area, it can absorb free water on its surface, which reduces the flow characteristics.
- The addition of low percentage GO in cement mortar promotes and enhances mechanical properties, such as compressive strength, split tensile strength, and flexural strength. Also, the modulus of elasticity of cement mortar is enhanced with the incorporation of a small amount of GO.
- The optimum amount of GO addition in the cement-sand mortar in terms of strength was 0.05% and 0.04% by weight of cement, for OPC and PPC based on both 1:2 and 1:3 cement-sand ratio mortars.
- The maximum improvement of compressive strength is noted by 20% and 13% for OPC based 1:2 and 1:3 cement-sand ratio mortars, after 28 days of curing, respectively. For PPC based cement-sand mortar, the maximum enhancement in compressive strength is observed by 12% and 9% for 1:2 and 1:3 ratio mortar respectively, after 28 days of

curing age (refer Fig. 5.3a – 5.3d). The results of UPV also support such improvement in strength (refer Fig. 5.7). The nano-reinforcing effect of GO is mainly responsible for the enhancement of such compressive strength of GO modified cement mortar.

- The addition of GO to OPC and PPC-based cement-sand mortar mixes led to significant enhancements in both split tensile and flexural strength. In OPC-based 1:2 ratio mortar, tensile strength and flexural strength are maximally enhanced by 27% and 26%, respectively. For OPC-based 1:3 ratio mortar, improvements reached 19% for split tensile strength and 15% for flexural strength. In PPC-based 1:2 ratio mortar, enhancements peaked at 22% for split tensile strength and 32% for flexural strength, while in PPC-based 1:3 ratio mortar, they are noted at 20% for split tensile strength and 20% for flexural strength (refer Fig. 5.4a – 5.5d). The GO shape is like a 2D nanosheets which act as a fibre in nano-scale to arrest the macro-cracks of the cement composites thereby improving the tensile and flexural strength of cementitious materials.
- The Young's modulus of GO modified mortar of OPC and PPC based cement-sand mortar is also enhanced (refer Fig. 5.6). The presence of denser hydration product and lower pore volume makes the improvement possible (refer Fig. 5.11a – 5.13b).
- The durability study also indicates that the optimum amount of GO addition in the cement-sand mortar was 0.05% and 0.04% by weight of cement, for OPC and PPC based on both 1:2 and 1:3 cement-sand ratio mortars as in the case of strength.
- The rate of water absorption of GO modified OPC and PPC based cement mortar is lower than the control sample (refer Fig. 5.8a – 5.8d). The amount of charge passing of the RCPT test procedure through the specimens is found lower for GO modified cement mortar with respect to the control. The less charge passing is possible for the presence of GO nanoparticles in hydration products of GO modified mortar samples (refer Fig. 5.9).

- The GO modified OPC and PPC based cement-sand mortar have almost similar resistance against acid attack compared to the control (refer Fig. 5.10a – 5.10d, and Table 5.13 -5.16).
- The MIP test result of OPC and PPC based cement mortar indicates that the incorporation of optimum amount of GO, by filling of large pore area reduces the total pore volume and refines the pore structure of cement mortar leading to the enhancement in the mechanical properties (refer Fig. 5.11a and 5.11b).
- The results of XRD analysis indicate the formation of more C-S-H gel in GO based cement mortar both in OPC and PPC with respect to their corresponding control mortar which is responsible for strength improvement (refer Fig. 5.12a and 5.12b)
- As per FESEM test, a distinct change is detected in the morphology of GO modified OPC and PPC based cement mortar as compared to their corresponding control where the former had a large amount of denser crystal (Fig. 5.13a 5.13b). In the presence of optimum amount of GO in cement mortar, more amount of denser, needle-shaped crystals are found which seem to be responsible for the higher mechanical and durability properties of GO modified cement mortar samples.
- The elemental analysis by EDX indicates that the percentages of carbon atoms and silicon atoms in cement mortar changed noticeably with the addition of a small amount of GO (refer Fig. 5.14a and 5.14b). The result helps to demonstrate that the GO could participate in the formation of crystals, and also regulate the formation and growth of needle-shaped crystals, thus further improving the mechanical properties such as compressive strength, tensile strength, etc.
- According to the present investigation, adding the ideal quantity of GO to cement-sand mortar enhances its overall strength and durability characteristics. It may be mentioned that this present research is restricted to a specific type of GO having a particular

Composition. The present study is limited to strength and short-term durability of cement (both OPC and PPC) sand mortar with appropriate amount of GO. Furthermore, it is common knowledge that GO is now more expensive than standard cement composites. It is expected that the price of GO will definitely reduce with more application of this material in different fields.

6.2 Future Scope of the Study

Based on this present experimental study, the following research areas may be suggested for future scope of study.

- Graphene oxide (GO) significantly reduces the workability of cement mortar when it is mixed with PPC or OPC cement mortar. To improve the workability of cement mortar including with GO, more study is required adding different admixtures.
- There is still much to be explored about the precise interaction between different types of GO and hydration products. To determine the actual relationship between GO and hydration products, more comprehensive and rigorous research needs to be done.
- There is still more to be discovered about the long-term durability of cement mortar, with the appropriate amount of GO.
- The behaviour of cement mortar with GO against fire can be a good area of research.
- The present research studies can be extended for concrete with GO addition.

Surajit Biswas
03/06/2024

Saroj Mandal
3/6/24

Dr. Saroj Mandal
Professor
Civil Engineering Department
JADAVPUR UNIVERSITY
Kolkata-32



Mechanical and micro-structural study of cement mortar with graphene oxide

Surajit Biswas¹ · Saroj Mandal¹

Received: 2 May 2022 / Revised: 27 June 2022 / Accepted: 5 July 2022
© The Author(s), under exclusive licence to Springer Nature Switzerland AG 2022

Abstract

The mechanical and micro-structure properties of cement sand mortar with and without graphene oxide (GO) was studied experimentally. Graphene oxide is a carbon based 2-D nano material which still needs detail investigation of its effect in cement mortar/concrete. In the present study, different proportions of GO, 0.03–0.06% by weight of cement, were incorporated into cement mortar. The measured fluidity was reduced by 23% with incorporation of 0.03% GO by weight of cement. The incorporation of 0.05% GO increased the compressive strength of mortar at 28 days by 20%. Similarly, the flexural strength of GO based mortar was also increased substantially compared to control mortar at 0.05% of GO addition. It was observed that rate of water absorption is reduced by GO addition into cement mortar. The addition of GO reduces the pore volume and refines the pore structure of cement mortar. These improvements in GO based mortar are mainly due to the formation of new hydration products as observed by FESEM analysis.

Keywords Graphene oxide · Mortar · Compressive strength · Flexural strength · Microstructure

1 Introduction

Cement is widely used as construction and building material. It is the principal binder in mortar/concrete as it holds the aggregates together in the presence of water by hydration. However, the brittle nature and low tensile strength are the major disadvantages of cement-based construction materials. To enhance its performances, recently researchers concentrated on using different types of additives and fibers. With the advancement of nanotechnologies, such as 0-D nanoparticles, 1-D nano-fibers and 2-D nano-sheets have drawn considerable attention because of their high mechanical properties with the high specific surface area.

It was noted that the mechanical properties of cementitious materials can be remarkably influenced by silica nanoparticles (0-D) [1–5]. It was observed that the durability, drying shrinkage and water permeability of cementitious materials were also influenced by the addition of such silica nanoparticles [3, 6, 7]. Addition of 10% nano-silica with dispersing agents, the compressive strength was increased

by 26% at 28 days curing [8]. Even, the incorporation of a small quantity of nano-SiO₂ particles into cement mortar enhanced the compressive and flexural strength by 10% and 25% respectively at 28 days [6]. It was established that the nano-SiO₂ particles filled the small pore of cement composite [9, 10]. Addition of a small amount of nano-SiO₂ into cement composite accelerated the hydration process and improved the strength and microstructure characteristics [6, 11–15]. A carbon nanotube (CNT) is a carbon-based 1-D nano material. It consists of rolled up single-layered carbon atom sheets. In general, CNTs are categorized into two types, single-layered and multi-layered and its diameters are 1–3 nm and 5–50 nm respectively [16]. However, it was noted that the addition of small amounts of CNTs increased the mechanical properties of cementitious materials [17–19]. Parveen et al. [20] reported that incorporation of a small amount of CNTs in cement mortar increased compressive strength and flexural strength up to 23% and 17% after 28 days. The main mechanism of incorporation of CNTs in the cement matrix is the filling of nano-size pore area, bridging the micro size capillary pores and the effects of nucleation [18]. Li et al. [21] concluded that enhancement of compressive strength, flexural strength as well as failure strain was improved due to the addition of CNTs.

✉ Surajit Biswas
Surajitce08@gmail.com

¹ Department of Civil Engineering, Jadavpur University,
Kolkata 700032, India

Table 1 Chemical composition OPC (53 grade)

Parameters	SiO ₂	Al ₂ O ₃	Fe ₂ O ₃	CaO	MgO	SO ₃	K ₂ O	Na ₂ O	Others
Percentage % (By mass)	21.94	4.95	3.74	62.33	2.08	2.22	0.56	0.32	1.89

Recently, carbon-based nanomaterial, Graphene oxide (GO) has drawn attention to incorporated into the cement matrix. It is a single-layered two-dimensional (2-D) nanomaterial consisting of various oxygen-containing functional groups such as hydroxyl, carbonyl, epoxy and carboxylic groups [22, 23]. In the aqueous solution, GO is conveniently dispersed due to the presence of different oxygen containing groups. These oxygens containing functional groups in GO's chemical structure is responsible for the enhancement of the chemical and physical properties of the different host materials [24]. It is well known that the specific surface area of GO is very high [25–28]. Thus, it can promote chemical and physical interaction with host materials such as cement composites [29]. It was accepted that in ceramic and polymer materials, GO can easily form composites and can promote the toughness by monitoring the microstructure of crystal [25, 29]. It may be mentioned that GO can be synthesized in large quantities by strong oxidation of inexpensive graphite powder [25]. However, it was concluded from previous study that introducing little amount of GO into cement paste can enhanced the mechanical properties such as compressive strength, tensile strength, and flexural strength. It not only increases the mechanical properties of cement composite, but microstructure of cement composite also promoted by introduced of GO in cementitious materials [31–33]. It was concluded by Gong et al. [34]; the incorporation of very small amount 0.03% of GO into cement paste by weight of cement, the compressive strength and tensile strength enhanced by around 40% and reduced the pore structure of cement paste. It was observed by Lv et al. [35] that the introduction of 0.03% of GO into cement composite increased the compressive strength, flexural strength and tensile strength by 38.9%, 60.7% and 78.6% respectively. According to Pan et al. [36], the incorporation of as little as 0.05% of GO by weight of cement reduced the workability of cement paste around 42%. The morphological study on the GO based cementitious material was concluded that the incorporation of GO in cement composite produced finer pore [37, 38].

In the present research work, the effects of addition of GO in cement-sand mortar, in terms of mechanical properties, fluidity behavior, and the micro-structural behavior are studied. The pore size distribution of GO based cement mortar was studied by Mercury Intrusion Porosimetry (MIP) test. The morphology of hardened GO based mortar was observed by using field emission scanning electron microscopy (FESEM), energy-dispersive X-ray spectroscopy (EDS) and X-ray diffraction (XRD). In the present study, the cement-sand mortar prepared with the addition of different

**Fig. 1** Powdered form of graphene oxide**Table 2** Technical properties of GO

Element	Carbon	Oxygen	Hydrogen	Others
Percentages (%) (By mass)	60–80	15–32	0–2	0–2

dosages of graphene oxide only, and no other chemicals or minerals were used.

2 Materials and methods

2.1 Materials

Ordinary Portland Cement (OPC) grade 53 confirming to IS: 269-2015 [39] was used throughout the experimental study. The chemical compositions of OPC obtained by chemical analysis are presented in Table 1. Locally available river sand of Grade-II as per IS: 383-2016 [40] and specific gravity of 2.66 was used. The two-dimensional GO in powdered form (Fig. 1) with 99% purity and black in colour was collected from M/s Ad-Nano Technologies Pvt. Ltd, Karnataka, India. The technical properties of GO obtained by EDS were presented in Table 2.

2.2 Mix proportion and curing

Table 3 showed the five numbers of mixtures with different percentage of GO addition. The water to cement ratio (by weight) and cement to sand ratio (by weight) were kept constant as 0.45 and 1:2 respectively for all mixtures. Initially,

Table 3 Details of different cement-sand mortar mixtures

Mixtures	Control	GOPC0.03	GOPC0.04	GOPC0.05	GOPC0.06
Water to cement ratio	0.45	0.45	0.45	0.45	0.45
Cement to sand ratio	1:2	1:2	1:2	1:2	1:2
GO (%)	0	0.03	0.04	0.05	0.06

the cement and sand were mixed thoroughly for 3–4 min in dry condition. Sonicated solution of required amount of water and GO was then mixed. The fresh mortar mix was placed into standard cube and prism mould and well compacted. The hardened cement mortar demolded after 24 h and placed in water for curing.

3 Sample preparation and testing

3.1 Flow test

The fluidity of all the fresh cement-sand mortar mixtures was measured by flow table test as per IS 4031 (7) [41]. The smaller flow table cone having top diameter 50 mm, bottom diameter 100 mm and height 50 mm was fixed firmly on a flow table at the center. The cone was filled with fresh cement-sand mortar. The final spread diameter of the mortar mix was measured after removing the cone (Fig. 2).

3.2 Sample for mechanical strength test and sorptivity test

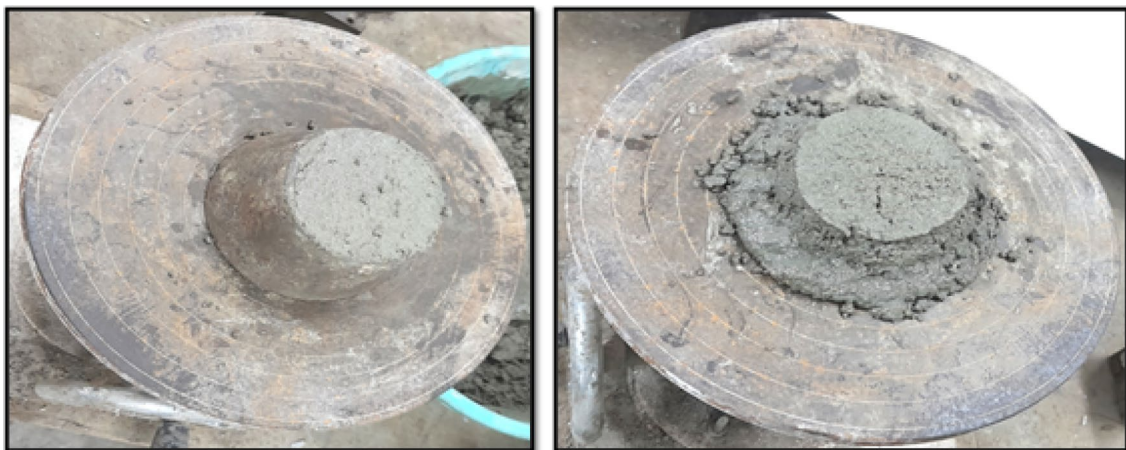
Standard mortar cube of size 70.6 mm × 70.6 mm × 70.6 mm was prepared for each mixture to determine compressive strength of cement-sand mortar mixes. Compressive strength of the mixes was determined at 3 days, 7 days and 28 days. The test set up has been shown in Fig. 3. The flexural

strength at 28 days was also measured on the prism sample size of 50 mm × 50 mm × 200 mm mortar bar for the five mixtures as per AASHTO T 67 [42]. The center point loading method was adopted for the determination of flexural strength as shown in Fig. 4.

For sorptivity test, similar mortar cubes of each side 70.6 mm were cast. Four sides of the mortar cube were painted through water proofing material. The testing was made as per ASTM C1585-04 [43]. This test provides unidirectional water absorption as a function of time. Figure 5 shows the experimental set up for the sorptivity test of mortar specimens. The prepared samples for different mixtures under water curing are shown in Fig. 6.

3.3 Sample for XRD analysis, FESEM and EDS analysis, MIP test

The broken parts of the samples tested at 28 days for compressive strength were dried, grinded and sieved to make the uniform particle size less than 5 µm for X-ray diffraction analysis in powder X-ray diffractometer (Bruker AXS Inc, Model D8, WI, USA) with a scan speed 0.5 s/step at 40 kV. The XRD spectrum was analyzed in the range $2\theta = 10^\circ$ to $2\theta = 70^\circ$ and the peak positions were marked and compared from JCPDS file. For FESEM (Field Emission Scanning Electron Microscope) analysis and EDS (Energy-Dispersive Spectra) analysis, the similar fine powder samples were diluted with ethanol (99.9%) to

**Fig. 2** Flow test of mortar

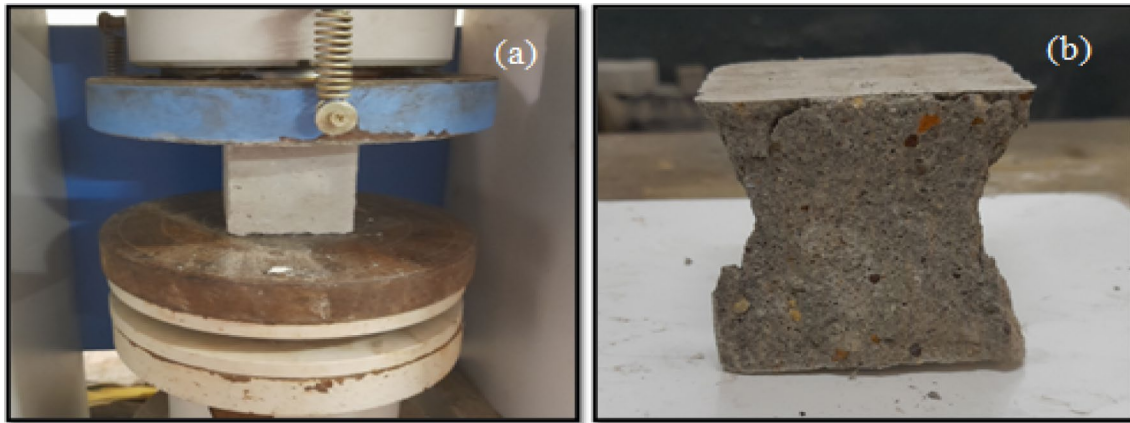


Fig. 3 Compressive strength test of mortar sample

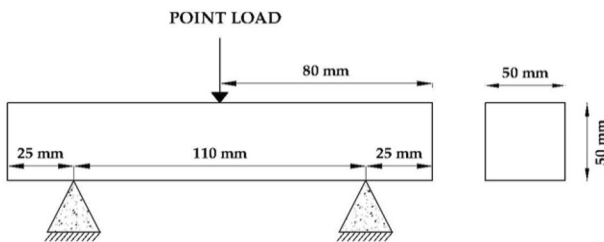


Fig. 4 Set up for center point loading for flexural strength

make a film on carbon tape and then kept under vacuum desiccators for evaporation. Finally, the dried samples were gold coated and analysed. The Mercury Intrusion Porosimetry (MIP) test was made for measuring pore size distribution on broken samples of size 3–6 mm particles in Quntachorme make Poremaster 60 after 28 days compression test. The broken pieces soaked in acetone to stop the hydration and were oven dried.

4 Results and discussion

In this section different test results of cement–sand mortar with and without GO are presented and discussed.

4.1 Flow test

Figure 7 showed the average fluidity in terms of final spread diameter in flow test of mortar with the addition of GO in different proportions. It was noted that the fluidity got reduced with the addition of GO in the cement mortar. The GO incorporation of 0.03% in cement mortar reduced the fluidity by 23% (maximum) compared to the control sample. Further addition of GO into cement mortar reduced the fluidity compared to control sample but increased compared to GOPC0.03 mixture. Therefore, the flow table test results indicate that the addition of GO into cement sand mortar reduces the fluidity compared to control sample, and maximum reduction in fluidity is observed at GOPC0.03.

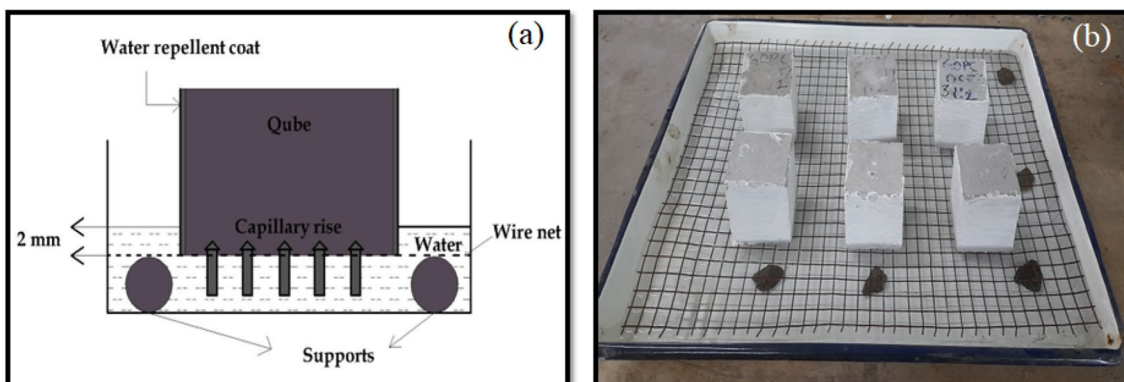


Fig. 5 Experimental set up of sorptivity test



Fig. 6 Cube and prism samples under curing

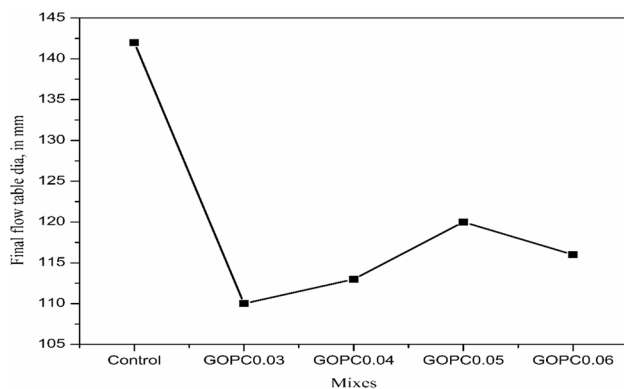


Fig. 7 Flow test results of different mixes

It is widely accepted that addition of GO into cement paste enhanced in viscosity and remarkably reduced the fluidity [34, 44]. According to Pan et al. [36] the incorporation of as little as 0.05% of GO by weight of cement reduce workability of cement paste around 42%. It was concluded by Gong et al. [34]; workability of cement paste reduced around 34% by the addition of 0.03% GO with water-cement ratio 0.5. It was reported by Long et al. [45] that incorporation 0.2% GO addition into cement sand mortar reduced the workability around 19% compare to control sample. This observation is in line with the accepted fact that 0.03% of GO is the threshold value of less workability of cement paste [46]. Also, it was accepted that addition of 0.05% of GO along with 0.8% water reducing agent, fluidity of cement past reduced 70% as compared to control sample [47]. It may be noted that GO has high specific surface area, hence, it allows to absorb free water on its surface leading to decrease in flow characteristic. It was also accepted that after mixing with cement composite, GO agglomerates became smaller in size thus entrapping large amounts of free water [48]. Sou et al. [49] reported that addition of 0.05% of GO with 0.5%

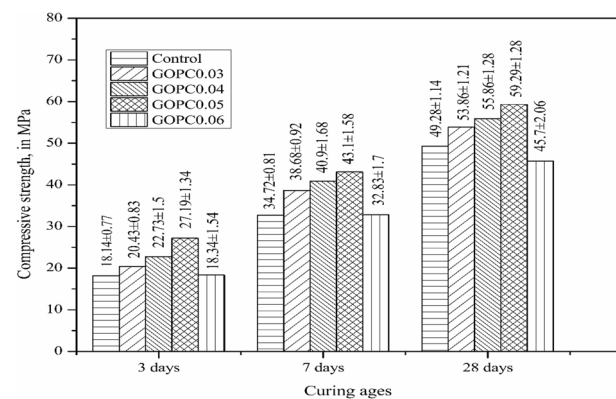


Fig. 8 Compressive strength of different mixes at different age

polycarboxylate-based superplasticizer [PCs], the fluidity of cement paste reduced around 52%. However, Liu et al. [50] concluded that incorporation of multilayer GO [MGO] with polycarboxylate-based superplasticizer [PCs] into cement mortar dose not reduced the fluidity. From this present study it was concluded that addition of GO reduced the fluidity of cement-sand mortar which similar to some previous studies [34, 35, 45–49] and 0.03% of GO is the threshold value for minimum fluidity.

4.2 Compressive strength

Figure 8 shows the compressive strength of cement-sand mortar mixtures (with and without GO) at the age of 3 days, 7 days and 28 days. The compressive strength of the mortar with GO up to 0.05% was increased compared to control mix (without GO) at all ages. However, the strength was decreased with further addition of GO (0.06%). At the age of 3 days, it was observed that compressive strength of GO based mortar mixtures GOPC0.03, GOPC0.04 and

GOPC0.05 was increased by 12%, 25% and 49% respectively compared to control sample. The improvements in strength at 7 days of the same three mixes were 11%, 17% and 25% respectively. Similarly, at the age of 28 days the improvement in strength for the three mixes with GO was noted as 9%, 13% and 20% respectively. Furthermore, it was noted that the compressive strength of mortar with 0.06% GO was reduced by 7.8% compared to control at 28 days.

In an experimental study, the increase in compressive strength by Li et al. [46] was reported to be 14% of cement paste by addition of 0.04% GO. The enhancement of compressive strength in another study by Gowda et al. [51] was around 17% of cement mortar containing 0.1% of GO at 28 days curing age. Wang et al. [52] concluded that with the addition of 0.05% Graphene nano platelet into cement mortar, compressive strength increased around 7.5% after 28 days. It was reported by Lv et al. [35] that the introduction of 0.03% of GO into cement composite increase the compressive strength by 38.9%. According to Zhao et al. [53]; the compressive strengths of cement composite at different water to cement ratio ($w/c = 0.29, 0.36, 0.45$) were increased around 16.31–25.60% compared to control with addition of 0.022% GO. A study by Pan et al. [54] reported that the incorporation 0.05% of GO increased the compressive strength of cement paste around 16% at 28 days. Abdullah et al. [55] concluded that the compressive strength of cement-sand mortar increased 29% with the addition of 0.05% GO with 7% silica fume. Another study by Liu et al. [50] reported that with the incorporation of 0.04% MGO with PCs, compressive strength increased around 5.85% compared to control sample after 28 days curing. It was concluded by Shang et al. [44] that incorporation 0.04% of GO into cement paste with water-cement ratio 0.4 enhanced the compressive strength around 15% compare to control sample. In the present study compressive strength increased around 20% by addition of 0.05% GO into cement-sand mortar at the age of 28 days.

4.3 Flexural strength

Figure 9 indicates the variations of flexural strength at 28 days of cement-sand mortar with and without GO. It was observed that flexural strength was increased by 11%, 21% and 26% for GOPC0.03, GOPC0.04 and GOPC0.05 respectively, compared to control sample. The maximum flexural strength of OPC based mortar at 0.05% addition of GO was 6.09 MPa compared to that of a control sample as 4.83 MPa. On further addition of GO (at 0.06%), the flexural strength decreased compared to '0.05% GO addition' case. According to Abdullah et al. [55]; flexural strength of cement-sand mortar increased 13% with the addition of 0.05% GO with 7% silica fume. The increase in flexural strength in a study by Li et al. [56] was reported to be 15%

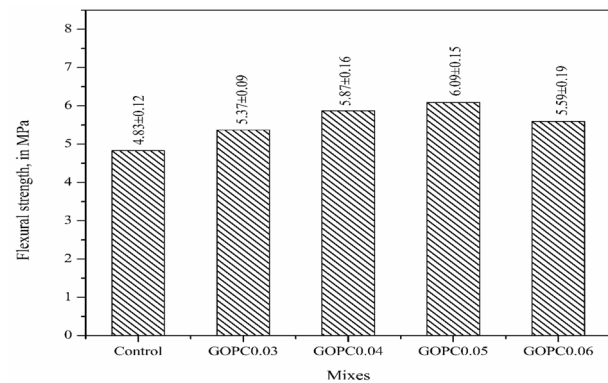


Fig. 9 Flexural strength of different mixes at 28 days

at 28 days in cement mortar containing 0.04% GO. Another study by Kim et al. [57] reported that incorporation of 0.05% GO flakes with superplasticizer at 28 days, flexural strength increased around 23%. The increase in flexural strength in another study by Gowda et al. [51] observed that around 12% at 28 days in cement mortar containing 0.1% GO. According to Lv et al. [37]; the flexural strength of cement mortar increased around 60% with addition of 0.03% GO along with polycarboxylate superplasticizer ($w/c = 0.36$). It was concluded by Lv et al. [35] that the introduction of 0.03% of GO into cement composite increased the flexural strength by 60.7%. Birenboim et al. [58] reported that the flexural strength increased around 70% at 28 days with addition of 0.05% GO with the presence of a superplasticizer. Another study by Liu et al. [50] reported that the incorporation 0.04% of MGO with PCs increased the flexural strength of cement-sand mortar. In this experimental study maximum enhancement of flexural strength noted 26% with the addition of 0.05% GO without any superplasticizer.

From the study of Abdullah et al. [55], it was concluded earlier that 0.05% GO along with 7% silica fumes, the compressive strength and flexural strength increased 29% and 13% in cement-sand mortar. But in our study, there is no addition of silica fumes/PCs where compressive strength and flexural strength was reported as 20% and 26% respectively which proves 0.05% GO itself has the ability to perform well. Based on the compressive and flexural strength results, the optimum percentage of addition of GO was notes as 0.05% for the present study. Thus, the sorptivity and the microstructure study was made both for control and for GOPC0.05 and compared.

4.4 Sorptivity test

Figure 10 shows the water absorption rate of GOPC0.05 and control sample mixes. The Primary absorption rate was considered up to 24 h of testing period ($294 \text{ sec}^{1/2}$) and secondary absorption rate is considered up to 10 days with

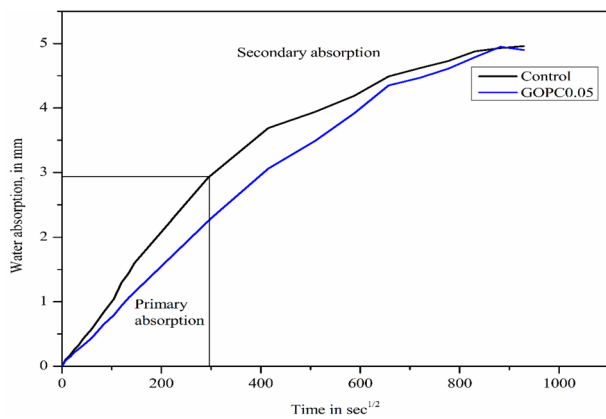


Fig. 10 Water absorption rate of control and GOPC0.05 mixes

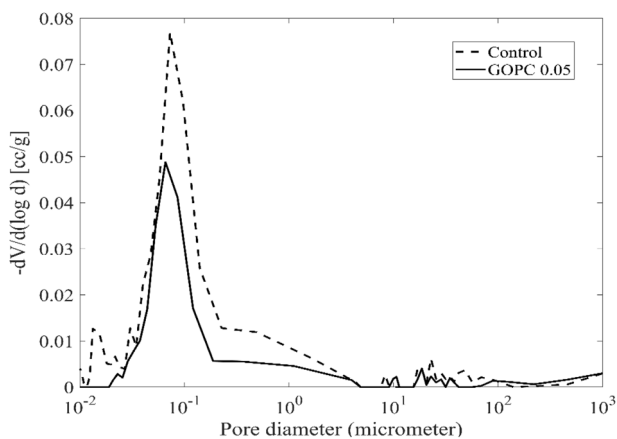


Fig. 11 Pore size distribution of control and GOPC0.05

24 h interval. Both at primary stage and secondary stage, the water absorption rate of GOPC0.05 mix was comparatively lesser than that of the control sample. This is due to the improved microstructure with lesser interconnected pore volume in GOPC0.05 showed by MIP test result. A similar conclusion was reported by Gowda et al. [51] in another study. The initial rate of water absorption for GO (by 0.1% weight of cement) based cement mortar was little less than control and the secondary rate (up to 8 days) of absorption found to be fluctuating.

4.5 Mercury Intrusion Porosity (MIP) test

Figure 11 shows the pore size distribution for both GOPC0.05 and control mortar sample in terms of $-dV/d(\log d)$ versus pore diameter (d) where V is pore volume. The intruded amount of mercury into pores is less in the GOPC0.05 compared to the control sample consistently. The large diameter pores were filled by GO agglomerates and the peak of the intruded amount of mercury shifted

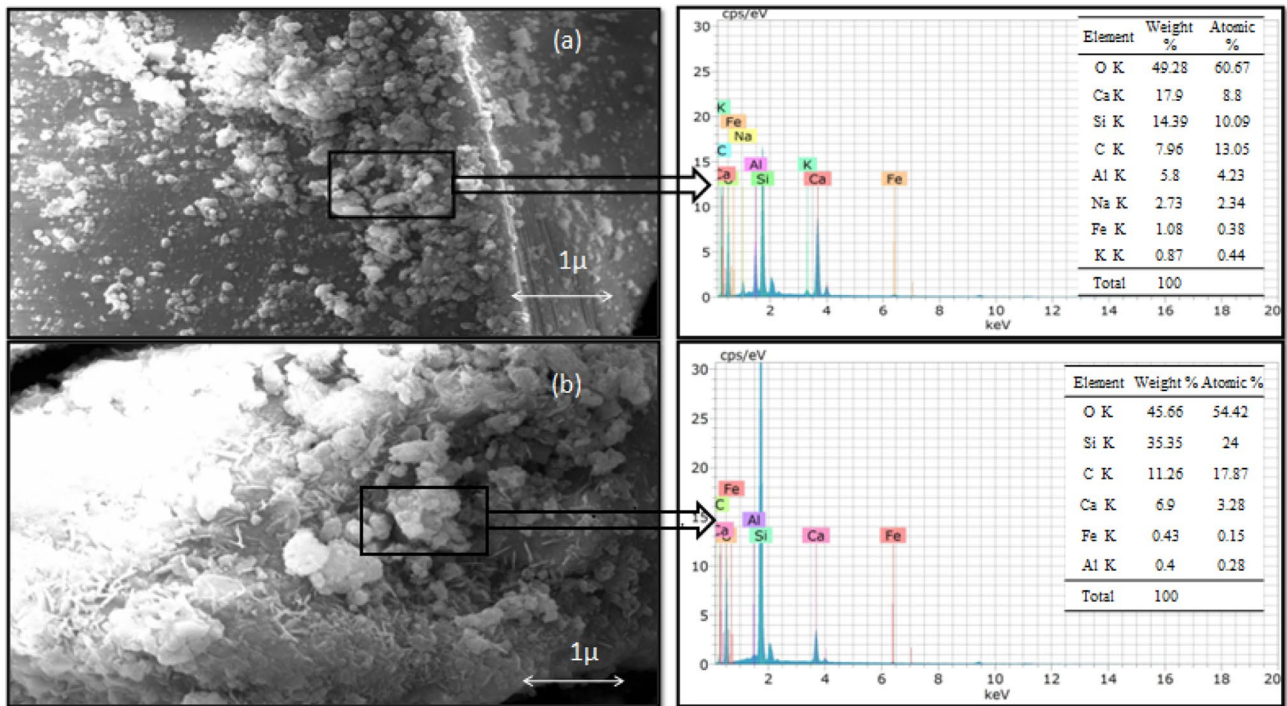
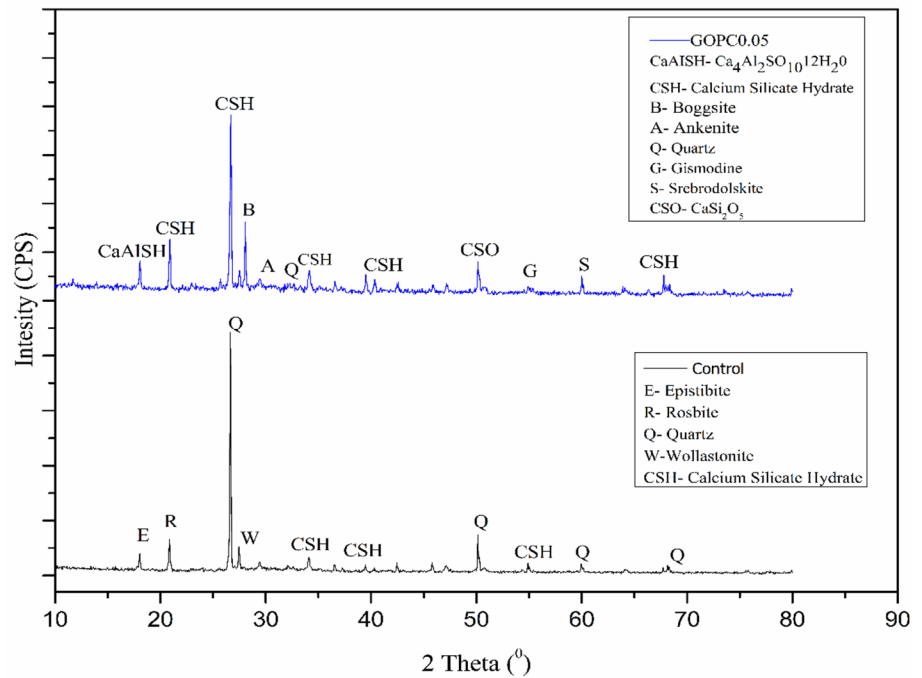
towards the finer pore diameter with the addition of GO into control cement-sand mortar. It indicates the modification of pore size distribution with the addition of GO, thereby increase the gel pore volume of calcium silicate hydrate gel compared to the control sample [34]. Similar refinement of cement composite by addition of GO also reported by Gong et al. [34] and Li et al. [46]. From the experimental study of Diamond [59] and Halamickova et al. [60], it was evident that the peak of the MIP test curve is related to critical pore size, which showed strong correlation with the permeability of material and diffusivity.

4.6 XRD analysis

The XRD analysis results of GOPC0.05 and control sample were presented in Fig. 12. It was clearly indicated that the higher and more peaks were observed for C–S–H (JCPDS CARD: 14-0035) in GOPC0.05 than control sample at different values of 2θ . The significant picks are appeared at $2\theta = 18.05^\circ, 20.9^\circ, 26.7^\circ, 28.05^\circ, 30.75^\circ, 34.15^\circ, 39.5^\circ, 50.15^\circ, 54.9^\circ, 60.0^\circ$ and 67.8° . New compounds $\text{Ca}_4\text{Al}_2\text{SO}_{10}12\text{H}_2\text{O}$ (JCPDS CARD:45-0158), Boggsite (JCPDS CARD: 42-1379), Ankerite (JCPDS CARD: 41-0586), Gismondine (JCPDS CARD: 20-0452), Srebrodolskite (JCPDS CARD: 038-0408) and CSO (JCPDS CARD:15-0130) are formed due to incorporation of GO in cement mortar. Thus, the early strength improvement was substantially more due to the formation of Ankerite and Gismondine. Gismondine generally provides thermal stability and prevents decomposition of cement gel at high temperature.

4.7 FESEM analysis

The morphology examined by field emission scanning electron microscope (FESEM) and EDS was shown in Fig. 13a, b for control and GOPC0.05 mixes respectively. A distinct change was observed in morphology of cement mortar incorporating 0.05% of GO compared to control featuring large amount of denser and needle shape crystal. For morphological analysis Zhu et al. [61] also reported the similar results by TEM analysis for cement paste with the addition of 0.03% of GO. A significant difference of the elementary compositions as per EDS analysis was also noted. The enhancement of silicon atoms in GOPC0.05 was more than two times greater than that of the control sample. Kang et al. [62] concluded the similar report. It was concluded that incorporation of 0.03% GO into cement paste, the Si concentration increased around 16.9% compared to control sample. However, it indicates that addition of GO was favorable to interlocked cement hydration products such C–S–H gel and produced a more compacted microstructure of cement mortar, which leads

Fig. 12 XRD analysis results of GOPC0.05 and control sample**Fig. 13** FESEM image and EDS analysis of cement-sand mortar **a** control sample and **b** GOPC0.05

to the enhanced mechanical properties. It was accepted that large amount of densified, needle and rod-shaped hydration products such as C–S–H produced by addition of GO into cement mortar [46, 59]. It seems that this has modified the pore structure of cement mortar with GO as

noted in the MIP results. It was reported earlier by Meng et al. [63] that incorporation of GO into cement paste, the exothermic peak value increased by 9.8% than that of the control sample. The presence of GO in cement paste increased hydration of cement paste and promotes the

C–S–H nucleation and growth by strong interaction with cement surface. Another experimental study indicated [64] that addition of Graphene nanoplatelets accelerates the hydration reaction and causes more heat generation. It may be possible that the presence of GO enhances the mobility of ions in cement mortar, which subsequently increases the interaction of water with the cement particles and promotes the growth and formation of C–S–H into cement-sand mortar.

5 Conclusion

The effects of addition of GO in cement–sand mortar, in terms of mechanical properties, fluidity behavior was studied. The micro-structural behavior of cement mortar with/without GO was examined by MIP, XRD, FESEM and EDS analysis. In this study, the cement-sand mortar prepared with the addition of different dosages of graphene oxide only, and no other chemicals or minerals or dispersion agents were used. Based on this study, it was found that incorporation of a small amount of GO enhanced the mechanical and morphological properties of cement-sand mortar. It was noted that the addition of GO reduced fluidity of cement mortar due to formation GO agglomerates which have high specific surface area and high free water entrapment capacity. For fluidity 0.03% of GO is the threshold value. Incorporation of GO, by filling of pore area reduces the total pore volume and refine the pore structure of cement mortar leading to the enhancement in the compressive strength. An optimum percentage (0.05%) of GO increases compressive strength by 49%, 25% and 20% at 3 days, 7 days and 28 days respectively. Similarly, the flexural strength of mortar with 0.05% GO addition was 26% more than the control. The reduction in strength was also noticed at 0.06% of GO addition at all ages. Appropriate amount denser hydration products with new compounds were observed into GO based mortar by FESEM, EDS and XRD analysis. Thus, the rate of primary and secondary water absorption of GO based cement mortar is lesser than control sample. Therefore, the effects GO in cement-based composites has great potential for cementitious materials.

Funding The authors declare that no funds, grants, or other support were received during the preparation of this manuscript.

Declarations

Conflict of interest The authors declare that they have no conflict of interest.

References

1. Isfahani FT, Redaelli E, Lollini F, Li W, Bertolini L (2016) Effects of nanosilica on compressive strength and durability properties of concrete with different water to binder ratios. *Adv Mater Sci Eng*. <https://doi.org/10.1155/2016/8453567>
2. Kumar A, Singh G (2018) Effect of nano silica on the fresh and hardened properties of cement mortar. *Int J Appl Eng Res* 13:11183–11188
3. Givi AN, Rashid SA, Aziz FNA, Salleh MAM (2011) The effects of lime solution on the properties of SiO₂ nanoparticles binary blended concrete. *Compos Part B* 42:562–569
4. Horszczaruk E, Mijowska E, Cendrowski K, Mijowska S, Sikora P (2014) Effect of incorporation route on dispersion of mesoporous silica nanospheres in cement mortar. *Constr Build Mater* 66:418–421
5. Sanchez F, Sobolev K (2014) Nanotechnology in concrete—a review. *Constr and Build Mater* 24:2060–2071
6. Ji T (2005) Preliminary study on the water permeability and microstructure of concrete incorporating nano-SiO₂. *Cem Concr Res* 35:1943–1947
7. Senff L, Hotza D, Repette WL, Ferreira VM, Labrincha JA (2010) Mortars with nano SiO₂ and micro-SiO₂ investigated by experimental design. *Constr Build Mater* 24:1432–1437
8. Qing Y, Zenan Z, Li S, Rongshen C (2006) A comparative study on the pozzolanic activity between nano-SiO₂ and silica fume. *J Wuhan Univ Technol Mater Sci Ed* 21:153–157
9. Zhuang C, Chen Y (2019) The effect of nano-SiO₂ on concrete properties: a review. *Nanotechnology* 8:562–572
10. Li H, Xiao HG, Yuan J, Ou J (2004) Microstructure of cement mortar with nanoparticles. *Compos Part B* 35:185–189
11. Jo BW, Kim CH, Tae GH, Park JB (2007) Characteristics of cement mortar with nano-SiO₂ particles. *Constr Build Mater* 21:1351–1355
12. Lin DF, Lin KL, Chang WC, Luo HL, Cai MQ (2008) Improvements of nano-SiO₂ on sludge/fly ash mortar. *Waste Manag* 28:1081–1087
13. Lin KL, Chang WC, Lin DF, Luo HL, Tsai MC (2008) Effects of nano-SiO₂ and different ash particle sizes on sludge ash–cement mortar. *J Environ Manag* 88:708–714
14. Li G (2008) Properties of high-volume fly ash concrete incorporating nano-SiO₂. *Cem Concr Res* 34:1043–1049
15. Schoepfer J, Maji A (2009) An investigation into the effect of silicon dioxide particle size on the strength of concrete. *ACI Spec Publ* 45:258–267
16. Agrawal S, Raghuveer MS, Ramprasad R, Ramanath G (2007) Multishell carrier transport in multiwalled carbon nanotubes. *IEEE Trans Nanotechnol* 6:722–726
17. Zou B, Chen SJ, Korayem AH, Collins F, Wang CM, Duan WH (2015) Effect of ultrasonication energy on engineering properties of carbon nanotube reinforced cement pastes. *Carbon* 85:212–220
18. Konsta-Gdoutos MS, Metaxa ZS, Shah SP (2010) Multi-scale mechanical and fracture characteristics and early-age strain capacity of high-performance carbon nanotube/ cement nano composites. *Cem Concr Compos* 32:110–115
19. Siddique R, Mehta A (2014) Effect of carbon nanotubes on properties of cement mortars. *Constr Build Mater* 50:116–129
20. Parveen S, Rana S, Figueiro R, Paiva MC (2015) Microstructure and mechanical properties of carbon nanotube reinforced cementitious composites developed using a novel dispersion technique. *Cem Concr Res* 73:215–227
21. Li GY, Wang PM, Zhao X (2005) Mechanical behavior and microstructure of cement composites incorporating surface-treated multi-walled carbon nanotubes. *Carbon* 43:1239–1245

22. Cote LJ, Kim J, Tung VC, Luo J, Kim F, Huang J (2011) Graphene oxide as surfactant sheets. *Pure Appl Chem* 83:95–110
23. Kim J, Cote LJ, Huang J (2012) Two-dimensional soft material, new faces of graphene oxide. *Acc Chem Res* 45:1356–1364
24. Mohammed A, Sanjayan JG, Nazari A, Al-Saadi NTK (2018) The role of graphene oxide in limited long-term carbonation of cement-based matrix. *Constr. and Build. Constr Build Mater* 168:858–866
25. Zhu Y, Murali S, Cai W, Li X, Suk JW, Potts JR, Ruoff RS (2010) Graphene and graphene oxide: synthesis, properties, and applications. *Adv Mater* 22:3906–3924
26. Dikin DA, Stankovich S, Zimney EJ, Piner RD, Dommett GHB, Evmenenko G, Nguyen SBT, Ruoff RS (2007) Preparation and characterization of graphene oxide paper. *Nature* 448:457–460
27. Potts JR, Dreyer DR, Bielawski CW, Ruoff RS (2011) Graphene-based polymer nanocomposites. *Polymer* 52:5–25
28. Kuila T, Bose S, Hong CE, Uddin ME, Khanra P, Kim NH, Lee JH (2011) Preparation of functionalized graphene/linear low density polyethylene composites by a solution mixing method. *Carbon* 49:1033–1051
29. Zaaba NI, Foo KL, Hashima U, Tan SJ, Liua W, Voon CH (2017) Synthesis of Graphene oxide using modified hummers method: solvent Influence. *Procedia Eng* 184:469–477
30. Adak D, Sarkar M, Mandal S (2014) Effect of nano silica on strength and durability of flyash based geopolymer mortar. *Constr and Build Mater* 70:453–459
31. Lu Z, Li X, Hanif A, Chen B, Parthasarathy P, Yu J, Li Z (2017) Early-age interaction mechanism between the graphene oxide and cement hydrates. *Constr and Build Mater* 152:232–239
32. Lv S, Ma Y, Qiu C, Zhou QF (2013) Regulation of GO on cement hydration crystals and its toughening effect. *Mag Concr Res* 65:1246–1254
33. Chuah S, Pan Z, Sanjayan JG, Wang CM, Duan WH (2014) Nano reinforced cement and concrete composites and new perspective from graphene oxide. *Constr Build Mater* 73:113–124
34. Gong K, Pan Z, Korayem H, Qiu L, Li D, Collins F, Wang CM, Duan WH (2015) Reinforcing effects of graphene oxide on portland cement paste. *J Mater Civ Eng* 27:1–6
35. Lv S, Ma Y, Qiu C, Sun T, Zhou LJ, Q, (2013) Effect of graphene oxide nanosheets of microstructure and mechanical properties of cement composites. *Constr Build Mater* 49:121–127
36. Pan Z, Duan W, Li D, Collins F (2012) Graphene oxide reinforced cement and concrete, WO Patent App. PCT/AU2012/001, 582
37. Lv S, Liu J, Sun T, Maa Y, Zhou Q (2014) Effect of GO nanosheets on shapes of cement hydration crystals and their formation process. *Constr Build Mater* 64:231–239
38. Celik F, Canakci H (2015) An investigation of rheological properties of cement-based grout mixed with rice husk ash (RHA). *Constr Build Mater* 91:187–194
39. IS 269 (2015) Ordinary Portland Cement specification, Bureau of Indian Standards, New Delhi, India
40. IS 383 (2016) Coarse and fine aggregate for concrete specification, Bureau of Indian Standards New Delhi, India
41. IS: 4031 (Part 7) (1988) Methods of physical tests for hydraulic cement, Bureau of Indian Standard, New Delhi, India
42. AASHTO T 67-05 (2008) Standard method of test for standard practices for force verification of testing machines, standard published by American Association of State and Highway Transportation Officials
43. ASTM C 1585-04 (2020) Standard Test Method for Measurement of Rate of Absorption of Water by Hydraulic-Cement Concretes
44. Shang Y, Zhang D, Yang C, Yan L, Liu Y (2015) Effect of graphene oxide on the rheological properties of cement pastes. *Constr Build Mater* 96:20–28
45. Long WJ, Wei JJ, Ma H, Xing F (2017) Dynamic mechanical properties and microstructure of Graphene oxide nanosheets reinforced cement composites. *Nanomaterials* 407:1–19
46. Li X, Liu YM, Li WG, Li CY, Sanjayan JG, Duan WH, Li Z (2017) Effects of graphene oxide agglomerates on workability, hydration, microstructure and compressive strength of cement paste. *Constr Build Mater* 145:402–410
47. Wang Q, Wang J, Lv CX, Cui XY, Li SY, Wang X (2016) Rheological behavior of fresh cement pastes with a graphene oxide additive. *New Carbon Mater* 31:574–584
48. Li X, Korayem AH, Li C, Liu Y, He H, Sanjayan JG, Duan WH (2016) Incorporation of graphene oxide and silica fume into cement paste: a study of dispersion and compressive strength. *Constr Build Mater* 123:327–335
49. Suo Y, Guo R, Xia H, Yang Y, Yan F, Ma Q (2020) Study on modification mechanism of workability and mechanical properties for graphene oxide-reinforced cement composite. *Nanomater Nanotechnol* 10:1–12
50. Liu J, Zhao L, Chang F, Chi L (2021) Mechanical properties and microstructure of multilayer graphene oxide cement mortar. *Front Struct Civ Eng* 15:1058–1070
51. Gowda ST, Ranganathan RV (2017) Microstructure modification of cementitious composites for enhanced engineering properties using nano-graphene oxide layers. *The Ind Conc Journ* 91:34–44
52. Wang B, Jiang R, Wu Z (2016) Investigation of the mechanical properties and microstructure of graphene nanoplatelet-cement composite. *Nanomaterials* 6:1–15
53. Zhao L, Guo XL, Liu YY, Zhao Y, Chen Z, Zhang Y, Guo L, Shu X, Liu J (2018) Hydration kinetics, pore structure, 3D network calcium silicate hydrate, and mechanical behavior of graphene oxide reinforced cement composites. *Constr Build Mater* 190:150–163
54. Pan Z, He L, Qiu L, Korayem AH, Li G, Zhu JW, Collins F, Li D, Duan WH, Wang CM (2015) Mechanical properties and microstructure of a graphene oxide–cement composite. *Cem Concr Compos* 58:140–147
55. Abdullah A, Taha M, Rashwan M, Fahmy M (2021) Efficient use of Graphene oxide and silica fume in cement-based composites. *Materials* 14:1–14
56. Li X, Li C, Liu Y, Chen SJ, Wang CM, Sanjayan JG, Duan WH (2018) Improvement of mechanical properties by incorporating graphene oxide into cement mortar. *Mech Adv Mater Struct* 25:1313–1322
57. Kim B, Taylor L, Troy A, McArthur M, Ptaszynska M (2018) The effects of Graphene oxide flakes on the mechanical properties of cement mortar. *Comput Concr* 21:261–267
58. Birenboim M, Nadiv R, Alatawna A, Buzaglo M, Schahar G, Lee J, Kim G, Peled A, Regev O (2019) Reinforcement and workability aspects of Graphene-oxide-reinforced cement nanocomposites. *Compos Part B Eng* 161:68–76
59. Diamond S (2000) Mercury porosimetry: an inappropriate method for the measurement of pore size distributions in cement-based materials. *Cem Concr Res* 30:1517–1525
60. Halamickova P, Detwiler RJ, Bentz DP, Garbocz EJ (1995) Water permeability and chloride ion diffusion in Portland cement mortars: relationship to sand content and critical pore diameter. *Cem Concr Res* 25:790–802
61. Zhu X, Kang X (2020) Effect of Graphene oxide (GO) on the hydration and dissolution of alite in a synthetic cement system. *J Mater Sci* 55:3419–3433
62. Kang X, Zhu X, Shu X, Liu J (2022) Hydration of clinker phases in portland cement in the presence of Graphene oxide. *J Mater Civ Eng* 34:1–11
63. Meng S, Ouyan X, Fu J, Niu Y, Ma Y (2021) The role of graphene/graphene oxide in cement hydration. *Nanotechnol Rev* 10:768–778

64. Baomin W, Shuang D (2019) Effect and mechanism of graphene nanoplatelets on hydration reaction, mechanical properties and microstructure of cement composites. *Constr Build Mater* 228:1–12

Publisher's Note Springer Nature remains neutral with regard to jurisdictional claims in published maps and institutional affiliations.

Springer Nature or its licensor holds exclusive rights to this article under a publishing agreement with the author(s) or other rightsholder(s); author self-archiving of the accepted manuscript version of this article is solely governed by the terms of such publishing agreement and applicable law.

Effect of Graphene oxide Addition on Cement-Sand Mortar

Surajit Biswas¹, Saroj Mandal²

¹ Research scholar of Civil Engineering Department, Jadavpur University, Kolkata-700032, India,

² Professor of Civil Engineering Department, Jadavpur University, Kolkata – 700032, India,

Paper ID - 020076

Abstract

The effect of addition of graphene oxide (GO) to the cement-sand mortar on its fluidity and strength was investigated. The dosages of GO addition were varied from 0.03% to 0.06% by weight of cement. The GO was sonicated with required water for uniform mixing and added to the dry mixture of Ordinary Portland Cement and sand of proportion 1:2 (by weight). The incorporation of GO in cement- sand mortar reduced its fluidity compared to control mortar (without GO). A maximum reduction in fluidity of 32% was noted for the GO addition of 0.03%. The compressive strength of mortar was enhanced with the addition of GO (up to 0.05%). However, such enhancement was reduced with further addition of GO. The 0.05% of GO addition increased the compressive strength of mortar by 49.8%, 25.6% and 20.3% compare to that of control sample at 3 days, 7 days and 28 days respectively. The flexural strength of GO based cement sand mortar was also increased substantially compared to control mortar at 0.05% GO addition. More flake like hydration products were observed in GO based cement sand mortars by field emission scanning electron microscopy (FESEM).

Keywords: Graphene oxide, Cement mortar, Fluidity, Compressive strength, Flexural strength.

1. Introduction

Cement based construction materials are most widely used for building, road, bridge and various other types of civil engineering construction. However, it has its own limitation because of its lesser tensile strength and brittleness. By providing steel bars [1], it possible to increase its resistance against tension. The incorporation of different admixture [2] and fibres [1,2] are at present most valuable techniques to Improve its overall performance. Recently carbon-based nanomaterials such as carbon nanotubes (CNTs) and graphene have pulled the attention in improving the performance of such cementitious materials [2] because of their amazing physical and mechanical properties. It was shown that the addition of very less amount of carbon nanotubes (CNTs) increase the mechanical properties of cementitious materials [3,4] and enhanced also the mechanical and chemical properties of fly-ash based geopolymers [5].

Graphene (G) and graphene oxide (GO) are new members in the world of carbon based nanomaterial. Graphene is a single layered and considered as two dimensional (2D). GO is basically a graphene derivative and it has various oxygen-containing functional group such as hydroxyl, carbonyl, epoxy and carboxylic groups. It has huge surface area and high mechanical properties [6, 7].

This makes GO potentially more favourable than 0D nanomaterials and 1D nanotubes for altering various matrix properties.

The aim of the present research work is to incorporate GO in cement sand mortar at various dosages (0.03% to 0.06% by weight of cement) and to investigate its effect on mechanical properties of cement-sand mortar. The microstructure analysis of cement-sand mortar (with/without GO) was also performed by field emission scanning electron microscope (FESEM).

2. Materials and Experimental Methods

2.1 Materials

Ordinary Portland Cement (OPC) grade 53 confirming to IS: 12269-1987 [9] was used throughout the experimental study. The chemical compositions of OPC are presented in Table 1. Locally available river sand of Grade-II (as per IS: 383-2016) and specific gravity of 2.66 was used. The properties of GO collected from M/s Ad-Nano Technologies Pvt. Ltd, Karnataka, India was presented in Table 2.

*Corresponding author. Tel: +919679824362; E-mail address: surajitju18@gmail.com

Table-1. Chemical composition OPC 53 grade

Parameters	Percentages
SiO ₂	21.94
Al ₂ O ₃	4.95
Fe ₂ O ₃	3.74
CaO	62.33
MgO	2.08
SO ₃	2.22
K ₂ O	0.56
Na ₂ O	0.32
Others	1.89

Table-2. Technical properties of GO

Descriptions	Graphene oxide
Purity	>99%
Numbers of layers	1-3 layers
Average thickness (z)	0.8-1.6nm
Average lateral dimension (x & y)	5-10 μ m
Surface area	450m ² /g
Carbon	66%
Oxygen	32%
Others	2%

2.2 Mix Proportion and curing

To investigate the effects of addition of GO in cement mortar, cement sand ratio was taken as 1:2 and the water to cement ratio was kept as 0.45 for all the mixtures. The amount of GO added into cement sand mortar are 0.03%, 0.04%, 0.05% and 0.06% by weight of cement. The cement and sand was mixed thoroughly 3-4 minutes in dry condition. Sonicated mixture of require amount water and GO was added. Then the mortar was placed into standard steel mould and well compacted. The hardened cement mortar was demoulded after 24 hours and immediately placed in water for curing till testing. Details of different mixtures are shown in table 3.

Table-3. Details of different mixtures and its flow test results

Mix designation	Control	GOPC-3	GOPC-4	GOPC-5	GOPC-6
Cement (gm)	726	726	726	726	726
Sand (gm)	1452	1452	1452	1452	1452
GO % (by weight of cement)	0.00	0.03%	0.04%	0.05%	0.06%
% of flow (as per flow table test)	42	10	13	20	16
Reduction of flow %	-	23	20	15	18

3. Preparation of Cement Mortar Sample and Testing

3.1 Fluidity Test

The fluidity of cement sand mortar mixes with/without GO was measured by using flow table test as per IS: 4031 (part 7) – 1988 [10]. The dimensions of the con are top diameter 50 mm, bottom diameter 100 mm and height 50 mm. the con was fixed firmly on flow table. The fluidity was measured from the initial and final diameter after test.

3.2 Sample Preparation for Compressive Strength and Flexural Strength Test

To study the effect of addition of different doses of GO on the mechanical properties of cement mortar, the compressive strength tests were conducted using standard cement mortar cube specimens of size 70.6 mm \times 70.6 mm \times 70.6 mm [11]. For the compressive strength test, hardened cement mortars were tested at different ages of 3 days, 7 days and 28 days. Flexural strength test was also carried out on 50 mm \times 50 mm \times 200 mm cement mortar bar at different dosages of GO. These specimens were tested after 28 days water curing. The center point method was adopted for the determination of flexural strength (AASHTO T 67) (12) of span 150 mm.

3.3 Sample Preparation for FESEM Analysis

After compressive strength test at 28 days, the fragments of cement sand mortar with/without GO were crushed to powder separately and were examined under FESEM (INSPECT F50 SEM, FEI Europe BV, Eindhoven, the Netherlands) to obtain micrograph.

4. Result and Discussion

4.1 Fluidity Test

The results of flow table test for different mixes are tabulated in table 3. It is noted that the fluidity of cement mortar decreases with respect to control sample (without GO) with the addition of different percentage of GO. Maximum reduction in fluidity of 23% was observed for the incorporation of 0.03% of GO. The reduction in fluidity of GO based cement-sand mortar may be due to the high specific surface area of graphene oxide. Further, graphene oxide interacted with cement particles and thereby agglomerates and flocculation was formed. The large surface area of graphene oxide with high absorption of free water on its surface leads to the decrease in fluidity [3].

4.2 Compressive strength

Fig. 1 shows the compressive strength of cement-sand mortar sample with and without GO. It is noted that the compressive strength of cement mortar increases

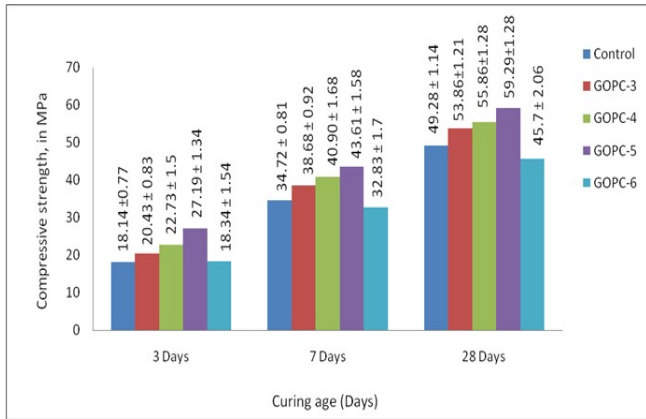


Fig 1. Compressive strength of different mixes at different ages

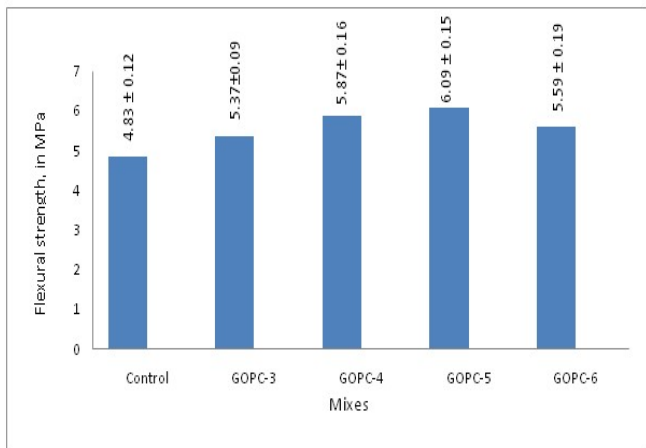


Fig 2. Flexural strength of different mixes at 28 days

prominently with the increase in GO addition up to 0.05% by weight of cement at all ages. However, with further addition (at 0.06% GO) the strength is decreased at all ages.

4.3 Flexural Strength

Fig.2 indicates the variations of flexural strength of cement sand mortar with and without GO. The maximum tensile strength at 0.05 addition of GO was 6.09 MPa compared to that of control sample of 4.83 MPa. Similar trend obtained as in the case compressive strength results.

4.4 Micro-Structural Analysis by FESEM

The FESEM images of cement sand mortar for control sample and GOPC5 are shown in Fig. 3 (a) and Fig. 3 (b) respectively. Large amount of flake like hydration products observed in GOPC-5 compare to control sample (without GO). The enhancement of compressive strength of GO based cement-sand mortar may be due to the presence of more such hydration product that fill the pore area of cement sand mortar and improve the pore structures. It has also noted that GO could have regulate have regulate the form of flower-like, polyhedral and lamellar hydration products of cement paste which form denser structures [13, 14].

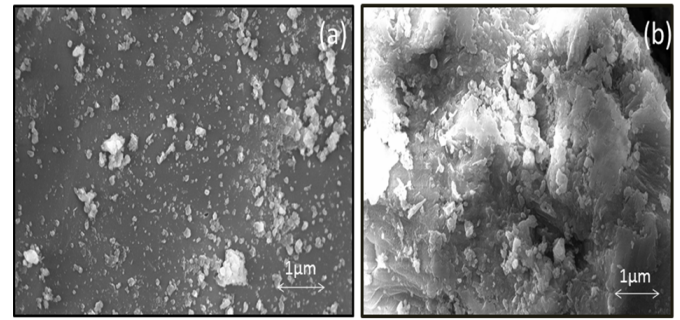


Fig3. FESEM image of cement-sand mortar (a) control sample and (b) GOPC-5

5. Conclusions

The fluidity of the cement sand mortar is reduced with the incorporation of GO. This reduction of fluidity is due to the formation of GO agglomerates which have high water entrapment capacity and high specific surface area. The maximum reduction of fluidity of GO based cement sand mortar noted at 0.03% addition of GO. Addition of GO also increases the compressive strength of cement sand mortar at different ages. The maximum enhancement of compressive strength was noted at 0.05% GO addition. Further, the enhancement in compressive strength is more pronounced at 3 days compared to 28 days. The tensile strength of cement sand mortar is also increased with the addition of GO and the optimum % of GO addition is noted as 0.05%. The improvement in strength seems to be due more refined pore structures with the formation of hydrated flake like product.

Disclosures

Free Access to this article is sponsored by SARL ALPHA CRISTO INDUSTRIAL.

References

- Pan Z., He L., Qiu L., Korayem A., Li G., Zhu W. J., Collins F., Dan Li, Duan W. H., Wang C. M.: Mechanical properties and microstructure of a graphene oxide–cement composite. *Cement & Concrete Composites* 58,140–147 (2015).
- Shang Y., Zhang D., Yang C., Liu Y., Liu Y.: Effect of graphene oxide on the rheological properties of cement pastes. *Construction and Building Materials* 96, 20–28 (2015).
- Li X., Liu Y. M., Li W. G., Li C. Y., Sanjayan J. G., Duan W. H., Li Z.: Effects of graphene oxide agglomerates on workability, hydration, microstructure and compressive strength of cement paste. *Construction and Building Materials* 145, 402–410 (2017).
- Konsta-Gdoutos M.S., Metaxa Z. S., Shah S. P.: Multi-scale mechanical and fracture characteristics and early-age strain capacity of high performance carbon nanotube/cement nano composites, *Cement Concr. Compos.* 32(2), 110–115 (2010).
- Siddique R., Mehta A.: Effect of carbon nanotubes on properties of cement mortars, *Constr. Build. Mater.* 50, 116–129 (2014).

6. Cote L. J., Kim J., Tung V.C., Luo J., Kim F., Huang J.: Graphene oxide as surfactant sheets, *Pure Appl. Chem.* 83, 95–110 (2011).
7. Kim J., Cote L. J., Huang J.: Two dimensional soft material: new faces of graphene oxide, *Acc. Chem. Res.* 45,1356–1364 (2012).
8. Chuah S., Pan Z., Sanjayan J. G., Wang C.M., Duan W. H. : Nano reinforced cement and concrete composites and new perspective from graphene oxide, *Constr. Build. Mater.* 73, 113–124 (2014).
9. _____ IS 12269: 2013. Ordinary Portland Cement, 53 Grade — Specification, Bureau of Indian Standards, New Delhi, India.
10. _____ IS: 4031 (Part 7) – 1988, Methods of Physical Tests for Hydraulic Cement, Bureau of Indian Standard, New Delhi.
11. _____ IS 10080 – 1982. Specification for vibration machine, Bureau of Indian Standards, New Delhi, India.
12. _____ AASHTO T 67-05. Standard method of test for standard practices for force verification of testing machines, standard published by American Association of State and Highway Transportation Officials.
13. Lv S., Liu J., Sun T., Ma Y., Zhou Q.: Effect of GO nanosheets on shapes of cement hydration crystals and their formation process, *Constr. Build. Mater.* 64, 231–239 (2014).
14. Lv S., Ma Yu., Qiu C., Sun T., Liu J., Zhou Q.: Effect of graphene oxide nanosheets of microstructure and mechanical properties of cement composites, *Constr. Build. Mater.* 49, 121–127 (2013).

RESEARCH ARTICLE | JULY 27 2023

Graphene oxide modified cement mortar

Surajit Biswas ; Saroj Mandal



AIP Conference Proceedings 2721, 020033 (2023)

<https://doi.org/10.1063/5.0153963>



CrossMark



AIP Advances

Why Publish With Us?

**25 DAYS**
average time
to 1st decision

**740+ DOWNLOADS**
average per article

**INCLUSIVE**
scope

[Learn More](#)

 AIP
Publishing

Graphene Oxide Modified Cement Mortar

Surajit Biswas^{1,a} and Saroj Mandal¹

¹Department of Civil Engineering, Jadavpur University, Kolkata-700032, India

^aCorresponding author: surajitce08@gmail.com

Abstract. An experimental study has been made for both Ordinary Portland Cement (OPC) and Portland Pozzolana Cement (PPC) based mortar with the addition of graphene oxide separately. The powdered graphene oxide (GO) in different proportions (0.03% to 0.06% by weight of cement) was ultra-sonicated with the part of the required mixing water before addition to the mortar. The optimum percentage of 0.05% and 0.04% of GO addition was achieved for OPC and PPC based mortar respectively in terms of strength criteria at different ages. The enhancement in strength of GO based cement mortar may be due to the refinement of pore structure in the mortar matrix

Keywords: Graphene oxide, compressive strength, flexural strength, cement-sand mortar.

INTRODUCTION

Cement is widely used in construction and building material. It is the principal binder in concrete as it holds the aggregates together in the presence of water by hydration. However, the brittle nature and low tensile strength are the major disadvantages of cement-based construction materials. To enhance the performances of the cementitious materials, recently researchers concentrated on using different types of additives and fibres. With the advancement of nanotechnology, such as 0D nanoparticles, 1D nano-fibers and 2D nano-sheets have drawn considerable attention because of their high mechanical properties with the high specific surface area. It was reported that the compressive strength, flexural strength and tensile strength of cementitious materials can be remarkably influenced by silica nano particles (0D) [1-4]. It was observed that the durability, drying shrinkage and water permeability of cementitious materials are also influenced by the addition of silica nanoparticles [2, 5, 6]. Addition of 10% nanosilica with dispersing agents, the compressive strength increased 26% after 28 days curing age [7]. Even, the incorporation of little amount of nano SiO₂ particles into cement composite improved the compressive strength and flexural strength after 28 days curing age 10% and 25% respectively [5]. It was accepted that the nano-SiO₂ particles filled the pore structure of cement composite [8, 9]. Addition of small amount of nano SiO₂ into cement composite accelerates the hydration process and improved the strength and microstructure characteristics [10-15]. Carbon nanotubes (CNTs) is a carbon based 1D nano materials. It consists of rolled up single layered carbon atom sheets. In general, CNTs are categorized into two types, single layered and multi layered and diameters are 1-3 nm and 5-50 nm respectively [16]. However, it was noted that the addition of small amounts of CNTs increased the mechanical properties of cementitious materials [17 - 19]. Parveen et al [20] showed that incorporation of a small amount of CNTs in cement mortar increased compressive strength and flexural strength up to 23% and 17% after 28 days. The main mechanisms of incorporation of CNTs in the cement matrix are the filling of nano-size pore area, bridging the micro size capillary pores and the effects of nucleation [18]. G.Y. Li et al [21] reported that enhancement of compressive strength, flexural strength as well as failure strain improved due to the addition of CNTs. The addition of CNTs improve the microstructure such as interracial interaction of CNTs and cement hydration and produced high strength, also improve the load transferred efficiency from cement to reinforcement. Recently, carbon-based nanomaterial, Graphene oxide (GO) has drawn attention to incorporate into the cement matrix. It is a single-layered two dimensional (2D) nanomaterial consisting of various oxygen-containing functional groups such as hydroxyl, carbonyl, epoxy and carboxylic groups [22, 23]. In the aqueous solution, GO can be conveniently dispersed due to the presence of different oxygen containing groups. These oxygen containing functional groups in GO's chemical structure is responsible for the enhancement of the chemical and physical properties of the different host materials [24]. GO has a high specific surface area and amazing mechanical properties such as ultra-high strength, flexibility [25-28]. Due to high specific surface area GO can promote chemical and physical interaction with host materials [29]. It

was accepted that with ceramic and polymer materials, GO can easily form composites and can promote the toughness by monitoring the microstructure of crystal [29, 30]. It may be mentioned that GO can be synthesized in large quantities by strong oxidation of inexpensive graphite powder [31]. However, GO has been widely used in various field such as energy storage materials [31], semiconductors [32] biological composites [33] and photo catalyst materials [34]. From previous study, it has been concluded that little amount of GO addition into cement paste can enhanced the compressive strength, tensile strength, and flexural strength. Not only increase the mechanical properties of cement composite, introduced of GO in cementitious materials, the microstructure of cement composite also promoted [35-37]. It was reported that incorporation of very small amount 0.03% of GO into cement paste increase the compressive strength and tensile strength around 40%, not only increase the compressive and tensile strength also reduced the pore structure of cement paste [38]. S. Lv et al [39] reported that introduction of 0.03% of GO into cement composite increase the compressive strength, flexural strength and tensile strength by 38.9%, 60.7% and 78.6% respectively. It was showed that incorporation of GO into cement composite, take an important role effectively to formation of the microstructure of hydration crystal, reduced brittleness and increased toughness significantly. The compressive strength and flexural strength were increased around 34% and 42% respectively by the introduction of very small amount 0.04% of GO by weight of cement into cement paste [40]. The incorporation of little amount 0.05% of GO into cement paste increase the flexural strength and compressive strength after 28 days, 41-58% and 15-33% respectively [42]. The investigation of the microstructure of GO based cementitious material was reported that incorporation GO in cement composite produce finer pore [40, 41]. It was observed the incorporation of as little as 0.05% of GO by weight of cement reduce workability of cement paste around 42% [42]. It is accepted that to wet the large specific surface area of GO agglomerates required more free water and lead to reduce the fluidity of cement composite. It was reported that introduction of GO into cement also influences the workability of cement composite and increase the viscosity of cement composite [43-45]. This are the clear indication that GO has a great potential to use into cement composite to reinforced. In author's knowledge, most of the earlier researchers investigated the effect of Graphene oxide on Ordinary Portland Cement. The objective of the present work is to compare the effect of GO addition in Ordinary Portland Cement based mortar and Portland Pozzolana Cement based mortar at various dosages such as 0.03%, 0.04%, 0.05% and 0.06% by weight of cement.

Table. 1. List of nomenclature used

Acronyms	Full Name
GO	Graphene Oxide
CNTs	Carbon Nano tubes
nano SiO ₂	Nano Silica
OPC	Ordinary Portland Cement
PPC	Portland Pozzolana Cement

MATERIALS AND EXPERIMENTAL METHODS

Materials

Ordinary Portland Cement (OPC) grade 53 and Portland Pozzolana Cement (PPC) confirming to IS: 269 - 2015 [46] and IS: 1489 (part-I) 2015 [47] respectively were used in this experimental study. The chemical compositions of OPC and PPC presented in Tables 2 and 3 respectively. Locally available river sand of Grade-II (as per IS: 383- 2016) and the specific gravity of 2.66 was used. The properties of GO collected from M/s Ad-Nano Technologies Pvt. Ltd, Karnataka, India was presented in Table 4. Fig 2 shows the bulk GO black in colour.

Table 2. Chemical composition (% by weight) of Ordinary Portland cement (OPC) grade 53

	SiO ₂	Al ₂ O ₃	Fe ₂ O ₃	CaO	MgO	SO ₃	K ₂ O	Na ₂ O	LOI
%	21.94	4.95	3.74	62.33	2.08	2.22	0.56	0.32	1.89

Table 3. Chemical composition (% by weight) of Portland Pozzolona cement.(PPC)

	SiO ₂	Al ₂ O ₃	Fe ₂ O ₃	CaO	MgO	SO ₃	LOI
%	30	8.0	5.2	42.4	1.65	2.45	3.6

**FIGURE 1.** Graphene oxide**Table 4.** Technical properties of Graphene Oxide.

Purity	> 99 %
Numbers of layers	1-3 layers
Average thickness (z)	0.8-1.6 nm
Average lateral dimension (x & y)	5-10 µm
Surface area	450 m ² /g
Carbon	66%
Oxygen	32%
Others	2%

Mix proportion and curing

For all the mixes with and without GO, the cement-sand ratio by weight was taken as 1:2 and water: cement ratio kept 0.45. The amount of GO added into cement sand mortar was 0.03%, 0.04%, 0.05% and 0.06% by weight of cement in different mixes for both OPC and PPC. GO solution was made by GO with water at a ratio of 1:10 and sonicated the mixture for around 45- 60 minutes by ultrasonic probe sonicator. Details of different mixtures using OPC and PPC are shown in Table 4 and Table 5 respectively. At first, in dry condition, the cement and locally available sands were mixed thoroughly for 3-4 minutes to get a uniform mixture. Then the sonicated mixture of appropriate quantity of GO and water was added to the dry mix. Then the mortar was placed into the different standard mould and well compacted. The hardened cement mortar was demoulded after 24 hours and placed in water for curing till testing.

Table 5. Details of different mixtures Ordinary Portland cement (OPC) mortar.

Sl No	Mix designation	Cement (gm)	Sand (gm)	GO %
1	Control	726	1452	0
2	GOPC-3	726	1452	0.03%
3	GOPC-4	726	1452	0.04%
4	GOPC-5	726	1452	0.05%
5	GOPC-6	726	1452	0.06%

Table 6. Details of different mixtures Portland Pozzolona (PPC) mortar.

Sl No	Mix designation	Cement (gm)	Sand (gm)	GO %
1	Control	726	1452	0
2	GOPC-3	726	1452	0.03%
3	GOPC-4	726	1452	0.04%
4	GOPC-5	726	1452	0.05%
5	GOPC-6	726	1452	0.06%

PREPARATION OF CEMENT MORTAR SAMPLE AND TESTING

Sample preparation for compressive strength test

To study the effect of addition of different amount of GO (such as 0.03%, 0.04%, 0.05 and 0.06%) on the mechanical properties of both type of cement mortars (such as OPC and PPC) with and without GO, the compressive strength tests were conducted using the standard cement mortar cube specimens of size 70.6 mm ×70.6 mm ×70.6 mm. The compressive strength tests were conducted at different curing ages of 3 days, 7 days and 28 days of harden cement mortar.

Sample preparation for flexural strength test

Flexural strength test was also carried out on 50 mm ×50 mm ×200 mm cement mortar bar at the same dosages of GO at 28 days of curing age. The center point loading method was adopted for the determination of flexural strength (AASHTO T 67) [48] of span 150 mm. Six samples were tested for each set of test results. For center point method, the mortar bar supported at two ends at a distance of 25mm from the edges. Load applied at the midpoint of clear span. Load is gradually increased until failure of mortar bar. The modulus of rupture reported as flexural strength. Fig.3 shows a set up of center point loading system.

RESULTS AND DISCUSSION

Compressive strength

Fig. 4 and Fig. 5 show the compressive strength of harden cement-sand mortar sample with and without GO using OPC and PPC respectively at the age of 3 days, 7 days and 28 days. After 3 days curing age, it was

observed that compressive strength of OPC based cement sand mortar GOPC-3, GOPC-4 and GOPC-5 increase around 12%, 25% and 49% respectively compared to control sample. At 7 days curing age increased the compressive strength around 11%, 17% and 25% for GOPC-3, GOPC-4 and GOPC-5 respectively. After 28 days curing age maximum increment of compressive strength observed for GOPC-5 around 20%. The compressive strength of GOPC-3 and GOPC-4 after 28 days noted 9% and 13% compared to control sample respectively. For GOPC-6, compressive strength observed at 3 days same as control sample and 7 days it slightly decreased.

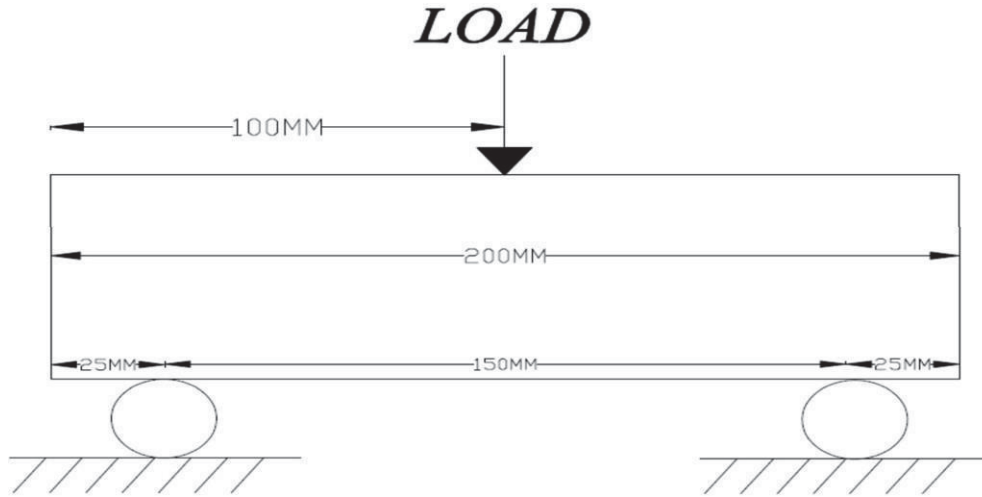


FIGURE 2. Set up for center point loading

After 28 days compressive decreased around 7.8% compare to control sample for GOPC-6. It was noted that the compressive strength of OPC based mortar was increased with the addition of GO up to 0.05% by weight of cement at all ages. Further addition (at 0.06% of GO) the strength was decreased at all curing ages. On the other hand, the compressive strength improvement observed for PPC based cement sand mortar GOPPC- 3, GOPPC-4 and GOPPC-5 at 3 days 9%, 26% and 13% respectively compared to control sample. At 7 days curing age increased the compressive strength around 7%, 15% and 10% for GOPPC-3, GOPPC-4 and GOPPC-5 respectively. After 28 days curing age maximum increment of compressive strength observed for GOPPC-4 around 12%. The compressive strength of GOPC-3 and GOPC-5 after 28 days noted 6% and 9% compared to control sample respectively. Other hands, the effect of compressive strength of GOPPC-6 similar to GOPC-6. After 28 days decrease around 9% compared to the control sample. It was noted that compressive strength improvement for PPC based cement sand mortar maximum at the dosage of 0.04% by weight of cement.

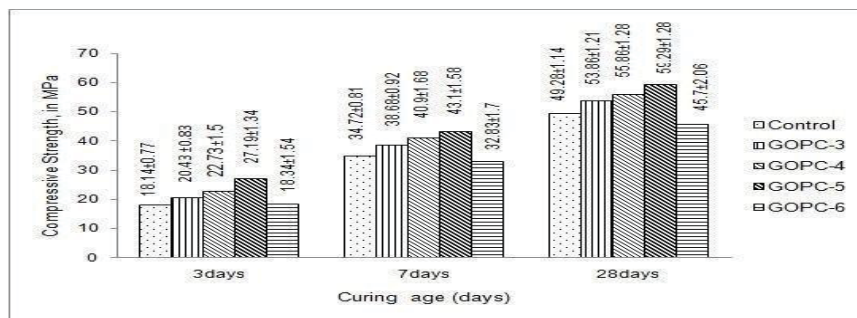


FIGURE 3. Compressive strength of different mixes of OPC based mortar at different ages.

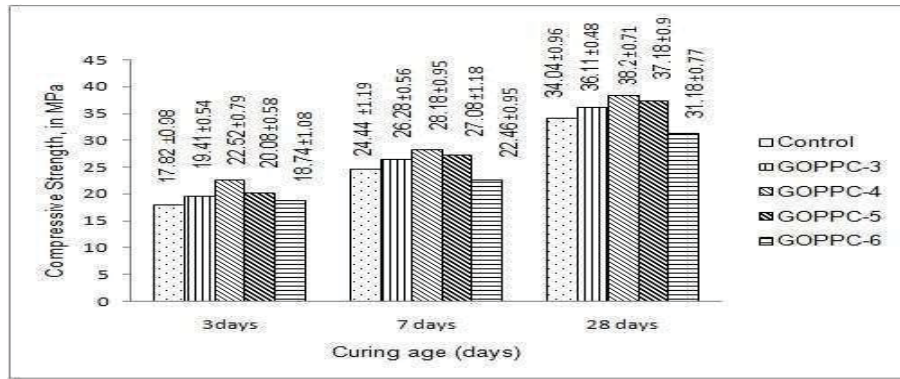


FIGURE 4. Compressive strength of different mixes of PPC based mortar at different ages.

Flexural strength

Fig.6 and Fig.7 indicates the variations of flexural strength of cement sand mortar with and without GO using OPC and PPC respectively. For OPC based cement sand mortar, it was observed that tensile strength increases 11 %, 21% and 26% for GOPC-3, GOPC-4 and GOPC-5 compare to control sample respectively. It was noted that the maximum tensile strength of OPC based mortar at 0.05% addition of GO was 6.09 MPa compared to that of a control sample of 4.83 MPa. Further addition of GO, for GOPC-6 increased the tensile strength compare to control sample but decrease compare GOPC-5. Other hand tensile strength of PPC based cement sand mortar increased after 28 days 17%, 32% and 21% for GOPPC-3, GOPPC-4 and GOPPC-5 compare to control sample respectively. MPa Further addition of GO, for GOPPC-6 increased the tensile strength compare to control sample but decrease compare GOPPC-4. For PPC based mortar, the maximum tensile strength at 0.04% addition of GO was 5.6 MPa compared to that of a control sample of 4.23 MPa. The behavior of tensile strength was similar to that of compressive strength results for both OPC and PPC based mortars.

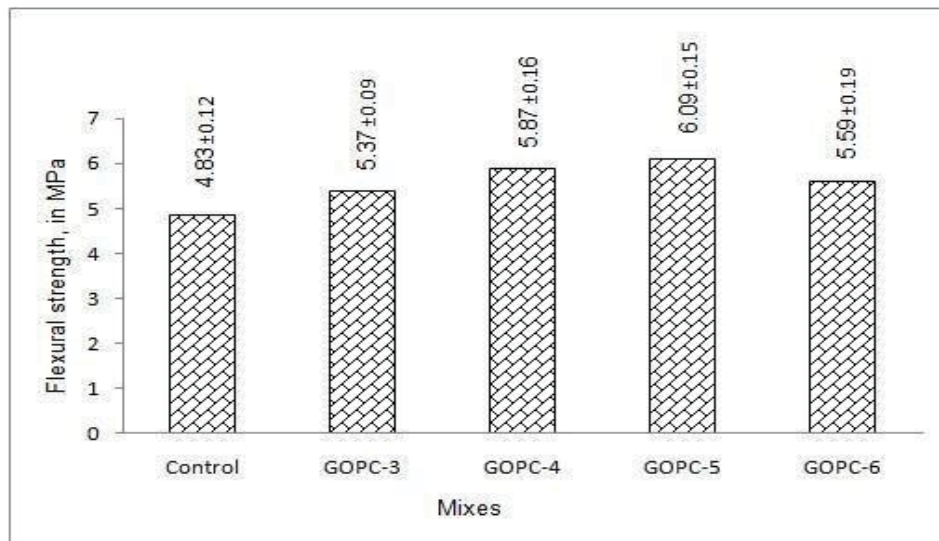


FIGURE 5. Flexural strength of different mixes of OPC based mortar at 28 days.

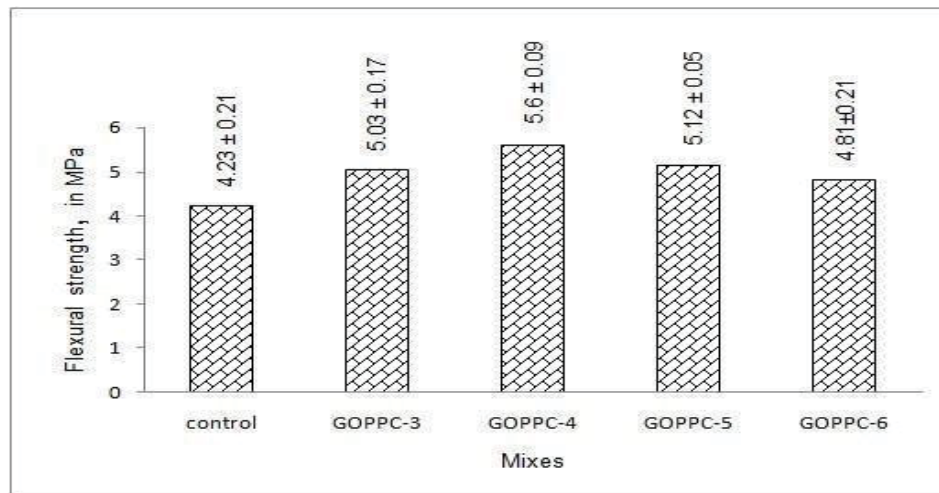


FIGURE 6. Flexural strength of different mixes of PPC based mortar at 28 days

CONCLUSION

Addition of GO increases the compressive strength of cement sand mortar of both types of cement OPC and PPC at different ages. The maximum enhancement of compressive strength of OPC and PPC was noted at 0.05% and 0.04% GO addition respectively. The enhancement of compressive strength of GO based cement mortar compare to the control sample is noted as 20% and 12% for OPC (0.05%) and PPC (0.04%) respectively at 28 days curing age. The flexural strength of cement sand mortar of OPC and PPC is also increased with the addition of GO. The optimum strength was noted at 0.05% and 0.04% of GO addition for OPC and PPC based mortar respectively. The enhancement of flexural strength of GO based cement mortar compare to control sample is noted as 26% and 32% for OPC (0.05%) and PPC (0.04%) respectively at 28 days curing age. The enhancement in strength of GO based cement mortar is supposed to be due to the refinement of pore structure in the mortar matrix by GO agglomerates. However more micro-structural study is needed for the effective use in different cement-based materials.

REFERENCES

1. H. Li, H. G. Xiao and J. Ou, A study on mechanical and pressure-sensitive properties of cement mortar with nanophase materials. *Cem and Concr Res.* 2004, 34 (3), 435- 438.
2. N. Givi, A. A. Rashid, S. Aziz, F. N. A. Salleh and M. A. Mohd, The effects of lime solution on the properties of SiO₂ nanoparticles binary blended concrete. *AGRIS science*, 2011, 42 (3), 562-569.
3. E. Horszaruk, E. Mijowaska, K. Cendrowski, S. Mijowaska and P. Sikora, Effect of incorporation route on dispersion of mesoporous silica nanospheres in cement mortar. *Construction and Building Materials*, 2014, 66, 418 - 421.
4. N. Sanchez, K. Sobolev, Nanotechnology in concrete – A review, *Constr. And Build Materials*, 2010, 24 (11) : 2060 –2071.
5. T. Ji, Preliminary study on the water permeability and microstructure of concrete incorporating nano-SiO₂. *Cem and Concr Res*, 2005, 35 (10) :1943–1947.
6. L. Senff, D. Hotza, W. L. Repette, V. M. Ferreira and J.A. Labrincha, Mortars with nano SiO₂ and micro-SiO₂ investigated by experimental design. *Constr and Build Mater.*, 2010, 24 (8): 1432–1437.
7. Y. Qing, Z. Zenan, S. Li and C. Rongshen, A comparative study on the pozzolanic activity between nano-SiO₂ and silica fume. *J Wuhan Univ Technol – Mater Sci Ed.*, 2008, 21 (3): 153–157.
8. C. Zhuang, and Y. Chen, The effect of nano-SiO₂ on concrete properties: a review, *Nanotechnology*, 2019, 8 (1) : 562 – 572.

9. H. Li, H.G. Xiao, J. Yuan and J. Ou, Microstructure of cement mortar with nanoparticles. *Compos Part B*, 2004, 35(2):185–189.
10. B.W. Jo, C.-H. Kim, Tae. G-h and J.B. Park, Characteristics of cement mortar with nano-SiO₂ particles, *Constr. Build. Mater.* 2007, 21 : 1351–1355.
11. H. Li, H. G. Xiao, J. Yuan and J. Ou, Microstructure of cement mortar with nanoparticles, *Compos. Part B: Eng.* 2004, 35 (2): 185–189.
12. D.F. Lin, K.L. Lin, W.C. Chang, H.L. Luo and M.Q. Cai, Improvements of nano-SiO₂ on sludge/fly ash mortar, *WasteManage.* 2008, 28 : 1081–1087.
13. K.L. Lin, W.C. Chang, D.F. Lin, H.L. Luo and M.C. Tsai, Effects of nano-SiO₂ and different ash particle sizes on sludge ash–cement mortar, *J. Environ. Manage.* 2008, 88 (4), 708–714.
14. G. Li, Properties of high-volume fly ash concrete incorporating nano-SiO₂, *Cem. Concr. Res.*, 2004, 34 (6) : 1043–1049.
15. J. Schoepfer and A. Maji, An investigation into the effect of silicon dioxide particle size on the strength of concrete, *ACI Spec. Publ.*, 2009 267 45–58.
16. S. Agrawal, M. S. Raghuvver, R. Ramprasad and G Ramanath, Multishell carrier transport in multiwalled carbonnanotubes. *IEEE Trans Nanotechnol*; 2007, 6 (6):722 –726.
17. B. Zou, S. J. Chen, A. H. Koryem, F. Collins, C. M. Wang and W. H. Duan,: Effect of ultrasonication energy onengineering properties of carbon nanotube reinforced cement pastes, *Carbon* 85, 2015, 212–220.
18. M.S. Konsta-Gdoutos, Z.S. Metaxa, and S.P. Shah, Multi-scale mechanical and fracture characteristics and early-age strain capacity of high performance carbon nanotube/ cement nano composites, *Cement Concr. Compos.* 2010 32 (2), 110–115.
19. R. Siddique and A. Mehta, Effect of carbon nanotubes on properties of cement mortars, *Constr. Build. Mater.*, 2014, 50,116–129.
20. S. Parveen, S. Rana, R. Fanguiero and M.C. Paiva, Microstructure and mechanical properties of carbon nanotubereinforced cementitious composites developed using a novel dispersion technique, *Cem. Concr. Res.*, 2015, 73 215–227.
21. G. Y. Li, P. M. Wang and X. Zhao, Mechanical behavior and microstructure of cement composites incorporating surface- treated multi-walled carbon nanotubes, *Carbon*, 2005, 43, 1239–1245 (2005).
22. L.J. Cote, J. Kim, V.C. Tung, J. Luo, F. Kim and J. Huang, Graphene oxide as surfactant sheets, *Pure Appl. Chem.*, 2011, 83, 95–110.
23. J. Kim, L.J. Cote, J. Huang, Two dimensional soft material: new faces of graphene oxide, *Acc. Chem. Res.*, 2012, 45, 1356–1364.
24. A. Mohammeda, J.G. Sanjayan , A. Nazari and N.T.K. Al-Saadi,: The role of graphene oxide in limited long-termcarbonation of cement-based matrix, *Constr. Build. Mater.*, 2018, 168, 858–866.
25. Y. Zhu, S. Murali, W. Cai, X. Li, J. W. Suk , J. R. Potts, R. S. Ruoff,: Graphene and graphene oxide: synthesis, properties, and applications, *Adv. Mater.* 22 (35) 3906 – 3924 (2010).
26. D.A. Dikin Dmitriy, S. Stankovich, E. J. Zimney, R. D. Piner, G. H. B. Dommett1, G. Evmenenko, S. B. T. Nguyen and R. S. Ruoff, Preparation and characterization of graphene oxide paper, *Nature*, 2007, 448 (7152) 457 – 460.
27. J. R. Potts, D. R. Dreyer, C. W. Bielawski and R. S. Ruoff, Graphene-based polymer nanocomposites, *Polymer*, 2011,52 : 5 – 25.
28. T. Kuila, S. Bose, C. E. Hong, Md E. Uddin, P. Khanra, N. H. Kim and J. H. Lee, Preparation of functionalized graphene/linear low density polyethylene composites by a solution mixing method, *Carbon*, 2011, 49 : 1033 – 1051.
29. F. Ling, L. Hong-bo, Z. Yan-hong and L. Bo, Technology research on oxidative degree of graphite oxide prepared byHummers method. *Carbon*, 2005, 4 : 10–2.
30. W. S. Hummers, Jr. and R. E. Offeman,: Preparation of Graphitic Oxide, *J. Am. Chem. Soc.* 1958, 80 : 1339 – 1339.
31. Z. Lu, D. Hou, B. Xu and Z. Li,: Preparation and characterization of an expanded perlite/ paraffin/ graphene oxide composite with enhanced thermal conductivity and leakage-bearing properties, *RSC Adv.*, 2015, 5 (130) 107514 – 107521.
32. X. Gong and W. Y. Teoh,: Modulating charge transport in semiconductor photocatalysts by spatial deposition of reduced graphene oxide and platinum, *J. of Catal.*, 2015, 332, 10 1– 111.
33. N. Mahmoudi and A. Simchi, On the biological performance of graphene oxide modified chitosan/polyvinyl pyrrolidone nanocomposite membranes: In vitro and in vivo effects of graphene oxide, *Mater. Sci. Eng.*, 2017, C 70 121 – 131.
34. Z. Lu, G. Chen, W. Hao, G. Sun and Z. Li, Mechanism of UV-assisted TiO₂/reduced graphene oxide

- composites with variable photo degradation of methyl orange, *RSC Adv.* 2015, 5 (89), 72916–72922.
35. Z. Lu, X. Li, A. Hanif, B. Chen, P. Parthasarathy, J. Yu and Z. Li, Early-age interaction mechanism between the graphene oxide and cement hydrates, *Construction and Building Materials*, 2017, 152 : 232–239.
 36. S. Lv, Y. Ma, C. Qiu and Q.F. Zhou, Regulation of GO on cement hydration crystals and its toughening effect, *Mag.Concr. Res.* 2013, 65, 1246–1254 (20).
 37. S. Chuah, Z. Pan, J. G. Sanjayan, C. M. Wang and W. H. Duan, Nano reinforced cement and concrete composites and new perspective from graphene oxide, *Constr. And Build. Mater.*, 2014, 73, 113–124.
 38. K. Gong, Z. Pan, H. Korayem, L. Qiu, D. Li, F. Collins, C. M. Wang and W. H. Duan: Reinforcing effects of grapheneoxide on portland cement paste, *Journal of. Mater. Civ. Eng.* 2015, 27(2), A4014010.
 39. S. Lv, Y. Ma, C. Qiu, T. Sun, J. Liu and Q. Zhou, Effect of graphene oxide nanosheets of microstructure and mechanical properties of cement composites, *Construction and Building Materials*, 2013, 49:121 – 127.
 40. S. Lv, J. Liu, T. Sun, Y. Maa and Q. Zhou: Effect of GO nanosheets on shapes of cement hydration crystals and their formation process, *Construction and Building Materials*, 2014, 64, 231 – 239.
 41. F. Celik, and H. Canakci, An investigation of rheological properties of cement-based grout mixed with rice husk ash(RHA), *Constr. Build. Mater.* 2015, 91, 187–194.
 42. Z. Pan, W. Duan, D. Li and F. Collins, Graphene oxide reinforced cement and concrete, WO Patent App. PCT/AU2012/001, 582, 2012.
 43. Z. Pan, L. He, L. Qiu, A. H. Korayem, G. Li, J. Wu Zhu, F. Collins, D. Li, W. H. Duan and M. C. Wang, Mechanical properties and microstructure of a graphene oxide-cement composite, *Cement & Concrete Composites*, 2015, 58, 140– 147.
 44. H. Elzbieta, M. Ewa, R. J. Kalenczuk, A. Malgorzata and M. Sylwia, Nanocomposite of cement/graphene oxide – impact on hydration kinetics and Young’s modulus, *Constr. Build. Mater.* 2015, 78 234–242.
 45. Y. Shang, D. Zhang, C. Yang, Y. Liu, and Y. Liu, Effect of graphene oxide on the rheological properties of cement pastes, *Construction and Building Materials*, 2015, 96, 20 – 28.
 46. IS 269: 2015. Ordinary Portland Cement specification, Bureau of Indian Standards, New Delhi, India.
 47. IS: 1489 (Part 1) – 2015, Portland Pozzolana Cement - Specification, Bureau of Indian Standard, New Delhi.
 48. AASHTO T 67-05. Standard method of test for standard practices for force verification of testing machines, standard published by American Association of State and Highway Transportation Officials.